NOVEL OLIGOMERIC BIODEGRADABLE CROSSLINKERS FOR HYBRID BIOMATERIAL FABRICATION FOR REGENERATIVE PURPOSES

Von der Fakultät für Lebenswissenschaften

der Universität Leipzig

genehmigte

D I S S E R T A T I O N

zur Erlangung des akademischen Grades

Doctor rerum naturalium

Dr. rer. nat.

vorgelegt von

Diplom-Pharmazeut Christian Kascholke

geboren am 02.07.1988 in Pößneck

Dekan: Prof. Dr. Tilo Pompe

Gutachter: Prof. Dr. Michaela Schulz-Siegmund

Prof. Dr. Karsten Mäder

Tag der Verteidigung: 01.06.2018

» Erfolg ist kein Zufall. Es ist harte Arbeit, Ausdauer, Lernen, Studieren, Aufopferung, jedoch vor allem, Liebe zu dem, was du tust oder dabei bist zu lernen. «

Edison Arantes do Nascimento (Pelé)

BIBLIOGRAPHISCHE DARSTELLUNG

Christian Kascholke

Novel Oligomeric Biodegradable Crosslinkers For Hybrid Biomaterial Fabrication For Regenerative Purposes

Fakultät für Lebenswissenschaften

Universität Leipzig

Dissertation

204 Seiten, 276 Literaturangaben, 43 Abbildungen, 7 Tabellen

The synthesis of extracellular matrix(ECM)-like biomaterial matrices is a promising strategy for tissue regeneration purposes. In this context, macromer-based materials offer great promise due to high design flexibility and versatile processability. This thesis aims at illustrating the advantages of the macromer-based concept by the establishment of two different material platforms: I) a gelatin-derived hydrogel system that allows for post-fabrication modification and II) a rigid glass-based hybrid material. To this end, two types of macromers were synthesized and characterized for chemical composition, molecular weight and reactivity. Low molecular-weight and chemically defined oligomers with adjustable composition were obtained. A set of hydrazide-reactive and anhydride-containing macromers was designed as a cross-linking building block for gelatin-derived hydrogels, while hybrid scaffolds were obtained from multi-armed lactide-based macromers and a sol-gel silica glass. Different strategies were investigated to adjust material macroporosity and applicability of PEG-porogen-leaching (hydrogel) as well as indirect rapid prototyping (hybrid glass) was demonstrated. Flexibility of the macromer-based material concepts was shown by successful processability of numerous dual-component formulations and relevant structure-property relationships were identified. In both concepts, material mechanics were controlled by macromer composition, molecular weight and concentration as well as material porosity. For the macromer/glass hybrids, *in vitro* degradation revealed continuous weight loss controlled by oligo(lactide) content and matrix hydrophilicity. Post-fabrication functionalization potential of the hydrogels was studied and reversible and triple-tunable hydrazide immobilization was shown which was controlled by hydrogel ketone content, hydrazide ligand concentration and medium pH. Precise adjustability of both macromer-based concepts offers great promise for material tailorability for versatile regenerative purposes.

TABLE OF CONTENTS

CHAPTER 1 1
Introduction

CHAPTER 2 17
Materials and Methods

CHAPTER 3 37
Dual-Functional Hydrazide-Reactive and Anhydride-Containing Oligomeric Hydrogel Building Blocks

CHAPTER 4 74
Dual Scale Porosity Adjustment of Oligomer-Cross-Linked Gelatinous Hydrogels

CHAPTER 5 93
Biodegradable and Adjustable Sol-Gel Glass Based Hybrid Scaffolds from Multi-Armed Oligomeric Building Blocks

CHAPTER 6 138
Discussion

CHAPTER 7 166
Summary

CHAPTER 8 171
Zusammenfassung

REFERENCES 176

APPENDIX 192
List of Abbreviations
Curriculum Vitae
List of Publications
Declaration of Authorship
Acknowledgements

CHAPTER 1

Introduction

1.1 BIOMATERIALS IN REGENERATIVE MEDICINE

Reviewing the annual reports given by the Scientific Registry of Transplant Recipients (SRTR) in collaboration with the Organ Procurement and Transplantation Network (OPTN), one realized that within the last 15 years the number patients awaiting transplantation in the USA increased from 80.000 to more than 120.000. In contrast, the number of performed transplantations stagnated at around 30.000 per year. Currently, every 10 minutes someone is added to the national transplant waiting list, but on average, 22 people die each day while waiting for a transplant.[1] Furthermore, the outcome of transplantations is often complicated by diseases, infections and/or rejection of the tissue by the host.[2] In case of bone, for example, which is the second most transplanted tissue after blood, allo- and xenografts suffer from immune rejection, reduced bioactivity and the risk of pathogen transmission.[3] Therefore, autografts still remain as the gold standard, but limited availability and donor site morbidity are significant disadvantages.[4] In that regard and with respect to the rise of age-related problems due to increased life expectancy of the population, there is a need for new strategies in regenerative medicine.[5] Biomaterial matrices were developed to foster tissue regeneration by mimicking the key characteristics of the extracellular matrix (ECM).[6] While different natural materials, such as hyaluronan, collagen, hydroxyapatite and calcium phosphates were initially used,[7,8] synthetic biodegradable polymers were developed within the last three decades.[9,10] The establishment of new synthesis strategies allowed for development of a great variety of polymeric materials with highly adjustable properties.[11,12] The spectrum of material characteristics was further enlarged by chemical modification of natural polymers and by creation of organic/inorganic hybrid materials.[3,13,14] Bioconjugation strategies offer great promise to specifically decorate materials of predefined network properties with functional molecules.[15] The application of mild conditions enables immobilization of complex ECM components, such as adhesion ligands, growth factors and other peptidic or GAG derivatives.[16] Reversible conjugation reactions further allow for controlled release of immobilized derivatives mediating long-term effects of surrounding cells and tissue.[17]

1.2 MACROMER-BASED MATERIALS

The originally used synthetic materials were linear polymers that were synthesized by e.g. radical or ring-opening polymerization. Among these, biodegradable polyesters, such as polycaprolactone (PCL), polylactide (PLA), polyglycolide (PGA) and their copolymers, are most widely studied for use in regenerative purposes as they offer sufficient mechanical stability and biodegradability.[18] By contrast, the macromer-based material design is based on the synthesis of reactive derivatives with low or intermediate molecular weight which can be cross-linked into a polymeric network. To be more specific, the IUPAC (International Union of Pure and Applied Chemistry) Compendium of Chemical Terminology defined macromer (or better: macromonomer) as oligo- or polymeric molecules of which each have one end-group that acts as a monomer molecule, so that each polymer or oligomer molecule contributes only a single monomer unit to a chain of the product polymer.[19] The key principle of this approach is the synthesis of chemically well-defined macromers which allows for a considerably higher control over properties of the finally cross-linked polymeric network when compared with linear polymers.

The application of versatile chemical strategies enabled development of a great variety of macromer structures. Biodegradable backbones were synthesized by the introduction of oligo- or polymeric ester and anhydride segments, or by using peptidic or glycosidic derivatives (Figure 1-1A). Two general synthetic strategies were established to fabricate a cross-linked macromer-based material: I) introduction of polymerizable functional groups (Figure 1-1B) and II) combination of chemical complementary functionalities that can take part in a conjugation reaction (Figure 1-1C).[20] The first strategy can be achieved by oligo- or polymer functionalization with (meth)acrylate functions enabling polymerization by heat or UV light. These functionalities can be introduced into a wide range of molecules as hydroxy and amino groups can react easily with (meth)acryloyl chloride or (meth)acryloyl anhydride, respectively. To this end, a great variety of natural components, such as hyaluronan[21,22], collagen[23], gelatin[21,24], heparin[25,26] and chitosan[27], as well as synthetic derivatives, including poly(ethylene glycol)(PEG)-derived polymers[28], PLA[29] and PCL[30], were processed into polymeric networks after (meth)acrylation. Reactive carbon-carbon double bonds can also be incorporated by coupling of maleic anhydride to amine functions[31], and by introduction of fumaric acid units

within[32] or at the end[33,34] of an oligo- or polymer chain. Functionalization with tri(m)ethoxysilane groups is another activation strategy which can be realized by reaction of hydroxy-, amino- or carboxy-bearing molecules with isocyanato- or glycidyl-functionalized silane-coupling agents.[35–37] Besides homopolymerization, hydrolysis and condensation of the alkoxysilanes can be used to produce covalently cross-linked (class II) organic/inorganic hybrid matrices by combination with a tetraethoxysilane(TEOS)-derived silica sol.[3,38]

On the other hand, several synthetic approaches have been established to form polymeric networks by reaction of complementary functional groups (Figure 1-1C). In that regard, click reactions were discovered as promising strategy as they are characterized by high reactivity, bioorthogonality, high specificity and high yield.[39] Typically, they occur under mild conditions and in presence of other functional groups that can be found within the biological milieu, such as alkenes, amides, disulfides, esters and phosphodiesters.[16] Enhanced synthetic effort, however, can be noted as a drawback of click chemistry as usually two different chemical functionalities have to be introduced into the macromers. In this regard, the reactions of aldehydes or ketones with hydrazides and hydrazines forming hydrazones are interesting, because they were described as *effectively* bioorthogonal,[16] but can be incorporated much easier.[40] Formation of hydrazone-cross-linked networks from several natural precursors[41,42] and synthetic building blocks[43,44] was reported. Aldehydes and ketones can be further converted into oxyamines by reaction with oximes, although oxime functionalization is challenging.[16,45] Many naturally occurring components bear amino functions (e.g. lysine-containing peptides or proteins) which can also be used for covalent cross-linking by anhydrides[46] or succinimide esters[47].

Overall, when selecting a cross-linking chemistry, one has to consider the presence of appropriate functional groups together with the targeted conditions and kinetics of the cross-linking reaction as well as toxicity of the reactive compounds. While (meth)acrylate functionalization is comparatively easy, their polymerization has to be initiated by heat or light.[11] In contrast, click chemistry permits network formation under physiological conditions and even in presence of cells, but macromer functionalization can be quite laborious and/or cost-intensive.[39,48]

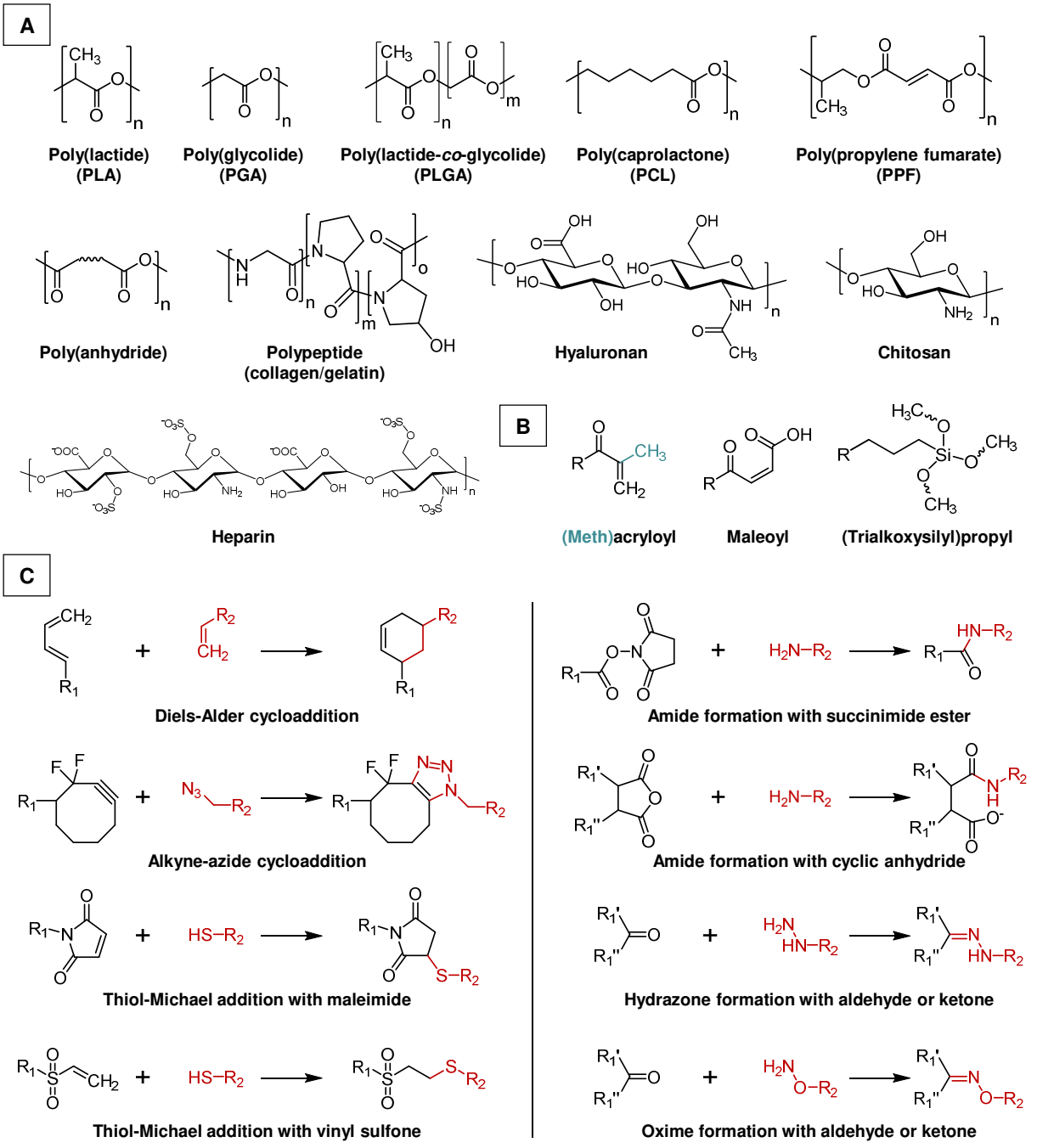

Figure 1-1. Macromer chemistry. (A) Oligo- or polymeric structures typically found in biodegradable (i.e. hydrolytically and/or enzymatically cleavable) macromers. (B) Polymerizable functionalities commonly introduced into hydroxy-, amino- and/or carboxy-bearing structures to enable macromer cross-polymerization. (C) Selected conjugation reactions (click reactions (left) and others (right)) used for covalent cross-linking of macromers with corresponding functional groups. Modified according to Fakirov et al.[10], Puppi et al.[5], Nimmo et al.[49], Hacker et al.[20] and McKinnon et al.[50]

1.3 MACROMER PROCESSABILITY

With respect to the development of biomaterials for regenerative applications, materials are wanted that can be tuned in size, shape and porosity in order to afford precise adjustment to the implant site, which in turn requires flexible material processability.[3,51] Due to the high molecular weight of conventional linear polymers, such as polyesters, their processability is limited and usually requires the application of heat or strong organic solvents.[10,18] Some polymers, e.g. high molecular-weight polymethacrylates, are even completely insoluble in commonly used organic solvents.[52] Besides reduced processability, this also hinders physico-chemical polymer characterization that is preferably performed in solution, such as in $^{1}H/^{13}C$ NMR spectroscopy and size exclusion chromatography.

In that regard, macromers are advantageous as they are soluble in commonly used solvents, even in high concentrations, due to their low or medium molecular weight.[53] This allows for excellent physico-chemical characterization in solution and opens potential for application of a great variety of processing techniques. For example, cross-linked hydrogel matrices can be fabricated from low viscous macromer solutions and the use of water resistant, such as clickable, functionalities enables *in situ* gelation in aqueous environment.[20,49] Sufficient flow properties of a fluid macromer offers potential for solvent-free processing even at ambient temperature.[54]

Due to the increase of molecular weight, macromer cross-linking is usually characterized by rising viscosity. This offers potential for generation of homogeneously distributed macropores by addition of a second inert phase that acts as space holder and can be leached after polymerization.[10] This concept was successfully applied by using solid (e.g. salt-leaching)[55] or semi-solid phases (e.g. solid lipid templating)[56], or a liquid which is immiscible with the macromer solution as reported for high molecular-weight poly(ethylene glycol) in aqueous solution.[57]

3D-printing methods are of increasing interest for precise adaption of material porosity.[58] While melt-extrusion-based methods were established to fabricate porous constructs from meltable, thermo-stable polymers, macromer solutions can be processed in more versatile manner.[59] Extrusion-based printing is enabled when solutions of reactive precursors gel within several seconds to form a stable strand. In this case, the cross-linking kinetics have to be adequately

adapted to ensure strand stability while avoiding blockage of the extrusion nozzle.[59] Fast-gelling formulation can also be processed by macromer extrusion into a bath of a cross-linking agent or by UV-cross-linking subsequently after printing.[60] Adequate macromer processability further allows for application of a variety of other 3D-printing methods, including stereolithography[2] or direct inkjet printing of a macromer solution and subsequent cross-linking.[61] Indirect 3D-printing is another promising technique in which 3D-printed structures act as templating matrices enabling precise indirect adjustment of material dimensions and porosity.[2] To this end, a macromer solution of middle or high viscosity is required which is polymerized after filling into the 3D-printed structure and the porous specimen can be obtained by subsequent template leaching. As this method imposes fewer requirements on viscosity and cross-linking kinetics when compared to direct printing, such an indirect printing approach offers potential for processing of a great variety of macromer-based systems including those, which do not allow for direct printing.

Taken together, the illustrated processing techniques make more or less specific demands on the viscosity of macromer dispersions or solutions which strongly depends on molecular weight and hydrophilicity of the macromer and can be adapted by type and amount of the applied solvent as well as temperature.[62] In addition, some procedures require precisely adjusted cross-linking kinetics, especially with regard to the time point of initiation and viscosity growth rate, which depend on: I) macromer molecular weight, type, concentration and content of reactive functionalities, II) solvent viscosity and hydrophilicity, III) initiator type and concentration as well as light intensity (UV-polymerization) or temperature (heat-induced polymerization), and IV) mixing time point and order of macromer components.[59]

1.4 TAILORABILITY OF MACROMER-BASED MATERIALS

Tunability of material properties is a key concern of modern biomaterial research in order to meet tissue-specific requirements of the implant site as good as possible.[63] In case of conventional linear polymers, material characteristics can be adjusted by copolymerization of different monomers and/or post-synthesis polymer modification, e.g. by grafting.[11,64–66] While tailorability of the polymer architecture is limited when a simple free-radical polymerization is used, controlled radical polymerization (CRP) methods including atom transfer radical

polymerization (ATRP) and reversible addition-fragmentation transfer (RAFT) have been established to afford better control over molecular weight, polymer structure, and controllable incorporation of versatile macromolecules.[14] However, as the properties of these conventional polymers are merely adaptable by modification of polymer composition, material tunability, especially the possibility to independently control specific characteristics, is limited. In contrast, the macromer concept allows for integration of reactive functionalities (almost) independently of the oligomer structure resulting in an enhanced degree of engineering freedom and therefore opens potential for improved fine-tuning of the cross-linked networks.[53] The following sections will illustrate the extent and importance of precise tailorability of macromer-based materials with the help of relationships between selected parameters.

1.4.1 Molecular weight vs. cross-linking degree

Independent control over molecular weight of the macromer chain and cross-linking degree of the polymerized network is often favored as both parameters influence mechanical properties and material degradation.[38] Both variables further control mesh size of cross-linked hydrogels which in turn determines solute diffusibility within these matrices.[63] An independent control is possible when reactive functionalities are introduced at different positions along the oligo- or polymer chain. This can be achieved, for example, by (meth)acrylation or tri(m)ethoxysilane functionalization of structures with repeating hydroxy or amino groups, such as hyaluronan or gelatin.[21,36] The same is valid for silanization of carboxy-bearing molecules[37] which are further accessible for carbodiimide-mediated dihydrazide cross-linking.[67] Macromer synthesis by copolymerization with reactive monomers in varying ratios is another strategy to decouple macromer molecular weight from cross-linking degree of the polymeric network, but is linked to the condition that the macromer chain length can be adjusted independently of macromer composition.[68]

1.4.2 Mechanical properties vs. porosity

When adapting to a certain tissue, biomaterials usually have to meet specific criteria with regard to mechanical stability and pore structure as both control cytocompatibility, while mechanical stability is further important for load-bearing applications.[69] This is clearly comprehensible when

highlighting the characteristics of cancellous bone, which offers an open porous structure, but simultaneously exhibits a certain mechanical stability (Figure 1-2).[69,70]

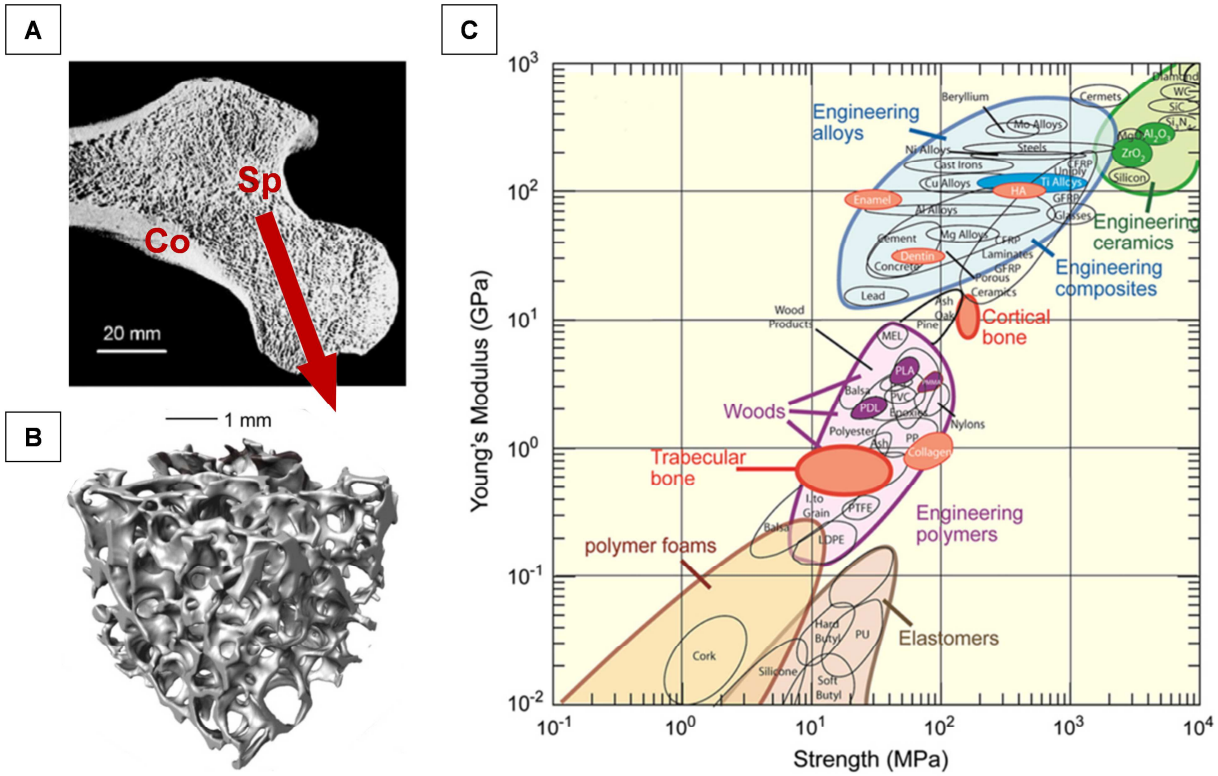

Figure 1-2. Porosity and mechanical properties of bone tissue. (A) Section of a femur head illustrating the compact shell of cortical (compact) bone (Co) and the porous cancellous (spongy) bone (Sp) inside. (B) µCT image of cancellous bone removed from the femur proximal of the knee joint highlighting the open-porous structure of this tissue. (C) Mechanical properties of cancellous (trabecular) and cortical bone in comparison with a variety of different types of engineered materials illustrating the effect of composition and microstructure on material mechanics. Modified according to Fratzl et al.[71], Jones et al.[3] and Fu et al.[72]

In this context, engineering (cancellous) bone is challenging, because an increase of material porosity usually correlates with a reduction in mechanical stability.[4,73] This demonstrates the importance of independent control over these two material characteristics, which can be achieved when porosity of the material is adjusted independently of macromer chemistry. In this regard, the above illustrated versatility of macromer processability is advantageous and enables application of different templating strategies (section 1.3) that allow for porosity adjustment to a

specific target value, while mechanical properties can be adapted by variation of macromer composition and/or concentration.[53,74]

1.4.3 Degradability vs. mechanics

Besides porosity and mechanical properties, degradability is a key characteristic of a material determining its potential for regenerative applications. Biodegradability can be mediated by introduction of hydrolytically degradable groups, such as esters, amides or anhydrides,[75] or enzymatically cleavable functions, e.g. glycosidic bonds or matrix metalloproteinase(MMP)-cleavable peptides.[76] Macromer-based materials can be rendered degradable by two general strategies: I) introduction of degradable monomers into the oligo- or polymer chain or II) macromer cross-linking via cleavable functions. Although the latter approach is beneficial for controlled release of immobilized ligands,[77] it is, however, not suitable to decouple degradative and mechanical properties as degradation would accordingly reduce the cross-linking density and therefore impair material mechanics. In fact, such an independent control is highly relevant for load-bearing applications, but its realization is often critical, because the introduction of cleavable domains, such as (hydrophobic) oligo- or polyester units, usually have significant impact on mechanical properties.[78,79] Nevertheless, the combination of two or more different macromers opens potential to decouple the content of degradable functionalities as controlled by macromer composition from the network properties which can be adjusted by the ratio and concentrations of both building blocks. In this context, sol-gel-derived organic/inorganic hybrid glasses are promising materials in which degradable macromers of different composition and reactivity can be covalently integrated into a pre-cured silica sol in varying ratios.[74 80]

1.4.4 Functionalization vs. predefined material properties

An ideal biomaterial would closely mimic the physiological environment with regard to physico-chemical network properties and biological functionality.[6] This objective, however, is overall quite challenging because of the complex nature of the extracellular matrix (ECM), what is composed of divers structure proteins (e.g., collagen, elastin), adhesion (glyco)proteins (e.g. fibronectin, laminin), glycosaminoglycans as well as embedded growth factors, cytokines and chemokines (Figure 1-3A).

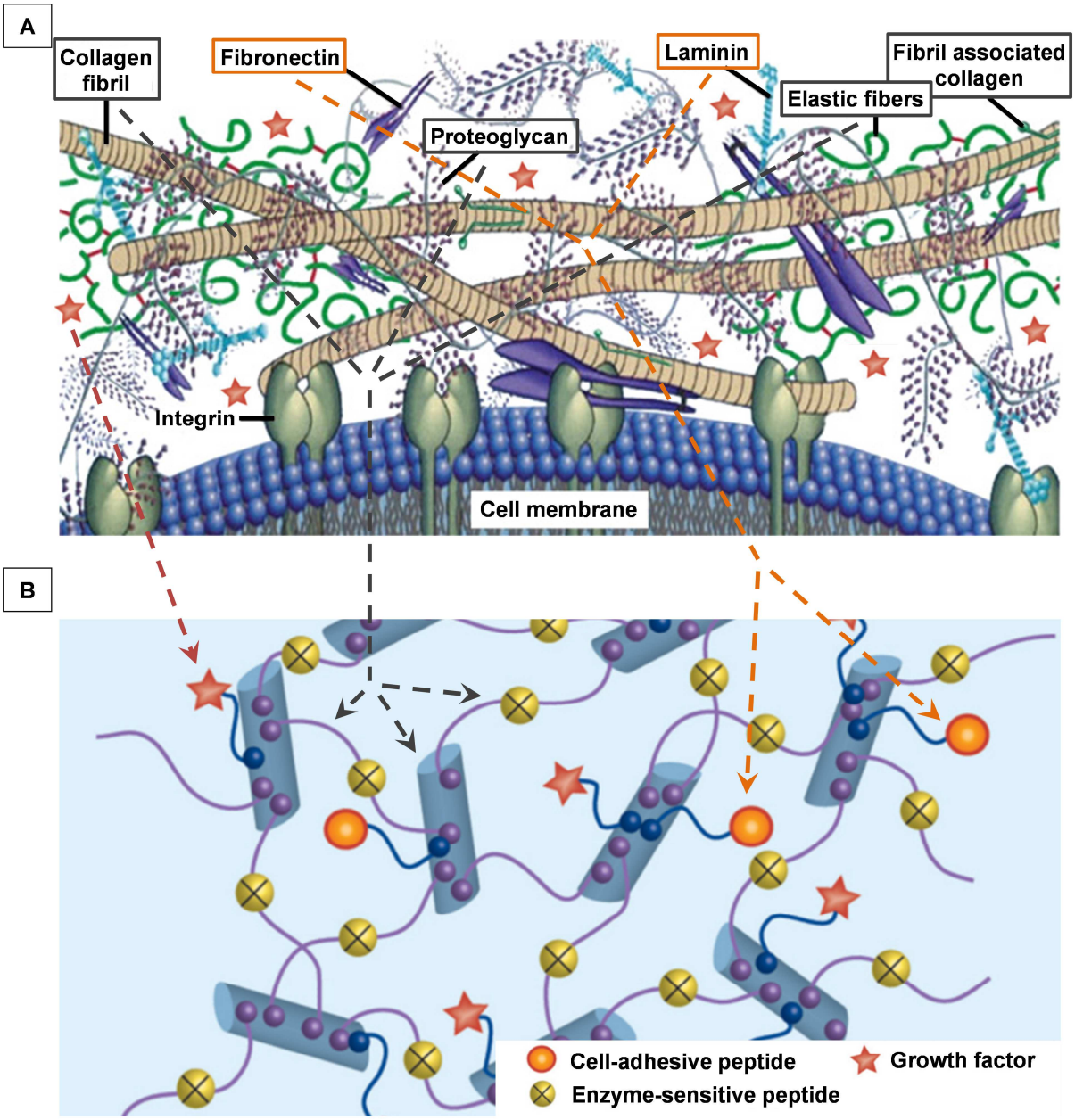

Figure 1-3. (A) Representative illustration of the ECM structure composed of versatile fibrous and branched components, and the cellular interaction with ECM biomolecules, including the integrin-binding fibronectin and laminin. (B) Model of a biomimetic synthetic hydrogel. Macromer chemistry and cross-linking density control network properties. Matrix functionality is mediated by immobilized cell-adhesive peptides and growth factors. Modified according to Aamodt et al.[81] and Zhu et al.[82]

While the viscoelastic properties of the ECM, which mainly result from the structural components, can be closely resembled by hydrogels,[82] it is crucial to mimic further functional

properties. Nevertheless, the integration of relevant functional ECM elements, such as cell binding motifs or growth factors, into hydrogels of appropriate viscoelasticity is a common approach (Figure 1-3B).[2] To this end, unspecific loading is the easiest way which, however, offers limited loading capacity and can merely mediate short-term effects due to burst release. These drawbacks can be counterbalanced by bioconjugation of ECM components or derivatives to matrix structures.[16,83] In order to fabricate precisely tunable materials, it is desirable that the covalent material functionalization would not significantly affect the predefined network properties. In that regard, macromers have outstanding potential, because macromer functionalization with two generally different chemical functionalities enables decoupling of functionalization and cross-linking chemistries (Figure 1-1, Figure 1-4D-E).[20] For example, Kaga and co-workers have synthesized dual-functional dendron-polymer conjugates, which can be processed into hydrogels by UV-cross-linking of methacrylate groups, while alkyne functionalities are accessible for covalent post-fabrication functionalization with azide-containing ligands.[84] The macromer concept further offers potential to introduce certain functionality directly into the macromer structure and/or to cross-copolymerize specific linker molecules that can act as anchors for subsequent bioconjugation.[53,85]

1.4.5 Structure-property relationships

The above illustrated examples demonstrate the potential of macromers as building blocks for the design of highly adjustable materials. While the physico-chemical material properties are tunable by macromer chemistry and molecular weight (Figure 1-4A-C), the introduction of additional reactive sites allows for functionalization of the pre-fabricated (cross-linked) material (Figure 1-4D-E). Such a combination of different chemical strategies offers potential for multiple levels of control over biochemical and biomechanical properties.[86,87] In terms of material versatility, the independent control over different material characteristics serves as a key advantage of macromer-based materials. This is visualized in Figure 1-4 as all of the illustrated strategies for adjustment of material characteristics (A-E) can be generally combined with each other.

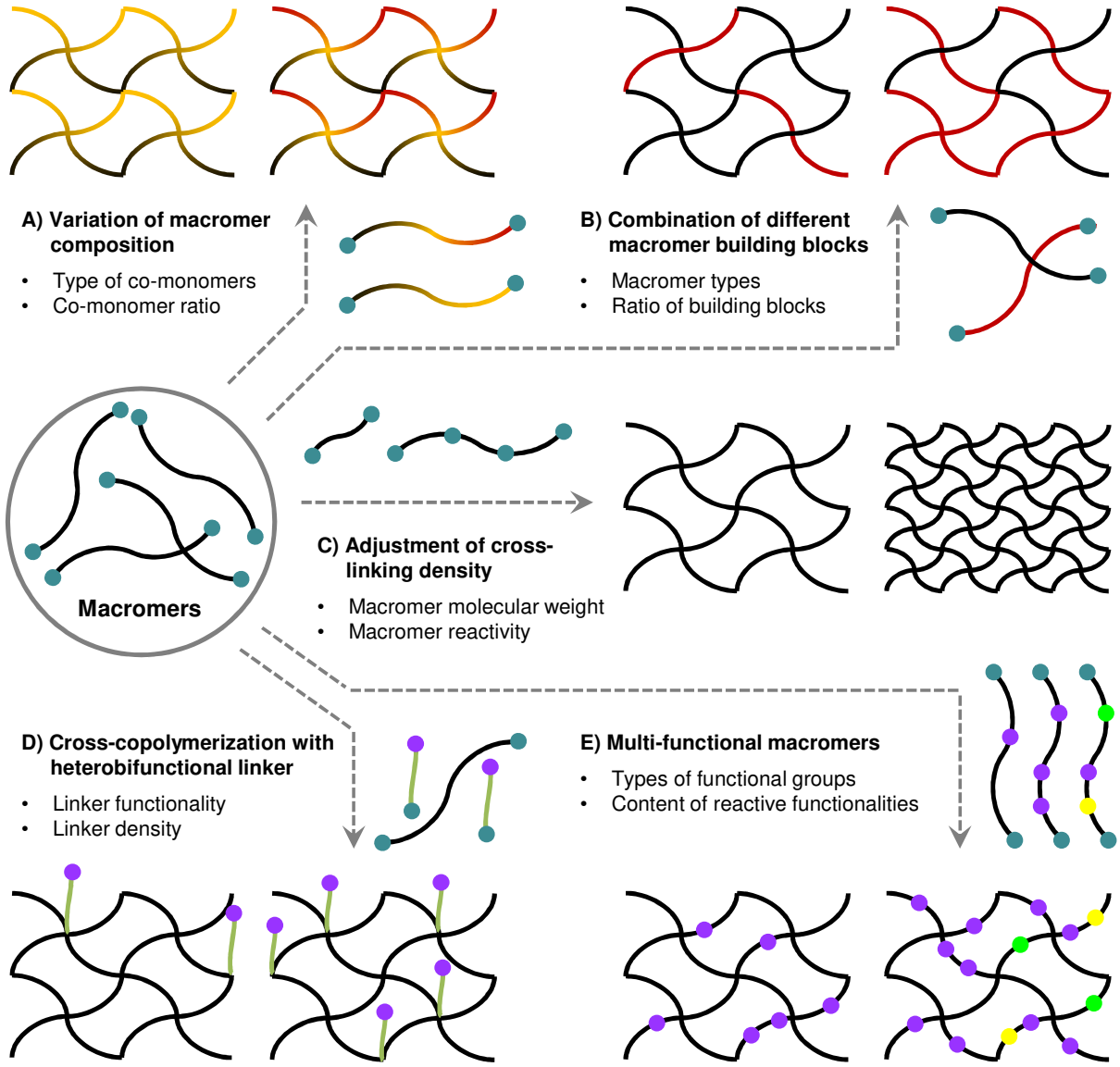

Figure 1-4. Illustration of tunability of a macromer-based material platform (here: linear derivative with reactive groups labeled turquois). Chemistry and corresponding hydrophilicity of a macromer-based material is generally adaptable by chemical composition of the macromers (A) and/or by combination of different macromer building blocks (B). Mechanical properties strongly depend on the cross-linking density which can be controlled by macromer molecular weight and/or content of reactive functionalities (C). Covalent post-fabrication strategies can be realized by cross-copolymerization with heterobifunctional linkers (D) and/or polymerization of macromers containing more than one functionality (multi-functional macromers) (E). Modified according to Singh et al.[88] and Hacker[89].

Even though it is impossible to adapt all material characteristics completely independently of each other, the macromer concept offers several possibilities for the fine-tuning of different material properties.[74] In this context, detailed knowledge of the impact of key macromer and

process variables on matrix properties is important to thoroughly understand a certain material. Macromer-based materials are particularly suitable for determination of such structure-property relationships due to the versatile processability of chemically well-characterized precursors. Excessive investigations of correlations between synthesis parameters, macromer structure and material properties were performed by the lab of Julian R. Jones (Imperial College London) for gelatin-silica hybrid scaffolds.[74] Nearly all variables of interest significantly affected cross-linking kinetics as well as porosity, mechanics and cytocompatibility of the hybrid glasses indicating tailorability of these material properties.

1.5 AIMS OF THE THESIS

A macromer-based material concept is characterized by two main advantages: I) versatile processability of chemically well-defined macromers enabling applicability for a wide range of material fabrication methods and II) versatile and precise control over different material properties. Both characteristics are highly relevant when aiming at fine-tuning of biomaterials for a specific regenerative application. The flexibility of macromer-based material platforms motivated their use in order to advance strategies of macromer processing into cross-linked hydrogel and hybrid glass matrices with highly tunable properties. To this end, two different macromer concepts were investigated with regard to different key aspects.

A) Oligomer-cross-linked gelatinous hydrogels

This hydrogel concept is based on covalent cross-linking of macromolecules that contain amino groups by anhydride-containing macromers. The previously established oligo(PEDAS-*co*-NiPAAm-*co*-MA) (oPNMA) macromers can effectively cross-link gelatinous peptides of low and medium molecular weights (Collagel (11 kDa), gelatin 50 Bloom) into hydrogel matrices, while long-chained gelatin (160 Bloom) is processable into microparticles.[90,91] Cytocompatible and cell-adhesive matrices were obtained in which the natural component provided biological activity and specific degradability, and the synthetic building block controlled network properties via content of reactive anhydride groups. Potential of covalent matrix functionalization by partial anhydride derivatization with amino-functionalized ligands prior to the cross-linking reaction has been demonstrated.[90] As anhydride functionalities are consumed for matrix formation and

functionalization, this strategy, however, is characterized by limited degree of functionalization and an alteration of cross-link density.

To this end, it was aimed to introduce a second functionality into the hydrogel-forming macromers. It is assumed that this strategy will enable decoupling of covalent matrix functionalization from cross-linking chemistry. In detail, reactive methyl ketone functionalities will be incorporated into the established oligomer-cross-linked hydrogel system by an exchange of the monomer NiPAAm by diacetone acrylamide (DAAm) to yield oligo(PEDAS-*co*-DAAm-*co*-MA) (oPDMA) macromers. It is intended to investigate reactivity of the incorporated ketone functionality on the macromer level as well as in the hydrogel state by secondary dihydrazide cross-linking and immobilization of model hydrazide and hydrazine derivatives, including hydrazido-functionalized hyaluronan. Furthermore, as previous cell culture experiments indicated good biocompatibility but limited cell migration into the depth of the hydrogel mactrices,[91,92] different strategies to enhance material porosity will be followed. Poly(ethylene glycol) will be applied as porogen introducing macroporosity by phase separation, while gelatin with increased molecular weight will be used to enhance hydrogel mesh size.

B) Sol-gel hybrid glass scaffolds from multi-armed macromers

This material concept is based on covalent integration of differently structured silane-functionalized macromers into a TEOS-derived silica sol. These hybrids are cross-linked by linear, three- and four-armed oligo(ethylene oxide)-derived cross-linkers which controlled hybrid properties via total content and oligo(ethylene oxide) content.[54] The implementation of an indirect rapid prototyping method enabled the production of macroporous, pore-interconnected scaffolds with controlled architecture. It is known from the literature that bioactive glass-based materials are often characterized by insufficient degradability.[93,94] This issue, however, has not been addressed by the hybrid glass platform yet.

This motivated the introduction of degradable oligoester functionalities into this hybrid glass system in order to control its degradability. In detail, oligo(D,L-lactide) units will be introduced into three- (TMPEO, Tx) and four-armed (PETEO, Px) ethoxylated alcohols. It is aimed to perform long-term degradation studies in order to characterize tailorability of the hydrolytic material degradation. The impact of macromer chemistry, macromer content in the hybrid, and

material porosity on mechanical properties as well as degradability of the hybrids will be assessed and correlated.

The main aspects of this work are:

1) To synthesize two sets of biodegradable, multi-armed macromers by using free-radical polymerization and ring-opening polymerization combined with established activation strategies. The synthesis setups will be tuned toward high macromer yields which will be required for processing into biomaterials with relevant sizes.

2) To physico-chemically characterize purified oligomeric macromers with regard to chemical composition, molecular weight and reactivity in order to yield well-defined macromer structures. NMR spectroscopy, size exclusion chromatography (GPC) and wet chemistry will be applied.

3) To characterize macromer processability into covalently cross-linked hybrid matrices by mixing with counterpart oligomeric components. This work will focus on a soft gelatin-derived hydrogel system for versatile biomedical applications as well as a rigid hybrid glass material for hard tissue regeneration. Sets of different formulations will be investigated in order to characterize the range of macromer processability and to establish structure-property relationships.

4) To investigate strategies for the adjustment of material porosity. Besides the adaption via cross-linking density, porogen-leaching and 3D-printing approaches will be followed in order to introduce macroporosity and to enable a decoupling of porosity and chemical (nano)structure of the cross-linked network.

5) To determine key material properties relevant for regenerative applications, including mechanical properties by compression tests and oscillation rheology, *in vitro* matrix degradability, as well as material cytocompatibility in indirect and direct contact experiments.

6) To identify strategies for covalent functionalization of the hybrid materials. Post-fabrication functionalization via specifically introduced chemical functionalities is favored enabling effective material decoration (almost) independently of the physico-chemical matrix properties.

CHAPTER 2

Materials and Methods

2.1 INTRODUCTORY COMMENT

This chapter illustrates materials and methods used in this work for synthesis and characterization of two types of biodegradable macromers. Their processing into cross-linked hybrid matrices is also described and methods for material characterization are further illustrated.

Dual-functional macromers that act as building blocks and cross-linkers for gelatinous hydrogel fabrication were synthesized by free radical polymerization (section 2.2, Chapter 3). Degradable multi-armed macromers as used for development of sol-gel glass-based hybrid scaffolds were synthesized by ring-opening polymerization and subsequent silanization (section 2.4, Chapter 5). Both chapters have been published and contain experimental sections in their original form. However, as these parts had to be written fairly condensed, sections 2.2 and 2.4 were used to provide further details on selected methods related to the published chapters.

In addition, strategies for porosity adjustment of oligomer-cross-linked gelatinous hydrogels are presented in Chapter 4. As this chapter has not been published by now, the corresponding materials and methods were completely illustrated herein (section 2.3).

Unless otherwise stated, experiments were conducted in triplicate and the data was expressed as means ± standard deviation (SD). Single-factor analysis of variance in conjunction with Tukey's Post Hoc test was performed to assess the statistical significance ($p < 0.05$) within data sets.

2.2 ADDITIONAL INFORMATION ON METHODS OF CHAPTER 3: DUAL-FUNCTIONAL HYDROGEL BUILDING BLOCKS

2.2.1 Synthesis of oPDMA oligomers

Oligo(PEDAS-*co*-DAAm-*co*-MA) (oPDMA) macromers were synthesized according to a previously established protocol.[90,95,96] Comonomer mixtures of pentaerythritol diacrylate monostearate (PEDAS), diacetone acrylamide (DAAm), and maleic anhydride (MA) were copolymerized by free radical polymerization after initiation with 2,2´-azobis(2-methylpropionitrile, AIBN) at 60 °C under a nitrogen atmosphere in THF. Comonomers were reacted in a 1:20 molar ratio of PEDAS to DAAm plus MA and the resulting oligomers were abbreviated oPDMA-z with z representing the molar feed of MA in the comonomer mixture relative to 1 mol PEDAS.

In detail, comonomers were weighed into 50 mL polypropylene tubes (BD Falcon, VWR International, Dresden, Germany). PEDAS and MA were weighed together into one tube, while DAAm amount was divided into two further tubes (Table 2-1). The weighing procedure was completed as quickly as possible in order to minimize exposure of the monomers to humidity. Comonomers were dissolved in freshly distilled THF and were subsequently transferred into a 500 mL round-bottom flask equipped with cooler, vacuum connection and drying tube.[96] The mixture was immediately purged with nitrogen (100 mL/min) and after heating to 60 °C, the reaction was initiated with AIBN to enable polymerization for 18 h under constant stirring (600-800 rpm, funnel-shaped swirl, total batch volume: 400 mL, total molar comonomer amount: 0.24 mol, total comonomer concentration: 0.6 mol/L). For product isolation, solution volume was reduced to 50-70 mL using a rotary evaporator (40 °C, 350-200 mbar, Heidolph, Schwabach, Germany) and the oligomer was precipitated in a 10-fold excess of diethyl ether (500 mL Erlenmeyer flask), followed by centrifugation in 50 mL tubes (4000 rpm / 2 min, last step: 7830 rpm / 1 min, centrifuge 5430, Eppendorf), drying under nitrogen stream at ambient temperature (3 h) and further vacuum drying overnight (MD 4C NT membrane pump, Vacuubrand, Wertheim, Germany). Oligomer purification was repeated twice by dissolution in 50 mL dichloromethane and subsequent precipitation in diethyl ether. Finally, the oligomers

were dried in technical vacuum (RZ6 oil pump, Vacuubrand, Wertheim, Germany) for at least one week to remove solvent residues.

Table 2-1. Compositions of the comonomer reaction feeds as used for synthesis of oPDMA oligomers.

	Composition of reaction feed							
	Molar ratio[a]				Absolute weight [g]			
	PEDAS	DAAm	MA	AIBN	PEDAS	DAAm	MA	AIBN
oPDMA-2.5	1	12.5	2.5	2 mol%	5.837	33.844	2.802	0.788
oPDMA-5		15	5			29.009	5.603	
oPDMA-7.5		12.5	7.5			24.174	8.405	
oPDMA-10		10	10			19.339	11.207	

[a]Molar comonomer ratio and AIBN to comonomer ratio based on a total molar comonomer amount of 0.24 mol.

2.2.2 Purification of DAAm before use

DAAm was usually purchased from Sigma-Aldrich (Seelze, Germany) and appeared as white flakes (diameter: ~ 0.5 cm) that were used for oPDMA synthesis as received. Due to its hygroscopic nature,[97] contact to humidity had to be carefully reduced by fast weighing and immediate nitrogen flushing of its solution in THF. For the same reason, an opened bottle was not used for more than 24 h and purged with nitrogen after each withdrawal. In 2014, however, new DAAm batches were obtained from the supplier that did not fully dissolve in THF anymore (Table 2-2). After a series of trials, this was attributed to a fraction of already polymerized DAAm in the batches that was not soluble in any common solvent. Besides solubility, batches classified as ‘usable’ and ‘unemployable’ significantly differed in their appearance and solution coloration which was attributed to the inhibitor(s) supplemented by the manufacturer to improve storage stability. Although the specific inhibitor chemistry is not known, aromatic (e.g. benzene) derivatives are known to introduce characteristic coloration.[11] To this end, a correlation with type and/or concentration of the applied inhibitor was assumed, but not further analyzed.

Table 2-2. Characteristics of different DAAm batches as obtained from Sigma-Aldrich.

Batch code	Place of manufacture	Appearance	Solubility in THF	Oligomer appearance	Batch assessment
MKBC5891V	Japan	white flakes	transparent solution within 5-10 min	grey-white	Usable
MKBR4094V	China	brown-white crystalline powder	incompletely soluble, rose-brown supernatant	rose-brown with green and grey-white fractions	Unemployable

Inquiries revealed that the DAAm batches were produced at different locations. Although certificates of analysis (IR, carbon and nitrogen content) and our own ^{1}H NMR analysis confirmed DAAm structure (soluble fraction), insufficient solubility rendered copolymerization of the monomer without further purification impossible. Three strategies for monomer purification were pursued:

- I: Removal of insoluble DAAm crystals by centrifugation and/or filtration
- II: Extraction and recrystallization of the soluble fraction of DAAm after dissolution in acetone, chloroform, ethyl acetate, THF or toluene
- III: Purification of the soluble fraction of DAAm by dissolution in THF or toluene and subsequent precipitation in cyclohexane, diisopropyl ether, n-heptane, n-hexane, petrol ether or petroleum benzene

Even though most strategies did not yield completely THF-soluble DAAm (insoluble fraction and/or gelation), two promising strategies were identified to isolate a defined amount of soluble DAAm from batch 'MKBR4094V'.

2.2.2.1 Removal of the insoluble fraction of DAAm. This approach aimed at dispersing DAAm in THF and using the soluble fraction directly for oligomer synthesis. Following this strategy, however, the fraction of insoluble DAAm had to be quantified in order to enable precise adjustment of the comonomer ratio. To this end, DAAm was dissolved in freshly distilled THF (50% (w/v)) in a 50 mL tube and was further incubated at 60 °C (temperature used for radical polymerization) for 10 min under gentle shaking. The fraction of insoluble DAAm was

gravimetrically assessed after separation by centrifugation (7830 rpm for 5 min), drying under nitrogen flushing at ambient temperature (3 h) and further vacuum drying overnight. A fraction of insoluble DAAm of 13.0 ± 0.6 wt% was obtained. Based on these results, a fresh solution of DAAm in THF could be accordingly prepared which is applicable for oPDMA synthesis by volumetric dosing (oPDMA batch abbreviated as D-Sep).

2.2.2.2 Recrystallization of DAAm in toluene. DAAm was dissolved in toluene (technical grade, AppliChem, Darmstadt, Germany) to obtain a concentration of 50% (w/v). After shaking and vortexing for 10 min at ambient temperature, insoluble DAAm was separated by centrifugation (7830 rpm for 3 min) and the soluble fraction was further filtered using 0.45 µm PTFE filters (VWR International). The obtained clear solution was immediately frozen at -20 °C overnight to enable crystallization of DAAm. The formed crystals were separated from the frozen solutions by centrifugation (7830 rpm for 1 min) and were subsequently vacuum-dried overnight at ambient temperature (oil pump). Recrystallized DAAm appeared as white-brown amorphous powder and could be used for oPDMA synthesis as described above (section 2.2.1, oPDMA batch abbreviated as D-Tol).

2.2.2.3 Change of supplier. In addition, DAAm was purchased from two other sources, i.e. Santa Cruz Biotechnology (Heidelberg, Germany, LOT: G1912, synthesized oPDMA abbreviated as D-SCBT) and TCI (Eschborn, Germany, LOT: DBMFJ-JD, synthesized oPDMA abbreviated as D-TCI). Morphology and solubility of these batches were comparable to that of the 'usable' batches from Sigma (Table 2-2).

2.2.2.4 Characteristics of oPDMA test batches. In order to evaluate the applicability of the different DAAm batches for oPDMA synthesis, a set of oPDMA-7.5 derivatives was synthesized and characterized by gel permeation chromatography (GPC), ^{1}H NMR and alkalimetric titrations (Chapter 3).[90,98] Molecular weight characteristics of all synthesized oligomer batches were comparable to each other and met the typical range of previous oPDMA-7.5 batches (M_n: 2800-3100 Da, $Đ_M$: 1.60-1.70) (Figure 2-1A). When oligomer compositions were compared, almost equal MA content and similar degrees of DAAm incorporation were detected (Figure 2-1B), although the applied quantitative ^{1}H NMR evaluation was biased by generally broad and partially overlapping signals.[98] Determination of MA content by alkalimetric titrations served as more valid characterization of MA incorporation as a measure of oligomer reactivity.

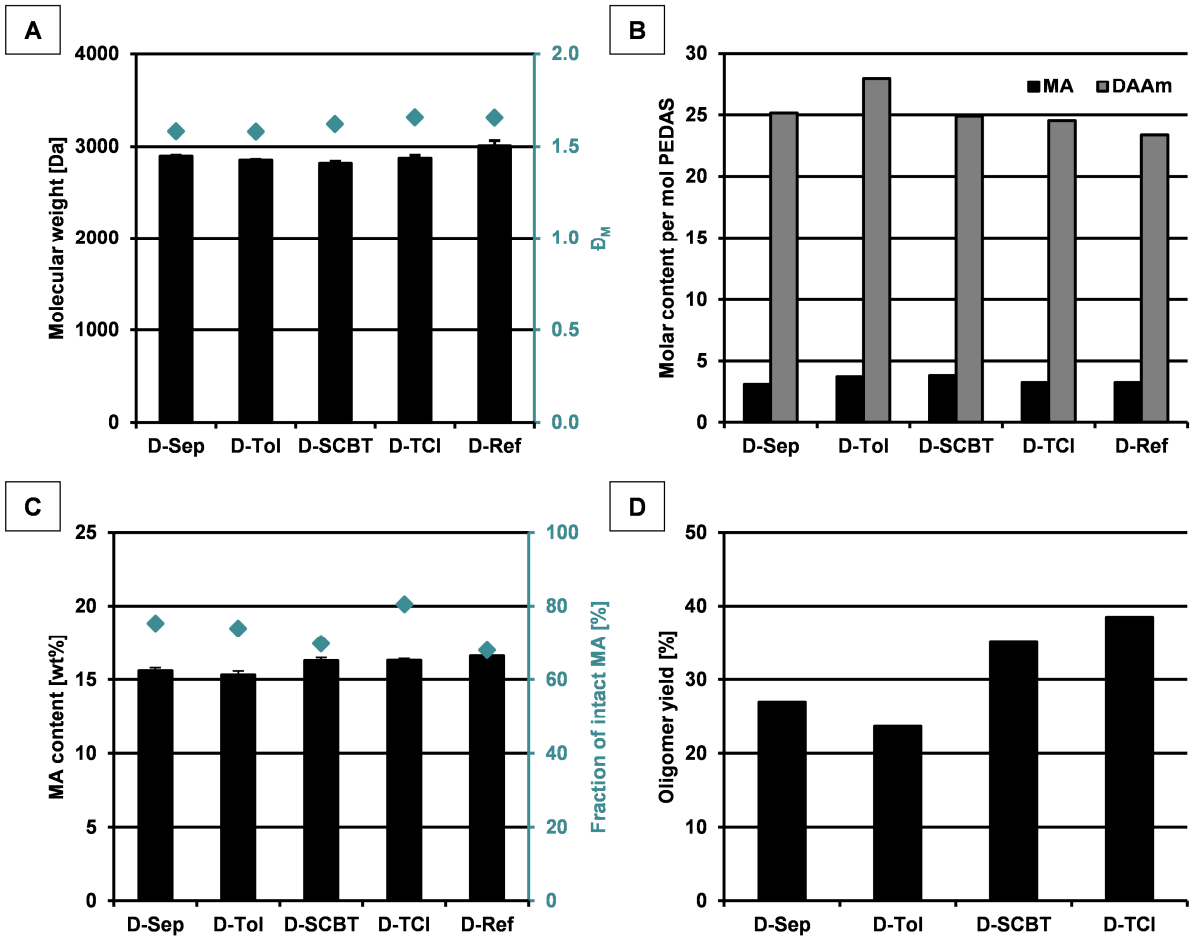

Figure 2-1. Molecular weight, composition and yield of oPDMA-7.5 oligomers as synthesized from different DAAm batches (D-X). (A) Molecular weight characteristics as determined by size exclusion chromatography (GPC), (B) oligomer composition as determined by ^{1}H NMR, (C) maleic anhydride (MA) content as well as fraction of chemically intact anhydride units, and (D) yield of synthesized oligomer. DAAm was obtained from Sigma and was further purified before use (D-Sep: separation of the insoluble fraction by centrifugation, D-Tol: recrystallized in toluene), or purchased from SCBT or TCI. A THF-soluble DAAm batch from Sigma served as reference for oligomer synthesis (D-Ref).[98]

Results for DAAm batches obtained from other suppliers were in accordance with our experiences from previous Sigma-derived batches (MA content: 16-17 wt%, intact MA: 65-80%) and the most reactive derivative, characterized by high MA content combined with high intactness of incorporated anhydrides, was obtained from TCI-derived DAAm (Figure 2-1C). However, although MA intactness was inconspicuous, the purified DAAm batches yielded reduced MA conversion which is in accordance with enhanced DAAm conversion (D-Sep, D-Tol, Figure 2-1B). SCBT- and TCI-derived DAAm further resulted in an appropriate amount of

the synthesis product, but DAAm purification caused reduction of oligomer yield which typically exceeded 30% when reference DAAm batches were applied (Figure 2-1D). When having a closer look at the GPC traces, appearance of the main peak (17-22 min) was almost equal in all oPDMA batches (Figure 2-2). However, broad signals of small intensity (11-16 min) were exclusively observed in oligomers that had been synthesized from purified DAAm indicating high-molecular weight by-products (~ 250-300 kDa) (Figure 2-2A-B).

Taken together, the applied purification protocols were generally suitable to remove insoluble fractions from the critical DAAm batches which resulted in clear monomer solutions in THF with adjustable concentration. The monomer could be copolymerized with MA and PEDAS in a manner that was comparable to previous batches and to derivatives which were obtained by using DAAm from other suppliers. GPC analysis, however, demonstrated the existence of high molecular weight by-products in oligomers from purified Sigma batches (D-Sep and D-Tol). Even though the extent of oligomer cross-linking was quite low and did not cause solubility issues, the presence of these by-products might introduce inhomogeneity into cross-linked hydrogel matrices that would be prepared from these oligomers. Reduced anhydride reactivity in oligomer batches D-Sep and D-Tol further might result in reduced cross-linking density which would negatively affect hydrogel stiffness. In conclusion, the effectiveness of the purification protocols is questionable. A change of the DAAm supplier was detected as best strategy to maintain quality of the established oligomeric cross-linkers. With respect to oligomer yield and anhydride reactivity, TCI-derived DAAm acted as the most promising monomer which was therefore used for further oPDMA syntheses.

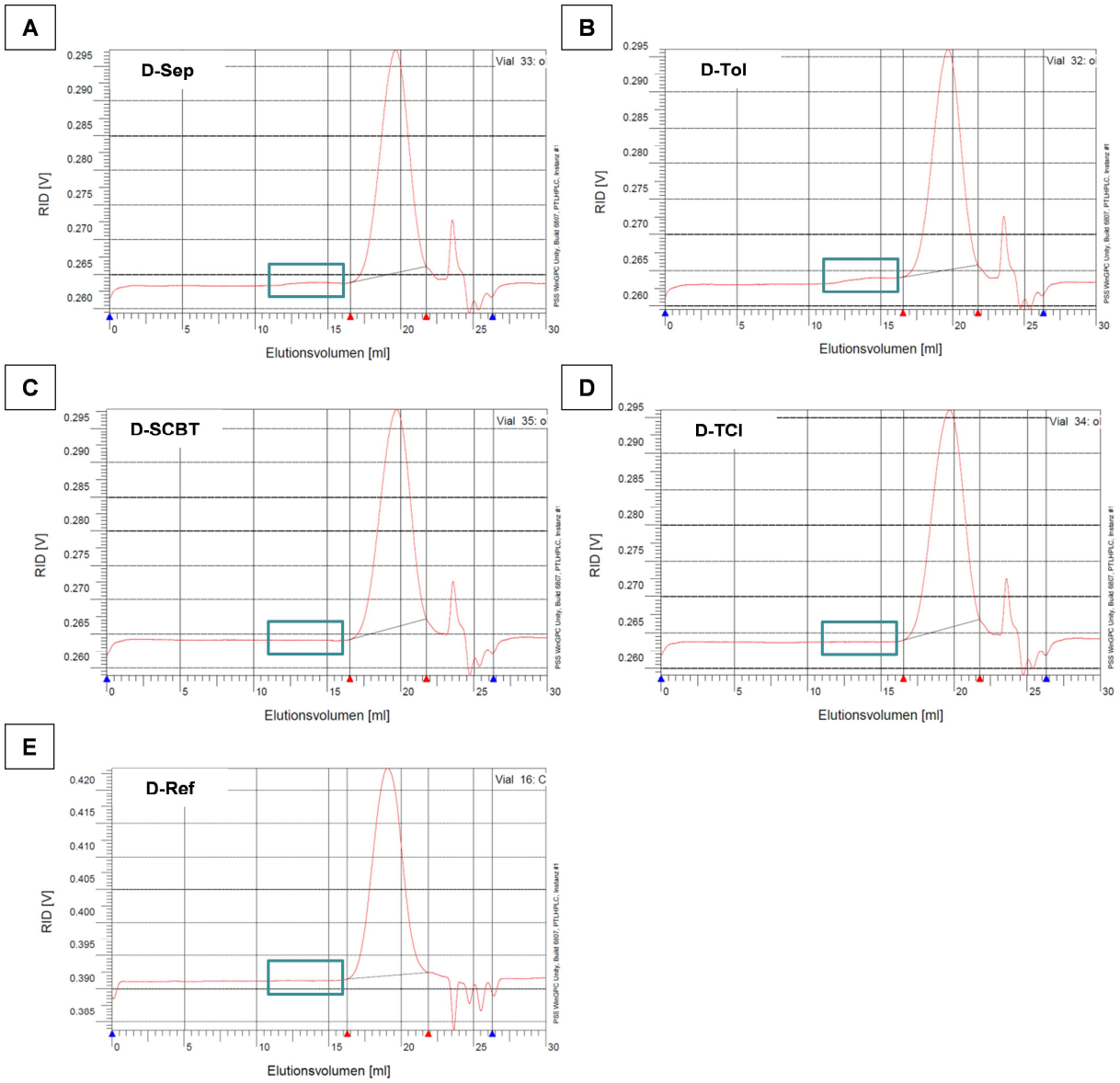

Figure 2-2. GPC traces of oPDMA-7.5 oligomers synthesized from different DAAm batches (D-X). Chromatograms were obtained in THF (1 mL/min) and molecular weight was determined relative to polystyrene standards.[98] DAAm was obtained from Sigma and further purified (D-Sep: separation of the insoluble fraction by centrifugation (A), D-Tol: recrystallized in toluene (B)), or purchased from SCBT (C) or TCI (D). An oPDMA-7.5 batch synthesized from 'usable' DAAm is shown for comparison (E). Blue-framed boxes highlight the range in which high-molecular weight by-products may appear, such as in the chromatograms of D-Sep (A) and D-Tol (B).

2.2.3 Synthesis and characterization of acid-soluble macromer derivatives (oPDMA^{+DEED})

Acid-soluble *N,N*-diethylethylenediamine(DEED)-derivatized oPDMA macromers were synthesized in order to investigate the acid-catalyzed formation of DNP-hydrazones in solution.

For oPDMA^{+DEED} synthesis, 1 g of oPDMA was dissolved in 3 mL of acetone. After incubation with DEED and TEA (each in equimolar ratio to intact anhydrides) for 4 h, the solution was precipitated in 40 mL diethyl ether, centrifuged (7830 rpm for 1min) and further dried under nitrogen stream at ambient temperature (2 h) and in vacuum overnight. For zeta potential analysis, colloidal macromer dispersions were prepared by dropwise addition of 9 mL water into 1 mL of macromer solution in acetone (20 mg/mL). Zeta potential was determined after 1:10 dilution with water using a Zetasizer 3000 HSa (Malvern, Herrenberg, Germany). Dispersions of unmodified (pristine) oPDMA-z macromers served as controls (n = 5).

2.2.4 Derivatization of oPDMA-derived macromers and hydrogels with 2,4-dinitrophenyl-hydrazine (DNPH)

2.2.4.1 Macromer derivatization with DNPH. In order to determine the potential of hydrazine immobilization to oPDMA oligomers, a DNPH solution was supplemented with different amounts of acid-soluble oPDMA^{+DEED} in 0.1 M HCl solution containing 50 mM KCl (pH 1).

In detail, 50 µL of DNPH stock solution (0.356 mg/mL) were incubated with varying volumes of oPDMA^{+DEED} stock solution (30 mg/mL) in a total volume of 500 µL for 5 min to obtain molar ketone/hydrazine ratios ranging from 0 to 100. Oligomer ketone content was indirectly calculated from M_n (GPC) together with MA content (conductometric titration) and the molar ratio of MA to PEDAS (from ^{1}H NMR). UV/Vis absorption spectra were recorded at 300-600 nm and absorbance ratio $A_{367\ nm}/A_{340\ nm}$ indicating the degree of hydrazone formation was determined using an Evolution 201 spectrophotometer (Thermo Fisher Scientific, Schwerte, Germany).

2.2.4.2 Hydrogel derivatization with DNPH. Lyophilized hydrogel discs (Ø = 7 mm) were rehydrated with PBS for 24 h (150 rpm, orbital shaker Heidolph Rotamax 120, Heidolph, Schwabach, Germany) and further incubated with DNPH solutions (0.25 mg/mL) at pH 1, 3, 5 and 7.4. Medium of pH 1 was composed of 108.4 mM HCl solution containing 50 mM KCl and PBS containing 0.01% (w/v) sodium azide was used as medium of pH 7.4. Buffer solutions of

pH 3 and 5 were prepared using 25 mM KH_2PO_4 and pH was adjusted using H_3PO_4 or KOH solutions.

In detail, 3 hydrogels were incubated with 5 mL DNPH solution in snap cap vials (5 mL) for 4 h followed by 4 washing steps, each with 5 mL of fresh medium for 20 min (orbital shaker, 150 rpm). After transfer to 48 well plates (Corning, Amsterdam, The Netherlands), stereomicroscopic images of hydrogels were taken (DS-2Mv digital camera, Nikon, Duesseldorf, Germany) and absorbance ratio $A_{405\ nm}/A_{340nm}$ was determined using a Tecan Infinite F 200 plate reader (Salzburg, Austria) equipped with appropriate absorption filters (450/10 nm, 340/35 nm). For determination of DNPH content, hydrogels were further hydrolyzed at pH 1 (500 µL per gel disc) for at least 70 days at room temperature. DNPH concentration was determined by UV/Vis spectroscopy using the Tecan plate reader at 340 nm and related to hydrogel dry weight (range: 2.0-3.8 mg). Control hydrogels were incubated at pH 7.4 without DNPH supplementation.

2.2.5 Hydrogel derivatization with and release of Alexa Fluor 350 hydrazide (AFH)

Lyophilized weight-adapted hydrogel discs (Ø = 5 mm) were rehydrated with PBS for 24 h (orbital shaker, 150 rpm) and further incubated with AFH solutions at pH 1, 3, 5 and 7.4 in media of above mentioned compositions (section 2.2.4.2). AFH stock solution (5 mg dissolved in 2.5 mL anhydrous DMSO) was diluted with medium of corresponding pH to obtain concentrations in the range of 1-200 µg/mL.

In detail, hydrogels were separately incubated with 100 µL of AFH solution in black 96 well plates (Corning) for 4 h followed by 5 washing step, each with 200 µL of fresh medium of corresponding pH for 18 h (1^{st} washing step) or 2 h (2^{nd}-5^{th} washing step) in order to remove adsorbed AFH (orbital shaker, 150 rpm). AFH content was determined by fluorescence spectroscopy using the Tecan plate reader (Ex: 360/35 nm, Em: 465/35 nm) and related to hydrogel dry weight. Calibration was performed by using 100 µL AFH solutions, while different measures for sample optical depth of the analyzed samples were considered:

- From well dimensions, a filling height of 2.92 mm was calculated for 100 µL of calibration solution and the calibration curve was normalized to sample optical depth to yield relative fluorescence units (RFU) per mm sample.

- Hydrogel thickness was individually determined by using a Physica MCR 301 rheometer (Anton Paar, Graz, Austria) with normal force control. Gels were placed on the bottom plate and position of the geometry (8 mm plate) was set to 2 mm. The gap was therefrom reduced in 0.05 mm steps and the position in which the normal force exceeded 0.05 N was defined as hydrogel thickness. Fluorescence intensity was accordingly normalized to hydrogel thickness which enabled quantification using the normalized calibration curve.

Derivatized hydrogels were further analyzed by fluorescence microscopy (Eclipse TE2000-S, Nikon, equipped with an Intensilight Fiber Illuminator C-HGFI and a DS-Ri2 digital camera) (filter: UV, exposure: 5 ms, gain: 17.1-fold). Control hydrogels were incubated at corresponding pH without AFH supplementation.

AFH release at pH 7.4 was investigated for selected formulations by incubation of AFH-derivatized gel discs in PBS. To this end, derivatized hydrogel discs were individually incubated with 200 µL PBS in a black 96 well plate (Corning) which was placed on an orbital shaker (150 rpm) after sealing with microplate sealing tape (Corning). After 1, 3, 5 and 7 days, medium was completely replaced by fresh PBS and AFH concentration was assessed from 100 µL media samples as described above.

2.2.6 Hydrogel derivatization with hydrazido-modified and ATTO-labeled hyaluronan (ATTO-hyHA)

Lyophilized weight-adapted hydrogel discs (Ø = 5 mm) were rehydrated with PBS for 24 h (orbital shaker, 150 rpm) and were further incubated with ATTO-hyHA solutions (10 mg/mL or 100 mg/mL) in PBS (containing 0.01% (w/v) sodium azide) at pH 7.4.

In detail, 3 hydrogels were incubated with 200 µL ATTO-hyHA solution in 500 µL Eppendorf tubes (orbital shaker, 150 rpm). After 20 h, hydrogels were washed threefold with 200 µL PBS over 20 h (4 h / 4 h / 12 h) to remove adsorbed HA (orbital shaker, 180 rpm). Immobilization of ATTO-labeled HA derivative was analyzed by fluorescence microscopy (filter: G, exposure: 2 s, gain: 31.4-fold). Additionally, derivatized gels were individually incubated with 100 µL of toluidine blue solution (2 mg/mL) in a 50:49:1 (v/v) mixture of ethanol, water and acetic acid (500 µL Eppendorf tubes) in order to stain immobilized HA.[99] After 30 min, gels were washed twice with 100 µL of the solvent mixture, twice with water and once with PBS (15 min each

step) before staining intensity was visually assessed. Control hydrogels were equally processed without ATTO-hyHA supplementation.

2.3 MATERIALS AND METHODS RELATED TO CHAPTER 4: POROSITY ADJUSTMENT OF OLIGOMER-CROSS-LINKED HYDROGELS

2.3.1 Materials

Diacetone acrylamide (DAAm, *N*-(1,1-dimethyl-3-oxobutyl)acrylamide), *N*-isopropylacrylamide (NiPAAm) Pentaerythritol diacrylate monostearate (PEDAS), 2,2'-azobis(2-methylpropionitrile) (azobisisobutyronitrile, AIBN) and 2,4,6-trinitrobenzenesulfonic acid (TNBS) were purchased from Sigma-Aldrich (Seelze, Germany). Maleic anhydride (MA), triethylamine (TEA) and poly(ethylene glycol) (average molecular weight (M_n) = 8000 Da, P8k) were obtained from Acros Organics (Geel, Belgium). Tetrahydrofuran (THF, refluxed over sodium and potassium and freshly distilled before use) and hydrochloric acid (HCl) 37% were obtained from VWR (Darmstadt, Germany). Diethyl ether, dimethylformamide (DMF), phosphate buffered saline (PBS), sodium bicarbonate and glutaraldehyde solution 25% were purchased from AppliChem (Darmstadt, Germany). Partially hydrolyzed gelatinous peptides (Collagel (type B, 11 kDa, LOT 895046, abbreviated COL) and gelatin 160 Bloom (type B, Lot 630253MI00, abbreviated G160)) were provided by Gelita AG (Eberbach, Germany). Deionized, ultrapure water was produced by a Milli-Q purifier system (Millipore Elix 10, Schwalbach, Germany).

2.3.2 Methods

2.3.2.1 Oligomer synthesis and characterization. Oligo(PEDAS-*co*-NiPAAm-*co*-MA) (oPNMA) and oligo(PEDAS-*co*-DAAm-*co*-MA) (oPDMA) macromers with different contents of maleic anhydride (MA) were synthesized as previously established.[90,98] Procedure of oPDMA synthesis is described in further detail in section 2.2.1 and was accordingly performed for synthesis of oPNMA oligomers. oPNMA-2, which was not described before, was synthesized from 5.837 g PEDAS, 23.279 g NiPAAm and 2.241 g MA which corresponds to a molar ratio of 1:18:2 (PEDAS:NiPAAm:MA). Synthesized oligomers were characterized with regard to chemical composition (^{1}H NMR, alkalimetric titrations) and molecular weight (GPC) according to previously established protocols (Table 2-3).[90,98]

Table 2-3. Compositions and molecular weight characteristics of synthesized oPNMA and oPDMA macromers.

Type	Macromer composition				Molecular weight[c]		
	NiPAAm/ DAAm content[a]	MA content[b]					
		[wt%]	Rel. to PEDAS	Intact MA [%]	M_n [Da]	M_w [Da]	$Đ_M$
oPNMA-1.75	18.8	7.4 ± 0.1	2.6	84.9	3413 ± 184	6054 ± 393	1.77 ± 0.03
oPNMA-2	18.4	8.5 ± 0.1	3.0	83.8	3723 ± 77	6663 ± 166	1.79 ± 0.03
oPNMA-7.5	15.4	20.5 ± 0.1	7.6	76.5	2705 ± 15	4528 ± 7	1.67 ± 0.01
oPDMA-7.5	23.4	16.6 ± 0.0	5.7	68.0	3008 ± 55	4974 ± 92	1.65 ± 0.00

[a]Molar NiPAAm or DAAm content per mol PEDAS as determined by ^{1}H NMR analysis.

[b]MA content as determined by conductometric titration. Total MA content of macromers is expressed as weight percent and relative to 1 mol PEDAS. Fraction of chemically intact anhydride functionalities as calculated from conductometric titration combined with Brown Fujimori titration.

[c]Molecular weight as determined by GPC in THF relative to polystyrene standards.

2.3.2.2 Fabrication of COL-derived hydrogels containing P8k. Oligomer-cross-linked hydrogels were fabricated following an adapted protocol from previous work (Table 2-4).[91,98] In detail, a solution of P8k and COL in water was prepared in a 50 mL polypropylene (PP) tubes (BD Falcon, VWR International, Dresden, Germany) by incubation in a water bath (40 °C) and intermediate shaking/vortexing for at least 1 h. The COL/P8k solution was sterile-filtered through polyethersulfone (PES) filters (0.22 µm, VWR) before use. Oligomer solutions in DMF were prepared in 15 mL PP tubes and cross-linking reaction was performed in 5 mL snap cap glass vials under aseptic conditions. In detail, oligomer solution was mixed with TEA before the COL/P8k solution was added. The vial was subsequently vortexed and gelation occurred within 5 s. After a drying period of 3 days at ambient temperature (2 d at atmosphere pressure and 1 d at 600 mbar), the cross-linked matrices were hydrated and washed for additional 2.5 days with PBS. Hydrogel discs of desired diameter were punched out, frozen at −20 °C, subsequently lyophilized, and rehydrated with PBS before experimental use. Hydrogels were named oPxMA-z/COL/P8k with x = D (oPDMA) or x = N (oPNMA) and corresponding solution concentrations

in the precursor mixture were provided in parentheses. Note, that the concentrations of all constituents were halved upon mixing of equal volumes of the precursor solutions.

Table 2-4. Reaction conditions as used for the fabrication of oPxMA/COL/P8k hydrogels.

oPxMA solution			COL/P8k solution			Catalyst	
Type	Conc [%]	Volume [µL]	COL conc [%]	P8k conc [%]	Volume [µL]	Type	Volume [µL]
oPNMA-7.5	5, 7, 9	200	22.5	0, 5, 10	200	TEA	50
oPDMA-7.5	7, 9						

2.3.2.3 Fabrication of G160-derived hydrogels. G160-derived hydrogels were generally fabricated as described in section 2.3.2.2, but the (P8k-free) peptide solution was prepared in a water:DMF mixture of 1:1 (v/v). As the G160 solutions showed sol-gel transition upon cooling from 40 °C to room temperature, their temperature was kept at 40 °C until use to enable cross-linking in the sol state. Due to the overall low solution concentrations, increased volumes of precursor solutions were used without changing the total volume ratio of precursor solutions and catalyst (COL:oPNMA:TEA = 4:4:1) (Table 2-5). Control hydrogels were accordingly prepared with glutaraldehyde (GTA) instead of oPNMA. Different amounts of the dialdehyde were used to obtain molar concentrations of aldehyde groups (GTA) that were equal to that of the intact anhydride functionalities of corresponding oPNMA solutions. Hydrogels were named oPNMA-z/G160 of $GTA_{eq\ oPNMA\text{-}z}$/G160 and corresponding solution concentrations in the precursor mixture were provided in parentheses.

2.3.2.4 Hydrogel characterization. Physico-chemical properties of fabricated hydrogels were determined by previously described methods.[91] Hydrogel leachables and swelling behavior were gravimetrically assessed. For determination of water leachable components, dry weight (DW) of fabricated and subsequently freeze-dried gels was assessed and theoretical dry weight (theoretical masses of all constituents in the precursor mixture) (TW) was calculated. As the peptide precursor solution for fabrication of oPxMA/COL/P8k gels was supplemented with P8k, another theoretical dry weight ($TW_{w/o\ P8k}$) was calculated which is based on the assumption that P8k was completely removed from the gel matrix during washing and hydration and which

therefore did not consider the theoretical mass of P8k in the mixture. Leachables after fabrication were calculated as (TW – DW) / TW (leachables I) or ($TW_{w/o\ P8k}$ – DW) / $TW_{w/o\ P8k}$ (leachables I*). For the determination of water content, immediately fabricated hydrogel discs (Ø = 8 mm) were punched out and weight in the swollen state (WW) was assessed. Water content I was calculated as (WW – DW) / DW. For calculation of hydrogel leachables and water content after rehydration (II), wet weight after rehydration in PBS (WW2) as well as dry weight after another lyophilization step (DW2) were determined. Leachables II were calculated as (DW – DW2) / DW and water content II was calculated as (WW2 – DW2) / DW2. Hydrogel stiffness was investigated rheologically after rehydration of lyophilized gel discs (Ø = 8 mm, amplitude: 1%, G′ reported at 1 Hz) and hydrogel thickness was determined from the measurement gap that resulted from normal force control (0.2 N). The cross-linking degree of cross-linked hydrogels was calculated from the residual free amino groups of COL or G160 as determined by a standard TNBS assay (absorbance at 346 nm).

Table 2-5. Reaction conditions as used for the fabrication of oPNMA/G160 hydrogels.

oPNMA solution			G160 solution		Catalyst	
Type	Conc [%]	Volume [µL]	Conc [%]	Volume [µL]	Type	Volume [µL]
oPNMA-1.75	3	300	6.25	300	TEA	75
			7.5			
			8.75			
	5		7.5			
	7		7.5			
oPNMA-2	3		7.5			
	5		7.5			
	7		6.25			
			7.5			
			8.75			

2.4 ADDITIONAL INFORMATION ON METHODS OF CHAPTER 5: DEGRADABLE SOL-GEL GLASS BASED HYBRID SCAFFOLDS

2.4.1 Synthesis of degradable three- and four-armed oligomers

Degradable three- or four-armed oligomers of different molecular weight and chemical composition were synthesized by ring-opening polymerization from different oligovalent alcohols as core molecules and defined feeds of D,L-lactide following an adapted protocol from previous work.[53]

In a typical synthesis, 10-30 mmol of tri- (TMPEO, Tx) or tetravalent alcohol (PETEO, Px) were combined with the corresponding molarity of D,L-lactide to equal 3, 4.5 or 6 lactic acid units per hydroxyl group of the core molecule, which corresponds to batch sizes of 23.5-26.5 g. For example, T170LA6 and T1014LA3 were synthesized from 3.00 g T170 + 22.89 g lactide and 14.50 g T1014 + 9.27 g lactide, respectively. Reactants were weighed into a 250 mL round bottom flask which was placed inside a paraffin bath (150 °C) after sealing with a silicon plug and application of nitrogen purge (100 mL/min). Ring-opening polymerization was initiated after 15 min by volumetric (dropwise) addition of tin(II) 2-ethylhexanoate ($Sn(Oct)_2$, 0.273 mol% per hydroxy group[100]) and maintained at 150 °C for 16 h (250 rpm), while nitrogen purge was stopped 30 min after initiation. After cooling at ambient temperature for 5-10 min, the warm product was dissolved in acetone to yield 40-50 mL solution which was further precipitated in 400-500 mL (1:10 ratio) of saturated aqueous sodium chloride solution (brine) (1 L beaker, 700 rpm). After phase separation for 3 h in a separatory funnel, the lower phase (brine) was separated and the transparent and viscous (upper) phase (oligomer product) was dissolved in acetone and the precipitation step was repeated. During method development, deionized water, n-hexane and diisopropyl ether (DIPE) were also used as precipitation media. The product was finally dissolved in acetone (solution volume ~ 100 mL), transferred into a 100 mL Erlenmeyer flask with ground glass joint and was subsequently dried using a rotary evaporator at reduced pressure at 40 °C. When no acetone was removable at 1 mbar, the water bath was heated to 80 °C and drying was continued for 3 h. Until further use, the flask was sealed with a silicon plug and was stored in the fridge. Before use, the flask was either warmed to rt (low viscous

oligomers, e.g. T1014LA3) or heated to 50 °C (high viscous oligomer, e.g. T170LA6). The oligomers were abbreviated as TxLAy or PxLAy with x representing the nominal molecular weight of core component (M_n) and y representing the theoretical number of repeating lactic acid units per side chain.

2.4.2 Degradation of hybrid scaffolds

Selected hybrid glass formulations were sterilized by dry heat (160 °C, 2 h) inside 5 mL snap cap vials which were sealed with aluminum foil. After determination of the initial dry weight (w_0) (135-150 mg) and sample dimensions (electronic caliper: range (mean ± SD), height: 6.58-7.51 mm (7.01 ± 0.18 mm), diameter: 5.42-6.48 mm (6.00 ± 0.21 mm)), initial dry volume (v_0) was calculated. Samples were immersed in 5 mL (v_{medium}) of PBS containing 0.01% (w/v) sodium azide inside a 5 mL screw cap vial in order to obtain a ratio v_{medium} / w_0 of > 30:1, which is in accordance with ISO 15814:1999(E). Application of reduced pressure (100-200 mbar) for 2-3 h together with repeated shaking enabled complete wetting of the porous specimens. Vials were sealed and placed on an orbital shaker (100 rpm) at 37 °C. Medium was exchanged twice per week followed by pH measurement using an Orion 3 Star pH meter (Thermo Fisher Scientific, Schwerte, Germany) equipped with a N6000 BNC electrode (SI Analytics, Weilheim, Germany) after two-point calibration (buffer solutions with pH 4 and pH 7, AppliChem). At defined time points (usually in intervals of 7 d, 14 d or monthly), samples were removed and weight and volume were determined immediately after careful removal of droplets from the sample surface with a paper towel (w_{wet} and v_{wet}) as well as after vacuum drying to constant weight (w_{dry} and v_{dry}). Remaining dry weight and volume (w_{dry}/w_0 * 100% or v_{dry}/v_0 * 100%) were calculated in order to determine material loss. Mass- and volume-related water content ($(w_{wet} - w_{dry})/w_{dry}$ or $(v_{wet} - v_{dry})/v_{dry}$) were determined to characterize swelling behavior. Determination of mechanical properties of dried specimens and fabrication of LA-free T1014-containing control scaffolds were done as previously described.[54]

2.4.3 Multiple linear regression analysis of hybrid mechanics data

Multiple linear regression with backward exclusion of independent variables was performed using SPSS statistical software package (IBM, version 24.0) to determine the factors that statistically significantly affected compressive strength and compressive modulus ($p < 0.05$).

The following oligomer-specific parameters were used as predictors in this analysis:

- Valence (N): absolute value (3 (TxLAy) or 4 (PxLAy)) [nondimensional]
- Total molecular weight (M_n(total)): M_n as determined by GPC [Da]
- Oligolactide-derived molecular weight (M_n(LA)): M_n(total) multiplied with relative LA content in the non-silanized oligomer (w/w) as determined by ^{1}H NMR [Da]
- Oligo(ethylene oxide)-derived molecular weight (M_n(EO)): M_n(total) multiplied with relative EO content in the non-silanized oligomer (w/w) as determined by ^{1}H NMR [Da]
- Total content of oligomer in hybrid (C): content of the non-silanized oligomer in the silica sol [wt%]

In order to derive a regression model by backward exclusion, all listed predictors were included in the first stage of analysis and then sequentially excluded. In each subsequent stage, the predictor with the smallest partial correlation was excluded when it did not significantly contribute to the model. Only hybrid formulations for which compressive strength or compressive modulus could be determined were considered. The following parameters were used to characterize each stage of the model:

- R^2: regression coefficient of the model indicating to which extent the included predictors account for the total variance of the model
- β: standardized coefficient of the predictor indicating the influence of the corresponding predictor to the outcome
- p: Probability value used to determine the level of significance to which the corresponding predictor contributes to the model. A p value below 5% was considered as statistically significant.

CHAPTER 3

Dual-Functional Hydrazide-Reactive and Anhydride-Containing Oligomeric Hydrogel Building Blocks

C. Kascholke[a,#], T. Loth[a,#], C. Kohn-Polster[a,#], S. Möller[b,#], P. Bellstedt[c], M. Schulz-Siegmund[a,#], M. Schnabelrauch[b,#], M. C. Hacker[a,#]

[a] Institute of Pharmacy, Pharmaceutical Technology, Leipzig University

[b] Biomaterials Department, INNOVENT e.V., Jena

[c] Institute of Organic Chemistry and Macromolecular Chemistry, Friedrich-Schiller University Jena

[#] Collaborative Research Center (SFB/Transregio 67), Matrixengineering, Leipzig and Dresden

Biomacromolecules **2017**, 18, 683-694

3.1 ABSTRACT

Biomimetic hydrogels are advanced biomaterials that have been developed following different synthetic routes. Covalent post-fabrication functionalization is a promising strategy to achieve efficient matrix modification decoupled of general material properties. To this end, dual-functional macromers were synthesized by free radical polymerization of maleic anhydride with diacetone acrylamide (*N*-(1,1-dimethyl-3-oxobutyl)acrylamide) and pentaerythritol diacrylate monostearate. Amphiphilic oligomers (M_n < 7.5 kDa) with anhydride contents of 7-20% offered cross-linking reactivity to yield rigid hydrogels with gelatinous peptides (E = 4-13 kPa) and good cell adhesion properties. Mildly reactive methyl ketones as second functionality remained intact during hydrogel formation and potential of covalent matrix modification was shown using hydrazide and hydrazine model compounds. Successful secondary dihydrazide cross-linking was demonstrated by an increase of hydrogel stiffness (> 40%). Efficient hydrazide/hydrazine immobilization depending on solution pH, hydrogel ketone content as well as ligand concentration for bioconjugation was shown and reversibility of hydrazone formation was indicated by physiologically relevant hydrazide release over 7 days. Proof-of-concept experiments with hydrazido-functionalized hyaluronan demonstrated potential for covalent aECM immobilization. The presented dual-functional macromers have perspective as reactive hydrogel building blocks for various biomedical applications.

3.2 INTRODUCTION

Biomimetic hydrogels are promising materials for biomedical applications as they contain cell-responsive moieties for improved biological performance. Integration of extracellular matrix(ECM)-derived structures, such as fibronectin, laminin and proteoglycans, into these soft biomaterials is a fundamental strategy to promote cell adhesion and proliferation.[101–103] ECM components can implement further properties to a semi-synthetic hydrogel, including enzymatic degradation and controlled interactions with growth factors as well as cytokines in order to specifically regulate cellular response. In this regard, multi-functional macromers are promising building blocks for hydrogel engineering, while one functionality supports network formation and other functionalities can promote chemical matrix modification or bioconjugation.[20] Post-

fabrication functionalization strategies allow for an orthogonal control over material fabrication and modification chemistry which enables high functionalization degree using high-yield reactions under mild conditions, such as click chemistry, and the realization of predefined material properties.[49,84]

We have established a hydrogel platform consisting of an anhydride-containing oligomer that can covalently cross-link amine-containing macromolecules, such as gelatin materials, here addressed as gelatinous peptides.[90,91] The effective incorporation of the oligomeric precursors into the cross-linked matrix as hydrogel building blocks allows for a broad adjustment of physico-chemical material properties. This dual-component material concept proved suitable for the formulation of cytocompatible, cell-adhesive hydrogels in which the natural component provided biological activity and specific degradability, and the synthetic building block controlled network properties via content of reactive groups for covalent cross-linking. The polyanionic character of the hydrogel matrix offers potential for non-covalent immobilization by electrostatic interactions. Partial pre-derivatization of the anhydride-containing oligomers also enabled covalent matrix modification. This strategy, however, is accompanied by loss of anhydride reactivity and may therefore result in altered hydrogel properties. Limited loading capacity is another drawback of this conjugation strategy.

It is the purpose of the study to extend material engineering and bioconjugation possibilities of this hydrogel platform. To this end, the versatility of the applied free radical polymerization chemistry was used to control macromer chemistry by variation of comonomer type and ratio. We present a dual-functional reactive oligomer in order to decouple hydrogel network formation by chemical cross-linking and covalent matrix functionalization. The oligomeric macromers were synthesized from pentaerythritol diacrylate monostearate (PEDAS), diacetone acrylamide (DAAm) and maleic anhydride (MA) to yield oligo(PEDAS-*co*-DAAm-*co*-MA) (oPDMA) that form hydrogel matrices by anhydride-mediated cross-linking of collagen hydrolysate (i.e. gelatin) as previously established.[91] First cell culture experiments illustrated the biological potential of these oPDMA-derived gels, since a pro-melanotic effect on melanocytes when cultivated on the cross-linked matrices was shown that was considered superior to other gel substrates including a commercial full-length collagen wound dressing (Collagen Cell Carrier®).[104] These results motivated for extended physico-chemical and biological hydrogel characterization, while we especially focus on the mildly reactive, fully cytocompatible methyl

ketone groups (from DAAm) that are incorporated to the materials as second functionality which can be chemically modified post hydrogel fabrication.

The specific reactivity of ketones and aldehydes towards hydrazides[105] and hydrazines[106] under mild conditions is known and the applicability of these specific conjugation reactions for hydrogel design was reported by several groups with the general focus on hydrazide derivatives.[50,107] Such a conjugation yields an acylhydrazone, but for simplification the term "hydrazone" was used irrespective of hydrazone substitution in this paper. Taking a closer look at this conjugation chemistry, hydrazide to hydrazone conversion has been used as cross-linking strategy for hydrogel formation, while simple dihydrazide cross-linking[67,108] was extended toward fabrication of homopolymeric[41,44,109] and heteropolymeric[17,110,111] networks from correspondingly functionalized macromeric precursors. The formed hydrazones could be cleaved pH-dependently[16,105] which allowed for subsequent degradation of cross-linked hydrogels and/or controlled release of covalently immobilized drugs.[16,112,113] Almost all previously presented concepts are based on aldehydes as carbonyl compounds which can be explained by a high reactivity combined with sufficient stability of this function in aqueous environment.[114] However, general applicability of carbonyl-hydrazide/hydrazine conjunction as attempted with ketone-containing oPDMA macromers here was assumed from a study of Patenaude and colleagues, in which biocompatible and mechanically stable hydrazone-cross-linked pNiPAAm-based hydrogels were fabricated using (methyl) ketone-functionalized precursors.[44]

This study aimed at synthesizing a series of oPDMA macromers and characterization of their dual functionality. Effective hydrogel formation with partially degraded gelatinous peptides is aspired and physico-chemical properties and cytocompatibility of the gels are to be determined. The ketone reactivity of the macromers will be evaluated by secondary dihydrazide cross-linking and by immobilization of well-detectable hydrazide and hydrazine probes. Equilibrium-driven release of the immobilized hydrazide probe and conjugation of hydrazido-functionalized hyaluronan (ATTO-hyHA) are assessed to further illustrate the potential of post-fabrication hydrogel modification via keto-hydrazide conjugation chemistry.

3.3 MATERIALS AND METHODS

3.3.1 Materials

Diacetone acrylamide (DAAm, *N*-(1,1-dimethyl-3-oxobutyl)acrylamide), 2,4,6-trinitrobenzene-sulfonic acid (TNBS), adipic acid dihydrazide (ADH), *N,N*-diethylethylenediamine (DEED), Dulbecco's modified eagle medium (DMEM) low glucose without phenol red, 1-ethyl-3-(3-dimethylaminopropyl)carbodiimide (EDC), *N*-hydroxysuccinimide (NHS) and toluidine blue were purchased from Sigma-Aldrich (Seelze, Germany). Deuterated chloroform ($CDCl_3$) and dimethyl sulfoxide (DMSO-d_6) were obtained from Armar Europa (Leipzig, Germany). Diethyl ether, sodium bicarbonate, phosphate buffered saline (PBS), hydrochloric acid (HCl) 37%, ethanol absolute and acetic acid glacial were purchased from AppliChem (Darmstadt, Germany). Partially hydrolyzed gelatinous peptide (Collagel type B, 11 kDa, LOT 895046, abbreviated COL) was provided by Gelita AG (Eberbach, Germany). Sodium chloride (NaCl), monobasic potassium phosphate (KH_2PO_4), sodium cyanoborohydride ($NaCNBH_3$), potassium chloride (KCl) and potassium hydroxide (KOH) were obtained from Acros Organics (Geel, Belgium). Fetal calf serum (FBS), penicillin/streptomycin (P/S) and trypsin were purchased from PAA Laboratories (Pasching, Austria). Alamar Blue reagent and calcein-acetoxymethyl (calcein-AM) were obtained from Invitrogen (Darmstadt, Germany). 2,4-Dinitrophenylhydrazine (DNPH) and phosphoric acid (H_3PO_4) 85% were purchased from Merck (Darmstadt, Germany). Alexa Fluor 350 hydrazide (AFH) and anhydrous dimethyl sulfoxide (DMSO) were obtained from Life Technologies (Darmstadt, Germany). Native high molecular weight hyaluronan (HA, from Streptococcus, M_w = 1.1 MDa, molecular-weight dispersity $Đ_M$ = 4.8) was purchased from Aqua Biochem (Dessau, Germany) and fluorescence marker (ATTO 633-NH_2) was obtained from ATTO-TEC (Siegen, Germany).

3.3.2 Methods

3.3.2.1 Macromer synthesis and characterization. Oligo(PEDAS-*co*-DAAm-*co*-MA) (oPDMA) macromers were synthesized according to a previously established protocol.[90] Briefly, comonomer mixtures of pentaerythritol diacrylate monostearate (PEDAS), diacetone acrylamide (DAAm), and maleic anhydride (MA) were copolymerized by free radical polymerization after

initiation with 2,2´-azobis(2-methylpropionitrile) at 60 °C under a nitrogen atmosphere in THF. Comonomers were reacted in a 1:20 molar ratio of PEDAS to DAAm plus MA and the resulting oligomers were abbreviated oPDMA-z with z representing the molar feed of MA in the comonomer mixture relative to 1 mol PEDAS (Table 3-1). The macromers were precipitated repeatedly with diethyl ether and further vacuum-dried. Molecular weight was determined by GPC in THF relative to polystyrene standards (PSS Polymer Standards Service GmbH, Mainz, Germany) and chemical compositions were verified by ^{1}H NMR, conductometric as well as Brown Fujimori titration.[90] ^{13}C NMR spectra were recorded in DMSO-d_6 (100 mg/mL) containing 0.03% (v/v) tetramethylsilane (TMS) as internal shift reference (Mercury Plus 300 MHz, Varian, Darmstadt, Germany). The pH-dependent temperature responsiveness of aqueous oPDMA solutions containing 200 mM sodium chloride was determined rheologically.[90]

3.3.2.2 Hydrogel fabrication. Cross-linked hydrogels were prepared following established protocol.[91] In brief, 200 µL of aqueous COL solution were cross-linked with 200 µL of macromer dissolved in DMF in the presence of 50 µl TEA. Weight-adapted hydrogels (w_{COL} + w_{oPDMA} = 63 mg) were prepared following a slightly modified protocol in which hydrogel volumes were adjusted to yield equivalent dry weights without changing building block concentrations or total volume ratio (COL:oPDMA:TEA = 4:4:1). After a drying period of 3 days, the cross-linked matrices were hydrated and washed for further 2.5 days with PBS. Hydrogel discs of desired diameter were punched out, frozen at -20 °C, subsequently lyophilized and rehydrated with PBS before experimental use. Hydrogels were named oPxMA-z/COL with x = D (oPDMA) or x = N (oPNMA) and corresponding solution concentrations were provided in parentheses.

3.3.2.3 Hydrogel characterization. Hydrogel composition and physico-chemical material properties were determined by previously described methods.[91] Hydrogel stiffness was investigated rheologically (Ø = 8 mm, G´ reported at 1 Hz). The cross-linking degree of cross-linked hydrogels was calculated from the residual free amino groups of COL as determined by a standard TNBS assay (absorbance at 346 nm) and hydrogel leachables and swelling behavior were gravimetrically assessed. COL content of the hydrogels was determined by HPLC after acidic gel hydrolysis at 60 °C and further o-phthalaldehyde (OPA, Sigma Aldrich) derivatization of the corresponding amino acids (absorbance at 335 nm). The oPDMA content was calculated

as the difference between hydrogel dry weight corrected by the PBS salt content and the COL content.

3.3.2.4 Hydrogel cytocompatibility. Indirect cytocompatibility tests and cell behavior in direct contact experiments were performed using γ-irradiated (13.5-16.5 kGy) oPxMA-7.5/COL hydrogel (3.5%/15%) discs (Ø = 11mm). Briefly, media samples conditioned with hydrated hydrogels (secondary extracts: 1 mL of fresh DMEM to the hydrated gel discs for 24 h at 37 °C) were prepared[91] and assessed for cytotoxicity on L929 mouse fibroblasts with a standard Alamar Blue assay as previously described.[115] Direct contact experiments were performed with human adipose tissue-derived stem cells (hASC) as follows: Lyophilized hydrogel discs were rehydrated with cell culture medium (CM: 89% DMEM, 10% FBS, 1% P/S) for 24 h at 37 °C , subsequently incubated with 30,000 cells per gel disc followed by dynamic cultivation using a horizontal shaker (70 rpm, 37 °C, 5% CO_2). After day 1 and day 3, cell number and proliferation was assessed by Alamar Blue assay. In more detail, discs were washed with PBS, hydrated with fresh CM and 10% Alamar Blue reagent was added. The reduction to resorufin (red) by viable cells was quantified after 6 h at 37 °C under gentle shaking using a Tecan Infinite F 200 plate reader (Salzburg, Austria) equipped with a fluorescence filter set (Ex: 570/8 nm, Em: 610/10 nm). Confocal laser scanning microscopy (CLSM) was performed after live cells were stained with calcein-AM.[91]

3.3.2.5 Post-fabrication cross-linking of hydrogels with adipic acid dihydrazide (ADH). Rehydrated weight-adapted oPDMA-5/COL hydrogel (5.5%/7.5%) discs (Ø = 8 mm) were incubated with 2 mL of buffered solution at pH 5 (25 mM KH_2PO_4) or pH 7.4 (PBS) containing 7.5% (w/v) ADH. Reductive stabilization of the formed hydrazone bonds was attempted by addition of 1.35% (w/v) $NaCNBH_3$ to yield a molar ratio of $NaCNBH_3$:hydrazide of 1:2.[113] Control groups were prepared in pure buffer and corresponding oPNMA/COL hydrogels served as ketone-free control matrices. Effects of ADH incubation on hydrogel stiffness were investigated by oscillation rheology (Physica MCR 301 rheometer, Anton Paar, Graz, Austria). Experiments were performed under normal force control (0.1 N). Storage modulus (G´), loss modulus (G´´), and complex viscosity (η*) were recorded during a time sweep with an amplitude of 1% and a frequency of 1 Hz. Storage moduli after 100 sec were reported. Hydrogel stiffness was determined before (t0) as well as after 2 h, 18 h, 66 h, and 210 h of contact with ADH.

3.3.2.6 Hydrogel derivatization with DNPH. Rehydrated weight-adapted oPxMA-7.5/COL hydrogel (3.5%/7.5%) discs (Ø = 7 mm) were incubated with DNPH solutions (0.25 mg/mL) at pH 1, 3, 5 and 7.4. Medium of pH 1 was composed of 0.1 M HCl solution containing 50 mM KCl and PBS was used as buffer of pH 7.4. Buffer solutions with pH 3 and pH 5 were prepared from 25 mM KH_2PO_4 solution by pH adjustment with H_3PO_4 and KOH. In detail, hydrogels were incubated with DNPH solution for 4 h followed by 4 washing steps within 80 min (orbital shaker, 150 rpm). After transfer to 48-well plates (Corning, Amsterdam, The Netherlands), stereomicroscopic images of hydrogels were taken (DS-2Mv digital camera, Nikon, Duesseldorf, Germany). The absorbance ratio $A_{405\ nm}/A_{340\ nm}$ was determined from derivatized hydrogels using the Tecan plate reader equipped with appropriate absorption filters (340/35 nm and 405/10 nm). DNPH content was determined after hydrogel hydrolysis over more than four weeks at pH 1 (0.1 M HCl, rt) by UV/Vis spectroscopy using the Tecan plate reader at 340 nm and expressed relative to hydrogel dry weight. Control hydrogels were incubated at pH 7.4 without DNPH supplementation.

3.3.2.7 Hydrogel derivatization with fluorescent hydrazide (AFH). Rehydrated weight-adapted hydrogel discs (Ø = 5 mm) were incubated with AFH solutions at pH 3, 3.5, 4, 4.5, 5 and 7.4. Buffers with pH 3-5 were prepared from 25 mM KH_2PO_4 solution by pH adjustment with H_3PO_4 and KOH, and PBS was used as buffer of pH 7.4. In more detail, AFH stock solution (5 mg dissolved in 2.5 mL DMSO) was diluted with corresponding medium to obtain AFH concentrations in the range of 1-200 µg/mL. Hydrogels were incubated with AFH solution in black 96-well plates (Corning) for 4 h followed by 5 washing step over 26 h in order to remove adsorbed AFH (orbital shaker, 150 rpm). Derivatized hydrogels were analyzed post washing by fluorescence microscopy (Eclipse TE2000-S, Nikon, equipped with an Intensilight Fiber Illuminator C-HGFI and a DS-Ri2 digital camera). Hydrogel AFH content was determined by fluorescence spectroscopy using the Tecan plate reader (Ex: 360/35 nm, Em: 465/35 nm) and related to hydrogel dry weight. Control hydrogels were incubated at corresponding pH without AFH supplementation. AFH release at pH 7.4 was investigated for selected formulations by incubation of AFH-derivatized gel discs in 200 µl PBS on an orbital shaker (150 rpm). After 1, 3, 5 and 7 days, medium was completely exchanged and AFH concentration was assessed.

3.3.2.8 Synthesis of hydrazido-modified and ATTO-labeled hyaluronan (ATTO-hyHA). Functionalized GAG derivative was synthesized from HA that was thermally degraded (180 min)

as previously described.[116] Firstly, carboxyl groups were functionalized with ADH to obtain hydrazido-modified HA (hyHA).[117,118] Briefly, 1.25 mmol HA were dissolved in 50 mL deionized water overnight. After addition of an aqueous ADH solution (5 mmol) and pH adjustment to 4.7 with HCl (0.1 M), EDC and NHS (each 2.5 mmol, dissolved in water) were added and the pH was tuned to 8. The solution was stirred for 5 h at rt and further dialyzed against NaCl (0.3 M, 3 days) as well as deionized water (~ 3 days, until conductivity < 5 µS) to remove salt residues, followed by filtration, lyophilization and vacuum drying (yield: 80-85%). Chemical structure of hyHA was analyzed by ^{1}H and ^{13}C NMR spectroscopy (Bruker Avance III 400 MHz, Billerica, MA). Secondly, fluorescently labeled hyHA derivative (ATTO-hyHA) was synthesized by coupling of ATTO 633-NH_2 to reducing termini of HA following established protocol.[119] In detail, 250 mg hyHA were dissolved in 20 mL deionized water and pH was adjusted to ~ 8 with NaOH (0.1 M). After ATTO 633-NH_2 addition (0.6 µmol in DMSO), the reaction mixture was stirred for 6 h at rt and further purified as described above for hyHA (yield: 85%).

3.3.2.9 Hydrogel derivatization with ATTO-hyHA. Rehydrated weight-adapted oPxMA-7.5/COL hydrogel (3.5%/7.5%) discs (Ø = 5 mm) were incubated with ATTO-hyHA solutions in PBS at pH 7.4 (10 mg/mL or 100 mg/mL). After 20 h, hydrogels were washed threefold with PBS for further 20 h to remove adsorbed HA (orbital shaker, 180 rpm). Immobilization of ATTO-labeled HA derivative was analyzed by fluorescence microscopy. Additionally, derivatized gels were incubated with toluidine blue solution (2 mg/mL) in a 50:49:1 (v/v/v) mixture of ethanol, water and acetic acid in order to stain immobilized HA.[99] After 30 min, gels were washed with the solvent mixture, water and PBS within 75 min before staining intensity was visually assessed. Control hydrogels were equally incubated without ATTO-hyHA supplementation.

3.3.2.10 Statistics. Unless otherwise stated, experiments were conducted in triplicate and the data was expressed as means ± standard deviation (SD). Single-factor analysis of variance in conjunction with Tukey's Post Hoc test was performed to assess the statistical significance ($p < 0.05$) within data sets.

3.4 RESULTS AND DISCUSSION

3.4.1 Amphiphilic, oligomeric oPDMA macromers with tunable composition. Oligo(PEDAS-*co*-DAAm-*co*-MA) (oPDMA) macromers were synthesized by free radical polymerization from pentaerythritol diacrylate monostearate (PEDAS), diacetone acrylamide (DAAm) and maleic anhydride (MA) (Figure 3-1A). MA integrates amine-reactive anhydride functionalities and PEDAS was used according to a previously established macromer design concept in a low molarity in order to balance the MA-mediated oligomer and hydrogel hydrophilicity by the lipophilic stearate domain and to increase hydrogel stability.[90,120–122] Reactive methyl ketones were incorporated by DAAm as third co-monomer, which is known to form copolymers with a variety of other comonomers.[123] The acrylamide structure may further support alternating copolymerization with MA,[68] which is desired for oPDMA synthesis in order to achieve an efficient incorporation of both (anhydride and ketone) functionalities. Different monomer feed ratios were used and macromers were abbreviated oPDMA-z with z representing the molar feed ratio of MA related to 1 mol PEDAS (Table 3-1). Molecular weights (M_n) ranged between 2300 Da and 7400 Da and an indirect correlation with MA feed was found, as expected from our experience with the synthesis of oPNMA that contains *N*-isopropylacrylamide (N) instead of D.[90] NMR analysis revealed characteristic signals derived from the constituent comonomers (Figure 3-1). ^{13}C NMR spectra offered typical ketone signals of DAAm at 206-211 ppm, which did not suggest any modification of these reactive groups upon copolymerization (Figure 3-1B). Anhydride carbons were generally detected in the range of 171 ppm to 176 ppm. Signals at 178-182 ppm were assigned to carboxylic acid functions and therefore indicated partial hydrolysis of anhydride units during macromer synthesis and purification. Furthermore, no C=C signals were found in the range of 120 ppm to 140 ppm (not shown) which suggests efficient purification and removal of monomer residues. The efficiency of the applied purification protocol was also confirmed by the absence of proton signals at 5.45-6.35 ppm in ^{1}H NMR spectra (Figure 3-1C). Proton NMR allowed for determination of the macromer composition with the help of five characteristic integrals (I_1-I_5), in which I_2 was set to equal 28 protons of the fatty acid chain of PEDAS.[90] The content of DAAm was calculated from I_3 and corresponding values were obtained from I_5 (Table 3-1). DAAm integration was generally controlled by DAAm feed in all synthesized oligomers. For oPDMA-2.5, total DAAm content

(85.5%) correlated well with the reaction feed (83.3%). The absolute DAAm contents decreased for oPDMA-5 to oPDMA-10, but not to the extent preset by the corresponding reaction feeds. Determination of MA content from NMR, particularly from I_4, was unreliable due to strongly overlapping signals. As established for related oPNMA oligomers,[90] a valid determination of MA content was achieved by alkalimetric titrations (Table 3-1). Importantly, anhydride content of the oligomers correlated well with MA feed. While MA was efficiently copolymerized in oPDMA-2.5 (low MA feed), its conversion decreased with increasing MA feeds which suggests a preferential alternating MA-DAAm copolymerization that has previously been reported for other MA-acrylamide systems.[68] In accordance with ^{13}C NMR results, titrations also confirmed partial anhydride hydrolysis, but 68-72% of the anhydride groups remained intact (Table 3-1). These values are approximately ten percentage points lower as established for corresponding oPNMA, which is attributed to the hygroscopic nature of DAAm.[97] Accordingly, increasing water signals were found in ^{1}H NMR spectra with increasing DAAm feeds (Figure 3-1C). Synthesized oPDMA macromers were not immediately soluble in water, but upon base-catalyzed anhydride hydrolysis clear solutions were obtained at pH values above 4.5. Temperature responsiveness in aqueous environment, which is characteristic for DAAm-containing copolymers,[124] was also observed for oPDMA and investigated rheologically. Phase transition temperatures ranged between 53 °C and 90 °C and correlated with MA content and medium pH (Figure 3-S1). Taken together, copolymerization of PEDAS, DAAm and MA yielded amphiphilic oligomers with molecular weights (M_n) below 7500 Da, more specifically below 3000 Da when relative MA feed above 5 was employed. The low molecular weight is advantageous to enable controlled formation of a versatile platform of cross-linked hydrogels with gelatinous peptides. The peptide material used here (COL) was also characterized by low molecular weight (11 kDa). Dual functionality was achieved by efficient incorporation of chemically intact anhydride as well as ketone groups into the oligomer chains. The reduction of anhydride reactivity by 20-30% is already known for other maleic anhydride-containing oligomers, but especially for higher MA oligomers still a MA feed-dependent reactivity towards amines can be expected.[90,91] In contrast, macromer ketone functions remained unchanged, which did not suggest any need for a ketal protection strategy as previously reported for copolymerization of a ketone-functionalized NiPAAm-derived monomer.[44] In comparison to analogous oPNMA macromers[90], higher molecular weights, higher acrylamide (DAAm) integration and reduced MA contents were found

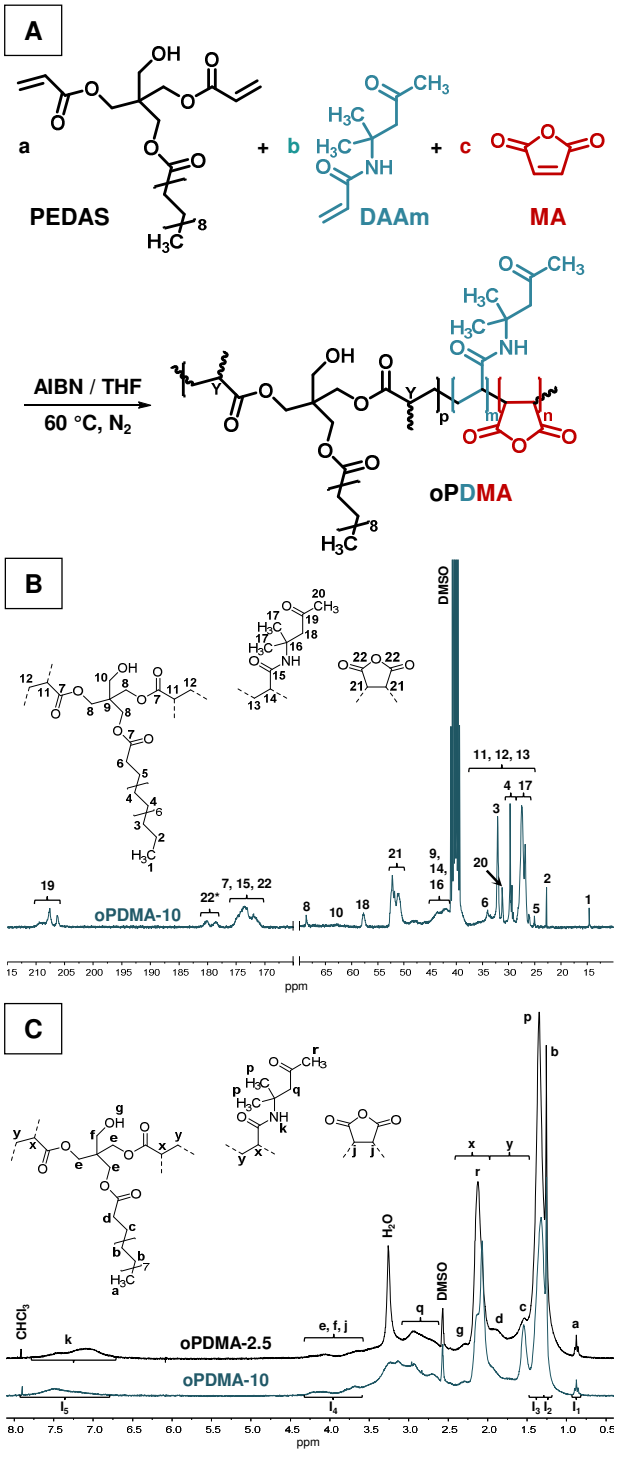

Figure 3-1. Synthesis scheme and NMR spectra. (A) Synthesis of oPDMA macromers by radical copolymerization (Y indicates possible branching sites). (B) Representative ^{13}C NMR spectrum of oPDMA-10 macromer. Label '22*' refers to carbon signals from hydrolyzed anhydride units. (C) ^{1}H NMR spectra of two oligomers with extreme MA contents. I_1–I_5 represent the integrals used to determine macromer composition.

Table 3-1. Compositions and molecular weight characteristics of synthesized oligo(PEDAS-*co*-DAAm-*co*-MA) macromers (oPDMA-z).

Type	Macromer composition							Molecular weight (GPC)		
	Reaction feed (molar ratio)			DAAm content (rel. to PEDAS)[a]	MA content[b]			M_n [Da]	M_w [Da]	$Đ_M$[c]
	PEDAS	DAAm	MA		[wt%]	Rel. to PEDAS	Intact MA [%]			
oPDMA-2.5	1	17.5	2.5	21.2 (85.5%)	7.0 ± 0.0	2.6	68.5	7373 ± 128	12257 ± 218	1.66 ± 0.02
oPDMA-5	1	15	5	24.0 (80.8%)	13.0 ± 0.1	4.7	71.5	4014 ± 57	6512 ± 78	1.62 ± 0.01
oPDMA-7.5	1	12.5	7.5	23.4 (77.7%)	16.6 ± 0.0	5.7	68.0	3008 ± 55	4974 ± 92	1.65 ± 0.00
oPDMA-10	1	10	10	21.7 (74.6%)	19.6 ± 0.1	6.4	68.6	2359 ± 23	3807 ± 17	1.61 ± 0.01

[a]Molar DAAm content per mol PEDAS and (calculated total molar DAAm content) as determined by ^{1}H NMR analysis using integral I_3.

[b]MA content as determined by conductometric titration. Total MA content of macromers is expressed as weight percent and relative to 1 mol PEDAS. Fraction of chemically intact anhydride functionalities as calculated from conductometric titration combined with Brown Fujimori titration.

[c]Molecular-weight dispersity $Đ_M = M_w/M_n$.

for oPDMA. These differences are attributed to a so-called H-bonding effect,[68] which results in sterically hindered amide functions during oPDMA copolymerization and ultimately may have shifted the chain growth reaction from alternating MA-acrylamide copolymerization toward DAAm homopolymerization (and DAAm-PEDAS copolymerization). Molecular weight and MA content data revealed an average PEDAS incorporation of < 2 units per oligomer chain for oPDMA-5 to oPDMA-10, but the comparatively high molecular weight of oPDMA-2.5 indicated significantly higher PEDAS conversion together with potentially increased branching. In consequence, further experiments mainly focused only on uniformly structured oPDMA-5, -7.5 and -10 macromers.

3.4.2 Rigid oPDMA/COL-derived hydrogels with good cell adhesion properties. Macromers bearing two or more anhydride units per polymer chain are able to effectively cross-link amine-containing macromolecules, such as gelatin. In this work, we used a low molecular weight fraction of hydrolyzed gelatinous peptides (Collagel®, COL, 11 kDa) – a material that does not show a sol-gel transition and is therefore processable in high solution concentrations. Hydrogels were fabricated using a wide range of oPDMA to COL ratios according to a previously published protocol.[91] Depending on the cross-linker type, solution concentrations of 2.5-5.5% of oPDMA together with 7.5-15% of COL yielded stable, macroscopically homogeneous and uniformly transparent hydrogels indicating the absence of phase separated domains (Figure 3-S2). Inadequate stability of the hydrogel formulation was found for low MA content in the mixture (e.g. oPDMA-2.5/COL gels) and for comparably high number of reactive MA groups (e.g. oPDMA-10/COL gels). This is in accordance with the physico-chemical hydrogel properties that were determined for a systematically selected set of formulations from the oPDMA/COL platform (Figure 3-2A, Figure 3-S3). Formulations fabricated from oPDMA with low anhydride contents were instable, which was attributed to a lower cross-linking degree and enhanced leaching of oPDMA. In contrast, the cross-linking degree of formulations with anhydride-rich oPDMA was generally high, but the rapid reaction with COL resulted in macroscopically irregular hydrogels, increased COL leaching, enhanced swelling and reduced hydrogel stiffness. Similar correlations have previously been found for the oPNMA/COL hydrogel platform.[91,115] As one key property, storage modulus of the gels is now discussed in further detail. The values ranged between 200 Pa and 8500 Pa which, for reasons of comparison, corresponds to elastic moduli of 0.6-25.5 kPa (using the simplified estimation of E equals 3G´)[125] (Figure 3-2A). The highest storage moduli were obtained for oPDMA-5-derived gels which revealed cross-linking degrees of 55-60% and a correlation with oPDMA content was found that was statistically significant within oPDMA-5/COL (X%/Y%) formulations with Y = 7.5% or 17.5% ($p < 0.01$). For almost all formulations, a medium COL content of 12.5% was optimal (not significant). Cross-linker oligomers with increased anhydride contents did not automatically yield stiffer gels, storage moduli rather decreased from oPDMA-5- to oPDMA-10-derived matrices, which is clearly visible when oPDMA-z/COL (3.5%/Y%) formulations with the same COL concentration (Y = 7.5%, 12.5% or 17.5%) are compared ($p < 0.01$). This can be explained by decreasing oligomer molecular weights and an increased reactivity of the anhydride-containing oligomer

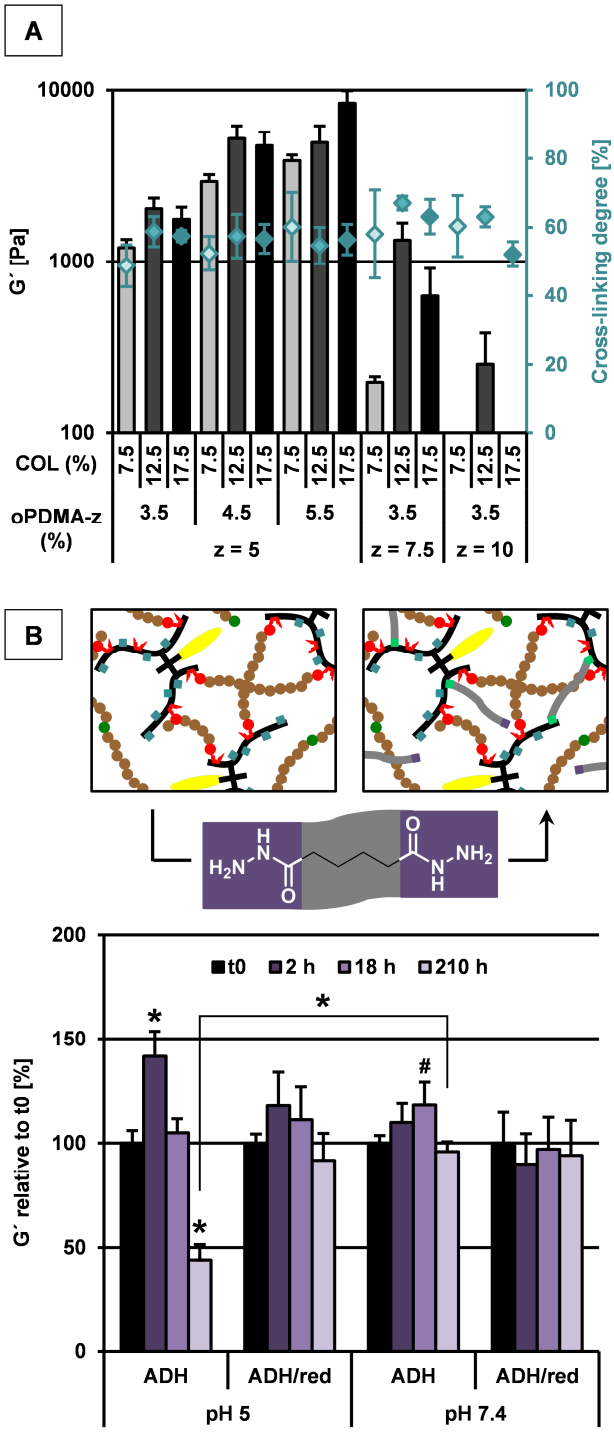

Figure 3-2. Stiffness of oPDMA/COL hydrogels and effect of secondary dihydrazide cross-linking as determined by oscillation rheology. (A) Storage modulus (n = 5) and cross-linking degree (n = 3) of different hydrogel formulations. (B) Effect of ADH treatment on storage moduli of oPDMA-5/COL (5.5%/7.5%) hydrogels (G´ = 3027 +/- 232 Pa). Storage moduli were expressed relative to initial G´ at t0. Hydrogels were incubated with ADH without (ADH) or with additional $NaCNBH_3$ treatment (ADH/red). Storage moduli of labeled groups differed statistically significantly from G´ at t0 or G´ of corresponding groups ($^{\#}p < 0.05$, $^{*}p < 0.01$) (n = 5).

which reduces gelling time during hydrogel formation and hinders chain orientation and effective amine-anhydride conversion in the gelation mix. Overall, macroscopically homogeneous hydrogels were obtained by balancing anhydride to amine ratios in the reaction mix and physico-chemical material properties were controlled by hydrogel composition. In general, oPDMA oligomers yielded stiffer hydrogels when corresponding formulations of oPDMA/COL and oPNMA/COL were compared[91] which might be caused by increased molecular weights and hydrophobicity of oPDMA over oPNMA. The obtained elastic moduli meet or even exceed the range of biologically relevant hydrogel mechanics[126] and hydrogel stability under physiological conditions was confirmed (Figure 3-S4).

Cell response to oPDMA/COL hydrogels was evaluated with indirect and direct contact experiments. A standard cell viability (LIVE/DEAD) assay using L929 fibroblasts revealed cytocompatibility of media samples conditioned with various hydrogel formulations. In order to mimic the application route to cell-containing systems, extracts of completely rehydrated hydrogels were analyzed. The representatively selected set of formulations offered oPDMA type and oPDMA/COL ratio as varying parameters. For all hydrogel types, fractions of live cells in the range of the live control were determined indicating the absence of toxic leachables (Figure 3-S5). Extract cytocompatibility was further confirmed by a metabolic assay (Alamar Blue), which revealed metabolic activities of more than 100% for a selected oPDMA/COL hydrogel formulation (Figure 3-3A). Direct contact experiments were performed by direct seeding of hASC on oPDMA/COL hydrogels, while the corresponding oPNMA-derived gel served as control matrices. Since hydrogel stiffness was detected as one key parameter affecting cell response,[126] materials of comparable storage moduli (4-4.5 kPa) and analogous composition were compared. After 3 days, a higher number of spread cells was found on oPDMA/COL hydrogels as compared to the analogous oPNMA/COL formulation (Figure 3-3B). This visual impression was quantitatively confirmed by the cell number in the gels which was significantly higher in the oPDMA/COL group after 3 days (Figure 3-3C). However, cells were preferably located densely on top of the gels and migration into the matrix was only observed at later time points (data not shown). Altogether, oPDMA/COL hydrogels showed excellent cytocompatibility and, in accordance with oPNMA/COL gels, potential cytotoxicity of anhydride residues vanished in the hydrogel state upon hydrolysis in aqueous medium.[91] The presence of reactive ketone functions in oPDMA was obviously not related to negative effects on environmental cells. These findings are in good agreement with a previous study on pNiPAAm-

based hydrogels from ketone-containing monomeric precursors.[44] In direct contact experiments, oPDMA/COL hydrogels supported adhesion and proliferation of hASC which confirmed previously seen positive effects of the same oPDMA/COL hydrogel formulation on phenotype during melanocyte cultivation.[104]

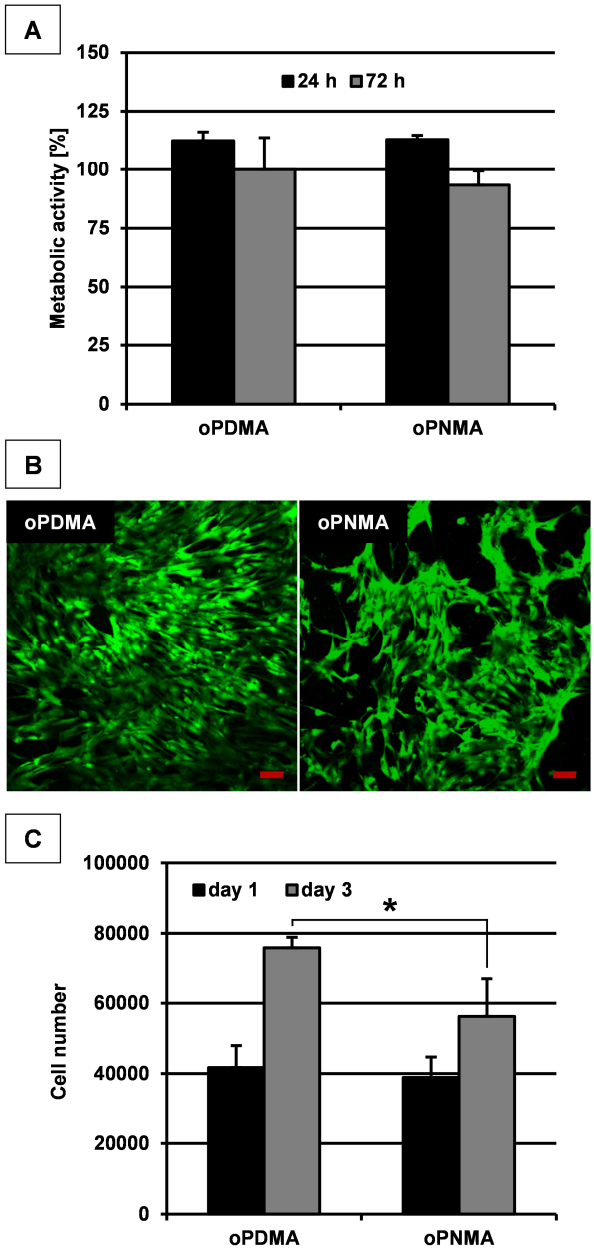

Figure 3-3. Hydrogel cytocompatibility and cell adhesion behavior. (A) Indirect cytocompatibility assay (Alamar Blue) of hydrogel medium extracts tested on L929 fibroblasts after 24 h and 72 h incubation (n = 4). (B-C) Attachment and proliferation of hASC on oPxMA-7.5/COL (3.5%/15%) hydrogels. (B) Stacked CLSM images at day 3 after calcein-AM staining (scale bars represent 250 µm) and (C) cell number after 24 h and 72 h of incubation (*$p < 0.01$) (n = 4).

3.4.3 Characterization of ketone reactivity: I. Effective post-fabrication cross-linking of oPDMA/COL hydrogels by ADH. The main objective of this study is based on efficient integration of reactive methyl ketones via oPDMA into cell-friendly hydrogel matrices in order to enable significant post-fabrication modification. These functionalities are supposed to remain unmodified during the hydrogel forming reaction of oPDMA with COL via covalent amide bond formation, because a conversion of ketones with amino groups during cross-linking would need strong acidic conditions and hydrogel formation is performed in presence of a base.[127] For functionalization experiments, hydrogel formulations were selected in which efficient oPDMA incorporation as hydrogel building block was realized (19-32 wt%). This criterion is also a key requirement of an effective post-fabrication functionalization of oPDMA methyl ketones. As a proof-of-principle experiment, secondary dihydrazide cross-linking of ready-to-use oPDMA/COL hydrogels was attempted. The ability of short-chained adipic acid dihydrazide (ADH) to cross-link two ketone functions with each other is widely used for stabilization of acrylic latexes,[105] and its effect on hydrogel stiffness was analyzed rheologically using a hydrogel formulation of intermediate stiffness (oPDMA-5/COL (5.5%/7.5%)) (Figure 3-2B). A significant increase of storage moduli by 18% at pH 7.4 was found after 18 h which was not observed when ADH was added to control group. Reductive hydrazone stabilization as intended by sodium cyanoborohydride supplementation did not change hydrogel stiffness at physiological pH. More pronounced effects of these treatments were found in mildly acidic environment (pH 5). Under these conditions, ADH cross-linking resulted in a highly significant G´ increase by 42%. The mildly acidic environment also induced a significant decrease of hydrogel stiffness after 210 h, which was attributed to hydrolytic gel degradation and accompanying water uptake (Figure 3-S4). ADH treatment with chemical reduction (by $NaCNBH_3$) prevented hydrogel destabilization which indicates a beneficial effect of the reduction step under slightly acidic conditions. Since no comparable ADH-mediated effects were found in corresponding ketone-free oPNMA/COL groups, successful post-fabrication dihydrazide cross-linking of oPDMA/COL hydrogels can be assumed. As a consequence of the chemical reversibility of hydrazone formation, ADH without reduction could only mediate chemical hydrogel stabilization for a comparably short time. In contrast, an ADH treatment in presence of a reducing agent resulted in long-term stabilization. Results are in agreement with literature, where acid-catalyzed hydrazone formation and efficient hydrazone to hydrazine reduction at pH 6 were reported.[16,113] Overall, ADH-mediated increase in storage modulus was limited which can be related to the effectiveness

of the gel-forming amine-anhydride-cross-linking. Additionally, steric limitations due to short chain length of ADH might have restricted an even more efficient cross-link formation between two oPDMA moieties (Figure 3-2B), that might be further improved by using longer-chained derivatives, such as PEG dihydrazide.[128]

3.4.4 Characterization of ketone reactivity: II. pH-dependent covalent phenylhydrazine immobilization to oPDMA/COL hydrogels. Post-fabrication cross-linking results motivated a more intensive analysis of methyl ketone reactivity in oPDMA. Initially, macromer-related experiments were performed with 2,4-dinitrophenylhydrazine (DNPH), which is commonly used for detection and quantification of ketones.[106,129] The acid-catalyzed formation of DNP-hydrazones was investigated in solution with *N,N*-diethylethylenediamine(DEED)-derivatized oPDMA[115] (Figure 3-S6A-C). A bathochromic shift of the absorption maximum suggested hydrazone formation and conversion degree was adjustable by the molar ketone to hydrazine ratio (Figure 3-S6D-E). In these experiments, DNPH coupling to macromeric anhydrides can be excluded due to complete consumption of these functions upon DEED coupling and hydrolysis of unreacted residues in oPDMA^{+DEED} which reflects the situation in the cross-linked gel network. Extent of DNPH immobilization to oPDMA/COL hydrogels (oPDMA-7.5/COL (3.5%/7.5%)) was investigated after gel incubation in DNPH solutions buffered at different pHs (Figure 3-4A). Stereomicroscopic images indicated yellow coloration of oPDMA/COL hydrogels, while ketone-free oPNMA/COL control gels remained uncolored (Figure 3-4B). Color intensity indirectly correlated with solution pH, but microscopic impressions are partly biased by significant gel shrinkage at pH < 5 (Figure 3-S4). The extent of covalent hydrazone formation within the hydrogels was assessed by quantification of the bathochromic absorbance shift using the ratio $A_{405\,nm}/A_{340\,nm}$ (Figure 3-4C). Absorption characteristics of pure hydrogel matrices were comparable ($A_{405\,nm}/A_{340\,nm}$ ~ 0.4) and independent of oligomer type (oPDMA or oPNMA). DNPH incubation of oPDMA-derived gels in acidic media resulted in strongly increased absorbance ratios of up to ~ 1.0 indicating hydrazone formation. For ketone-free oPNMA-based formulations only moderately enhanced values below 0.7 were found at pH < 5. Since covalent coupling to oPNMA/COL hydrogels can be excluded, this increase was assigned to alteration of absorption properties by syneresis. Total DNPH content of derivatized hydrogels was determined in solution after acidic gel hydrolysis (Figure 3-4D, Figure 3-S4). While effective and pH-dependent DNPH immobilization was identified in oPDMA/COL hydrogels, values measured for oPNMA/COL formulations remained on control level.

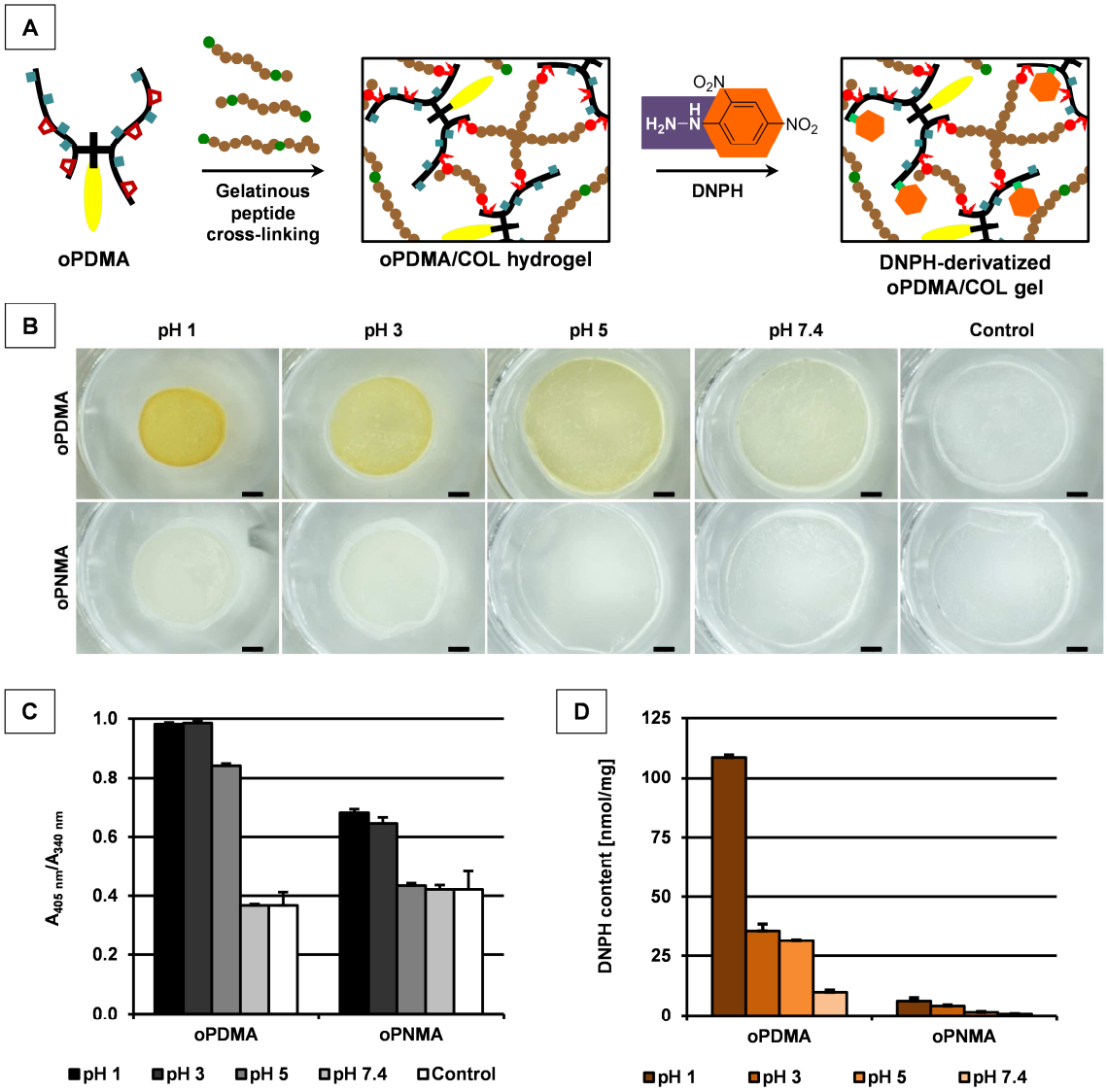

Figure 3-4. Hydrazine (DNPH) immobilization to oPxMA-7.5/COL hydrogels (3.5%/7.5%) in dependence on medium pH. (A) Schematic illustration of DNPH immobilization to pre-fabricated oPDMA/COL hydrogels. (B) Stereomicroscopic images of DNPH-derivatized hydrogels (scale bars represent 1 mm). (C) Absorbance ratio (405 nm to 340 nm) as determined in derivatized hydrogels. (D) DNPH content in hydrogels as determined from gel hydrolyzates.

Altogether, increasing DNPH amounts were detected in oPDMA-derived hydrogels with decreasing media pH. Congruently, the degree of covalent immobilization (hydrazone formation with methyl ketones of oPDMA) also increased which is in agreement with literature data.[106,129] In hydrogel post-fabrication derivatization experiments, comparatively low molar ketone to hydrazine ratios (1.0 to 2.4) were used. Taking data on hydrazone formation with soluble

oPDMA^{+DEED} into account, which required far higher molar ratios for quantitative conversion (Figure 3-S6E), the extent of hydrazone conversion can be further improved when gel formulations with higher ketone contents are used. Nevertheless, maximum DNPH content of oPDMA/COL gels at pH 1 corresponds to 61% of overall presented hydrazine which suggests effective DNPH retention from solution. Indeed, strong acidic conditions are not favored for post-fabrication modifications in view of morphological hydrogel changes and low biocompatibility as well as reduced stability of biologically active macromolecules at these conditions. Compatibility with mildly acidic conditions (pH 4-6), however, was confirmed for a variety of relevant ECM compounds, such as HA[40], transforming growth factor beta (TGF-β)[130], fibroblast growth factor (FGF)[131], vascular endothelial growth factor (VEGF)[132], platelet derived growth factor (PDGF)[133] and bone morphogenetic protein 2 (BMP-2)[134]. In order to put the results in further perspective, the value of DNPH for determination of maximum ketone reactivity is questionable as the dinitrophenyl group reduces hydrazine nucleophilicity and therefore reactivity.[106] Even though higher conversion rates can be expected for aliphatic hydrazines,[50] their difficult implementation on biomolecules is a considerable drawback.[135]

3.4.5 Characterization of ketone reactivity: III. Triple-tunable covalent hydrazide coupling to oPDMA/COL hydrogels. Hydrazides are promising functionalities for covalent immobilization to oPDMA/COL gels under mild conditions as indicated by ADH cross-linking experiments (Figure 3-2B). Furthermore, dihydrazide coupling to carboxylic acids[40] and hydrazinolysis of corresponding esters[16] or amides[136] have been reported as convenient strategies to introduce these functional groups to certain molecules. In order to determine the potential of hydrazide immobilization to oPDMA-derived hydrogels, a stable fluorescent hydrazide (AFH) with high detection sensitivity was used (Figure 3-5A). Experiments were predominantly focused on an environmental pH of 7.4 to fully maintain hydrogel integrity and simulate physiological conditions (Figure 3-S4A). Fluorescence micrographs of AFH-incubated hydrogels (oPxMA-5/COL (5.5%/15%)) clearly indicated stronger fluorescence intensity in oPDMA samples for AFH concentration above 10 µg/mL as compared to ketone-free oPNMA control group (Figure 3-5B). This suggests low unspecific AFH immobilization (oPNMA controls) and concentration-dependent covalent AFH immobilization to oPDMA/COL hydrogels. Hydrogel cross-sections further demonstrated homogeneous AFH distribution in all groups (Figure 3-S7A). Cross-linked matrices showed no considerable autofluorescence which enabled a direct AFH quantification in

derivatized hydrogels (Figure 3-5C). Results confirmed the microscopic impressions and a linear correlation between solution concentration of AFH and its content in washed oPDMA/COL hydrogels was found. Release experiments at pH 7.4 indicated effective and loading-dependent AFH release from derivatized oPDMA/COL hydrogels over 7 days in micromolar range (Figure 3-5D). Relative hydrazide release from these matrices was almost independent of the initial loading (Figure 3-5E) which indicates that AFH was released by hydrazone hydrolysis. Significant AFH loading was even detected after 7 days suggesting further release potential over a longer period of time (Figure 3-S7B). Influence of pH on AFH immobilization to hydrogels was investigated with a selected AFH solution concentration of 10 µg/mL (Figure 3-S8). In comparison with pH 7.4, reduced AFH contents were recorded in oPDMA groups at pH 3.5 to 5, but increased values were found at pH 3. This group, however, might have been biased by hydrogel syneresis and therefore enhanced fluorescence intensity due to gel shrinkage (Figure 3-S4). In order to investigate the tunability of AFH immobilization by the third parameter of keto group content of the hydrogel, selected oPDMA/COL formulations with varying ketone contents were analyzed at pH 7.4. Fluorescence micrographs indicated composition-dependent differences with the strongest fluorescence signal for formulation oPDMA-7.5/COL (3.5%/7.5%) (Figure 3-5F). The amounts of AFH in the hydrogels correlated with their theoretical ketone contents (Figure 3-5G).

Taken together, significant covalent AFH immobilization to ketone-containing hydrogels was shown which was tunable by matrix composition, available AFH amount and medium pH. AFH coupling performed best at pH 7.4. Although hydrazide to hydrazone conversion is generally acid-catalyzed,[16] McKinnon et al., for example, also found rapid formation of bis-aliphatic hydrazones at pH 7.4.[50] A catalytic effect of aniline on hydrazone formation at neutral pH as described in literature[137] was not investigated here, but might be a promising strategy to further improve hydrazide immobilization potential of oPDMA/COL hydrogels under physiological conditions. In accordance with kinetic studies[50,138], our findings demonstrate, that the chemical equilibrium of hydrazone formation in oPDMA-containing hydrogel bulk can be shifted by both hydrazide and ketone concentration. The latter parameter is highly relevant in terms of cost-efficient hydrogel decoration with hydrazido-functionalized bioactive components and proposes high loading rates when ketone-rich hydrogels are employed. This in turn can be realized as the incorporation of DAAm in oligomers and ultimately in oPDMA-based hydrogels did not impair

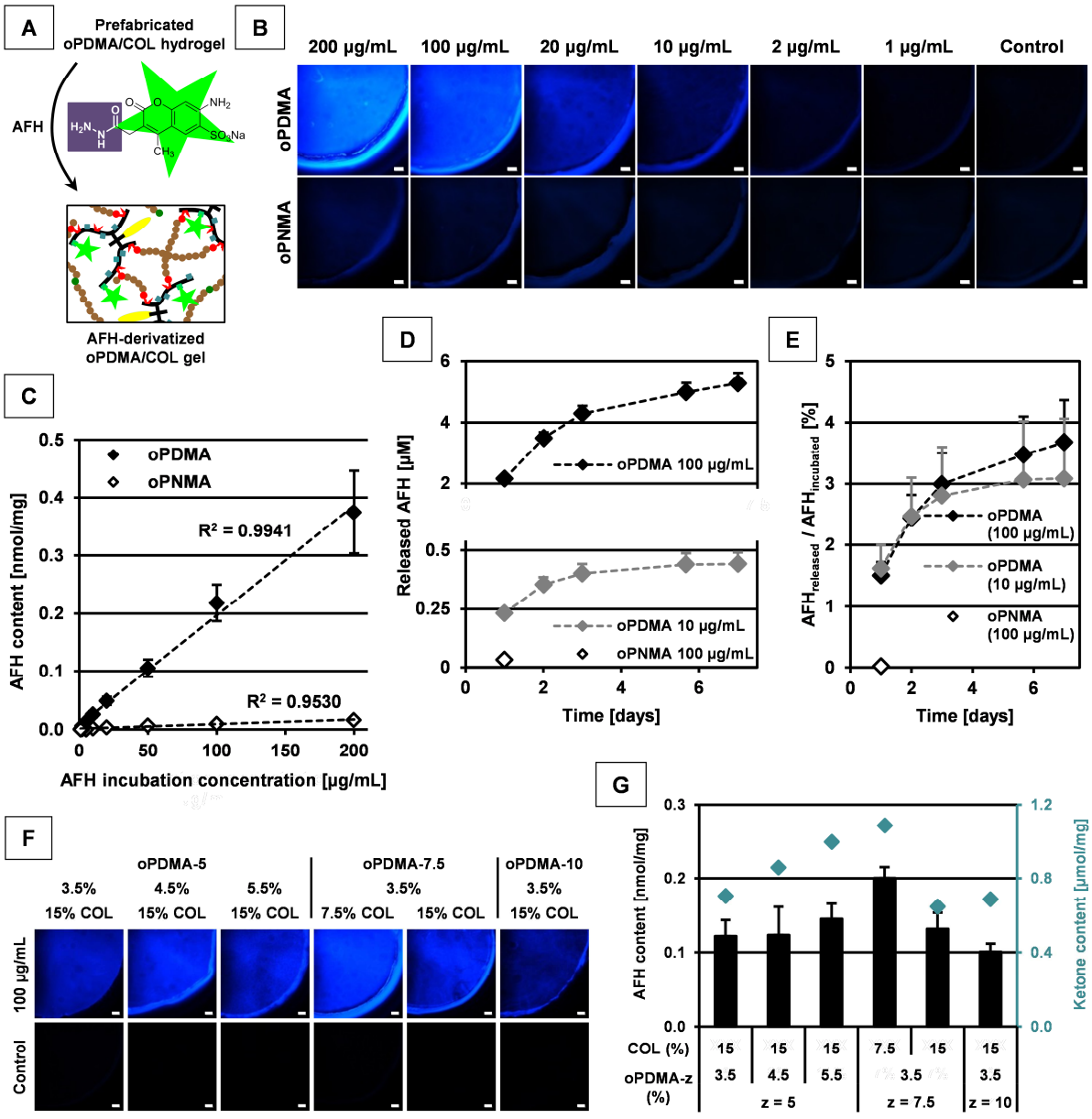

Figure 3-5. Hydrogel derivatization with fluorescent hydrazide (AFH). (A) Schematic illustration of AFH immobilization to oPDMA/COL hydrogels. (B-E) Characterization of concentration-dependent AFH coupling to oPxMA-5/COL hydrogels (5.5%/15%) at pH 7.4 and release in PBS. (B) Fluorescence micrographs, (C) AFH content as determined in derivatized hydrogels post washing and (D-E) AFH release from derivatized hydrogels at pH 7.4 over 7 days. (F-G) Characterization of hydrogel composition-dependent AFH immobilization to oPDMA/COL gels at pH 7.4. (F) Fluorescence micrographs and (G) AFH content (post washing) as determined in derivatized hydrogels. AFH contents in (C) and (G) are corrected for hydrogel autofluorescence as measured for AFH-free controls. Scale bars represent 250 µm.

material cytocompatibility, but rather improved cell adhesion and proliferation. However, adjustment of the hydrogel ketone content while maintaining the general physico-chemical hydrogel properties is limited in this approach, because the ketone content of the oligomer inversely correlated with anhydride content and reactivity (Table 3-1). Furthermore, macroscopically inhomogeneous gels were obtained for high oligomer concentrations or high-MA oligomers (Figure 3-S2, Figure 3-S3). The reversibility of hydrazone formation caused significant loading-dependent AFH release and can be generally used for controlled release applications.[16,107] Here, released AFH amounts at pH 7.4 ranged within 0.2-6 µM which meets or even exceeds the physiologically relevant range for several growth factors and chemokines, such as TGF-β[77,139], BMP-2[139] and SDF-1α[139,140], which are all biologically active in nanomolar concentrations.

3.4.6 Effective hydrazido-GAG immobilization to oPDMA/COL gels. As a biologically relevant molecule, hydrazido-functionalized HA was synthesized and exemplarily coupled to ketone-containing hydrogels (Figure 3-6A). Hydrazide functionalities were introduced to thermally degraded HA by ADH coupling to the C6-carboxyl groups of the D-glucuronic acid units (hyHA, M_w ~ 40 kDa, $Đ_M$ = 2.1). ^{13}C NMR analysis of hyHA derivative demonstrated the appearance of an additional C=O peak at 175.2 ppm as well as two methylene-derived signals at 25.7 ppm and 34.0 ppm, that all were referred to ADH moieties (Figure 3-6B). Typical ADH-related methylene signals in ^{1}H NMR spectra (1.55 ppm and 2.14 ppm) further indicated successful hydrazide functionalization and allowed for determination of the degree of substitution (DS = 0.1) (Figure 3-S9). For analytical purpose, the fluorescent label ATTO 633-NH_2 was coupled to reducing termini of hyHA to yield ATTO-hyHA and an ATTO content of 0.003 µg/mg suggested sufficient detectability of the HA derivative.

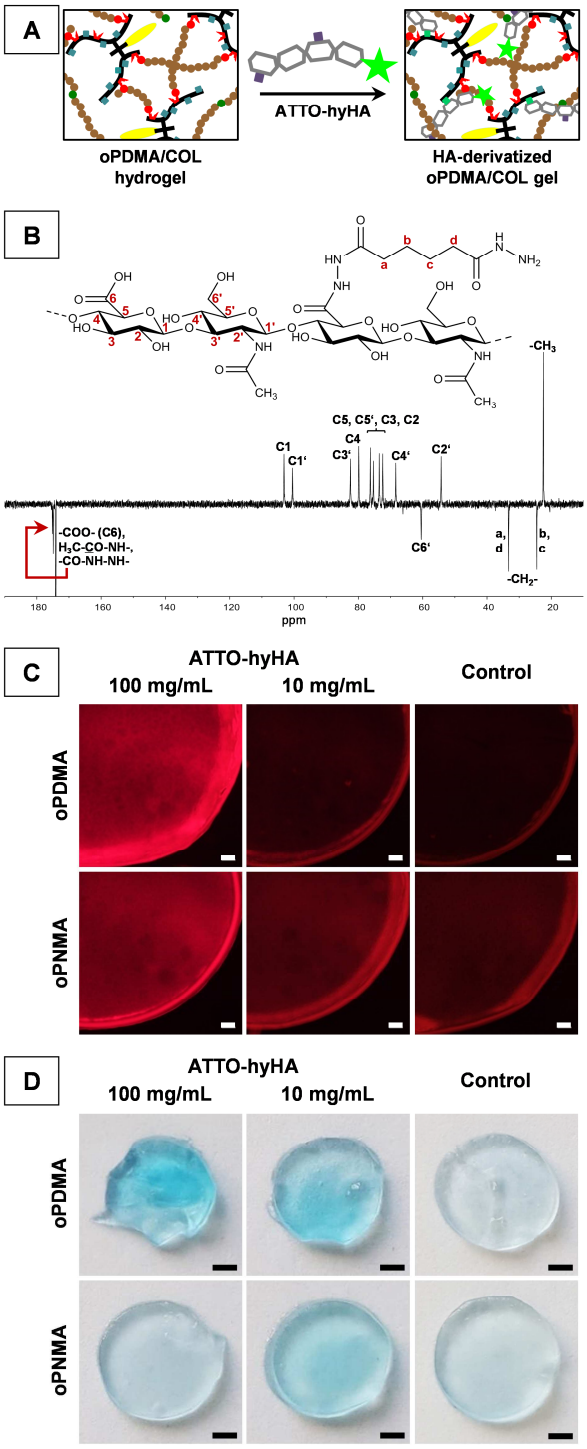

Figure 3-6. Hydrogel derivatization with fluorescent hydrazido-functionalized HA (ATTO-hyHA). (A) Schematic illustration of ATTO-hyHA immobilization to oPDMA/COL hydrogels. (B) ^{13}C-APT NMR spectrum of hydrazido-modified HA (hyHA). (C-D) Characterization of ATTO-hyHA immobilization to oPxMA-7.5/COL hydrogels (3.5%/7.5%) at pH 7.4. (C) Fluorescence micrographs of derivatized hydrogels (scale bars represent 250 µm) and (D) photographic images of derivatized hydrogels after toluidine blue staining (scale bars represent 1 mm).

Based on the results of AFH immobilization (Figure 3-5) and literature reports[50,138], ATTO-hyHA coupling to cross-linked hydrogels was performed under specifically selected conditions, i.e. incubation of ketone-rich oPDMA-7.5/COL (3.5%/7.5%) gels in highly concentrated hydrazide solutions (100 mg/mL) at pH 7.4 for 20 h. Fluorescence micrographs offered increased and concentration-dependent fluorescence intensity in oPDMA group, when gels were supplemented with ATTO-hyHA (Figure 3-6C). Cross sections further demonstrated homogeneous distribution of the immobilized hydrazido-HA derivative (not shown). In comparison, oPNMA-based gels generally showed higher autofluorescence, but no significant ATTO-hyHA accumulation was seen after incubation and washing due to the absence of reactive moieties. Toluidine blue staining of derivatized hydrogels was performed to directly visualize immobilized HA independent of the ATTO label (Figure 3-6D). Color intensity was strongly increased in ATTO-hyHA-incubated oPDMA/COL hydrogels, which illustrated the presence of HA in the gels and confirmed the findings from fluorescence microscopy. Taken together, the principal applicability of the presented covalent hydrogel functionalization concept toward bioconjugation of hydrazido-functionalized aECM was shown.

3.5 CONCLUSION

The presented dual-functional oligomers with reactive anhydrides as one key functionality show high cross-linking reactivity with gelatinous peptides. Rigid two-component hydrogels with adjustable composition and physico-chemical properties were formed. Currently, the introduction of the co-monomer DAAm in hydrogel-forming building blocks did not only raise any concerns on oPDMA/COL hydrogel cytocompatibility, but yielded formulations that showed superior cell-material interactions as compared to established oPNMA/COL gels. Hydrazide- und hydrazine-reactive methyl ketones were incorporated to oPDMA as second functionality. Their reactivity in cross-linked oPDMA/COL hydrogels opens potential for versatile post-fabrication functionalization strategies. The successful decoupling of covalent hydrogel modification from cross-linking reaction is a key property enabling efficient functionalization while maintaining pre-determined material properties. Triple-tunability of hydrazide immobilization holds promise for adjustable and cost-effective hydrogel modification. Functionalization with biologically active aECM components under physiologically relevant conditions enables engineering of biomimetic hydrogels and the reversibility of hydrazone formation offers potential for controlled release of immobilized derivatives.

3.6 ACKNOWLEDGEMENTS

Financial support by the German Research Council (DFG SFB/Transregio 67, projects A1, A2 and Z3) is gratefully acknowledged. Gelita AG generously provided Collagel® for this study. Confocal laser scanning microscopy of cell-laden hydrogels was performed at a Leica TCS SP5 STED with the kind assistance of Barbara Goettgens (Faculty of Biosciences, Pharmacy and Psychology, Leipzig University). We also thank Lothar Hennig (Department of Organic Chemistry, Leipzig University), Katharina Schwabe, Jonas Steiner and Saskia Krusch (Institute of Pharmacy, Leipzig University). L.H. and J.S. contributed to ^{13}C-NMR analysis of oPDMA macromers. K.S. contributed to direct contact cytocompatibility studies and S.K. assisted during DNPH immobilization to hydrogels.

3.7 SUPPORTING INFORMATION

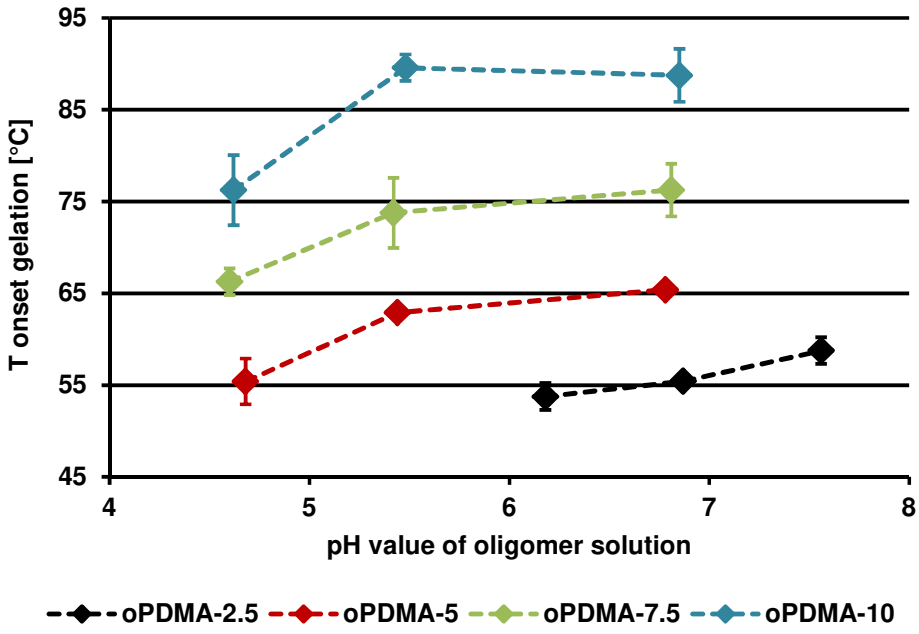

Figure 3-S1. Temperature responsiveness of oPDMA macromers. Phase transition temperature of aqueous macromer solutions containing 200 mM NaCl as determined by oscillation rheology at different pH values. The transition temperature increased with MA content of the oligomers due to the hydrophilicity of the carboxylate groups formed from the anhydrides upon dissolution of the oligomers in water. The interaction of the carboxylate groups with water is pH-dependent and reduced in acidic environments, which explains the drop in transition temperature at pH < 5.

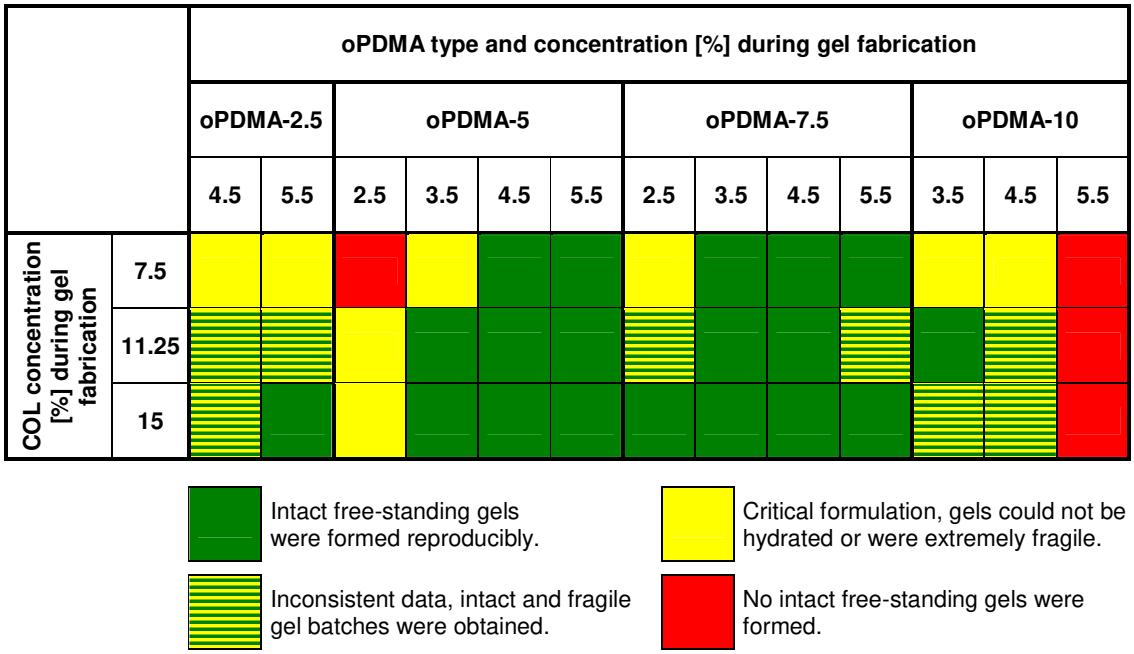

Figure 3-S2. Overview of investigated hydrogel formulations. Data was obtained from different experiments and color codes indicate hydrogel quality based on processability of constituent components, amount of leachables as well as general gel stability. Number of intact hydrogels generally increased with increasing MA content (oPDMA-2.5 to oPDMA-7.5), but rapid cross-linking in oPDMA-10/COL formulations due to high anhydride reactivity resulted in macroscopically inhomogeneous matrices.

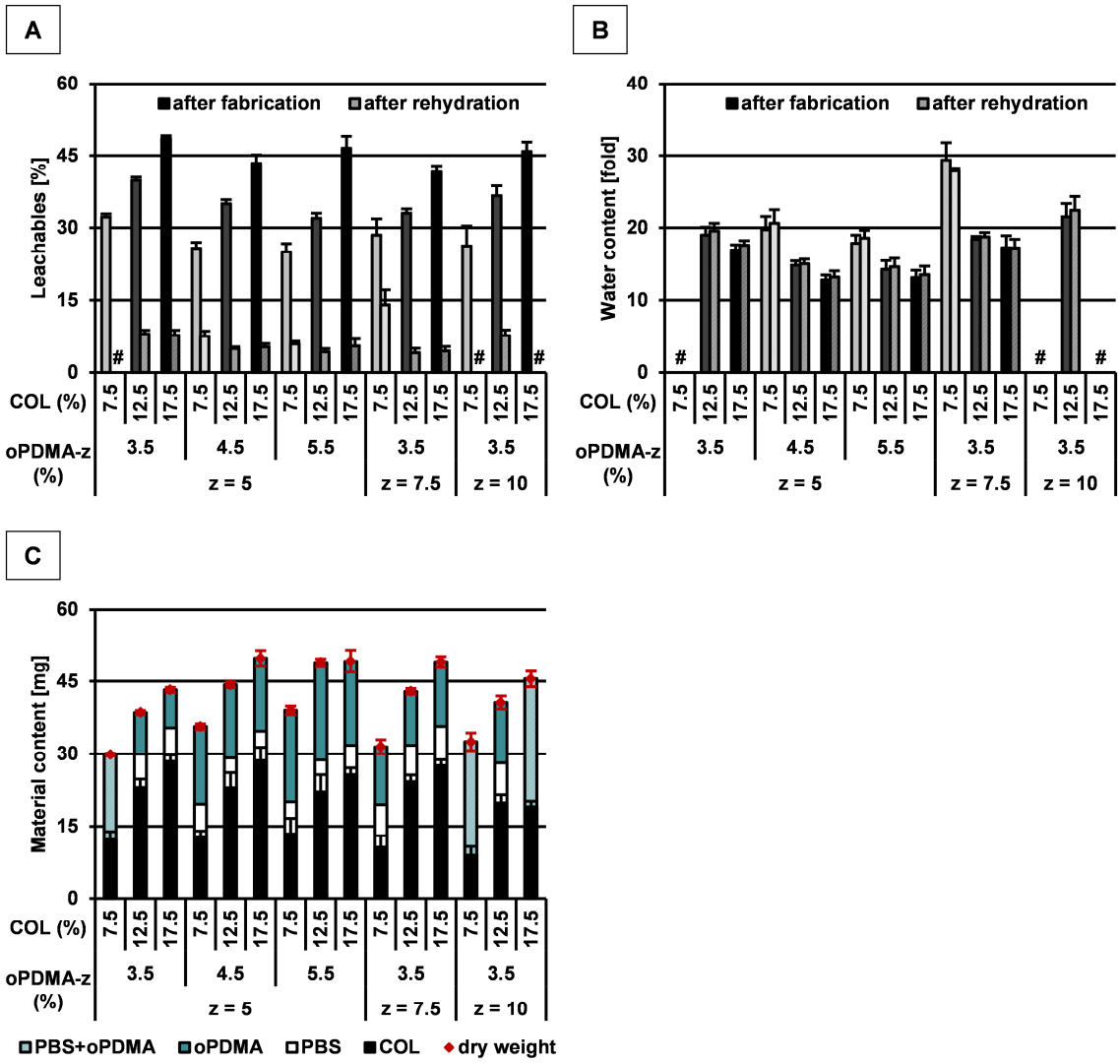

Figure 3-S3. Physico-chemical properties of a selected set of oPDMA/COL hydrogels. (A) Leachables and (B) water content of fabricated gels after hydration and after rehydration of freeze-dried gels (n = 5). (C) Chemical composition of hydrogels as determined by HPLC analysis (n = 5 (dry weights), n = 4 (COL content)). Label '#' refers to fragile formulations which were not analyzable due to high leachables and/or excessive swelling as a consequence of unstable and insufficiently cross-linked hydrogels. For formulations with low anhydride contents (3.5% oPDMA-5), oPDMA incorporation was reduced which is in line with low cross-linking degree and increased swelling (some formulations were even completely dissolved). For the highly reactive oPDMA-10 derivative, only low oligomer concentrations yielded processable hydrogels.

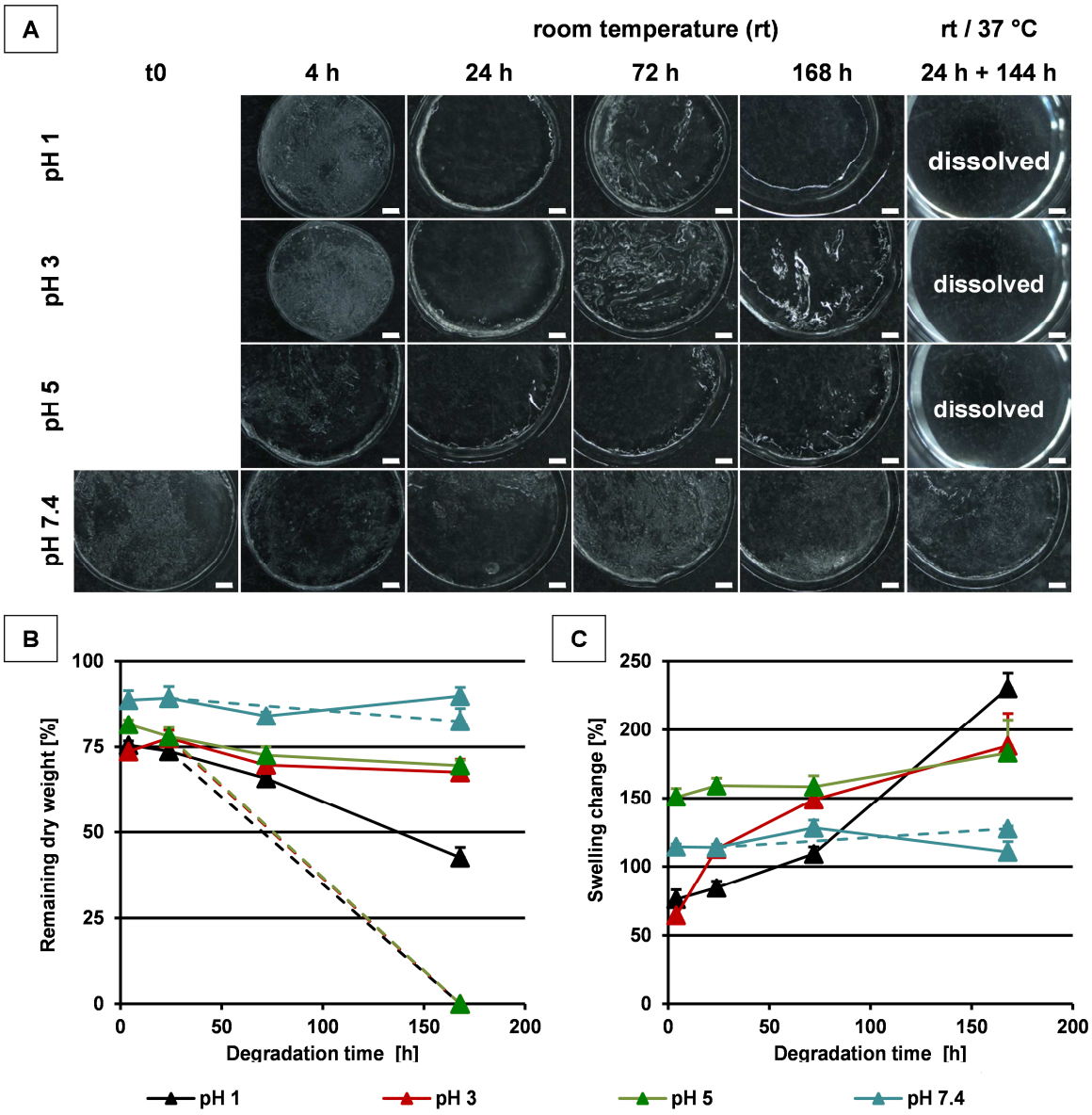

Figure 3-S4. pH-dependent degradation of a oPDMA-7.5/COL (3.5%/15%) hydrogel. (A) Gel morphology, (B) remaining dry weight and (C) swelling behavior in buffered media of different pH at room temperature (rt) (7 d, continuous lines) or at rt for 24 h followed by a 6 day period at 37 °C (dashed lines). The results confirmed hydrogel stability under physiological conditions, while comparably fast degradation of the matrices was observed in acidic buffers due to sensitivity toward acidic hydrolysis and osmolarity. The initial (4 h) reduction in dry weight was in accordance with hydrogel leachables corrected for a certain amount of buffer salts that remained in the freeze-dried gels. Swelling behavior correlated with the observed hydrogel shrinkage (pH 1, pH 3) or the reduced medium osmolarity (pH 5). After 7 days, significant degradation was observed in the acidic media and a correlation of medium acidity with weight loss and swelling was found. The results indicated pH-dependent hydrolytic amide cleavage of the cross-linked matrices.

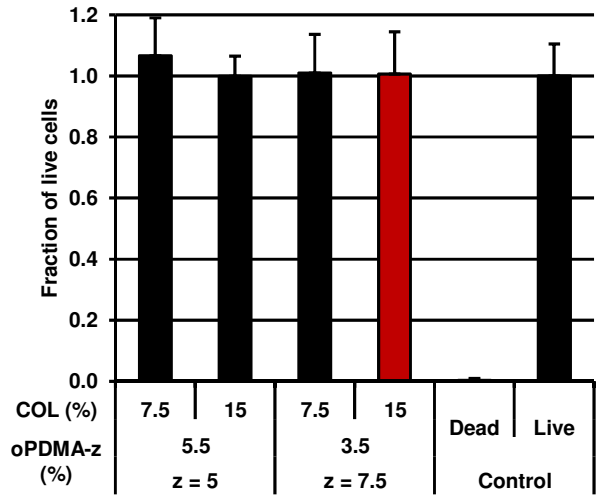

Figure 3-S5. Indirect cytocompatibility assay (LIVE/DEAD) of medium extracts tested on L929 fibroblasts after 24 h incubation (n = 5). For extracts which generally contained 4-8% hydrogel leachables, fractions of live cells in the range of the live control were found. The absence of toxicity was also confirmed for the oPDMA-7.5/COL hydrogel (3.5%/7.5%) formulation which was characterized by increased leachables (14%). The cytocompatibility of oPDMA/COL hydrogel extracts was further assessed by an Alamar Blue assay for a representatively selected formulation (red bar).

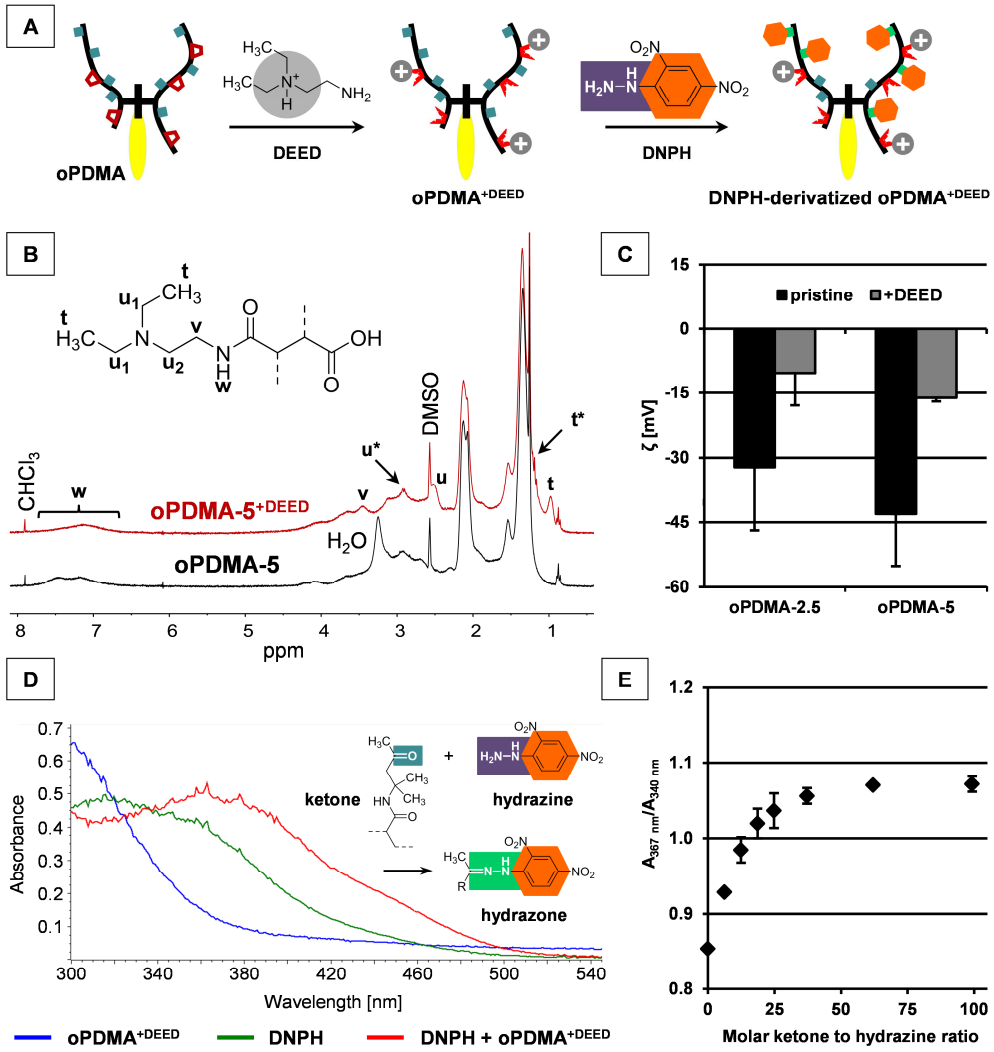

Figure 3-S6. Hydrazine (DNPH) immobilization to acid-soluble oPDMA macromer derivatives. (A) Schematic illustration of (B-C) oPDMA functionalization with DEED and (D-E) DNPH coupling to oPDMA^{+DEED}. (B) Representative ^{1}H NMR spectra of DEED-modified oPDMA and the corresponding pristine macromer. Label 'v' in oPDMA-5^{+DEED} spectrum (-CH_2-NH-) indicates covalent DEED functionalization and label '*' corresponds to protonated DEED moieties. (C) Zeta potential of colloidal dispersions as prepared from pristine and DEED-derivatized oPDMA macromers (n = 5). Increased values in the oPDMA^{+DEED} groups demonstrated successful introduction of positive charges by DEED into the macromer structure. (D) Representative UV/Vis absorption spectra of oPDMA-7.5^{+DEED} (30 mg/mL), DNPH (0.036 mg/mL) and DNPH+oPDMA-7.5^{+DEED} (0.036 mg/mL + 3 mg/mL) solutions at pH 1. The bathochromic shift of the absorption maximum in DNPH+oPDMA-7.5^{+DEED} (red curve) demonstrated DNP-hydrazone formation. The intersect of the DNPH and DNPH+oPDMA-7.5^{+DEED} spectra at ~ 340 nm indicated that only DNP residues contribute to the signal which allowed for DNPH quantification independent of chemical changes to the hydrazine group at pH 1. In combination with the absorption maximum of the DNP-hydrazone (367 nm), a quantitative estimation of the extent of hydrazone formation is enabled in solution using the absorbance ratio $A_{367\ nm}/A_{340\ nm}$ (spectrophotometer) or directly in derivatized hydrogels ($A_{405\ nm}/A_{340\ nm}$, plate reader). (E) Absorbance ratio $A_{367\ nm}/A_{340\ nm}$ of DNPH solutions supplemented with different oPDMA-5^{+DEED} amounts. The ratio was enhanced with increasing macromer concentration and plateaued for ketone to hydrazine ratios of above 60 which indicated the need of high ketone excess to shift the chemical equilibrium toward hydrazone formation.

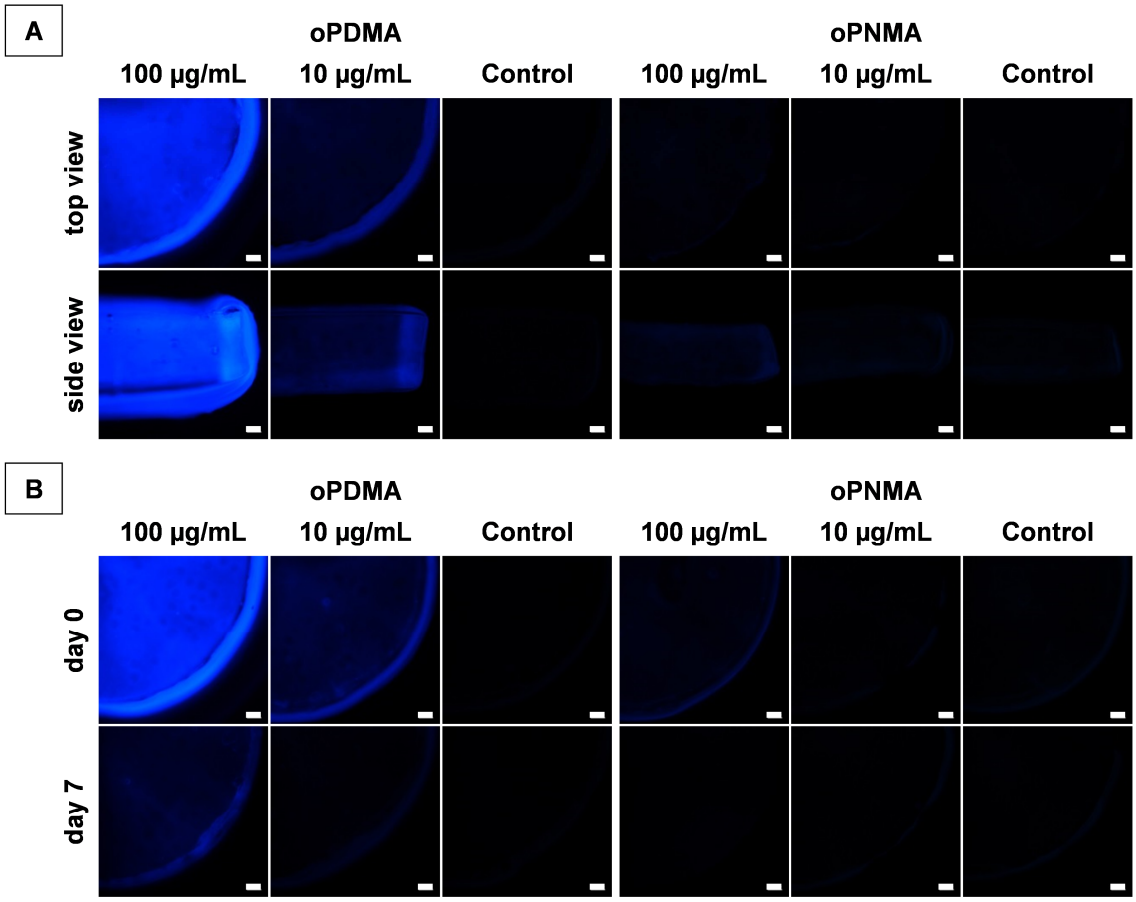

Figure 3-S7. Homogeneity of the AFH immobilization to oPxMA-5/COL (5.5%/15%) hydrogels and microscopic monitoring of the AFH release. (A) Fluorescence micrographs of selected AFH-derivatized hydrogels. The homogeneous fluorescence intensity in gel top view and in side view of gel cross sections demonstrated an even distribution of immobilized AFH. The higher fluorescence intensity on the gel boundaries is attributed to optical refraction effects as the extent of this phenomenon was dependent on the surface texture. (B) Fluorescence micrographs of AFH-derivatized hydrogels before (day 0) and after 7 days of AFH release. Reduction of the fluorescence intensity in derivatized oPDMA/COL hydrogels over time revealed significant but not yet completed release of covalently immobilized AFH within 7 days. Scale bars represent 250 µm.

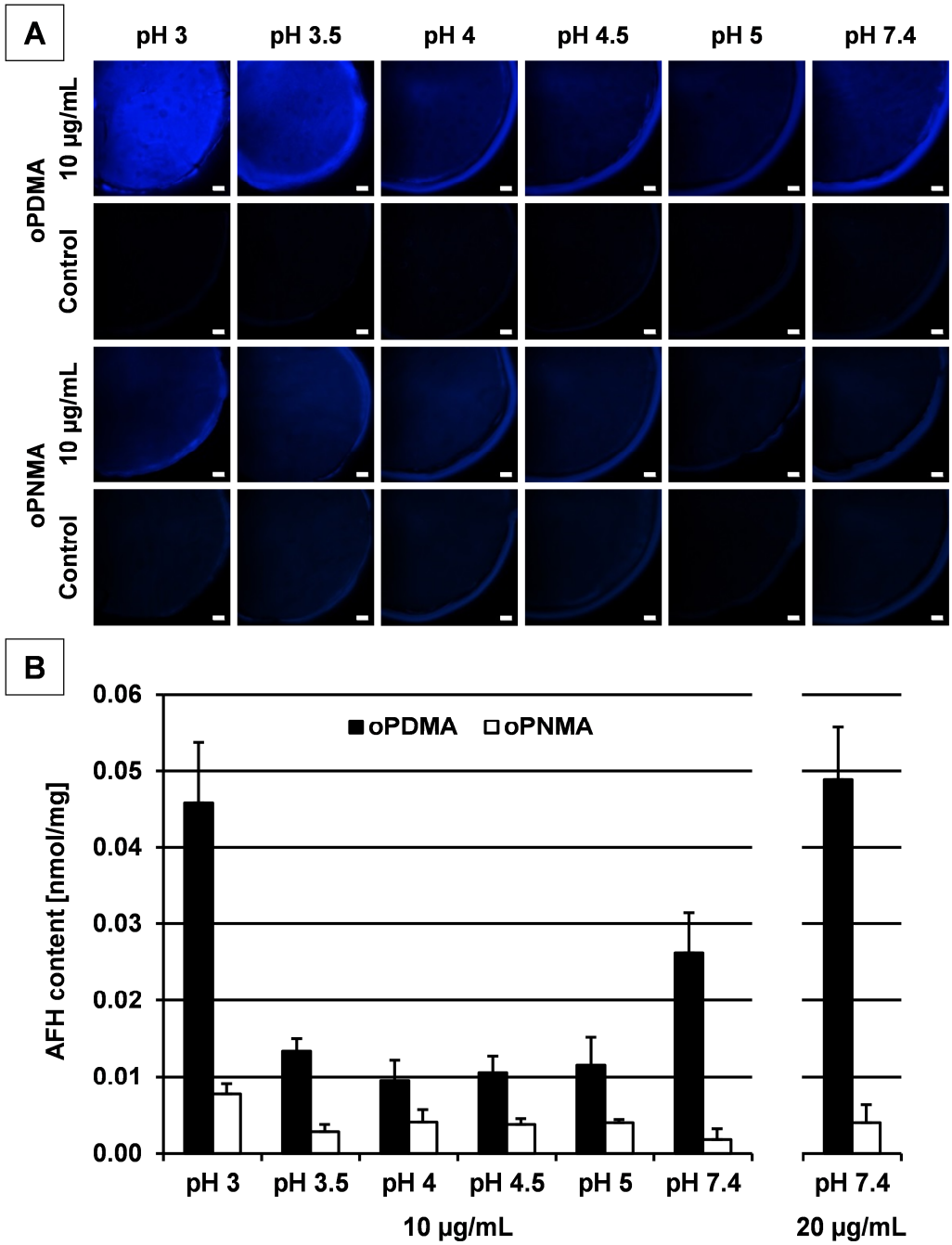

Figure 3-S8. Characterization of pH-dependent AFH immobilization (10 µg/mL) to oPxMA-5/COL (5.5%/15%) hydrogels. (A) Fluorescence micrographs and (B) AFH content as determined in derivatized hydrogels. Results of 20 µg/mL groups at pH 7.4 are shown for comparison. Scale bars represent 250 µm. The label 'control' in (A) refers to hydrogels that were incubated with plain buffer at corresponding pH. These groups enabled a correction for hydrogel autofluorescence when AFH content of the gels was calculated (B). Based on the observations that higher fluorescence intensities are observed not before pH values below 3.5 and considering that gel integrity is strongly affected in a pH-dependent manner below pH 5, we conclude that AFH immobilization is best performed at physiological pH.

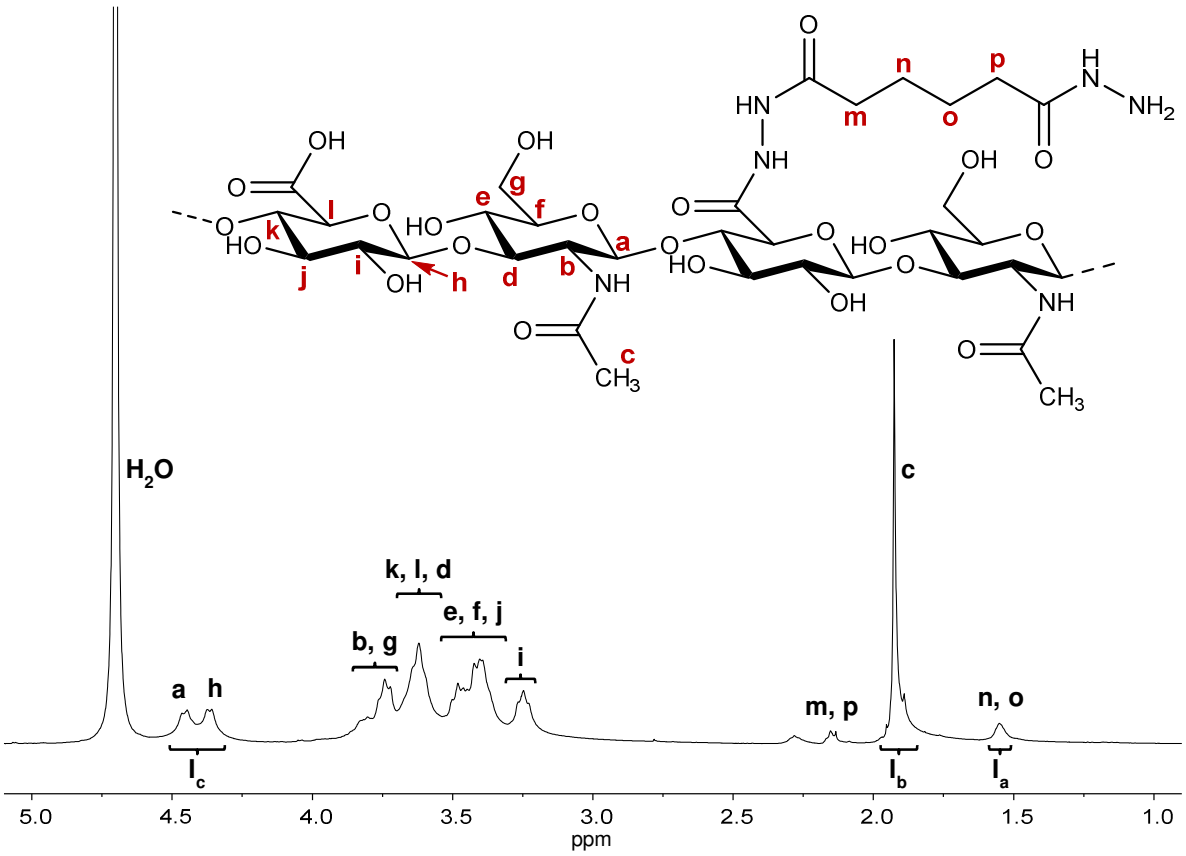

Figure 3-S9. ^{1}H NMR spectrum of hydrazido-functionalized HA (hyHA) as used for ATTO labeling. Methylene proton signals at 1.55 ppm and 2.14 ppm indicated ADH coupling to C6-carboxyl groups and thereby successful hydrazide functionalization of HA. I_a-I_c represent the integrals used to determine hyHA composition: While I_b/I_c (~ 1.5) served as HA-related control ratio, degree of substitution (DS) was calculated from ratio I_a/I_b (DS = 0.1).

3.8 SPECIFICATION OF THE AUTHORS' CONTRIBUTIONS TO:

C. Kascholke, T. Loth, C. Kohn-Polster, S. Möller, P. Bellstedt, M. Schulz-Siegmund, M. Schnabelrauch, M.C. Hacker, Dual-Functional Hydrazide-Reactive and Anhydride-Containing Oligomeric Hydrogel Building Blocks, *Biomacromolecules* **2017**, 18, 683-694, doi:10.1021/acs.biomac.6b01355.

Christian Kascholke (First Author)

Manuscript writing, oligomer synthesis and characterization, hydrogel fabrication, determination of ketone reactivity in oligomers and hydrogels (ADH cross-linking, immobilization of DNPH, AFH and ATTO-hyHA), thermogelation, degradation study

Tina Loth

Optimization of oligomer synthesis, establishment of hydrogel fabrication procedure, physico-chemical hydrogel characterization (stiffness: rheology, cross-linking degree: TNBS assay, composition: water content/HPLC), indirect cytocompatibility (LIVE/DEAD assay)

Caroline Kohn-Polster

Indirect cytocompatibility (Alamar Blue assay), direct contact experiments with hASC

Stephanie Möller

Synthesis of hydrazido-functionalized and fluorescently labeled HA (ATTO-hyHA)

Peter Bellstedt

NMR analysis of functionalized HA (^{1}H, ^{13}C)

Michaela Schulz-Siegmund

Cell culture know-how and access to analytical equipment, advice for experimental design and discussion

Matthias Schnabelrauch

Conceptual design and equipment of/for synthesis and characterization (GPC) of functionalized HA

Michael C. Hacker (Corresponding Author)

Conceptual design of hydrogel matrix cross-linked by dual-functional oligomers, advice for experimental design, discussion and manuscript review


Christian Kascholke

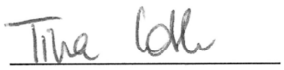
Tina Loth

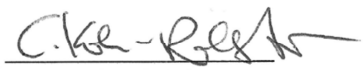
Caroline Kohn-Polster

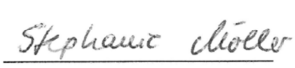
Stephanie Möller


Peter Bellstedt

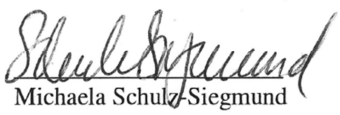
Michaela Schulz-Siegmund

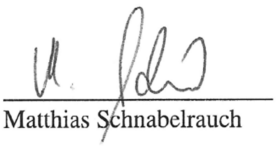
Matthias Schnabelrauch


Michael C. Hacker

CHAPTER 4

Dual Scale Porosity Adjustment of Oligomer-Cross-Linked Gelatinous Hydrogels

C. Kascholke[a,#], F. Tischer[a,#], M. Schulz-Siegmund[a,#], M. C. Hacker[a,#]

[a] Institute of Pharmacy, Pharmaceutical Technology, Leipzig University

[#] Collaborative Research Center (SFB/Transregio 67), Matrixengineering, Leipzig and Dresden

4.1 INTRODUCTION

Regenerative medicine aims at supporting the body in the healing of wounds and tissue defects through the delivery of cells, biomolecules and supporting structures to the appropriate site, independently or in synergy.[2] While the initial focus was directed to cell therapy, over time it was found that cells require a 3D biomaterial scaffold acting as cell guide and supporting template.[2,141] To this end, the scaffold should closely mimic the corresponding extracellular matrix (ECM), while material porosity was detected as crucial factor. In order to optimally support cellular ingrowth by enabling diffusion of physiological nutrients and gases to cells, and removal of metabolic waste, 100% interconnectivity is ideally required,[2,5] which means that all pores inside a material are connected to the environment.[142] Some general requirements can be drawn from the literature: The IUPAC defines three types of porosity based on the material pore size which are: macroporosity (> 50 nm), mesoporosity (2-50 nm) and microporosity (< 2 nm).[19] In context with regenerative medicine, it is often stated that a biomaterial requires macroporosity in order to allow for cell and tissue penetration.[57,143] This specification, however, is not thoroughly in accordance with the IUPAC definition, because the migration of cells is only enabled when the pore size exceeds the cell diameter by factor 5-10 which corresponds to the micrometer range.[2,144] For example, small pores of ~ 20 µm enable optimal fibroblast ingrowth, while larger pores are required for migration of hASC (20-125 µm) and cells involved in bone regeneration (100-250 µm).[145] These examples indicate that the pore structure needs to be specifically adapted to the characteristics of certain target tissue. A great variety of techniques was developed to introduce a pore structure into a biomaterial, including phase separation,[10] porogen leaching,[53,56] gas foaming,[36,146] emulsion freez-drying,[145] electrospinning,[147] direct[148,149] and indirect 3D-printing[54,150] (Chapter 5) as well as combination of different methods[2]. In that regard, dimensionally stable matrices that only swell to a low or moderate degree in physiological environment are beneficial to precisely adjust material pore structure. These materials are further accessible for common analytical methods to characterizes pore architecture and porosity, including optical methods/procedural imaging (e.g. scanning electron microscopy (SEM), micro-computed tomography (µCT)),[53,69,143,151] gravimetry[69] and mercury intrusion porosimetry (MIP)[36,37]. Especially the latter is an accurate and the most versatile method, but requires significant mechanical stability of the material.

The situation is significantly different in hydrogel matrices that can absorb from 10-20% up to thousands of times their dry weight in water.[152] This swelling which is strongly dependent on the characteristics of the surrounding medium, such as osmolality and pH, handicaps adjustment and characterization of hydrogel porosity. Hydrogels generally offer a porous architecture which is controlled by the structure of the hydrophilic polymer network, including molecular weight, cross-linking density and hydrophilicity.[153] Pores in the hydrogel network are typically nano-sized and therefore much smaller than a cell diameter. Consequently, they do not contribute to cell migration but rather control solute diffusion within the matrix.[63,154] The above listed techniques can generally be used to introduce macroporosity into a hydrogel matrix, but their overall low mechanical stability has to be considered and limits porogen-leaching approaches.[59] In addition, high sensitivity of hydrogel toward the environmental conditions may also reduce applicability of methods involving organic solvents and foaming agents. The high swelling degree could further result in insufficient removal of toxic additives.[155] To this end, freeze-drying is the most widely used method to generate a porous hydrogel structure under mild conditions by using ice crystals as porogen.

The main challenge in porosity assessment of hydrogel matrices is their characteristic swelling behavior together with their low mechanical stability.[7] To this end, determination of porosity in the (freeze-)dried state is generally the most valid method, but it is questionable to what extent the obtained results represent the situation in the swollen state.[156] Although MIP is a rather accurate technique for porosity determination of a porous solid, it cannot be applied for porosity determination in the hydrogels as the applied pressure likely leads to the rupture of scaffold during the analysis.[157] Nevertheless, several analytical methods have been established to characterize hydrogel porosity in the swollen state, but only three techniques were reported for direct determination, i.e. laser scanning microscopy,[91] magnetic resonance microscopy[157] and helium pycnometry[158]. Most methods are based on an indirect porosity assessment from physico-chemical hydrogel properties, such as swelling behavior and mechanics. Four important swelling parameters have been used to define the network structure of hydrogels: I) mass and volume swelling ratio, II) polymer volume fraction in swollen state, III) number average molecular weight between cross-links (M_c) and IV) network mesh size (ξ) (Figure 4-1). While parameters I and II can be determined by swelling experiments, III make use of the equilibrium swelling theory.[13,82] Network mesh size (IV) can be calculated from storage modulus by application of the rubber elasticity theory which holds true when a correlation between hydrogel stiffness and the

number of cross-links is found.[83] Otherwise, calculation of the molecular weight between two reactive functionalities in the macromer structure might be a rough estimation of ξ.[90] Further indirect methods characterize hydrogel porosity by diffusivity of labeled molecular probes (e.g. fluorescein-labeled dextran)[7] or model proteins (e.g. BSA or IgG)[57,83]. Finally, functional analysis of matrix porosity by investigation of cell migration ability in cell culture experiments serves as the best indirect method in order to characterize the regenerative potential of a biomaterial.[69]

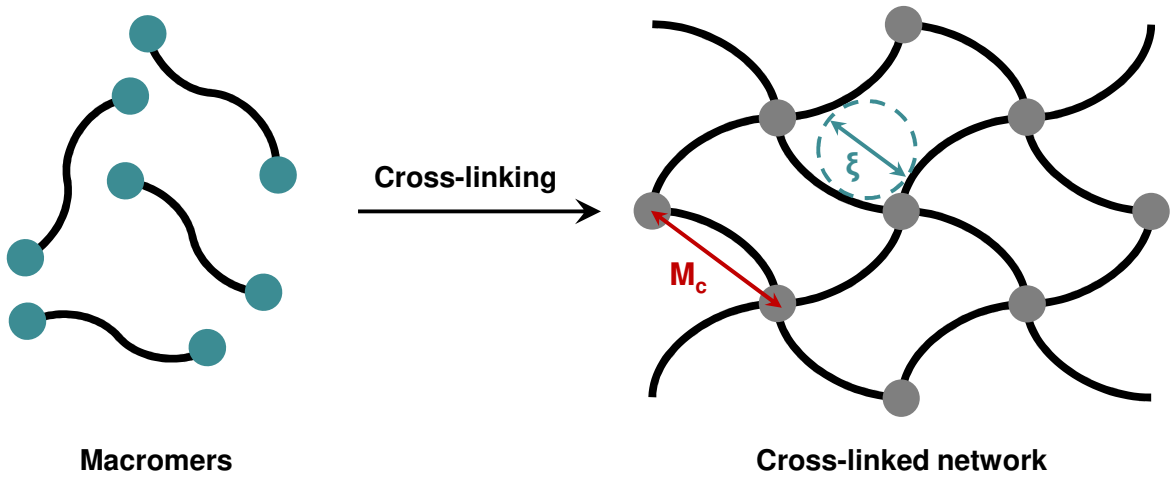

Figure 4-1. Schematic illustration of relevant network parameters of a cross-linked hydrogel network. The matrix is composed of oligo- or polymeric chains (black lines) cross-linked via reactive sites (turquois dots). M_c represents the number average molecular weight between two adjacent cross-links which is determined by the cross-linking degree. ξ represents the mesh size of the network indicating the distance between consecutive cross-linking points. Modified according to Zhu et al.[82]

We have established two hydrogel platforms consisting of anhydride-containing macromers (oPNMA or oPDMA) that covalently cross-link gelatinous peptides (Chapter 3).[90–92,95,96,98,115] As we aimed at developing flexible material platforms, the previous focus was directed toward physico-chemical characterization and the illustration of versatile material tunability. In that regard, a porous structure was detected and a correlation between hydrogel composition and pore size was found.[91] However, cell culture experiments indicated a dense cell layer on the gel surface, while only marginal cell migration was detected. Although pores of appropriate size (20-100 µm) were found,[145] this observation was attributed to inadequate pore distribution, because only small pores were detected in the outer layers of the gel that the cells have to pass first.

To this end, it is the purpose of this study to increase porosity of the established cross-linked hydrogel platforms. Previously, different attempts were performed to adjust porosity of oPNMA-derived matrices.[92] However, pore generation into pre-fabricated gels by using a custom-designed punch did not result in improved cell migration and the introduction of unidirectional porosity can be noted as significant disadvantage of this approach. As salt-leaching is generally applicable in aqueous solutions,[55] this strategy looked promising, but the resulting matrices were extremely fragile. In another attempt, cross-linked hydrogel matrices were fabricated in presence of poly(ethylene glycol) (M_n = 8000 Da, P8k) which can generate pores due to liquid-liquid phase separation with the macromer mixture.[57] The applied concentrations of 1.25% and 2.5% (w/v) were able to affect the final macroporous hydrogel structure in a concentration-dependent manner, but pore size was not significantly increased. Due to the promising results, this strategy was expanded in this work by application of enhanced P8k concentrations of 2.5-5% (w/v). A second approach was based on the previously found correlation between hydrogel pore size and molecular weight of the applied gelatinous component (COL (11 kDa) or gelatin 50 Bloom) which is in accordance with the previously proposed theory (Figure 4-1).[92] In order to further enlarge the structure of the cross-linked network, hydrogel fabrication with a higher molecular weight gelatin (160 Bloom, G160) was intended. This type of gelatin has previously been processed into oPNMA-cross-linked microparticles.[91,92] Applicability of both strategies was assessed regarding processability of the precursor mixtures and the potential to fabricate stable hydrogels matrices. Typical physico-chemical hydrogel characteristics were determined. Hydrogel stability was characterized by the fraction of leachables components and by cross-linking degree, swelling behavior was assessed by water content and hydrogel stiffness was determined rheologically. Although hydrogel porosity was not directly assessed, it was attempted to draw valid conclusions from the physico-chemical hydrogel characteristics.

4.2 MATERIALS AND METHODS

The experimental section of this chapter is integrated in Chapter 2 (section 2.3).

4.3 RESULTS AND DISCUSSION

4.3.1 Effect of P8k incorporation into COL-derived hydrogels

Anhydride-containing macromers (oPNMA or oPDMA) were synthesized that have been effectively cross-link gelatinous peptides into stable hydrogel matrices.[90,91,98] In particular, a low molecular weight gelatin (COL, 11 kDa) offered promising characteristics, such as the absence of sol-gel transition and processability in high concentrations, which resulted in the fabrication of a great variety of differently composed COL-derived hydrogels with tunable properties. However, cell culture experiments revealed marginal cell migration into the hydrogel bulk indicated insufficient porosity of these matrices, which is a crucial drawback in terms of a regenerative application. In order to improve material porosity, the integration of a porogen seemed promising, because the COL-derived offered comparatively high mechanical stability (elastic modulus of up to 13 kPa) that might allow for the application of such a templating method.[55] As the integration of a poly(ethylene glycol) (P8k) porogen offered promising results in previous experiments, this approach was advanced in this work.[92] Pore generation by PEG is based on liquid-liquid phase separation of high molecular weight PEG and cross-linker precursor solutions and was successfully applied in hydrogel engineering.[159,160] The principle of a porogen-leaching approach is the integration of an inert phase that can be leached after cross-linking. This applied to the utilized P8k as a reaction of the alcohol functions with the macromer anhydrides is not expected at room temperature,[96,161–163] while the water-soluble PEG can be leached during hydrogel washing and hydration in aqueous buffer.

While P8k was previously used in low concentrations (1.25% and 2.5% (w/v)), its content was increased to 2.5% and 5% (w/v) which is in accordance with a published protocol.[57] As the low molecular weight COL can be effectively cross-linked by highly reactive macromers, hydrogels were fabricated by cross-linking with oPxMA-7.5 derivatives (Table 2-3). The porogen was added into the aqueous COL solution and a two-phase system was obtained which could be

homogenized by vortexing immediately before cross-linking. Stable hydrogels could be fabricated without further adaption of the previously established fabrication procedure indicating the robustness of this method (Table 2-4).[91] This can be explained with the low molecular weight of the hydrogel building blocks together with the rapid cross-linking reaction. The resulting gelation within a few seconds enabled homogeneous integration of the P8k porogen.

The application of an extensive washing and hydration protocol over 3 days opened potential to effectively remove the incorporated porogen. In that regard, hydrogel leachables were determined indicating the fraction of water soluble components. Hydrogel leachables after fabrication (I) ranged between 30-50% and the values increased with increasing P8k content in all formulations (Figure 4-2A). This correlation was statistically significant for high porogen content and indicates successful removal of incorporated P8k. In order to further support this assumption, the parameter leachables I* was calculated which represents leachables corrected by the theoretical amount of P8k (Figure 4-2B). This parameter was not significantly affected by P8k addition in any hydrogel formulations indicating that the hydrogel building blocks (oPxMA and COL) were leached in a comparable extent independent of PEG incorporation. Taken the results of both parameters together, hydrogel leachables correlated with the amount of applied P8k demonstrating effective removal of the porogen. A similarly effective removal of P8k from a PCL matrix has been shown by Columbus et al.[144] Another leachables parameter (II) was calculated representing the fraction of dry weight that is leached by rehydration of freeze-dried gels (Figure 4-2C). Low values of only 4-8% indicate that non-cross-linked precursors were separated by the initial washing and hydration procedure, while the cross-linked matrices offer adequate stability indicating efficient cross-linking. As parameter leachables II did not significantly depend on the amount of incorporated P8k, a negative effect of the porogen addition on hydrogel stability can be excluded. Previous experiments demonstrated absent cytotoxicity of the leached non-cross-linked hydrogel fraction.[91,98] Cytocompatibility of the presented macroporous gels can also be assumed as the possible release of PEG residues would not have toxic effects.[164]

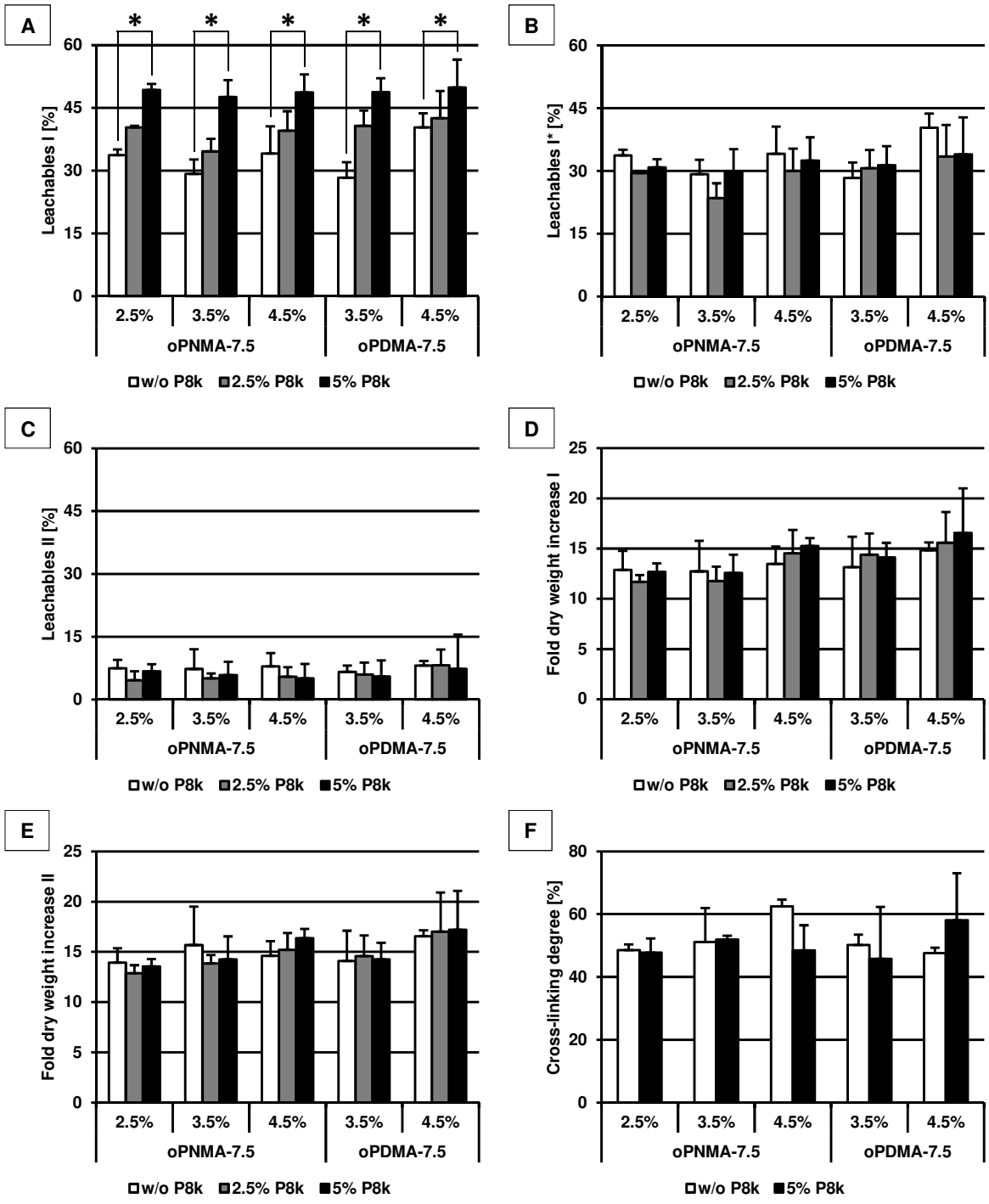

Figure 4-2. Hydrogel leachables, water content and cross-linking degree of fabricated oPxMA/COL/P8k formulations. (A) Leachables after hydrogel extraction/washing relative to all constituents of the precursor mixture (including P8k, I) or (B) relative to cross-linking precursors (excluding P8k, I*). Leachables of labeled groups differed statistically significantly from each other ($p < 0.05$). (C) Leachables II as determined after rehydration of freeze-dried gels in PBS and subsequent lyophilization. (D) Water content I as determined after fabrication and hydration of hydrogels and (E) water content II as determined after rehydration of freeze-dried gels in PBS (A-E: $n = 5$). (F) Cross-linking degree as determined by a standard TNBS assay ($n = 3$).

Water content of the hydrogels was determined in order to characterize swelling behavior of the cross-linked matrices. The oPxMA-7.5/COL hydrogels were able to absorb 12-17-fold of their dry weight of water when equilibrated in PBS, while no significant differences were detected across the formulations (Figure 4-2D-E). This shows homogeneous swelling independent of hydrogel composition and P8k content. Furthermore, water content after fabrication (Figure 4-2D) did not differ from that after rehydration of lyophilized gel disk (Figure 4-2E). This is in accordance with the low leachables II values and indicates network stability of the macroporous matrices.

Cross-linking density is another important parameter characterizing network properties that was determined by a standard TNBS assay (Figure 4-2F). Cross-linking degrees of 45-65% were obtained that varied between different hydrogel formulations, but no correlation with porogen content was detected. This confirmed the expected non-covalent P8k integration as any conversion of PEG-OH groups would have resulted in decreased cross-linking degree of amino functions and would have been determined by this method.[96,161–163]

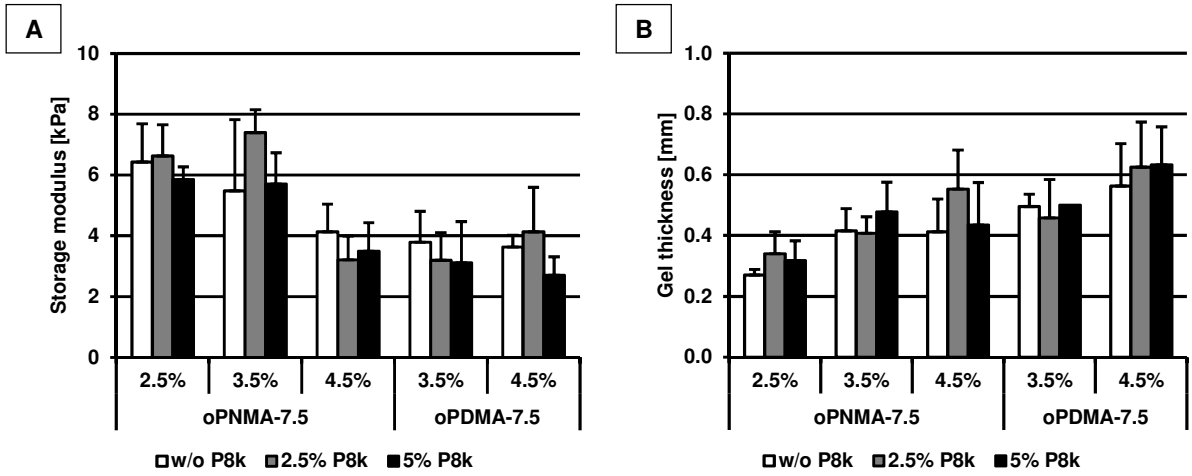

Figure 4-3. Rheological characterization of fabricated oPxMA/COL/P8k hydrogel formulations. (A) Storage modulus and (B) gel thickness as determined in a parallel plate setup under normal force control (0.2 N) at 1 Hz (n = 4).

Hydrogels were further analyzed by oscillation rheology (Figure 4-3). Hydrogel storage modulus (2.5-7.5 kPa) was dependent on oPxMA type and concentration, but did not correlate with cross-

linking degree (Figure 4-3A). This is in accordance with our previous results for oPxMA-derived matrices in which matrix homogeneity strongly affected hydrogel stiffness which is not necessarily reflected by the cross-linking degree.[91,98] Hydrogel stiffness remained unchanged upon P8k addition which is generally promising in order to enable decoupling of material porosity and mechanics.[165] Nevertheless, these results are in conflict with the characteristics of porous carbodiimide-cross-linked gelatin materials for which increased porosity resulted in decreased mechanics.[55,155] Such an inverse correlation between material porosity and mechanical stability has also been described for a variety of other (solid) materials.[4,73,166] One possible explanation for this discrepancy might be that formation of the cross-linked hydrogel network was not affected by the incorporation of comparatively low P8k amounts as indicated by the other physico-chemical hydrogel characteristics. This had likely resulted in comparable matrix viscoelasticity which was not altered by macropore generation.[167] Hydrogel thickness, determined as another indicator of hydrogel stability, correlated with the content of the oligomeric building blocks (oPxMA concentration) which was expected due to comparable relative swelling behavior (Figure 4-3B). Porogen application did not affect gel thickness which is in accordance with the leachables II and water content data. Gels were thicker than 0.25 mm which has been empirically determined as critical threshold for successful hydrogel handling.

Generally, physico-chemical characteristics were in accordance with previous findings for oPxMA/COL matrices indicating reproducibility of macromer synthesis and robustness of hydrogel fabrication.[91,98] Slight deviations were found in oPNMA-matrices, in which increased stiffness and reduced cross-linking densities were obtained when compared with previous data. These differences again confirmed an unclear correlation between both parameters and might be attributed to more homogeneous cross-linking in the current hydrogel formulations in which a COL batch of slightly higher molecular weight (11 kDa vs. 10.8 kDa) was used.

Taken together, incorporated P8k was effectively removed from the hydrogel matrix during fabrication by aqueous extraction, but did not affect the general physico-chemical properties. On the one hand, this could be expected as hydrophilic PEG residues would likely have significant effects on parameters such as water content and therefore gel thickness. On the other hand, significantly increased hydrogel porosity might also result in altered physico-chemical properties. Although porosity was not directly assessed, microscopic comparison of PEG-derived and conventional oPNMA-7.5/COL (3.5%/11.25%) formulations indicated an improved

interconnected pore structure together with enhanced surface porosity in the P8k-derived hydrogel.[168] Enhanced release of incorporated siRNA[168] and improved cell migration ability as indicated in collaborative experiments for different cell types, including hASC (not shown) are further powerful indicators of increased material porosity and the results confirmed previous data on this porogen-leaching strategy. Overall, phase separation by liquid-liquid immiscibility is a more promising method to generate homogeneous porosity when compared to a solid templating approaches, such as salt-leaching, due to increased stability of the dispersion.[55]

4.3.2 Characterization of G160-derived hydrogel matrices

Besides short-chained COL, successful hydrogel fabrication from another gelatin source with medium molecular weight (50 Bloom, G50) was previously demonstrated, especially by cross-linking using oPNMA with low anhydride contents. This has presumably resulted in increased mesh size (ξ) of these matrices (Figure 4-1),[169] although this parameter could not be quantified.[91] Nevertheless, previous LSM and SEM analyses indicated that G50 matrices offered increased pore size when compared to COL-derived formulations.[92] These findings motivated for extension of this concept by cross-linking of a high molecular weight gelatin (160 Bloom, G160) in order to further improve material porosity. Although hydrogel mesh size generally determines porosity on the nanoscale which generally is not relevant for cell penetration, improved diffusion of nutrients, gases and metabolic products, however, might positively affect cellular response.[2,5]

The application of G160 required low reactive macromers, i.e. oligomers with low anhydride content per molecule (Table 2-3), in order to fabricate homogeneously cross-linked matrices, because anhydride-rich oligomers would cause rapid gelation before the precursor mixture could be homogeneously mixed resulting in irregularly cross-linked clumps.[91] Based on previously established G50 matrices, i.e. oPNMA-1.75 and -2.5 (2.5-4.5%) + G50 (3.75-6.25%), similarly composed G160 formulations were screened with regard to their processability into homogeneous and stable hydrogel matrices (oPNMA-1.75, -2 and -2.5 (1.5-5.5%) + G160 (0.625-8.75%)). In order to cope with the sol-gel transition of G160 solutions, a critical characteristic of this high molecular weight gelatin, the solutions had to be processed above 30 °C in order to maintain a sol state.[158] Stable hydrogels were obtained when gelatin was dissolved in a 1:1 mixture of DMF/water (v/v), while G160 solutions in water were insufficiently cross-linked in the applied setup which can be explained with enhanced hydrolysis of reactive

anhydrides due to the increased water content. This is in accordance with our experiences form G50-derived matrices. During development of suitable hydrogel formulations from G160, three characteristic observations were made: I) high anhydride content (anhydride-rich macromer or high macromer concentration) resulted in inhomogeneous cross-linking, II) high G160 concentrations were not processable due to physical gelation, even at 37 °C, and III) insufficiently cross-linked matrices were obtained when comparatively low G160 concentrations were used. As known from other experiments, correlation III can be partially optimized when the fabrication procedure was scaled-up. To this end, the total material content was increased by factor 1.5, while solution concentrations and oPNMA/COL/base ratio were not changed (Table 2-5). A series of differently composed hydrogel were obtained by G160 cross-linking with oPNMA-1.75 and -2 macromers. When compared with G50-derived hydrogels, lower oligomer concentrations were processable into homogeneous matrices which can be explained with increased gelation of G160 formulations due to enhanced molecular weight.

Cross-linking by oPNMA macromers resulted in free-standing hydrogels which swelled in a manner that enable detachment from the bottom of the reaction vial (Figure 4-4A-B). Matrix homogeneity was macroscopically compared with that of glutaraldehyde(GTA)-cross-linked gels. GTA is a commonly used cross-linker of gelatin (Figure 4-4C-D).[170–172] In order to enable adequate comparison, GTA was applied in concentrations which correspond to the same equivalents of reactive functionalities as used for oPNMA cross-linking. GTA-cross-linking also resulted in the formation of insoluble matrices, but the gels were comparably thin and remained attached to the bottom of the fabrication vial. This can be explained with the significantly reduced material content in GTA-derived formulations due to its high reactive group to molecular weight ratio. Low material swelling was attributed to high cross-linking densities in the range of 100% which can be assumed for the applied conditions, i.e. GTA concentration of > 1 wt% and GTA to gelatin weight ratio of > 0.5.[171] When high GTA concentrations were used, the cross-linked matrices appeared turbid indicating inhomogeneous cross-linking which was not observed for the corresponding oPNMA-derived formulations (Figure 4-4B, D). As it was not the objective of this study to evaluate differences of matrix properties between oPNMA- and GTA-cross-linked derivatives, only oPNMA-derived formulations were further characterized. Nevertheless, we previously demonstrated that oPNMA macromers showed strong potential as functional alternative for GTA in the fabrication of microspheres.[92]

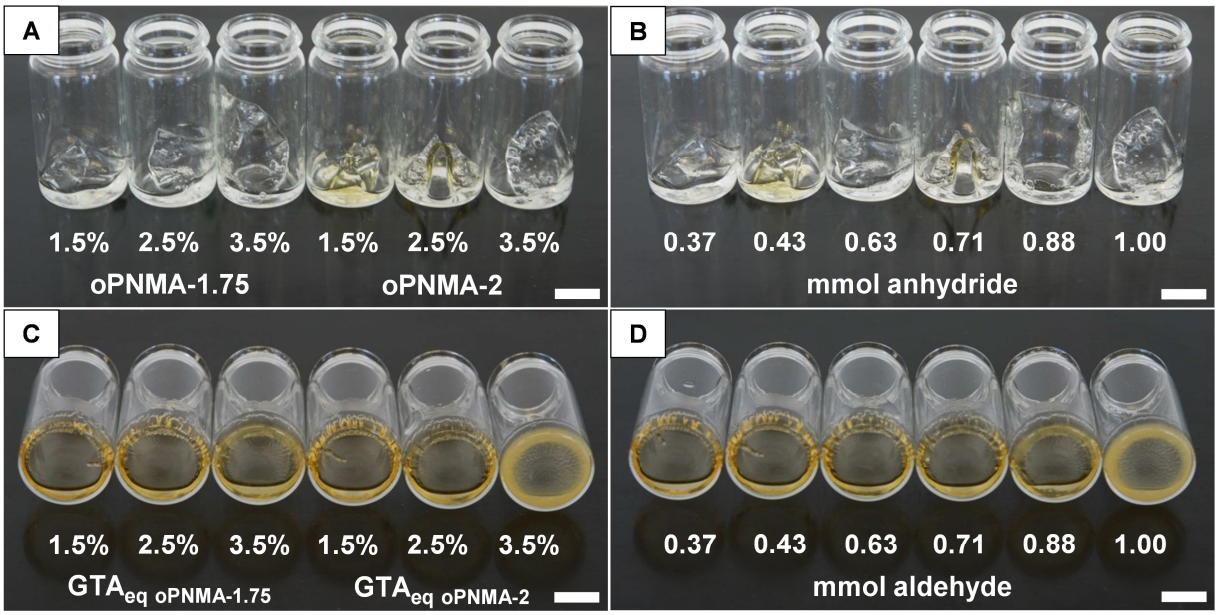

Figure 4-4. Morphology of fabricated G160-derived hydrogels containing 3.75% G160. (A, B) oPNMA/G160 hydrogel formulations as function of type and concentration of the cross-linking oligomer (A) and as function of the applied molar amount of anhydride functionalities (B). (C, D) GTA/G160 hydrogel formulations as function of oPNMA-z equivalents of GTA (C) and as function of the applied molar amount of aldehyde functionalities (D). Scale bars represent 1 cm.

In order to evaluate the effects of the incorporation of G160 building block on the physico-chemical material properties, hydrogel characteristics were assessed by the same methods as applied for characterization of P8k-containig formulations. The fraction of material that was leached during the hydration and washing of cross-linked matrices (leachables I, Figure 4-5A) ranged within only 2-12% which is significantly lower than typical leachables found in oPNMA-cross-linked COL and G50 formulations.[91] This generally indicated effective cross-linking, but might also be biased by reduced solubility or mobility of G160.

Rheological characterization offered comparatively high storage moduli (3-10 kPa) meeting the upper stiffness range of the established oPxMA-cross-linked matrices (Figure 4-5B).[91,98] These values, however, did not reflect the handling properties of the hydrogel discs (before lyophilization) that felt softer and comparable to oPNMA/G50 formulations. The reason for this discrepancy might be that previous data was determined from as-fabricated gel discs, while G160 matrices were characterized after lyophilization and subsequent rehydration. The processing steps had likely strengthened the hydrogels as known from literature and own experience with

COL-derived matrices which limits comparability with previous oPxMA-cross-linked matrices.[14] Nevertheless, the values corresponded to elastic moduli of 9-30 kPa (using the simplified estimation of E equals 3G′) which exceeded Young's moduli that have been reported for GTA-cross-linked gelatin (1.5-7.4 kPa)[173] or collagen (3.5-7.2 kPa)[174]. Stiffness further correlated with concentration of the hydrogel building blocks which confirmed previous findings.[91,98]

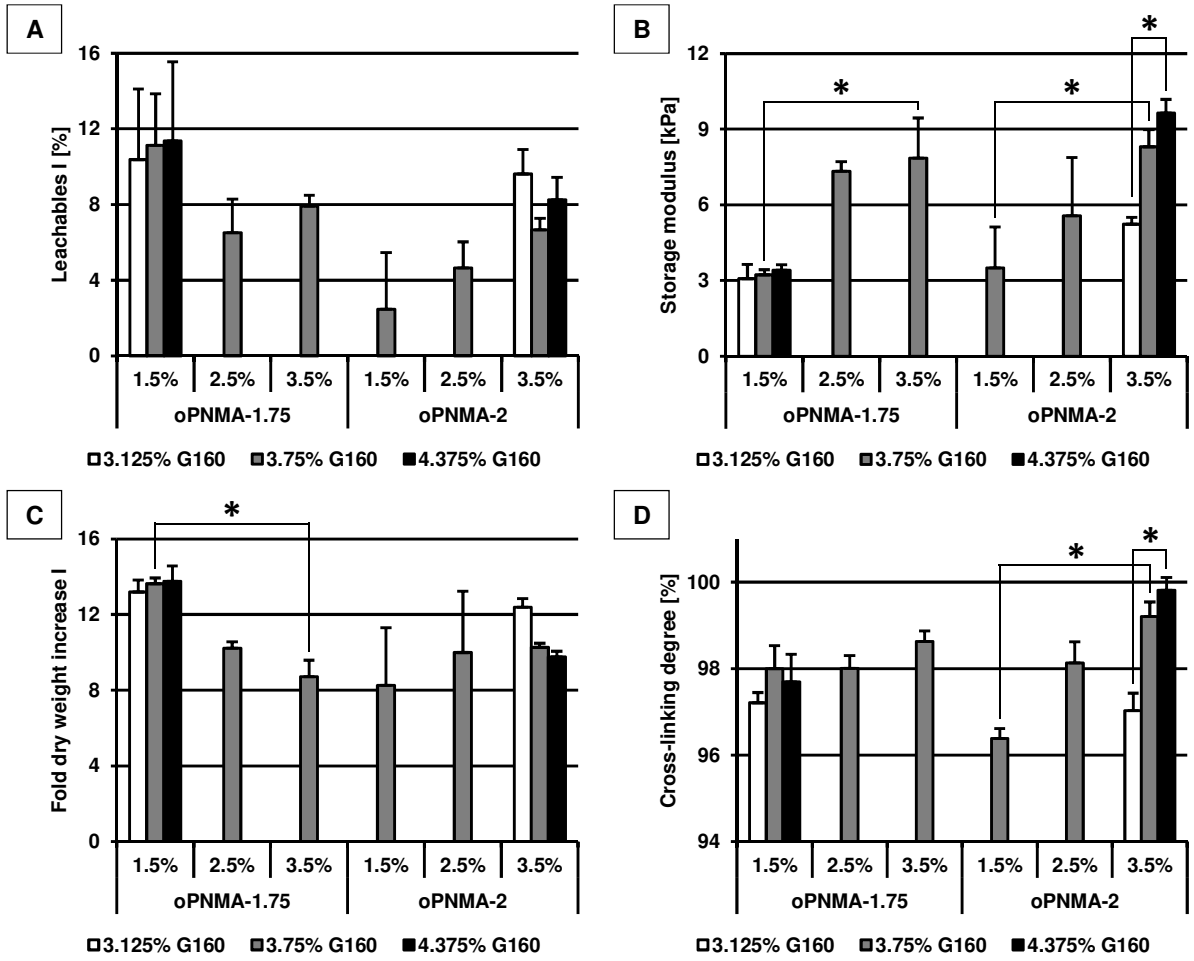

Figure 4-5. Physico-chemical properties of fabricated oPNMA/G160 hydrogels. (A) Leachables I and (C) water content I as determined after washing and hydration of fabricated hydrogels. (B) Storage modulus as determined by oscillation rheology (A-C: n = 5). (D) Cross-linking degree as determined by a standard TNBS assay (n = 3). Values of labeled groups differed statistically significantly from each other ($p < 0.01$).

Water content (I) was measured to determine swelling behavior and cross-linked G160 matrices were able to absorb 8-14-fold of their dry weight of water when equilibrated in PBS (Figure 4-

5C). While this swelling behavior matched the lower end of the range of other oPxMA-derived formulations,[91,98] the obtained indirect correlation between increased macromer concentration and decreased water content is in accordance with increased gel stiffness (Figure 4-5B).

The determination of the cross-linking degree of G160 in the hydrogels revealed high values of above 96% which have not been previously obtained for oPxMA-cross-linked COL and G50 hydrogels (Figure 4-5D).[91,98] Comparatively high values were reported for GTA-cross-linked gelatin matrices.[171] Effective cross-linking by oPNMA can thus be resumed. The results are further in line with high storage moduli and low swelling degree.[155] Furthermore, significant direct correlations between concentrations of building blocks, oPNMA and G160, in the hydrogel formulations and cross-linking degree were detected. This also correlates with increased hydrogel stiffness (Figure 4-5B).

Taken together, G160 was successfully processed into stable hydrogel matrices. To this end, a previously established hydrogel fabrication protocol was adapted in terms of concentrations of the oligomeric building blocks, volume of precursor mixture and processing temperature. The high molecular weight of the gelatin required low reactive macromers in order to afford homogeneous cross-linking. When compared to COL- and G50-derived matrices, the application of a higher molecular weight peptide component strongly increased cross-linking degree which resulted in decreased leachables and reduced water content.[91] In this context, it can be assumed that the investigated oPNMA/G160 formulations are characterized by an (almost) optimal balance of cross-linking kinetic, orientation of functional groups and precursor molecular weight. The high stiffness is a promising characteristic enabling the hydrogel to possibly withstand the stress exerted by a surgeon or when applied as wound dressing material. With respect to material porosity, we have previously experienced that the largest pores were found in hydrogels of low stiffness that offered high water contents.[91,92] To this end, the comparatively low swelling degree of the present G160 formulations might be in conflict with the formation of a highly porous, flexible network. Nevertheless, the hydrogel design concept based on long-chained gelatin combined with anhydride-containing macromers, that are characterized by a comparably high molecular weight per chemically intact anhydride unit,[90] suggest a fairly open nanoporous hydrogel network. Cell culture experiments further indicated improved performance of macrophages on oPNMA-1.75/G160 gels containing 3.75% gelatin which might serve as a functional proof of increased hydrogel porosity (data not shown).

4.3.3 Prospect: further strategies to improve hydrogel porosity

The presented strategies generally offer great promise to enhance hydrogel porosity. While P8k incorporation can be used to generate macroporosity, the application of long-chained building blocks opens potential to enhance hydrogel mesh size on the nanoscale. Additional parameters and methods are known that will allow for further optimization if needed. First possibility is the adaption of the applied freeze-drying process in which ice crystals act as porogens. It was demonstrated that pore size and morphology can be affected by cooling rate, temperature gradient and final freezing temperature.[158,175] Adjustment of the drying parameters offers further potential, but the effect on porosity was comparably low.[176] The application of repeated freeze-thawing or cryogenic treatment could also alter hydrogel structure.[13,14] We have previously investigated possible effects of the freezing temperature, that was usually set to -20 °C. Gels were also frozen at reduced temperature (-80 °C and -196 °C) which resulted in the formation of small pores, while freezing at -20 °C enabled formation of larger ice crystals forming larger pores (not shown).[92,170] To this end, the established protocol might already use the optimal freezing conditions for the formation of large-scaled pores. Secondly, we have detected that UV irradiation of freeze-dried oPxMA-cross-linked gels led to increased storage moduli (not shown). An effect on hydrogel porosity is therefore also possible.

Rapid prototyping is an upcoming approach which meanwhile also enables fabrication of precisely shaped and structured hydrogel matrices.[2,60,62] Our dual-component hydrogel concept may also offer potential for application of a freeform fabrication method due to the rapid cross-linking reaction,[59] although the establishment of such a technique is comparatively difficult and requires careful adjustment of cross-linking reaction and the deposition method.[60] In that regard, it has been demonstrated that gelation kinetics of the oPNMA/COL system are adjustable in order to enable fabrication of tubular structures by processing of the hydrogel building blocks from a double syringe delivery system equipped with a static mixing nozzle.[115] This offers promise for generative fabrication by extrusion bioprinting of a precursor mixture, while printing of a gelatin solution into a solution of the oligomeric cross-linker might serve as another possible strategy.[59]

4.4 CONCLUSION

Two different strategies were presented to enhance porosity of oPxMA-cross-linked gelatin matrices. One strategy focused on biologically relevant macroporosity of the gels by utilizing poly(ethylene glycol) (P8k) to allow for pore formation by phase separation and subsequent leaching of the porogen. In another approach focused on mesh size-related porosity, long-chained gelatin (G160) was cross-linked by low-reactive, high molecular weight macromers with the objective to widen mesh size and nanoporosity of the materials. Successful applicability of both methods was demonstrated by processability of all formulations into stable gels. Efficient P8k leaching from oPxMA/COL matrices was shown, while the porogen incorporation did not affect other physico-chemical hydrogel properties. Improvement of hydrogel porosity was at least indirectly shown improved cell migration and enhanced release of incorporated complexes indicating great promise of this porogen-leaching method. As the applied P8k amounts (2.5-5%) did not increase matrix fragility, the incorporation of even higher porogen concentrations might open potential for further enlarged macroporosity. In this context, PEG contents of up to 50% ((w/w) related to the total amount of hydrogel building blocks) were reported,[57] while the amounts applied in this study corresponded to only 16-36%. Adjustment of oligomer concentrations and phase homogenization conditions as well as change of porogen molecular weight were reported as further parameters of significant influence on hydrogel porosity.[53,57,144] Formation of G160-derived structures with enhanced mesh size was indicated by improved macrophage performance in cell culture experiments and it was demonstrated that highly cross-linked matrices were obtained. The high stiffness further might offer potential to combine both concepts that were investigated in this study. In that regard, a large mesh size would be advantageous for efficient leaching of even higher porogen amounts. The determination of hydrogel porosity, e.g. by CLSM imaging of hydrated networks,[91] is an important further objective in order to directly evaluate effects of the applied strategies on gel matrix porosity. In this regard, network interconnectivity is an important parameter, which can be characterized by the interconnectivity index (ICI). The ICI as established by Le et al. can be determined by micro-computed tomography (µCT) analysis and was originally defined for a trabecular network as: $ICI = \frac{Nd * NNd}{T * (NNdTm + 1)}$ (Nd: total number of nodes, NNd: node-to-node branches, NNdTm: number of node-to-termini branches, T: number of trees).[142,177,178] In case of a trabecular

network, for example, high interconnectivity is accompanied by high network fragmentation and results in an increased ICI. In the case that cell migration behavior into oPxMA-cross-linked matrices would be insufficiently addressed by any approach of porosity adaption, the development of *in-situ* gelling formulations might serve as a promising strategy for homogeneous cell distribution within the entire gel network, which will be subject of further investigations.

4.5 SPECIFICATION OF THE AUTHORS' CONTRIBUTIONS TO CHAPTER 4:

C. Kascholke, F. Tischer, M. Schulz-Siegmund, M. C. Hacker, Dual Scale Porosity Adjustment of Oligomer-Cross-Linked Gelatinous Hydrogels.

Christian Kascholke

Oligomer synthesis and characterization, experimental design, fabrication and characterization of G160-derived hydrogels, data evaluation

Franziska Tischer

Screening experiments for formulation of P8k-containing and G160-derived hydrogels, fabrication and characterization of P8k-containing hydrogels

Michaela Schulz-Siegmund

Access to analytical equipment, advice for experimental design and discussion

Michael C. Hacker

Conceptual design, advice for experimental design, discussion and chapter review

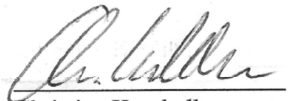

Christian Kascholke

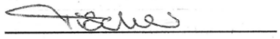

Franziska Tischer

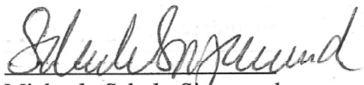

Michaela Schulz-Siegmund

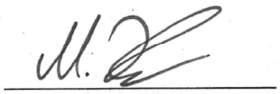

Michael C. Hacker

CHAPTER 5

Biodegradable and Adjustable Sol-Gel Glass Based Hybrid Scaffolds from Multi-Armed Oligomeric Building Blocks

C. Kascholke[a], S. Hendrikx[a], T. Flath[b], D. Kuzmenka[a], H.-M. Dörfler[b], D. Schumann[c], M. Gressenbuch[d], F. P. Schulze[b], M. Schulz-Siegmund[a], M. C. Hacker[a]

[a] Institute of Pharmacy, Pharmaceutical Technology, Leipzig University

[b] Department of Mechanical and Energy Engineering, Leipzig University of Applied Sciences

[c] Bubbles and Beyond GmbH, Leipzig

[d] DMG Chemie GmbH, Leipzig

Acta Biomaterialia **2017**, Accepted Manuscript, doi: 10.1016/ j.actbio.2017.09.024

5.1 ABSTRACT

Biodegradability is a crucial characteristic to improve the clinical potential of sol-gel-derived glass materials. To this end, a set of degradable organic/inorganic class II hybrids from a tetraethoxysilane(TEOS)-derived silica sol and oligovalent cross-linker oligomers containing oligo(D,L-lactide) domains was developed and characterized. A series of 18 oligomers (M_n: 1100-3200 Da) with different degrees of ethoxylation and varying length of oligoester units was established and chemical composition was determined. Applicability of an established indirect rapid prototyping method enabled fabrication of a total of 85 different hybrid scaffold formulations from 3-isocyanatopropyltriethoxysilane-functionalized macromers. *In vitro* degradation was analyzed over 12 months and a continuous linear weight loss (0.2-0.5 wt%/d) combined with only moderate material swelling was detected which was controlled by oligo(lactide) content and matrix hydrophilicity. Compressive strength (2-30 MPa) and compressive modulus (44-716 MPa) were determined and total content, oligo(ethylene oxide) content, oligo(lactide) content and molecular weight of the oligomeric cross-linkers as well as material porosity were identified as the main factors determining hybrid mechanics. Cytocompatibility was assessed by cell culture experiments with human adipose tissue-derived stem cells (hASC). Cell migration into the entire scaffold pore network was indicated and continuous proliferation over 14 days was found. ALP activity linearly increased over 2 weeks indicating osteogenic differentiation. The presented glass-based hybrid concept with precisely adjustable material properties holds promise for regenerative purposes.

5.2 STATEMENT OF SIGNIFICANCE

Adaption of degradation kinetics toward physiological relevance is still an unmet challenge of (bio-)glass engineering. We therefore present a glass-derived hybrid material with adjustable degradation. A flexible design concept based on degradable multi-armed oligomers was combined with an established indirect rapid prototyping method to produce a systematic set of porous sol-gel-derived class II hybrid scaffolds. Mechanical properties in the range of cancellous bone were narrowly controlled by hybrid composition. The oligoester introduction resulted in significantly increased compressive moduli. Cytocompatible hybrids degraded in physiologically

relevant time frames and a promising linear and controllable weight loss profile was found. To our knowledge, our degradation study represents the most extensive long-term investigation of sol-gel-derived class II hybrids. Due to the broad adjustability of material properties, our concept offers potential for engineering of biodegradable hybrid materials for versatile applications.

5.3 INTRODUCTION

Although bioactive glasses have been researched for almost half a century, the clinical establishment of glass materials for bone regeneration purposes, especially for treatment of large-scale bone defects, has not been realized.[3] Despite challenges associated with the fabrication of large-scale porous scaffolds, the adjustment of degradation properties to physiological requirements remains a critical issue.[51,94,179,180] For example, long-term investigations of BonAlive®, an approved pure inorganic glass with promising clinical results, offered significant particle residues after up to 14 years of implantation which might induce inflammation.[3,181] Slow *in vivo* degradation was also found for sintered 45S5 as well as sol-gel-derived 58S and 77S glasses, although the degradation rate of sol-gel glasses is generally enhanced.[93,94] Modification of the glass composition, e.g. by the introduction of borate which results in decreased chemical durability, is one possibility to control degradability of these inorganic materials.[179] However, the combination of the inorganic glass with a degradable organic component appears to be a more promising strategy to adjust material degradation over a broad range[3,94,182] and a wide variety of clinically relevant polymers was established during the last decades, including polyesters, polyorthoesters, polyphosphoesters, polyanhydrides, polycarbonates, polyamides and polyphosphazenes.[5,183] Among these, most attention has been paid to poly(α-hydroxy acids), such as (co-)polymers of lactic acid and/or glycolic acid, which are FDA-approved for various biomedical applications, including sutures, wound dressings and stents.[5,9] The degradable polymer matrix can be used to physically embed the inorganic glass particles and possibly prevent of self-catalyzed acidic polyester hydrolysis by the buffering capacity of released inorganic ions, which has been postulated as a major advantage of these composites in addition to increased toughness.[38,184–186] Nevertheless, the inorganic phase usually degrades much slower than the organic polymer which may lead to an immune response to released glass particles *in vivo*.[38,80,186] Furthermore, poor cell response and rapid loss of mechanical properties were reported as typical drawbacks of conventional composites.[3,37]

More homogeneous degradation behavior has been found in sol-gel-derived hybrids which behave as a single phase due to molecular interaction between the inorganic and organic components.[38,94] Degradation properties can be precisely controlled when the organic polymer is covalently incorporated in the hybrid structure (class II hybrid)[74] which can be achieved after polymer functionalization with 3-isocyanatopropyltriethoxysilane (ICPTES) (-OH group of the organic component) or 3-glycidoxypropyl trimethoxysilane (GPTMS) (-NH_2 or -COOH groups of the polymer).[35–37] Various (bio)degradable natural and synthetic polymers were covalently introduced into tetraethoxysilane(TEOS)-derived sol-gel hybrids, e.g. poly(γ-glutamic acid)[37,180], gelatin[36,74,151,187], chitosan[80,188], cellulose[189] and poly(ε-caprolactone)[35,190–192]. Lactic acid-based polymers have also been used for hybrid production,[193–195] but there has only been one report on TEOS-derived class II hybrids so far.[196] In such covalent hybrids, cross-linking degree can be controlled independently of the organic content which enables high tunability of hybrid properties, especially degradation profile and mechanics.[36,80] Material adjustability is important to precisely adapt a biomaterial to the implantation site-specific requirement, because remodeling time of a tissue is variable and depends on its type, anatomy and physiology.[51] Overall, only a few extensive degradation studies on class II hybrids were reported,[74,191,194] but none lasted longer than 140 days.[193]

We have recently established a class II hybrid material consisting of a TEOS-derived silica sol and synthetic oligovalent cross-linkers.[54,150] The implementation of an indirect rapid prototyping method further enabled the production of macroporous, pore-interconnected scaffolds of controlled architecture which are applicable for bone regeneration purposes. Mechanical properties were controlled by content and structure of the organic component and covered the range of cancellous bone.

It is the purpose of the study to extend the degradability of these glass-based hybrid materials by the introduction of (bio)degradable domains.[197] This approach adapts a design concept for a macromer platform composed of an ethoxylated alcohol core and hydrolytically degradable oligoester units.[53] This design enabled for broad adjustment of material properties of cross-polymerized scaffolds, such as mechanics and degradation profile. Herein, a set of 18 differently composed oligomers was synthesized by ring-opening polymerization from ethoxylated tri- or tetravalent alcohols and D,L-lactide. The oligomers were characterized with regard to chemical composition and molecular weight and activated by conversion with ICPTES of terminal

hydroxyl end groups. A large set of porous hybrid scaffold formulations were fabricated by mixing the macromers with a TEOS-based sol and subsequent indirect 3D-printing.[54] Mechanical properties of the obtained porous hybrids were determined by compression tests and correlation with structure and content of the oligomeric building block and material porosity was investigated. Long-term degradation properties were investigated over 12 months for a systematically selected set of formulations and correlations of the degradative behavior with hybrid chemistry were derived. Adhesion and proliferation behavior of human adipose tissue-derived stem cells (hASC) was further studied in order to demonstrate the applicability for regenerative purposes.

5.4 EXPERIMENTAL SECTION

5.4.1 Materials

3,6-Dimethyl-1,4-dioxane-2,5-dione (D,L-lactide, LA), tin(II) 2-ethylhexanoate (95%), polycaprolactone (PCL, M_n ~ 45,000), trimethylolpropane ethoxylates (TMPEO) (T170 (M_n ~ 170, specified ratio of ethoxy units (EO) per hydroxyl groups (OH): EO/OH = 4/15), T450 (M_n ~ 450, EO/OH = 14/6), T730 (M_n ~ 730, EO/OH = 23/5) and T1014 (M_n ~ 1014, EO/OH = 20/3)), pentaerythritol ethoxylates (PETEO) (P270 (M_n ~ 270, EO/OH = 3/4) and P797 (M_n ~ 797, EO/OH = 15/4)), trifluoroacetic anhydride (TFAA), maleic acid, Dulbecco's modified Eagle's medium (DMEM), dexamethasone, β-glycerolphosphate, ascorbic acid-2-phosphate, Triton X, p-nitrophenyl phosphate (pNPP, substrate for alkaline phosphatase (ALP)) and 4',6-diamidino-2-phenylindole (DAPI) were purchased from Sigma-Aldrich (Seelze, Germany). Acetone (technical grade), ethanol 96% (v/v), Dulbecco´s phosphate buffered saline (PBS) and sodium azide (NaN_3) were purchased from AppliChem (Darmstadt, Germany). Deuterated chloroform ($CDCl_3$) and dimethyl sulfoxide (DMSO-d_6) were obtained from Armar Europa (Leipzig, Germany). Diisopropyl ether (DIPE), 3-isocyanatopropyltriethoxysilane (ICPTES) and sodium chloride (NaCl) were purchased from Fisher Scientific (Schwerte, Germany). PicoGreen® and Alexa Fluor® 488 phalloidin were obtained from Life Technologies (Darmstadt, Germany). Tetrahydrofuran (THF, HPLC grade) and n-hexane (technical grade) were obtained from VWR (Darmstadt, Germany). Weigert's hematoxylin kit and Van Gieson's solution were purchased from Carl Roth (Karlsruhe, Germany).

5.4.2 Methods

5.4.2.1 Oligomer synthesis. Degradable three- or four-armed oligomers were synthesized by ring-opening polymerization from different oligovalent alcohols as core molecules (Figure 5-1A) and defined feeds of D,L-lactide following an adapted protocol from previous work.[53,198] In a typical synthesis, 10-30 mmol of tri- (TMPEO, Tx) or tetravalent alcohol (PETEO, Px) were combined with the corresponding molarity of D,L-lactide to equal 3, 4.5 or 6 lactic acid units per hydroxyl group of the core molecule (Figure 5-1B). Ring-opening polymerization was initiated by the addition of tin(II) 2-ethylhexanoate ($Sn(Oct)_2$, 0.273 mol% per hydroxyl group[100]) and

maintained at 150 °C for 16 h. After cooling to room temperature (rt), the product was dissolved in acetone and precipitated in saturated aqueous sodium chloride solution (brine). After phase separation for 3 h, the product (upper phase) was dissolved in acetone and the precipitation step was repeated. During method development, deionized water, n-hexane and diisopropyl ether (DIPE) were also used as precipitation media. The product was finally dissolved in acetone and subsequently dried using a rotary evaporator at reduced pressure. The oligomers were abbreviated as TxLAy or PxLAy with x representing the nominal molecular weight of core component (M_n) and y representing the theoretical number of repeating lactic acid units per side chain.

5.4.2.2 Silane-coupling reaction. Oligomers were functionalized with reactive silane groups using ICPTES in a bulk reaction as previously described.[54] Briefly, oligomeric intermediate and ICPTES were reacted at 120 °C for 3 h under continuous stirring in equimolar ratio of hydroxyl groups (oligomer) and isocyanate functions (ICPTES) (Figure 5-1B). Silanized macromers were abbreviated as TxLAy-Si or PxLAy-Si.

5.4.2.3 Proton nuclear magnetic resonance (^{1}H NMR) spectroscopy. ^{1}H NMR spectra were recorded on a Mercury Plus 300 MHz spectrometer (Varian, Darmstadt, Germany). Oligomer samples were dissolved in $CDCl_3$ (20 mg/mL) without or after addition of 5% (v/v) TFAA. Silanized macromers were dissolved in DMSO-d_6 (100 mg/mL) and maleic acid was added as internal standard (20 mg/mL).[54] Post-acquisition data processing was performed with the MestReNova 10 NMR software package (Mestrelab Research S.L., Spain).

5.4.2.4 Gel permeation chromatography (GPC). Molecular weight distributions of the non-silanized oligomers were determined by a SECcurity GPC system (Agilent Technologies, Boeblingen, Germany) with a series of analytical PSS SDV columns in THF relative to polystyrene standards (PSS Polymer Standards Service GmbH, Mainz, Germany).[53] The number average molecular weight (M_n) and molecular-weight dispersity ($Đ_M = M_w/M_n$) were reported.

5.4.2.5 Fabrication of hybrid scaffolds. Hybrid sol-gel scaffolds were produced by an indirect rapid prototyping method as previously established (Figure 5-4).[54,198] In brief, a silica sol was produced by TEOS hydrolysis and condensation (molar ratio H_2O:TEOS of 1.78:1) catalyzed by sulfuric acid, followed by controlled ethanol evaporation and subsequent curing for 7 days at 4 °C. For hybrid synthesis, the sol was mixed with triethoxysilane-functionalized macromers (TxLAy-Si or PxLAy-Si) at rt in specified ratios to obtain contents of the non-silanized oligomer

of 5-40 wt% relative to the silica sol (Figure 5-S3). The hybrid sol was filled into a PCL template cylinder and further cured in a saturated ethanol atmosphere for 6 days. After template leaching with THF, the scaffolds were washed with ethanol and dried under ambient conditions for at least 3 weeks.

5.4.2.6 Template characteristics. PCL template cylinders of 7.9 * 8.0 mm (d * h, inner diameter: 7.0 mm) with a layered grid structure were produced via rapid prototyping (Fused Deposition Modeling, FDM) using a Bioscaffolder® (SYSENG, Germany).[54] In order to obtain a scaffold porosity of 44%, templates with a calculated porosity of 56% were fabricated by extrusion of PCL using the following parameters: T_{melt} = 75 °C, inner needle (and measured strand) diameter: 0.178 mm (0.191 ± 0.020 mm), line spacing x-y: 0.43 mm, level spacing z: 0.14 mm. Porosity was further set to 46% (I), 64% (II) or 68% (III) using templates that were produced with modified parameters (inner nozzle diameter, measured strand diameter, line spacing x-y, calculated template porosity): (I) 0.330 mm, 0.359 ± 0.022 mm, 0.80 mm, 54%; (II) 0.330 mm, 0.381 ± 0.023 mm, 0.60 mm, 36%; (III) 0.250 mm, 0.278 ± 0.011 mm, 0.43 mm, 32%.

5.4.2.7 Micro-computed tomography (μCT), scanning electron microscopy (SEM) and mechanical testing. Scaffolds were scanned with a Scanco vivaCT 75 system (Scanco Medical, Brüttisellen, Switzerland). SEM imaging after gold sputter coating (CS 44 SEM, Cam Scan, Waterbeach, UK) and mechanical testing by compression (Zwick Z050 with a 50 kN load cell, Zwick GmbH & Co. KG, Ulm, Germany) of templates and/or scaffolds was performed as previously described.[54] Compressive modulus (slope of the linear part of the stress-strain curve) and compressive strength (maximum load) were determined. The exact dimensions of each cylindrically shaped scaffold were determined with an electronic caliper before compression and ranged within 6.58-7.51 mm (7.01 ± 0.18 mm) in height and 5.42-6.48 mm (6.00 ± 0.21 mm) in diameter.

5.4.2.8 Degradation of hybrid scaffolds. Selected hybrid formulations were fabricated as described above and sterilized by dry heat (160 °C, 2 h). After determination of the initial dry weight (w_0), samples were immersed in 5 mL (v_{medium}) of PBS containing 0.01% (w/v) sodium azide in order to obtain a ratio v_{medium} / w_0 of > 30:1, which is in accordance with ISO 15814:1999(E). Vials were placed on an orbital shaker (100 rpm) at 37 °C. Medium was exchanged twice per week followed by pH measurement using an Orion 3 Star pH meter (Thermo Fisher Scientific, Schwerte, Germany) equipped with a N6000 BNC electrode (SI

Analytics, Weilheim, Germany). At defined time points, samples were removed and weight was determined immediately after careful removal of droplets from the sample surface (w_{wet}) as well as after vacuum drying to constant weight (w_{dry}). Remaining dry weight (w_{dry} / w_0 * 100%) and water content ((w_{wet} – w_{dry}) / w_{dry}) were calculated. Mechanical properties of degraded samples were determined after drying as stated above. T1014-containing scaffolds were used as LA-free controls and were fabricated as previously described.[54]

5.4.2.9 Cell culture. For cell culture tests, T170LA3-20 scaffolds were fabricated using PCL templates of smaller height (3.0 * 7.9 mm (height * diameter)). Scaffolds were preincubated for 48 h in culture media (CM, DMEM high glucose, supplemented with 1% penicillin/streptomycin and 10% fetal calf serum (FCS)). Cell seeding was based on a method described previously.[54,199] Using spinner flasks, $3*10^5$ human adipose tissue-derived stem cells (hASC), isolated from lipoaspirates from healthy donors, were seeded per scaffold for 24 h in CM. Seeded scaffolds were transferred to 24-well plates (Corning, Amsterdam, The Netherlands), filled with 2 mL of osteogenic medium (OM, DMEM high glucose, supplemented with 1% penicillin/streptomycin, 10% FCS, 10 nM dexamethasone, 10 mM β-glycerolphosphate and 50 µM ascorbic acid-2-phosphate) and incubated at 37 °C and 5% CO_2 on an orbital shaker (1 cm orbit, 116 rpm). Medium was changed three times a week. Cells on tissue culture plastic (8000 cells/cm^2) served as two-dimensional control. Cell number was determined using Quant-iT™ PicoGreen® dsDNA Assay Kit (Invitrogen) on days 1, 8, 11 and 14 after seeding. For ALP analysis, scaffolds were ground to granules and cells were lysed in 0.1% Triton X solution. After addition of pNPP, the lysate was incubated at 37 °C and formation of p-nitrophenol representing ALP activity was detected by absorption measurement at 405 nm (Tecan Infinite F 200 plate reader, Salzburg, Austria). Cryosections were prepared after 28 days of culture using tissue freezing medium (Leica Microsystems Nussloch GmbH, Heidelberg, Germany) and a Leica cryostat CM1950 (Leica Microsystems, Wetzlar, Germany). The 10 µm thick sections were stained with DAPI/phalloidin or Weigert-Van Gieson to determine cell morphology and distribution as well as matrix formation.

5.4.2.10 Statistical analysis. Unless otherwise stated, experiments were conducted in triplicate and the data was expressed as means ± standard deviation (SD). Single-factor analysis of variance in conjunction with Tukey's HSD Post Hoc test was performed to assess any statistical significance ($p < 0.05$) within data sets.

For mechanics data, multiple linear regression with backward exclusion of independent variables was performed using SPSS statistical software package (IBM, version 24.0) to determine the relevant factors influencing compressive strength and compressive modulus. The following oligomer-specific parameters were used as predictors in this analysis: valence (N), total molecular weight (M_n(total)), oligo(lactide)-derived molecular weight (M_n(LA)), oligo(ethylene oxide)-derived molecular weight (M_n(EO)) and total content of oligomer in hybrid (C). In the backward exclusion linear regression model, all listed predictors were included in the first stage of analysis and then sequentially excluded. In each subsequent stage, the predictor with the smallest partial correlation was excluded when it did not significantly contribute to the model ($p < 0.05$).

.

5.5 RESULTS

5.5.1 Oligomer synthesis and characterization. A set of 18 differently composed oligomers was synthesized by ring-opening polymerization of varying feeds of D,L-lactide with tri- or tetravalent alcohols of different ethoxylation degrees (Figure 5-1A, B). The oligomeric three- or four-armed intermediates (TxLAy or PxLAy) were purified, isolated and characterized by ^{1}H NMR (Figure 5-1C). In TxLAy spectra, characteristic signals derived from protons of the trivalent alcohol appeared at 0.80-0.95 ppm (-CH_2-C**H$_3$**, triplett) and 1.35-1.45 ppm (-C**H$_2$**-CH_3). The methylene protons neighboring the ether or ester functions were generally found at 3.30-4.30 ppm in all spectra. Proton signals from non-terminal ethoxy (EO) units were detected at 3.50-3.80 ppm, which were clearly visible for oligomers with high EO content, such as P797LA3. In contrast, the intensities of these signals were significantly less in spectra of low ethoxylated oligomers, such as T170LA3 (Figure 5-1C). Protons derived from oligomerized lactic acid (LA) units generally appeared at 1.35-1.65 ppm (-C**H$_3$**) and 5.05-5.30 ppm (>C**H**-). Methine signals of terminal LA units were found at 4.25-4.45 ppm. No signals of stannous octoate protons and only small residues of unreacted lactide (1.65-1.70 ppm (-C**H$_3$**) and 5.00-5.10 ppm (>C**H**-)) and water (1.65-1.90 ppm) were found indicating efficiency of the applied purification protocol. ^{1}H NMR spectra further enabled determination of the oligomer composition. For TxLAy derivatives, integral values of LA-derived methyl protons (I_2) were related to that of the core alcohol (I_1), while I_3 and I_4 served as control integrals. Chemical composition of PxLAy oligomers could only be determined after addition of trifluoroacetic anhydride (TFAA), which resulted in separation of core and oligo(lactide) proton signals and the LA content was calculated from I_2 (LA protons) and I_5 (core protons) (Figure 5-S1).

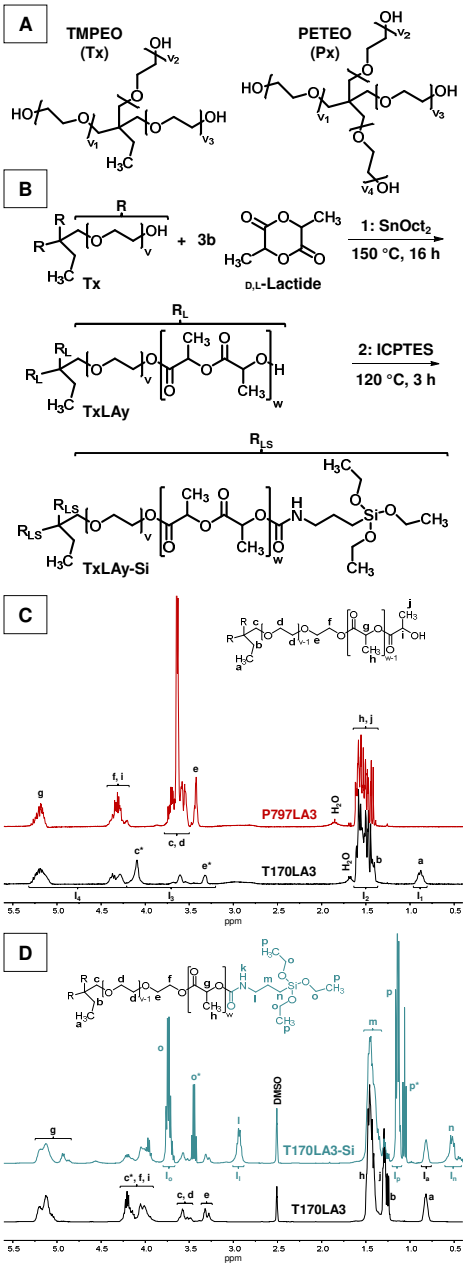

Figure 5-1. Synthesis scheme and ^{1}H NMR spectra. (A) Structure of tri- and tetravalent core alcohols as used for synthesis of reactive oligomers (B). (1) Ring-opening polymerization of D,L-lactide was initiated from trivalent alcohol in melt to yield TxLAy (x: M_n of core alcohol, y: number of lactic acid units per oligomer arm). (2) Silane functionalization of the oligomeric intermediates with ICPTES in melt. Note that composition of each oligomer arm is generally not equal due to statistical variations, but for simplification the abbreviations R (oligo(ethylene oxide) arm), R_L (oligo(lactide)-functionalized R) and R_{LS} (silanized R_L) were used without further differentiation. (C) Representative ^{1}H NMR spectra of three- (T170LA3) and four-armed (P797LA3) oligomers in $CDCl_3$. Label c* (and label e*) refer to methylene protons in α-position to ester hydroxyls in non-ethoxylated (or to core ethers in mono-ethoxylated) arms. (D) Representative ^{1}H NMR spectra of a silanized oligomer (T170LA3-Si) and the corresponding non-silanized derivative in DMSO-d_6. Labels o* and p* refer to alkyl protons of ethanol as released from ICPTES. Carbamate protons (k) were detected at 7.10-6.90 ppm (Figure 5-S2). I_x represent the integrals used to determine oligomer composition (C) and to characterize ICPTES functionalization (D).

For purification of the synthesized hydroxyl-terminated oligomers, different media were tested and efficiency was monitored by ^{1}H NMR. In terms of reactant solubility, water was detected as the most promising precipitation medium which resulted in absence of reactant signals in the corresponding oligomer spectra. Applicability of this purification protocol, however, was limited to the more hydrophobic of the synthesized derivatives. In hydrophilic derivatives purified by precipitation in water, considerably increased LA contents were found in the products (Figure 5-2). This was attributed to the solubility of hydrophilic oligomer fractions with low LA content which were removed from the polydisperse product. Purification with less hydrophilic diisopropylether (DIPE) or n-hexane yielded products of the desired composition, but ^{1}H NMR spectra showed insufficient reactant separation. When saturated sodium chloride solution (brine) was used as precipitation medium, the purification efficiency was comparable to that of water and relative LA conversions in the range of n-hexane-purified derivatives were obtained (0.96-1.18). Based on these results, brine was selected as best purification medium and only oligomers precipitated in brine were further analyzed and processed.

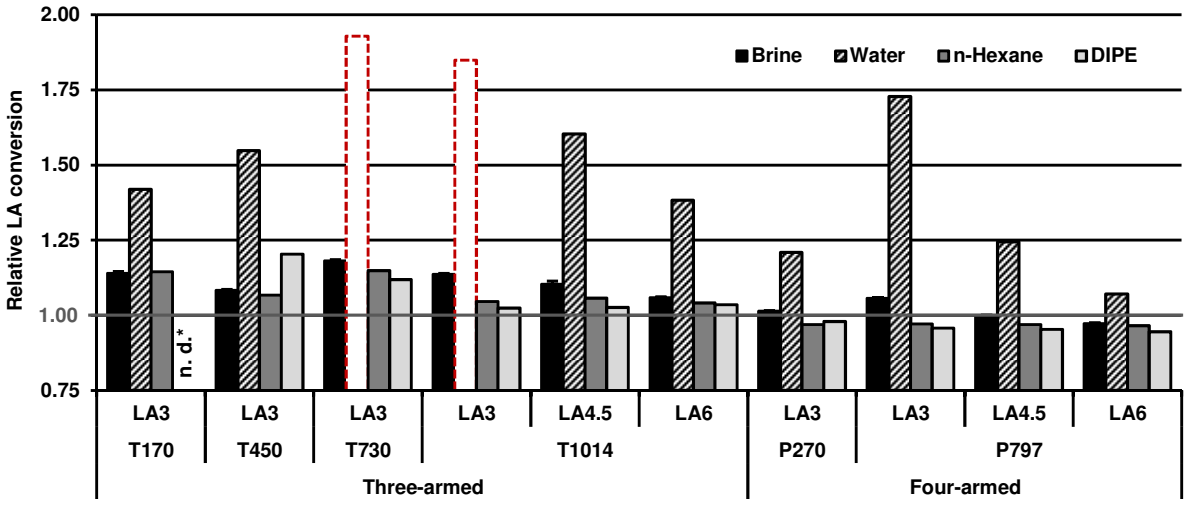

Figure 5-2. Composition of non-silanized oligomers after twofold precipitation in different media as determined by ^{1}H NMR. Relative lactide (LA) conversion represents the ratio of oligomer LA content and LA feed. Gray horizontal line (1.00) represents theoretical LA content of the oligomer. Labeled groups could not effectively been isolated (dashed red framed bar) or were completely soluble (n. d.*) in the corresponding medium.

Molecular weights of the oligomers were determined by GPC relative to polystyrene standards and ranged between 1100-3200 Da for TxLAy and 1500-3000 Da for PxLAy derivatives (Figure 5-3). When oligomers with the same tri- or tetravalent core alcohol and increasing LA content or those with the same length of the degradable block and increasing degree of ethoxylation were compared, molecular weights increased according to their chemical structure. Molecular-weight dispersities ($Đ_M$) were lower than 1.26 and decreased with increasing degree of ethoxylation down to 1.10. This expected correlation can be explained with increasing uniformity of the EO distribution within the molecule with increasing degree of ethoxylation.[53]

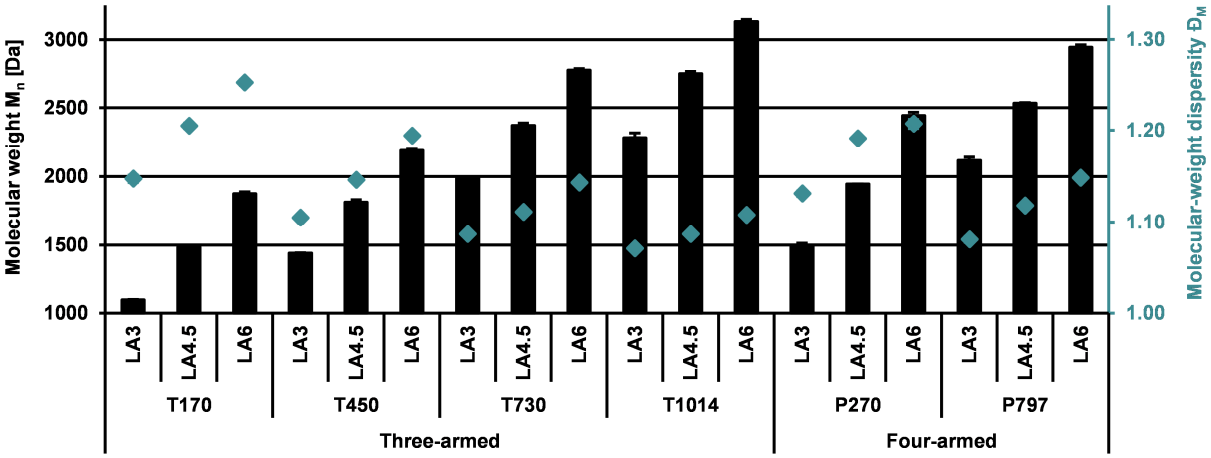

Figure 5-3. Molecular weight characteristics of the synthesized hydroxyl-terminated oligomers as determined by GPC analysis. Data represents the number average molecular weight M_n (bars, left y-axis) and molecular-weight dispersity $Đ_M$ (diamonds, right y-axis) relative to polystyrene standards. All values within groups of oligomers of the same core molecule and within groups of the same LA content per arm differed statistically significantly ($p < 0.01$).

5.5.2 Oligomer functionalization and hybrid scaffold fabrication. In order to enable covalent linkages between the organic oligomers and the TEOS-based glass sol, the hydroxyl-terminated oligomers were functionalized with 3-isocyanatopropyltriethoxysilane (ICPTES) (Figure 5-1B). Proton NMR analysis demonstrated successful ICPTES conjugation by formation of carbamate ester functions (Figure 5-1D, Figure 5-S2). The absence of two characteristic ICPTES-derived signals (l: 3.14-3.22 ppm, m: 1.51-1.57 ppm) in the spectra of silane-functionalized macromers indicated effective ICPTES conversion in three- and four-armed derivatives possibly accompanied by minor isocyanate hydrolysis. More than 80% of the ethoxy groups remained reactive toward the silica network after functionalization (as determined from the integral ratio $(I_o + I_p) / (I_l + I_n)$).

The silanized macromers were mixed with a pre-cured TEOS-derived silica sol that still contained unreacted ethoxy groups enabling covalent integration of the organic component (Figure 5-4A). The sol-gel curing process inside a 3D-printed PCL mold yielded negative replica of the template structure and after PCL leaching crack-free hybrid scaffolds with defined and uniform pore architecture were obtained (Figure 5-4B). The oligomers were incorporated in different ratios ranging from 5 to 40 wt% which corresponded to a content of the silanized macromers in the range of 7-55% (Figure 5-S3). Overall, 85 different hybrid scaffold formulations were fabricated with varying type and content of the oligomeric building block.

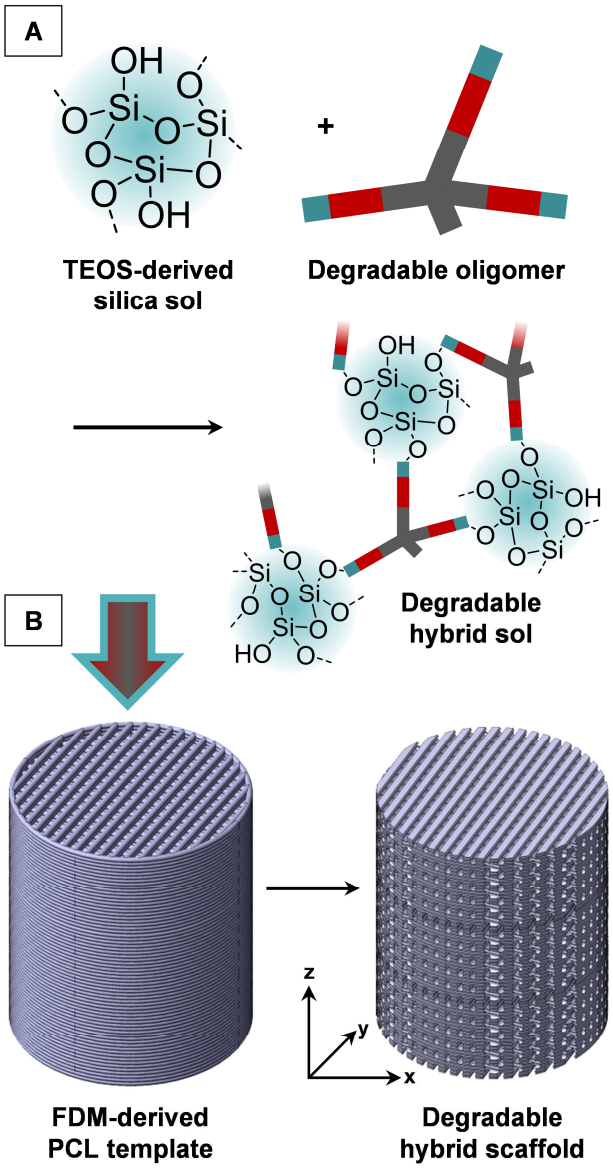

Figure 5-4. Schematic illustration of the hybrid scaffold fabrication process. (A) Hybrid sol production from silanized oligomers (TxLAy-Si or PxLAy-Si) and silica sol as obtained from TEOS hydrolysis and condensation. (B) 3D CAD models of FDM-derived PCL template and scaffold structure illustrating the scaffold fabrication procedure by indirect rapid prototyping.

5.5.3 Mechanical properties. Mechanical properties of the hybrid scaffolds were analyzed by uniaxial unconfined compression tests and correlation of compressive strength and modulus with cross-linker structure and hybrid composition was assessed. Highest compressive strengths were found for three-armed T170LA3-40 (30 ± 4 MPa) and four-armed P270LA3-40 (29 ± 7 MPa) hybrids, each containing the highest amount of the oligomer with the lowest molecular weight (Figure 5-S4A, C). In contrast, the maximum oligomer content of 40% yielded the lowest compressive moduli (≤ 50 MPa, in T730LA4.5-40 and P797LA6-40) (Figure 5-S4B, D). The highest compressive moduli were found for scaffolds containing 20% of three-armed T170LAy (530-585 MPa) or four-armed P270LA4.5 oligomers (716 ± 63 MPa). For scaffolds with three-armed derivatives, compressive strength was enhanced when oligomer content increased from 5 wt% to 20-30 wt% and plateaued or decreased for higher contents, while for PxLAy-containing formulations a clear decrease was found for contents above 20 wt% (Figure 5-5A). Independent of the oligomer valence, the highest compressive moduli were found for hybrids with 20 wt% oligomer and values decreased with increasing oligomer content (Figure 5-5B). In order to illustrate the correlation between mechanical properties and oligomer structure, data of the hybrids with 30 wt% oligomer was selected. Compressive strength generally was increased with increasing LA content (Figure 5-5C), decreasing EO content (Figure 5-5D) and decreasing molecular weight (Figure 5-5E). This correlation was independent of the oligomer valence and even more pronounced for compressive modulus data (Figure 5-5F-H). In order to combine the three oligomer-specific variables to one characteristic parameter, the ratio of LA content/EO content/M_n was calculated for each oligomer indicating the molecular balance of hydrophobic and hydrophilic domains (Figure 5-S5). Below a ratio of 0.003 mol/g, compressive strength and modulus were increased with increasing hydrophobicity, while mechanics tended to plateau or decrease for values higher than 0.010 mol/g.

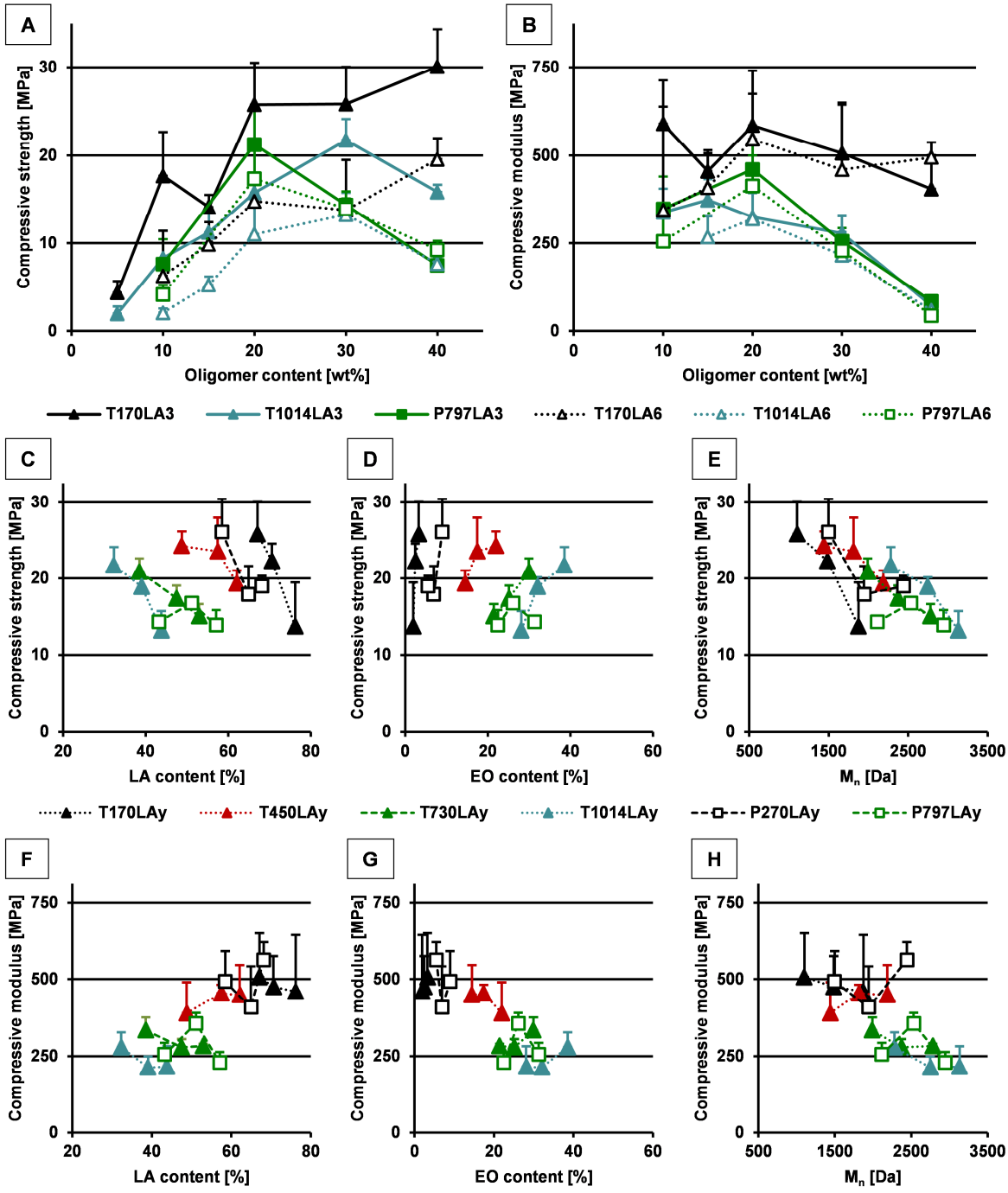

Figure 5-5. Mechanical properties of porous hybrid scaffolds in dependence of structure, composition and content (calculated for the hydroxyl-terminated precursor) of the oligomer. (A) Compressive strength and (B) compressive modulus as function of oligomer content. (C-E) Compressive strength and (F-H) compressive modulus of hybrid formulations with 30% oligomer as a function of oligomer LA content (C and F), EO content (D and G) and molecular weight (E and H) (n = 6).

5.5.4 Statistical analysis of compression test data. In addition to the correlations illustrated above for hybrids with 30% oligomer, we included all analyzed hybrid formulations in multiple linear regression models with backward exclusion of predictors of the compression test data to statistically analyze correlations between oligomer characteristics and mechanical properties of the hybrid scaffolds (Table 5-1).

Table 5-1. Results of multiple linear regression analysis of oligomer parameters on mechanical properties. M_n(total): total molecular weight of oligomer, M_n(LA): LA-derived fraction of M_n, M_n(EO): EO-derived fraction of M_n, C: total oligomer content in hybrid, N: number of oligomer arms (valence), R^2: regression coefficient of the model, β: standardized coefficient of the predictor, and p: level of significance.

Variables		Stage 1			Stage 2		
Depen-dent	Indepen-dent	R^2	β	p	R^2	β	p
Strength	M_n(total)	0.413	-0.048	0.867	0.414	-	-
	M_n(LA)		-0.315	0.098		-0.346	0.000
	M_n(EO)		-0.301	0.173		-0.337	0.000
	C		0.488	0.000		0.488	0.000
	N		0.162	0.000		0.163	0.000
Modulus	M_n(total)	0.436	0.564	0.047			
	M_n(LA)		-0.459	0.014			
	M_n(EO)		-0.919	0.000			
	C		-0.375	0.000			
	N		0.139	0.000			

Five predictors describing the hybrid composition were used: total oligomer content in hybrid (C), valence (N) and molecular weight of the oligomer (M_n), which was further subdivided into the LA- and EO-derived molecular weight fraction (M_n(LA) and M_n(EO)) in order to distinguish between hydrophobic and hydrophilic domains. While all independent parameters significantly ($p < 0.05$) contributed to the model for compressive modulus, M_n(total) did not significantly influence compressive strength ($p = 0.867$, stage 1). The last stage of each backward exclusion revealed highly significant contribution of all included predictors and absolute values of the

standardized coefficients (β) indicated C (or M_n(EO)) as the main factors of influence for compressive strength (and modulus). Regression coefficients (R^2), indicating contribution of the included predictors to the total variance of the model, were overall higher for compressive modulus as compared to compressive strength confirming results depicted for selected samples (Figure 5-5).

5.5.5 Effect of porosity on scaffold properties. The applied indirect rapid prototyping method enabled precise adjustment of scaffold architecture by variation of template structure. Four different scaffold porosities were generated by using templates with different strand diameter and varying strand spacing, and the effect on scaffold properties was investigated. SEM and μCT images showed that scaffold structure represented the negative replicate of the PCL template (Figure 5-6A, Figures 5-S6 and 5-S7). For template fabrication, two layers of PCL strands were extruded on top of each other before the next strand pair was deposited in perpendicular direction which determined the scaffold pore structure in the x-y level (XXYY pattern). The partial coalescence of the PCL strands further yielded pore interconnects in z direction and resulted in 100% pore interconnectivity. Analysis of the pore size indicated that the scaffold pores in x/y direction were 5-20% smaller than the expected diameter as predetermined by the PCL strands (Figure 5-6B). This can be explained by shrinkage of the hybrid structure during scaffold drying which is a result of evaporation of ethanol released during silane condensation. Nevertheless, scaffold structures exhibited no macroscopic crack formation. The comparison of the theoretical and final scaffold diameters revealed increasing shrinkage with increasing pore diameter, but no correlation with total scaffold porosity was found (Figure 5-6C). The stiffest formulation (T170LA3-40) was selected to investigate the effect of material porosity on mechanical properties of the hybrid scaffold. Mechanical parameters decreased from 30 MPa to 4 MPa (strength) and > 500 MPa to 120 MPa (modulus), when porosity increased from 44% to 68% (Figure 5-6D-F).

By analysis of all formulations with a theoretical porosity of 44%, composition-dependent shrinkage in the range of 8-21% was detected (Figure 5-S8). Increasing oligomer content generally reduced sol-gel-derived shrinkage by stabilization of the hybrid network due to increased degree of organic-inorganic cross-links which is in line with the observation of increased mechanical stability (e.g. T170LA3-40). This stabilizing effect of the oligomer on

hybrid structure, however, was reduced or even reversed with increasing molecular weight of the oligomer (Figure 5-3), which was referred to enhanced molecular flexibility.

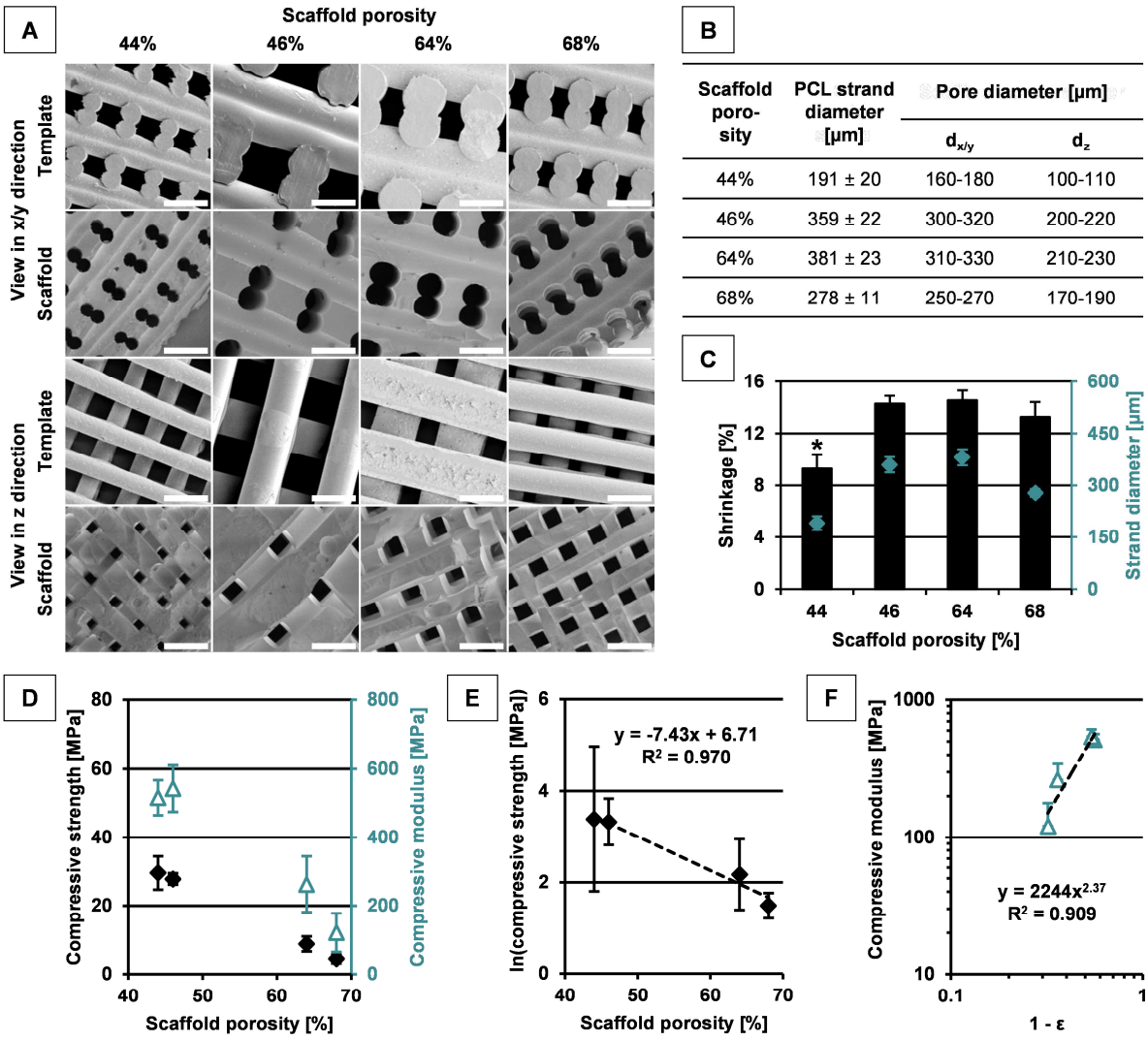

Scaffold poro-sity	PCL strand diameter [µm]	Pore diameter [µm]	
		$d_{x/y}$	d_z
44%	191 ± 20	160-180	100-110
46%	359 ± 22	300-320	200-220
64%	381 ± 23	310-330	210-230
68%	278 ± 11	250-270	170-190

Figure 5-6. Influence of material porosity on morphology and mechanical properties of T170LA3-40 scaffolds. (A) SEM images of PCL templates and corresponding hybrid scaffolds of different porosities. Scale bars represent 500 µm. (B) Strand diameters of PCL templates and diameter range of scaffold pores as determined from SEM images. Diameter $d_{x/y}$ representing the size of transverse and longitudinal pores in x/y direction and d_z indicating the minimal size of pore interconnects in scaffolds. (C) Shrinkage of scaffolds during fabrication as calculated from scaffold diameter and inner template diameter (bars, left y-axis) and strand diameters of PCL templates representing the theoretical pore diameter in the x/y direction (diamonds, right y-axis) (* indicates $p < 0.01$). (D-F) Mechanical properties of different porous T170LA3-40 hybrids. (D) Compressive strength and compressive modulus as a function of scaffold porosity, (E) logarithmic plot of compressive strength vs. porosity and (F) compressive modulus as a function of 1-ε with ε representing relative scaffold porosity (n = 6).

5.5.6 Degradation study. The diversity of the oligomer platform as established in this study is based on the modification of ethoxylated core molecules with varying length of oligomerized lactide domains. A selected set of representative formulations with varying oligo(lactide) content and hydrophilicity was investigated for *in-vitro* degradation in PBS at 37 °C. Stereomicroscopic images showed composition-dependent differences of the scaffold morphology (Figure 5-7A). While wet LA-free hybrids appeared transparent, the introduction of oligo(lactide) domains rendered the material opaque. Heat sterilization of T1014-based scaffolds resulted in a yellowish discoloration which was not found in the non-sterilized control (T1014-20-NS). The discoloration disappeared over the course of the degradation study and was also observed during oligomer synthesis in melt. As color intensity in the synthesized oligomers correlated with degree of core alcohol ethoxylation, the discoloration was attributed to thermal transformation products of additives or impurities of the ethoxylated core alcohols. For all formulations, significant dimensional changes were not detected before day 67. Thereafter, a correlation between volume decrease and LA content of the hybrid became apparent (T170LA6-40 > T170LA6-20 > T170LA3-20 > T1014LA3-20). Images further show the appearance of cracks in LA-free scaffolds upon drying which became larger with increasing degradation time. In order to detect the release of acidic degradation products, pH of incubation media was monitored and an initial pH decrease to 6.2 at day 7 was observed (Figure 5-7B). The initial acid release was strongest within the first 7 days and decreased until day 21. A second and more moderate pH decrease between days 21 and 42 was observed for LA-containing formulations which correlated with LA content. With increasing degradation time, the acid release was slowly reduced and no significant pH decrease was detected after 175 days. Profiles of dry weight over time showed continuous decrease of the residual mass without delay for all formulations (Figure 5-7C). The weight loss was accelerated with increasing LA content of the hybrids. LA-rich T170LA6-40 scaffolds completely degraded within 200 days, while degradation of the other LA-containing formulations was completed after approximately one year. LA-free T1014-derived hybrids lost more than 60% of their initial dry weight over the course of this study (368 days), which was not assumed from scaffold morphology (Figure 5-7A).

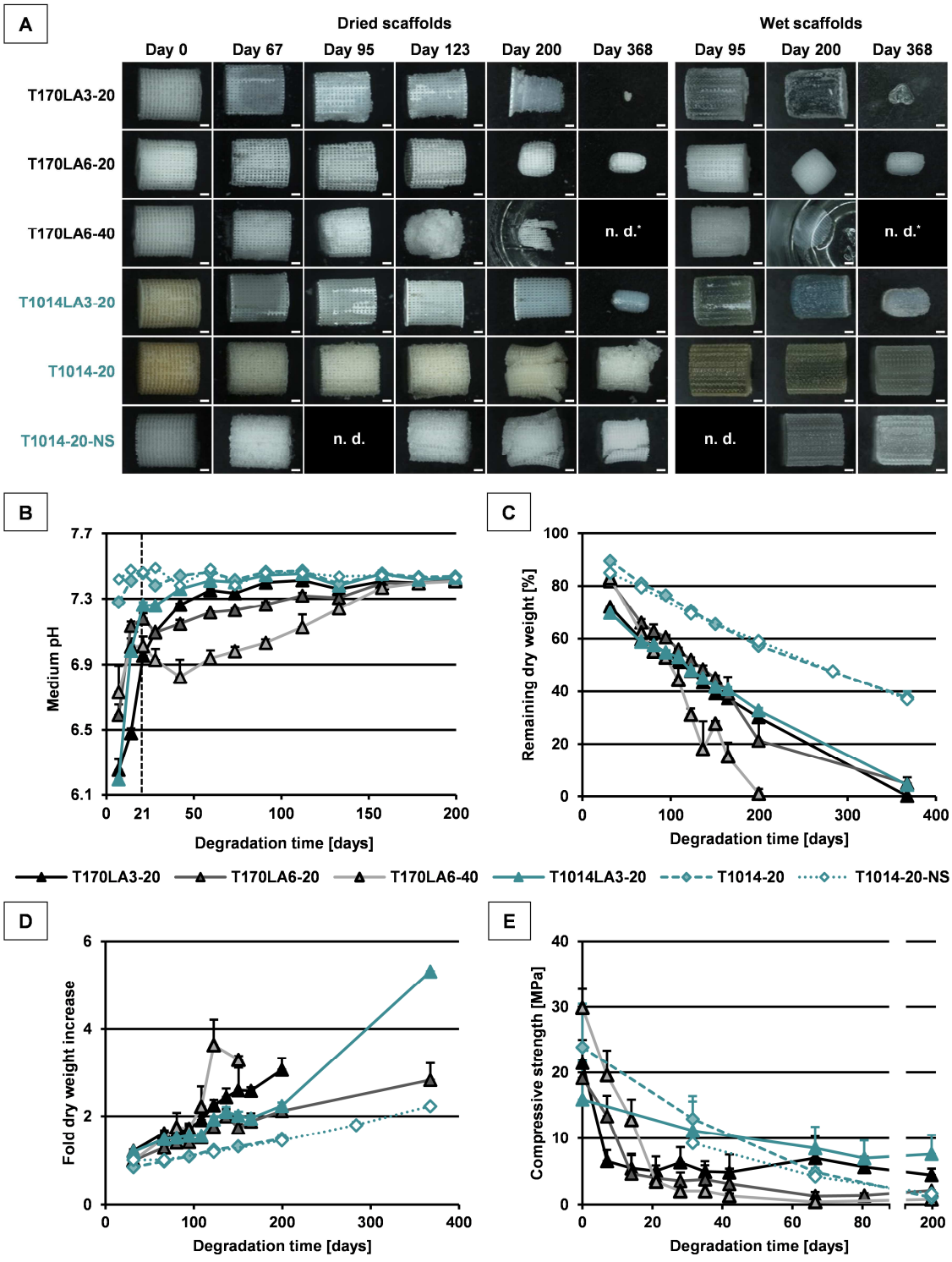

Figure 5-7. Degradation characteristics of selected hybrid scaffolds in PBS at 37 °C. (A) Stereomicroscopic images of wet and dried scaffolds at selected degradation time points. Missing images were not determined (n. d.) or could not be taken due to complete degradation (n. d.*). Scale bars represent 1 mm. (B) pH of degradation media at selected time points (medium pH was determined semi-weekly). (C) Remaining dry weight and (D) water content of the degraded scaffolds. (E) Compressive strength of dried scaffolds at selected time points (n = 5).

Water content correlated with dry weight loss but material swelling was comparably moderate (Figure 5-7D). In order to evaluate changes of mechanical properties over time, compressive strength of dried specimens was determined. Reduction of mechanical stability within the first 21 days was in accordance with the extent of initial acid release, but not directly correlated to the LA content of the oligomer fraction (Figure 5-7E). The decrease of compressive strength that was determined during degradation after week 3, however, correlated with LA content of the hybrids which was clearly visible for T170LAy-derived materials. T170LA6-derived hybrids completely lost their mechanical stability over the course of this study which is in accordance with the observed weight loss. A strong decrease of compressive strength was also determined for T1014-containing samples without oligomerized LA chains (< 2 MPa at 200 days), which was not expected from the remaining dry weight (~ 60%). Heat sterilization did not affect degradation behavior as the degradation profiles of T1014-20 (sterilized) and T1014-20-NS (non-sterilized) hybrids appeared congruent (Figure 5-7B-E).

5.5.7 Cell culture. Cytocompatibility of hybrid scaffolds was investigated by cell culture experiments with primary cells (hASC) and efficient dynamic seeding on T170LA3-20 hybrids was observed (seeding efficacy: 46.1 ± 5.8%). Linear increase of cell number within 14 days (R^2 = 0.9901) indicated continuous proliferation, while cell number was nearly doubled (Figure 5-8A). Microscopic images confirmed the ability of cells to infiltrate the entire pore network and attach to pore walls in a spread morphology (Figure 5-8C, D). While no ALP activity was detected in cells seeded on hybrid scaffolds in control medium (day 1), the activity continuously increased after transfer to osteogenic medium (R^2 = 0.9999) and significantly exceeded that of the 2D control after 14 days indicating osteogenic differentiation (Figure 5-8B). Weigert-Van Gieson staining further suggested significant and homogeneous matrix formation within the scaffolds (Figure 5-8E).

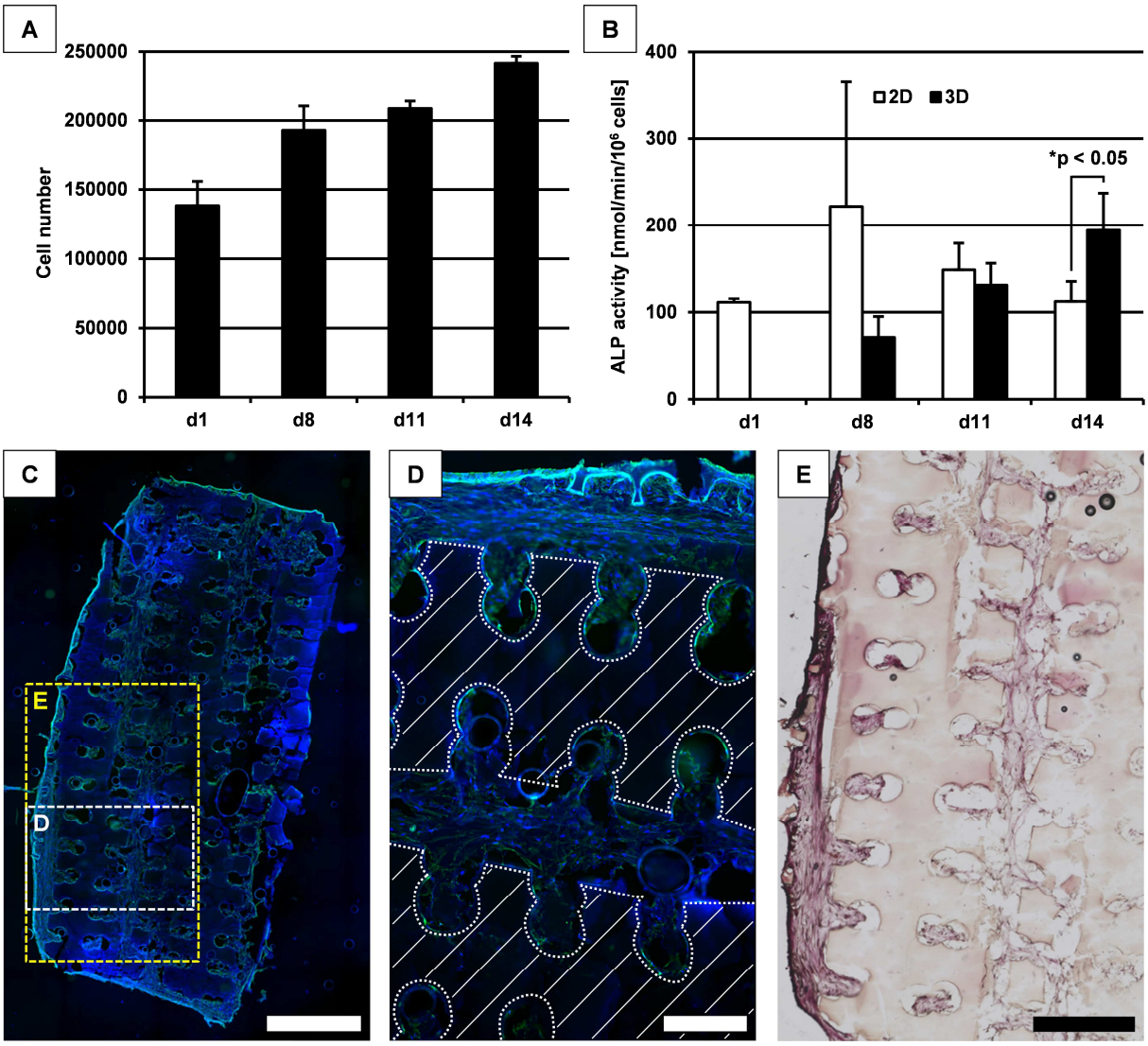

Figure 5-8. Adhesion and proliferation characteristics of hASC on T170LA3-20 scaffolds. (A) Cell number and (B) ALP activity over 14 days. Microscopic images of (C-D) DAPI/phalloidin-stained and (E) Weigert-Van Gieson-stained scaffold cryosections after 28 days. Dashed squares in (C) indicate the approximate location of histological segments (D) (white) and (E) (yellow) within scaffold section. Hatched areas in (D) highlight scaffold material and dashed lines indicate the location of transverse and longitudinal pores. Scale bars represent 1 mm (C), 250 µm (D) or 500 µm (E) (n = 4).

5.6 DISCUSSION

The presented organic/inorganic hybrid concept is based on a previously established material design in which silane-functionalized non-degradable oligovalent alcohols were covalently integrated into a TEOS-based silica sol upon curing.[54] With the motivation to introduce adjustable degradability into such hybrid material, the organic component was modified with hydrolytically degradable oligo(D,L-lactide) moieties by ring-opening polymerization starting from tri- or tetravalent alcohols. Lactide was incorporated in small quantity in order to obtain low molecular weight oligomers that enable high cross-linking degrees and adaptable material engineering.[53,79] A number of at least three repeating units of lactic acid was used which is minimally required to yield significant oligoester degradability.[200,201] In contrast to previously established methacrylated three-armed macromers of similar composition,[53] we here faced the challenge to isolate and purify the hydroxyl-terminated oligomers in order to make them available for stoichiometric functionalization with ICPTES. This strategy was preferred, because the oligomers can be best purified with aqueous medium, but low stability of the silanized products was expected in presence of water. While fractional precipitation of hydrophilic oligomers was observed in pure water, precipitation in brine combined the high purification efficiency of an aqueous precipitation medium with effective separation of the product (Figs. 1C, 2), which can be explained with decreased solubility of hydrophilic oligomers in saturated salt solutions (salting-out effect).[202] Proton NMR data illustrated that LA content of the oligomer was well controlled by LA feed. The effective removal of stannous octoate was another important aim of the purification protocol since residues of the catalyst could have initiated ester hydrolysis and/or transesterification during the following oligomer functionalization with ICPTES at 120 °C.[203] Stannous octoate was therefore used in a concentration at the lower end of the reported range[100] and the absence of significant catalyst and solvent signals in NMR confirmed the efficiency of the applied purification protocol. GPC data complemented the NMR results and demonstrated adjustability of the LA content in small increments (Figure 5-3). The adjustable oligomer composition together with the obtained molecular weight range of 1100-3200 Da opens potential for fabrication of hybrid materials with tunable material properties. Covalent integration of the macromers into the silica network was enabled by functionalization with ethoxysilane groups as previously shown[54] and the resulting reactive TxLAy-Si and PxLAy-Si

derivatives can be defined as macromers in our interpretation of the IUPAC definition.[19,53] Effective ICPTES conversion was detected which is in accordance with literature and our previous findings for LA-free hybrids.[54,204] Overall, successful synthesis of a set of reactive macromers with precisely adaptable molecular weight, hydrophilicity and content of degradable domains was shown.

The applied indirect rapid prototyping method was previously established to fabricate glass-based hybrids containing non-degradable organic macromers.[54] This method also enabled processing of the full set of synthesized LA-containing analogs in different hybrid compositions and was robust to the different viscosities of the sol mixtures that had to be filled into PCL molds. This is one significant advantage of indirect templating over direct printing. The efficient incorporation of the macromers as hybrid building block (content of up to 55 wt%) allowed for the desired adaption of scaffold mechanics as a function of cross-linking density and oligomer chemistry.[78,205] With regard to applicability for hard tissue regeneration, scaffolds should have an elasticity similar to the tissue it is intended to replace in order to avoid stress shielding, while material strength should meet or exceed the range of the target tissue to prevent fatigue or failure.[206,207] All formulations complied with the requirements for compressive strength of cancellous bone ($\geq$ 2-12 MPa), while more than 80% of the hybrids exactly met the published range of compressive modulus (50-500 MPa) (Figure 5-S4).[70,186] The broad range of mechanical properties that was obtained with the tested hybrid formulations indicates the outstanding adaptability of the presented material concept to different applications as commonly intended with sol-gel-derived class II hybrids.[3,192] The large set of data gathered here, further enabled the identification of correlations between mechanical properties and hybrid composition expanding the current knowledge on glass/organic class II hybrid materials (Figure 5-5, Figure 5-S5). Increased oligomer content resulted in increased compressive strength and decreased compressive modulus which is in accordance with literature.[187,192] These findings can be attributed to increased bridging of fracture-sensitive silica bonds (leading to improved strength) and decreased volumetric density of rigid Si-O-Si bonds (leading to reduced modulus).[54,208,209] The highest strength and stiffness were obtained for hybrids containing short-chained oligomers with low EO content and high LA conversion and can be explained by low oligomer flexibility.[53,79] These hybrids accordingly exhibited low shrinkage (Figure 5-S8). The correlation function further suggests that a combination of maximum compressive strength and modulus could be expected when cross-linker oligomers with LA/EO/M_n ratios of 0.003-0.011 mol/g were

used – theoretically, this would correspond to three-armed oligomers with a T180 or a T190 core (Figure 5-S5).

When mechanical properties were compared with those of corresponding LA-free hybrids, the introduction of oligo(lactide) domains yielded materials of comparable strength, but the maximum stiffness was significantly increased (Figure 5-S4)[54] which is in accordance with findings for purely organic matrices composed of PLA and PEG blocks.[78] No significant effect of oligomer valence (three- vs. four-armed macromers) was detected which is in accordance with the characteristics of analogous hybrids with non-degradable macromers.[54] Multiple linear regression analysis of all synthesized hybrid scaffolds confirmed the illustrated correlations and pointed out that the specific ratio of LA to EO domains in the oligomer better correlated with compressive strength and modulus as the total molecular weight. This demonstrates the importance of chain flexibility besides cross-linking density (Table 5-1).[53,79] The statistical analyses revealed total oligomer content and EO content as the main factors significantly influencing compressive strength and modulus, respectively, which is in agreement with previously found correlations for analogous LA-free hybrids.[54] An indirect correlation between organic content and material shrinkage was described by Tian et al. for PCL-containing, TEOS-derived sol-gel hybrids, but possible effects of the macromer molecular weight were not described.[35] The absence of macroscopic crack formation let us assume that scaffold shrinkage did not significantly affect material stability.

3D-Printing (fused deposition modeling) was used for fabrication of a well-defined XXYY-patterned template structure, which enabled fabrication of an open porous hybrid network structure[51] with comparatively large pore interconnects (60-70% of pore diameter). The lowest pore size of 100-110 µm as determined from the length of the squared pore interconnects corresponds to a pore diagonal of 140-155 µm (Figure 5-6A, B). Therefore, all pores were significantly larger than 100 µm enabling cell infiltration. The potential to create pores greater than 300 µm, a size recommended for sufficient scaffold vascularization,[51,69] has been shown. Indirect prototyping also enabled porosity adaptation within the physiologically relevant range of cancellous bone (50-90%[69]). An exponential correlation between scaffold porosity and compressive strength was found and the calculated slope of 7.43 (Figure 5-6E) is in accordance with literature and our previous findings for LA-free hybrids.[4,54,166] Furthermore, a power law relationship between compressive modulus and material porosity was identified as indicated by

logarithmic plot (Figure 5-6F) and the calculated exponent value of 2.37 is similar to that reported for poly(lactide-*co*-glycolide) (PLGA) scaffolds (2.4).[73] These findings suggest that hybrid mechanical properties is also controlled by 'scaffold porosity' independent of its composition and practicably independent of pore size.

Biodegradability is an important characteristic for material application in a regenerative application, but long-term degradation of organic/inorganic composites and hybrids have not yet been broadly investigated. In most studies, hybrid degradability has been assessed for not longer than 1-3 months. The longest investigation of class II hybrid degradation looked at a period of just 140 days.[193] This motivated a long-term degradation analysis of the presented hybrid matrices over more than a year *in vitro*. Scaffold degradation was well controlled by hybrid composition and weight loss correlated with content of degradable LA domains in the hybrids (R^2 = 0.932) (Figure 5-S9A). An even stronger correlation was obtained when the weight loss rate was depicted as a function of LA/EO weight ratio of the incorporated oligomer (R^2 = 0.984) (Figure 5-S9B) demonstrating the importance of hydrophilic domains for the control of water penetration into the lipophilic oligoester segments.[38,210] These findings are in accordance with degradation characteristics of purely organic PLA/PEG matrices,[200,211] but have not yet been described for hydrolytically degradable class II hybrids. The incorporation of enantiopure oligo(lactide) or other hydrolytically degradable oligoester domains would hold further promise to adjust material degradation, but was not investigated in this study.[53,212] Not only was the degradation time widely adjustable, the weight loss interestingly followed a linear kinetic in all formulations (0.2-0.5 wt%/d, R^2: 0.964-0.996) (Figure 5-7C), which has been reported for other class II hybrids.[187,190] This can be explained by hydrolysis of the inorganic Si-O-Si network[70,74] combined with oligoester cleavage in LA-containing formulations. The observed continuous matrix degradation is advantageous over the complex and less predictable degradation behavior of poly(lactide)-derived (organic) materials[9,193] in which abrupt release of acidic degradation products in late stages of bulk degradation can cause a strong inflammatory response.[182,186] Scaffolds completely degraded within 6-12 months which is a crude approximation of the *in vivo* degradation of hydrolytically degradable materials[75] and therefore covers a physiologically relevant time frame for bone regeneration.[3,51] In combination with only moderate material swelling during degradation (Figure 5-7A, D), the materials appear promising for application in confined defects. The observed strong decrease of compressive strength within the first 21 days (Figure 5-7E) which was comparable to that of another lactide-derived class II hybrid,[193]

correlated with initial medium acidification (Figure 5-7B), but no correlation with LA content of the hybrids was found. The mechanical destabilization was therefore attributed to sulfuric acid residues which presumably were not completely extracted from the hybrids by THF and ethanol during template leaching and might have initiated Si-O-Si hydrolysis upon scaffold incubation in PBS.[74,94] The existence of acid residues was indicated by the correlation between initial medium acidification and content of the sulfuric acid-containing silica sol that was used for hybrid fabrication (Figure 5-S9C). The extent of acid release within the first 21 days correlated with compressive strength of the hybrid and molecular weight of the oligomer suggesting that retention of the inorganic acid depended on cross-linking degree and distance between organic-inorganic cross-links in the hybrid network (Figure 5-S9D).[3,94] Mechanical properties, here reported in dry condition, naturally deteriorated upon degradation (Figure 5-7A, E). Nevertheless, especially formulations with low LA content (TxLA3) met the mechanical requirements of cancellous bone for more than 6 months[70,186] and many formulations maintained mechanical properties potentially suitable for osteochondral regeneration.[213,214] The observed initial loss of mechanical stability represents a limitation of the presented hybrid material. In order to enable use as load-bearing implant for hard tissue regeneration, the promising initial hybrids mechanics would have to be conserved over a longer time range.[51,166] One strategy to realize such properties involves a reduction of sulfuric acid residues in the hybrid. To this end, optimization of acid extraction or adjustment of the applied amount of catalytic acid to hybrid composition serve as possible strategies but would demand for a careful reformulation of the TEOS sol.[94]

In cell culture experiments, cytocompatibility of the degradable hybrid scaffolds with human stem cells was shown which confirmed the findings for analogous LA-free hybrids (Figure 5-8).[54] Pore sizes of significantly more than 100 µm enabled quantitative cell migration throughout the full scaffold volume. As the investigated scaffold architecture represented the lower end of adjustable material porosity (44%) and pore size, comparable or even improved cell behavior can be assumed for scaffolds with higher porosity (Figure 5-6). Continuously increasing ALP activity indicated potential for hASC differentiation toward the osteogenic lineage. With regard to hybrid composition, one of the formulations which offered mechanical and degradative properties compatible with cancellous bone, namely T170LA3-20, was exemplarily selected (Figure 5-S4, Figure 5-7C). A further key property of glass-based hybrid materials is their potential bioactivity enabling stable bond to host bone.[38] Although not investigated in this study,

the existence of oligoester functionalities in the presented hybrids might offer potential for apatite deposition without additional incorporation of calcium.[215] A lack of biomineralization for a specific hybrid formulation, on the other hand, would allow for consideration of target tissues other than bone that demand for precisely adjusted mechanical properties, such as cartilage or tendon.[216]

5.7 CONCLUSION

A platform of three- and four-armed degradable oligomers with adjustable content of oligo(D,L-lactide) domains and varying degrees of ethoxylation was synthesized, characterized and activated for covalent integration in TEOS-based glass hybrids. Macroporous scaffolds of predefined structures were fabricated from a series of hybrid combinations by an indirect rapid prototyping method. Uniform *in vitro* degradation of the hybrid scaffolds at a physiologically relevant rate of 0.2-0.5 wt%/d was determined which was controlled by oligoester content and material hydrophilicity. Precise adjustability of the mechanical properties (compressive strength: 2-30 MPa, compressive modulus: 44-716 MPa) covering the range described for cancellous bone and beyond was demonstrated. The set of different hybrid formulations enabled the identification of the parameters total content, oligo(ethylene oxide) content, oligo(lactide) content and molecular weight of the organic component as well as material porosity as factors that statistically affected mechanical properties. Direct contact experiments with hASC further revealed hybrid cytocompatibility. In summary, the combination of reproducible macromer synthesis together with a well-controlled scaffold fabrication process enabled the detection of relevant structure-property-relationships of the hybrid scaffolds which opens potential for tailoring material characteristics toward specific regenerative applications.

5.8 ACKNOWLEDGEMENTS

Financial support by the AiF Projekt GmbH (grant number: KF2734502MU1) and the German Research Council (DFG SFB/Transregio 67, project A1) is gratefully acknowledged. The authors thank Bernhard Rieger (Department of Mechanical and Energy Engineering, HTWK Leipzig) for access to the compression testing equipment, Ulf Anderegg (Department of Dermatology, Venereology and Allergology, Leipzig University) for support in the preparation of histological sections, Lothar Hennig (Department of Organic Chemistry, Leipzig University) for access to NMR spectroscopy and Ricardo Bernhardt (Max-Bergmann-Center of Biomaterials, Dresden Technical University) for support in µCT analysis. We also thank Jörg Lenzner (Department of Experimental and Semiconductor Physics, Leipzig University) for access to SEM, Rudi Loth

(Institute of Pharmacy, Leipzig University) for support in the initial phase of this work and Annett Starke (Institute of Pharmacy) for assistance in the degradation study.

5.9 SUPPLEMENTARY INFORMATION

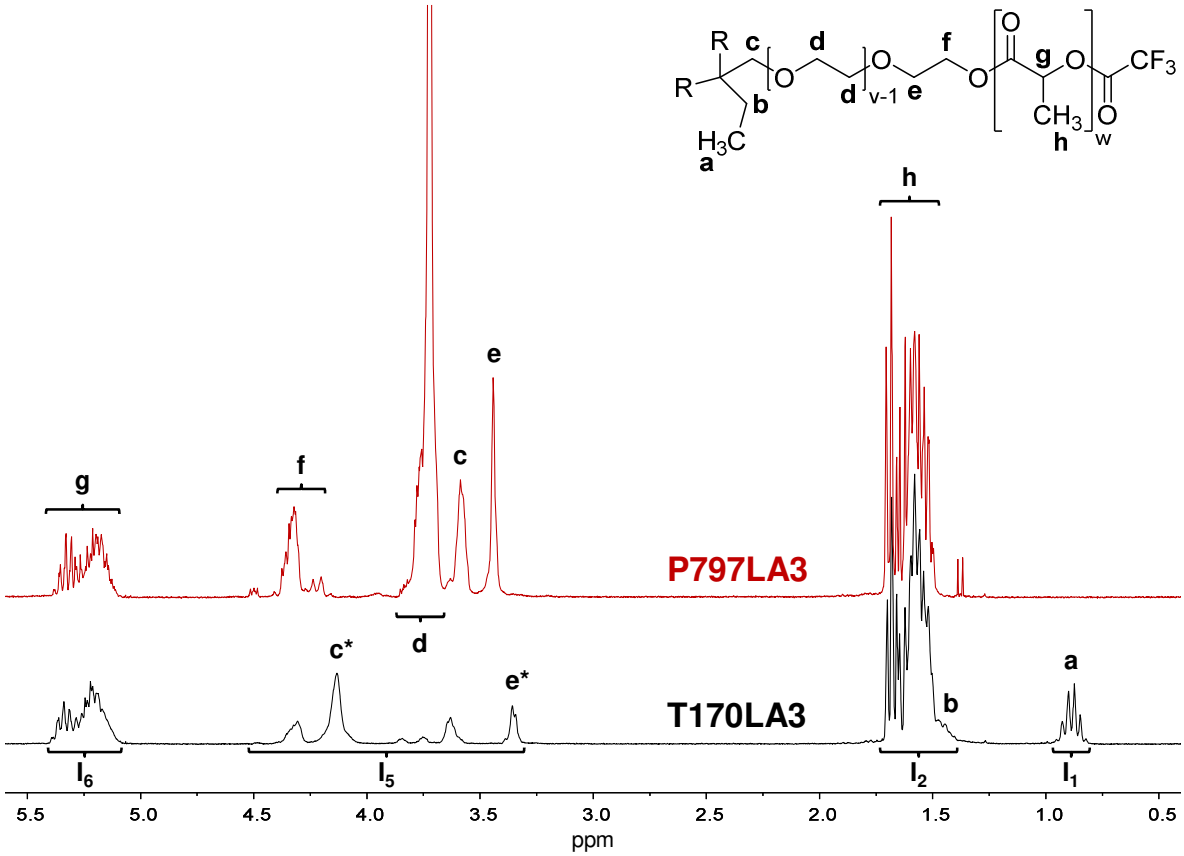

Figure 5-S1. Representative ^{1}H NMR spectra of three- (T170LA3) and four-armed (P797LA3) oligomers after derivatization with trifluoroacetic anhydride (TFAA) in $CDCl_3$. Label c* refers to methylene protons in α-position to ester hydroxyls in a non-ethoxylated arm. Label e* refers to methylene protons in α-position to core ethers in a mono-ethoxylated arm. I_x represent the integrals used to determine oligomer composition. TFAA supplementation enabled determination of PxLAy composition, because LA-related proton signals (g, h) were uniformly shifted without overlapping with core protons. LA content of PxLAy was determined from I_2 (LA-C**H**$_3$ protons) and I_5 (PETEO-C**H**$_2$- protons). Signals from residual water (1.65-1.90 ppm) disappeared upon TFAA addition due to its consumption for TFAA hydrolysis and formation of trifluoroacetic acid (10.5-11.2 ppm, not shown).

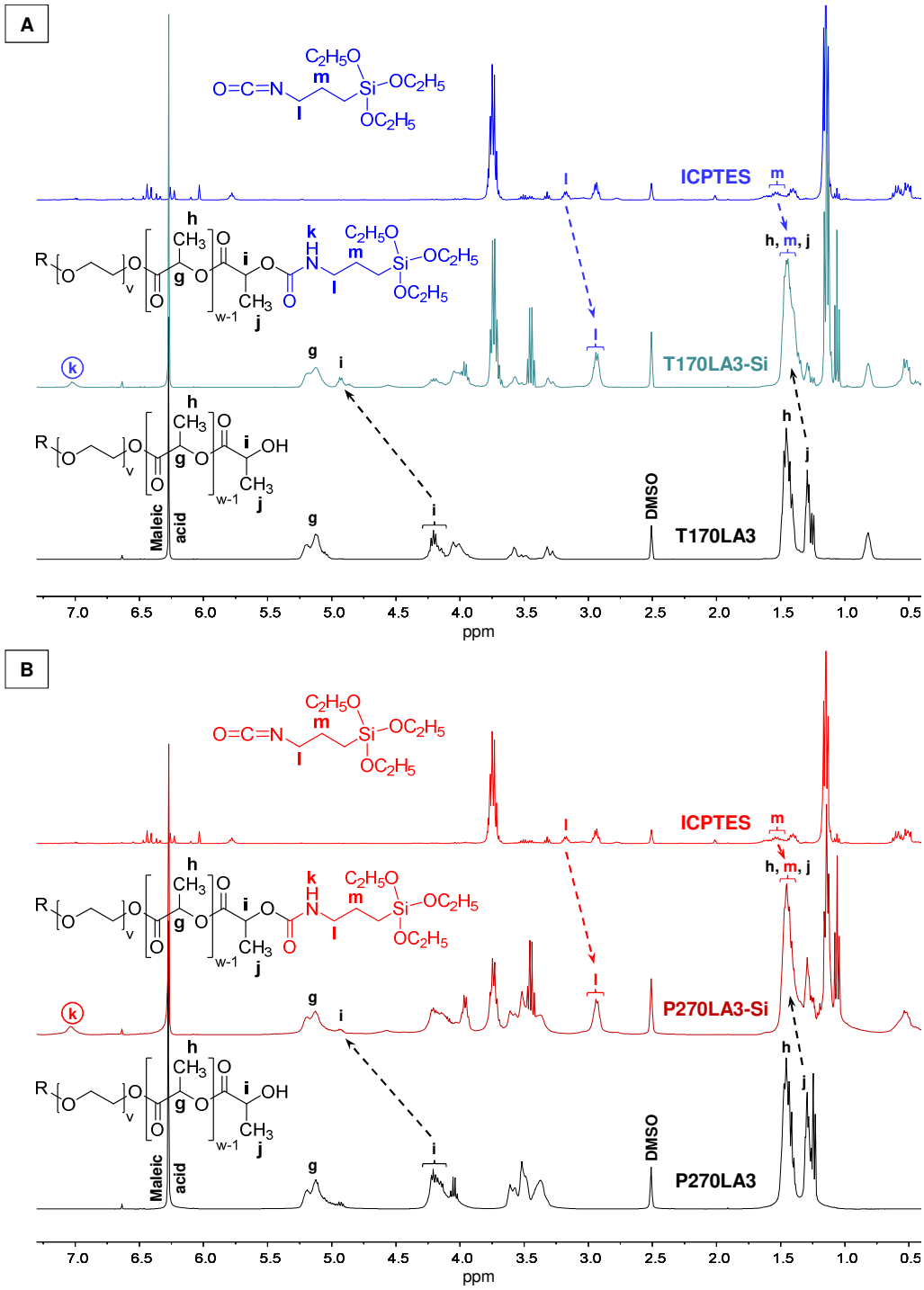

Figure 5-S2. NMR analysis of oligomer derivatization with 3-isocyanatopropyltriethoxysilane (ICPTES). Representative 1H NMR spectra of functionalized three-armed TxLAy-Si (A) and four-armed PxLAy-Si macromers (B) compared with pristine oligomers and ICPTES as determined in DMSO-d6. Upon derivatization of the oligomers with the silane-coupling agent, relevant signals significantly shifted (i, j, l, m) or newly appeared (k) illustrating conversion of ICPTES to the oligomers. Nearly complete disappearance of the ICPTES-derived signals at 3.14-3.22 ppm (l) and 1.51-1.57 ppm (m) indicated effective ICPTES conversion with three- and four-armed macromers possibly accompanied by minor isocyanate hydrolysis.

Oligomer type		Content of the non-silanized oligomer (w/w) in the silica sol					
		5%	10%	15%	20%	30%	40%
T170	LA3	T170LA3-5 *8.7*	T170LA3-10 *16.8*	T170LA3-15 *24.3*	T170LA3-20 *31.2*	T170LA3-30 *43.8*	T170LA3-40 *54.8*
	LA4.5	*	T170LA4.5-10 *15.2*	-	T170LA4.5-20 *28.7*	T170LA4.5-30 *40.8*	-
	LA6	*	T170LA6-10 *14.0*	T170LA6-15 *20.5*	T170LA6-20 *26.8*	T170LA6-30 *38.5*	T170LA6-40 *49.4*
T450	LA3	T450LA3-5 *8.0*	T450LA3-10 *15.4*	T450LA3-15 *22.5*	T450LA3-20 *29.1*	T450LA3-30 *41.3*	T450LA3-40 *52.3*
	LA4.5	*	T450LA4.5-10 *14.3*	-	T450LA4.5-20 *27.2*	T450LA4.5-30 *39.1*	T450LA4.5-40 *49.9*
	LA6	T450LA6-5 *6.9*	T450LA6-10 *13.5*	T450LA6-15 *19.9*	T450LA6-20 *26.1*	T450LA6-30 *37.7*	T450LA6-40 *48.4*
T730	LA3	T730LA3-5 *7.3*	T730LA3-10 *14.2*	T730LA3-15 *20.9*	T730LA3-20 *27.2*	T730LA3-30 *39.1*	T730LA3-40 *49.9*
	LA4.5	*	T730LA4.5-10 *13.5*	-	T730LA4.5-20 *25.9*	T730LA4.5-30 *37.5*	T730LA4.5-40 *48.3*
	LA6	*	*	T730LA6-15 *19.1*	T730LA6-20 *25.0*	T730LA6-30 *36.4*	T730LA6-40 *47.1*

T1014	LA3	T1014LA3-5 *7.0*	T1014LA3-10 *13.7*	T1014LA3-15 *20.1*	T1014LA3-20 *26.2*	T1014LA3-30 *37.9*	T1014LA3-40 *48.7*
	LA4.5	*	T1014LA4.5-10 *13.1*	-	T1014LA4.5-20 *25.3*	T1014LA4.5-30 *36.7*	T1014LA4.5-40 *47.5*
	LA6	*	T1014LA6-10 *12.7*	T1014LA6-15 *18.8*	T1014LA6-20 *24.7*	T1014LA6-30 *36.0*	T1014LA6-40 *46.6*
P270	LA3	P270LA3-5 *8.9*	P270LA3-10 *17.1*	-	P270LA3-20 *31.8*	P270LA3-30 *44.4*	P270LA3-40 *55.4*
	LA4.5	P270LA4.5-5 *8.0*	P270LA4.5-10 *15.5*	-	P270LA4.5-20 *29.1*	P270LA4.5-30 *41.3*	P270LA4.5-40 *52.3*
	LA6	*	*	-	P270LA6-20 *27.4*	P270LA6-30 *39.3*	P270LA6-40 *50.2*
P797	LA3	*	P797LA3-10 *14.9*	-	P797LA3-20 *28.3*	P797LA3-30 *40.3*	P797LA3-40 *51.3*
	LA4.5	P797LA4.5-5 *7.2*	P797LA4.5-10 *14.1*	-	P797LA4.5-20 *26.9*	P797LA4.5-30 *38.7*	P797LA4.5-40 *49.5*
	LA6	*	P797LA6-10 *13.5*	-	P797LA6-20 *25.9*	P797LA6-30 *37.5*	P797LA6-40 *48.3*

Figure 5-S3. Overview of the fabricated hybrid formulations. Code of the materials containing silanized macromers (TxLAy-Si or PxLAy-Si) as well as content (wt%) of silanized derivatives in the hybrid sol (italicized). Formulations without code were not investigated (-) or did not result in analyzable scaffolds (*).

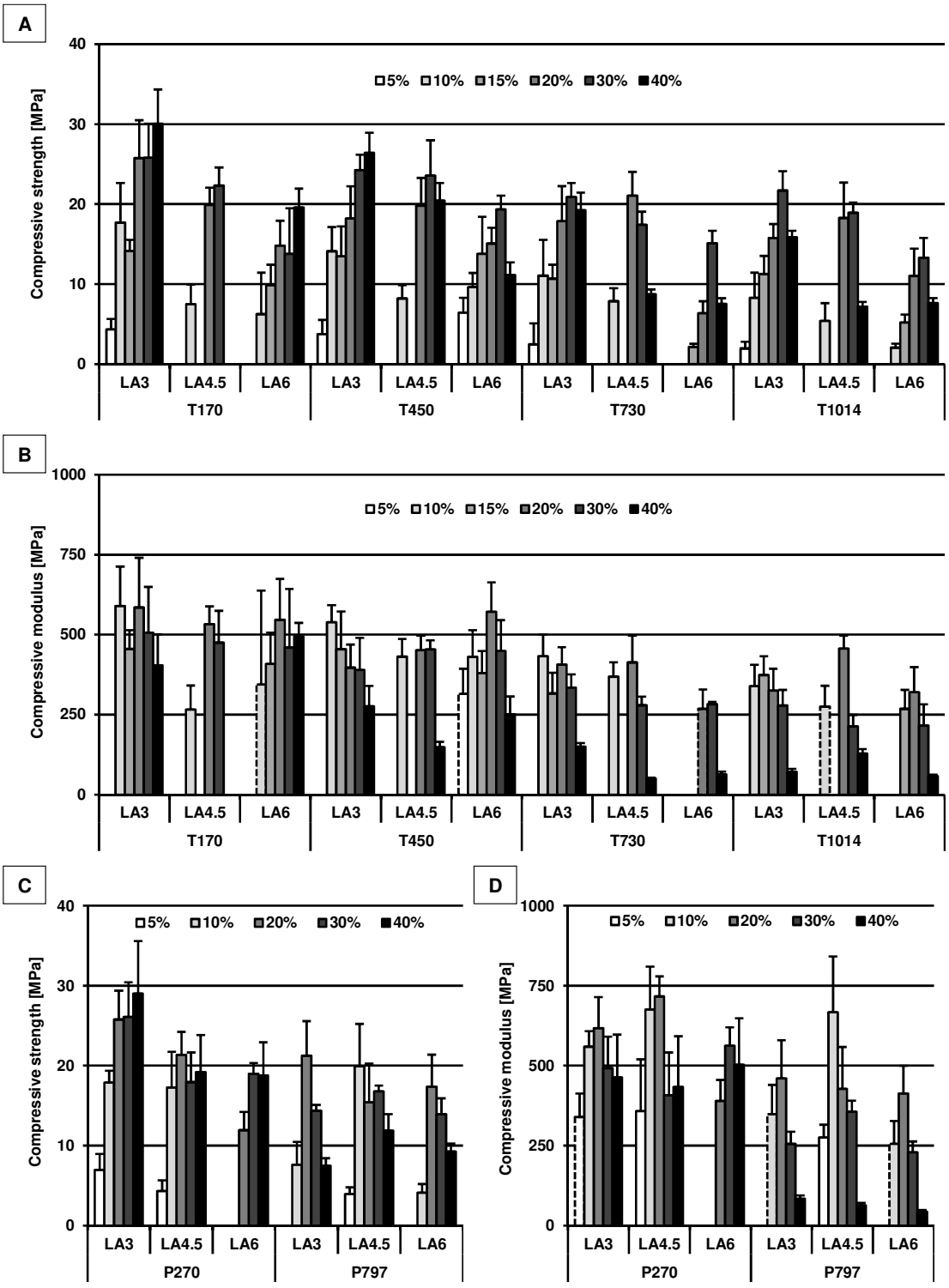

Figure 5-S4. Overview of the mechanical properties upon uniaxial compression of fabricated hybrid scaffolds in dependence of structure, composition and content of the organic oligomer. (A, C) Compressive strength and (B, D) compressive modulus of hybrids containing silanized three-armed TxLAy-Si (A, B) or four-armed PxLAy-Si (C, D) macromers. Dashed bars correspond to brittle scaffolds and represent compressive moduli as determined from comparatively jagged, hard to analyze stress-strain curves (n = 6).

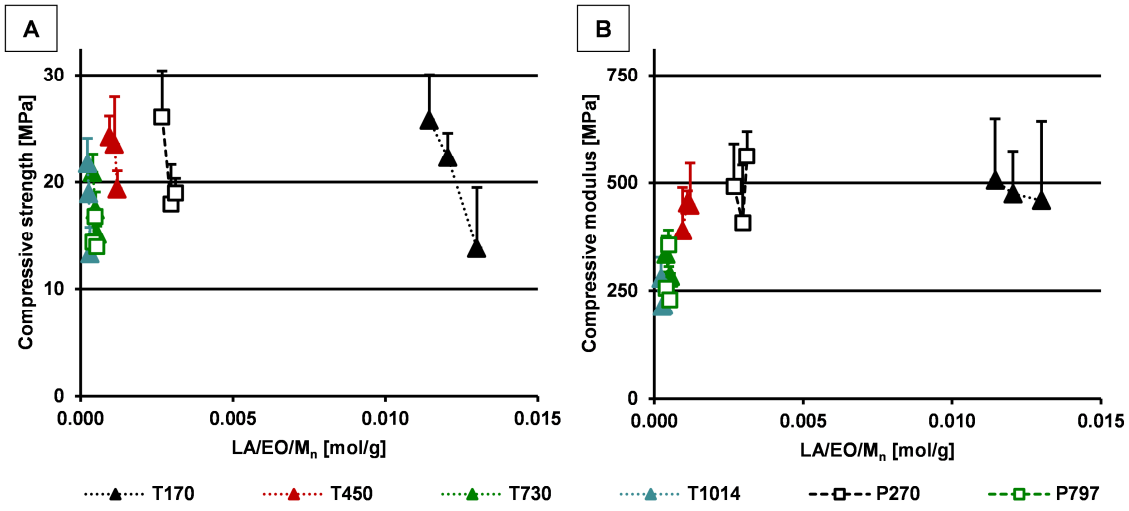

Figure 5-S5. Correlation between hybrid mechanics and structure characteristics of synthesized oligomers. (A) Compressive strength and (B) compressive modulus of scaffolds with 30% oligomer in dependence of the oligomer-specific ratio of LA content to EO content and molecular weight (M_n) expressing the molecular balance of hydrophilic and hydrophobic domains. At values below a threshold ratio of 0.003 mol/g compressive strength and modulus were increased with increasing hydrophobicity, while mechanics tended to plateau (modulus) or decrease (strength) for values higher than 0.011 mol/g. The correlation was more pronounced for compressive modulus which is in accordance with the data shown in Figure 5-5 (n = 6).

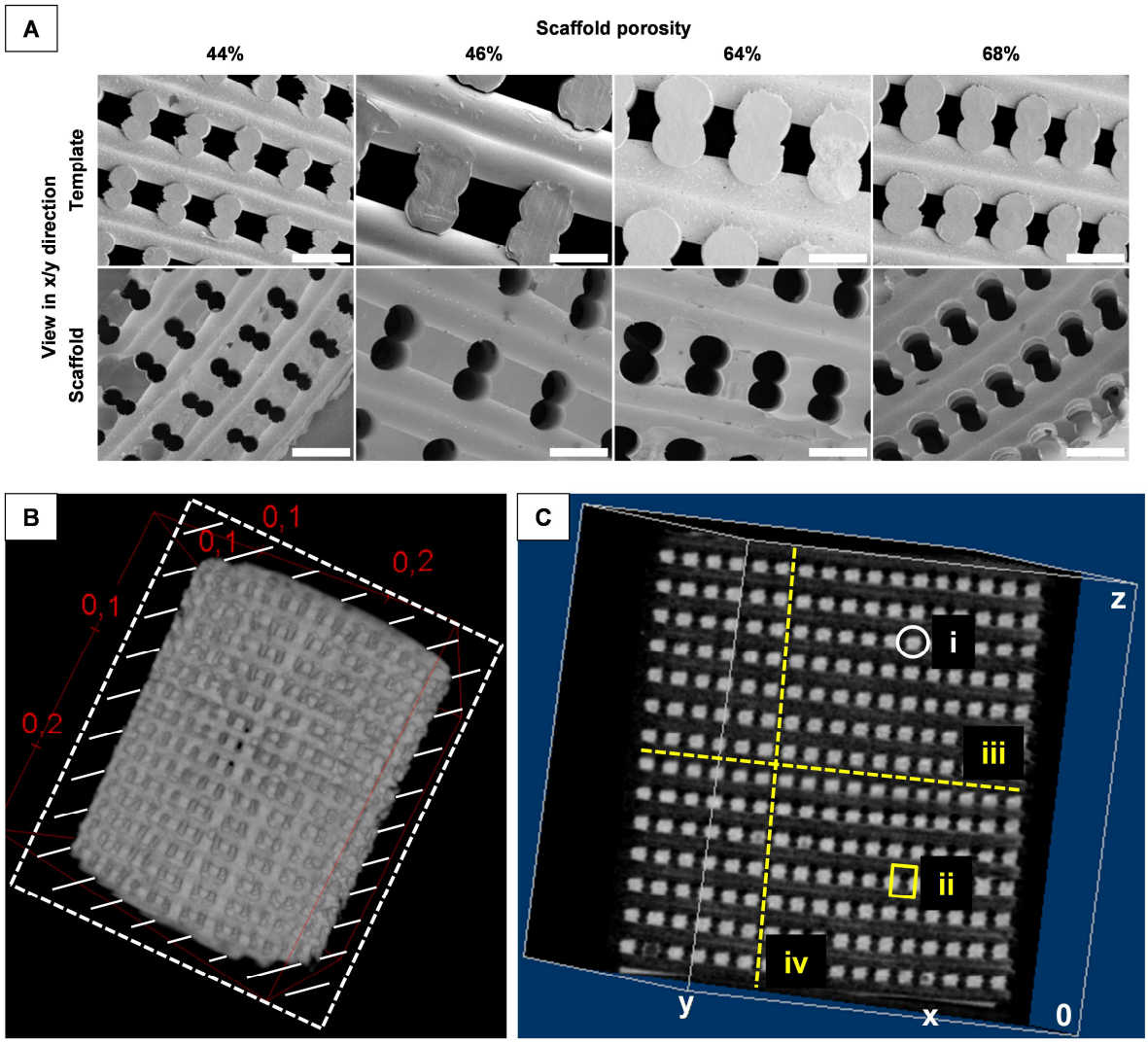

Figure 5-S6. Illustration of template and scaffold structure of T170LA3-40 scaffolds in x/y direction. (A) SEM images of PCL templates and corresponding hybrid scaffolds of different porosities. Scale bars represent 500 µm. (B-C) µCT images of T170LA3-40 scaffolds (porosity: 44%). (B) Scaffold side view indicating open channels (pores) in x/y direction. (C) Scaffold intersection plane (approximate location indicated by hatched plane in (B)) illustrating scaffold pore channels (dark areas) and scaffold material (bright areas, i). Pores in x (forward, ii) and y direction (horizontal, iii) as pre-determined by diameter and density of the PCL strand are interconnected in z direction (vertical, iv) due to partial coalescence of deposited PCL strands in the template structure. No template residues are visible.

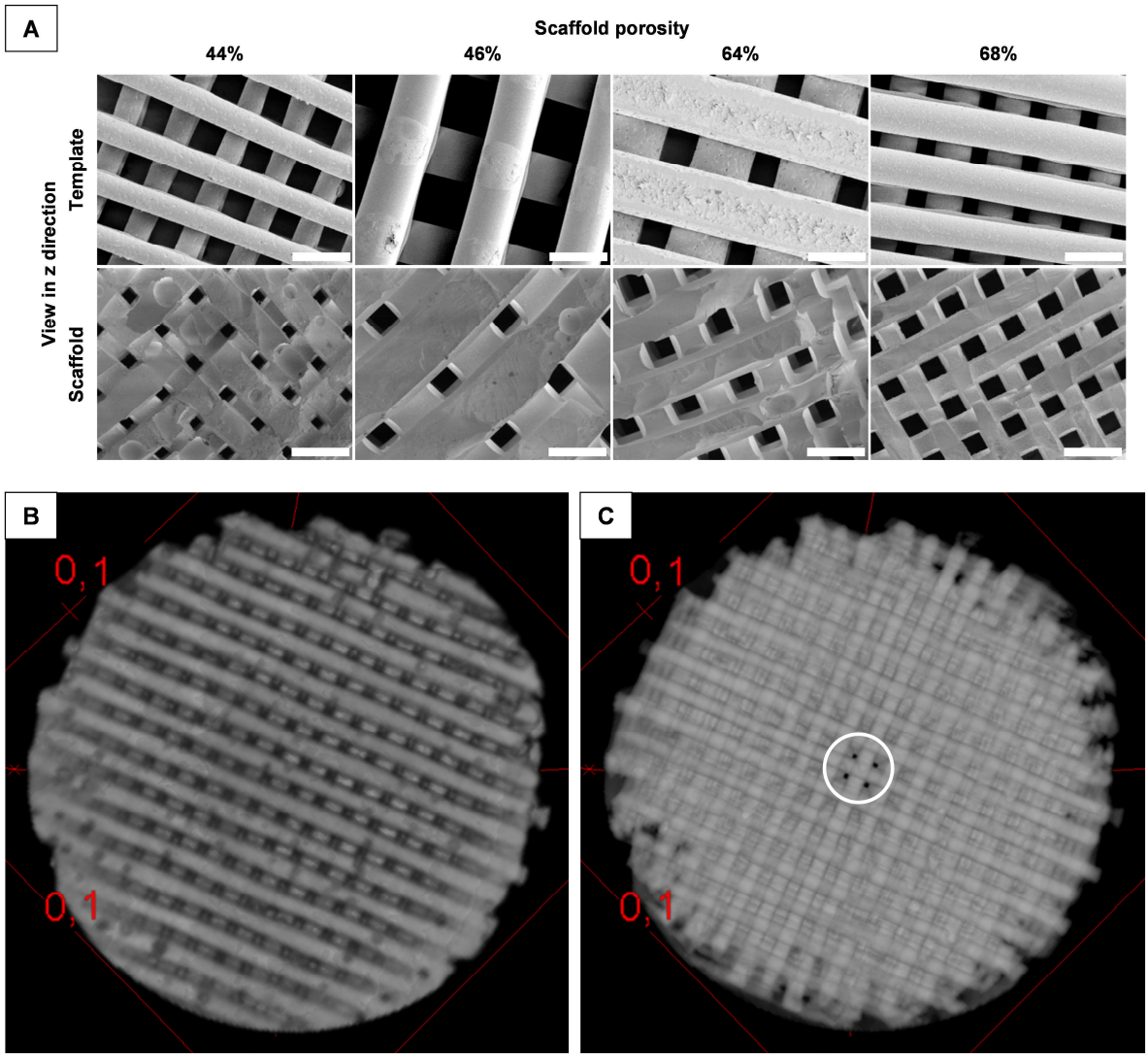

Figure 5-S7. Illustration of template and scaffold structure of T170LA3-40 scaffolds in z direction. (A) SEM images of PCL templates and corresponding hybrid scaffolds of different porosities. Scale bars represent 500 µm. (B-C) µCT reconstructions of T170LA3-40 scaffolds (porosity: 44%). Scaffold top view with low (B) and high (C) material transparency indicating the layered grid structure of scaffold pores. Dark dots in the center of (C) illustrate continuous pores in z direction (white circle) and the absence of template residues.

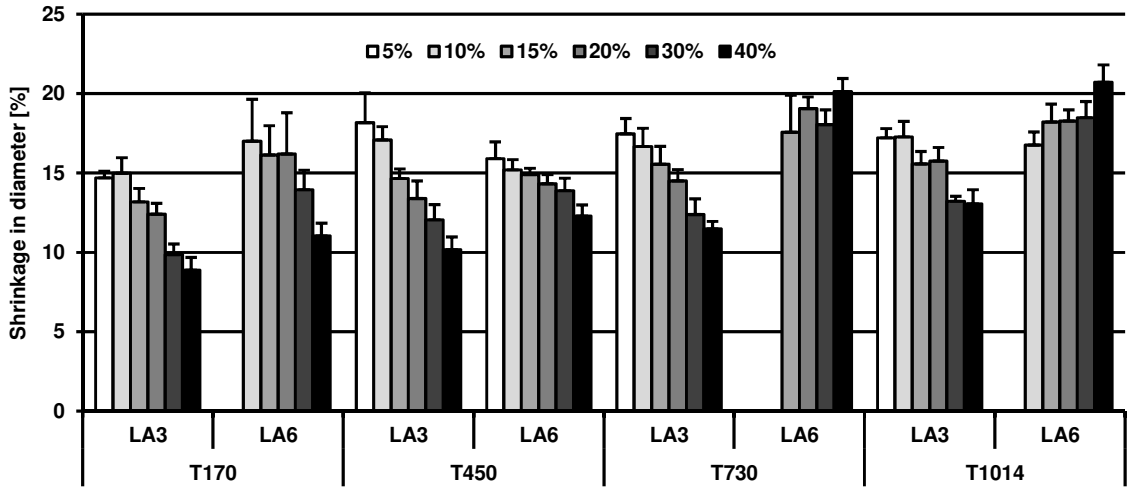

Figure 5-S8. Shrinkage expressed as relative decrease in scaffold diameter of selected three-armed hybrid scaffold formulations in dependence of oligomer type and content. Shrinkage was calculated from diameter of scaffold cylinders as determined after drying and theoretical diameter of the hybrids as predetermined by the PCL template (inner diameter: 7.0 mm). Degree of shrinkage was decreased with increasing oligomer content for oligomers with low or medium molecular weight. For hybrids that contained oligomers with high molecular weight (M_n > 2500 Da (TxLAy) or M_n > 2000 Da (PxLAy)), however, the shrinkage was either not significantly reduced (P270LA6, P797LAy (not shown)) or even enhanced (T730LA6, T1014LA4.5, T1014LA6) with increasing oligomer content which can be explained with increased flexibility of the oligomer (n = 6).

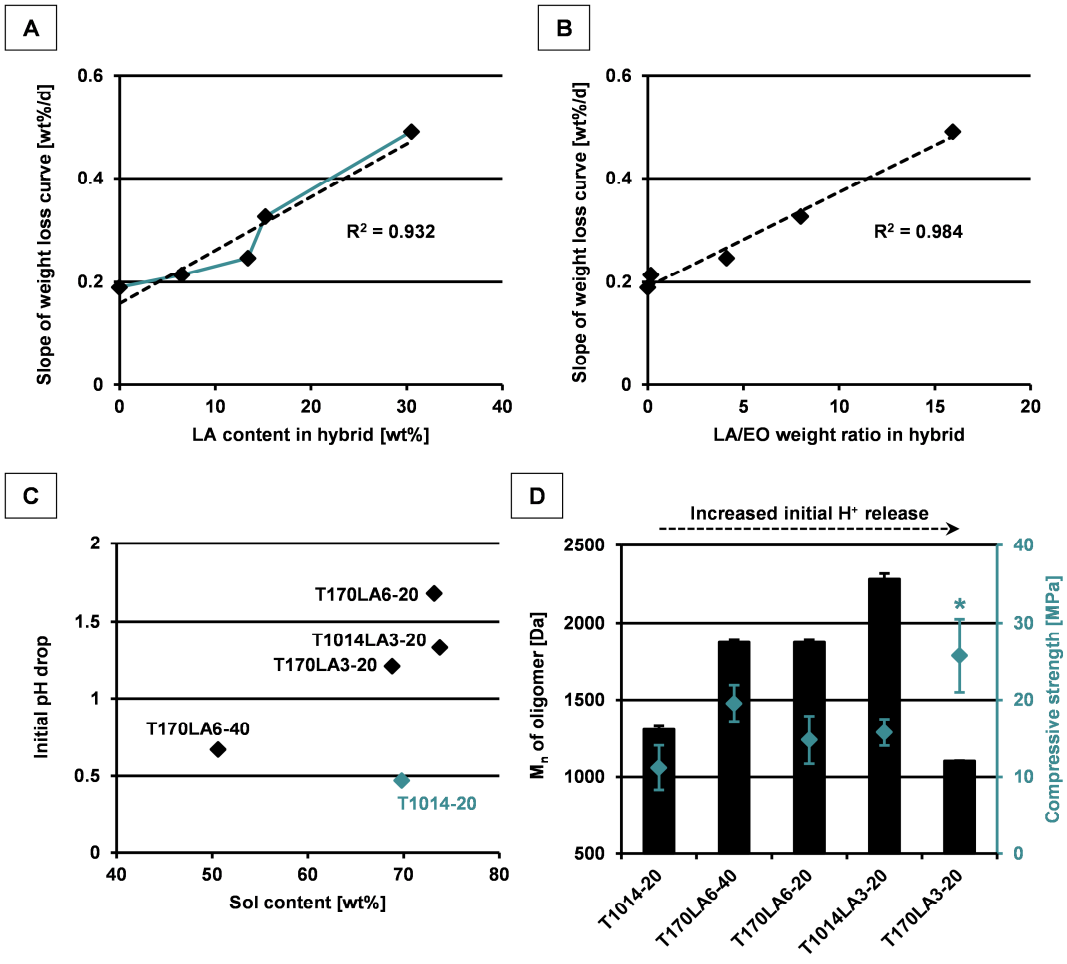

Figure 5-S9. Degradation kinetics and initial acid release of selected hybrid scaffolds. (A-B) Weight loss rate as determined from linear regression of the remaining dry weight curves (days 32-200, Figure 5-7C) as a function of LA content (A) and weight ratio of LA to EO units in the hybrids (B). LA-free hybrid scaffolds (T1014-20) degraded at a rate of 0.2 wt%/d. For LA-containing hybrids, the weight loss rate was enhanced with increasing content of degradable oligoester functions up to a level of 0.5 wt%/d for LA-rich T170LA6-40 scaffolds. In the illustration of the weight loss rate over LA content (A), a step was observed for medium LA content which was vanished when weight loss was shown as function of LA/EO ratio (B) indicating the importance of water penetration into the hybrid matrix before hydrolytic bulk degradation can occur. (C, D) Correlation of initial acid release from hybrids with oligomer structure and hybrid composition as determined by pH measurement of media samples (Figure 5-7B). (C) Difference of buffer and sample pH at day 3.5 as a function of sol content used for hybrid fabrication. (D) Extent of initial acid release within the first 21 days in dependence of molecular weight (M_n) of the oligomers (before silanization) (bars, left y-axis) (n = 3) and compressive strength of the corresponding hybrids (diamonds, right y-axis) (n = 6). Initial pH decrease of the LA-containing hybrids at day 3.5 correlated with content of the sulfuric acid-containing silica sol, while the small pH drop observed for T1014-20 scaffolds indicated effective extraction of sulfuric acid residues from the hydrophilic matrix during the template leaching procedure. Extent of acid release within the first 21 days was increased when materials of comparable compressive strength contained oligomers of higher molecular weight (T1014-20 to T1014LA3-20). The strongest acid release was determined for scaffolds with significantly ($p < 0.05$) increased compressive strength (T170LA3-20) suggesting that retention of the inorganic acid depended on cross-linking degree and distance between organic-inorganic cross-links in the hybrid network.

5.10 SPECIFICATION OF THE AUTHORS' CONTRIBUTIONS TO:

C. Kascholke, S. Hendrikx, T. Flath, D. Kuzmenka, H.-M. Dörfler, D. Schumann, M. Gressenbuch, F. P. Schulze, M. Schulz-Siegmund, M. C. Hacker, Biodegradable and Adjustable Sol-Gel Glass Based Hybrid Scaffolds from Multi-Armed Oligomeric Building Blocks, *Acta Biomaterialia* **2017**, Accepted Manuscript, doi: 10.1016/j.actbio.2017.09.024.

Christian Kascholke (First Author)

Manuscript writing, oligomer synthesis and characterization, degradation study, data evaluation

Stephan Hendrikx

Scaffold fabrication, mechanical testing, SEM and shrinkage analysis, cell culture experiments

Tobias Flath

Template design and production, mechanical testing, 3D CAD modeling, µCT evaluation

Dzmitry Kuzmenka

NMR analysis of ICPTES conversion, dry vs. wet scaffold mechanics

Hans-Martin Dörfler

Determination of scaffold porosity

Dirk Schumann

Conceptual design, silica sol design and production

Mathias Gressenbuch

Conceptual design, silica sol design

F. Peter Schulze

Conceptual design, template design, infrastructure for template fabrication

Michaela Schulz-Siegmund

Conceptual design, advice for experimental design, discussion and manuscript review

Michael C. Hacker (Corresponding Author)

Conceptual design, statistics on mechanical properties, advice for experimental design, discussion and manuscript review

Christian Kascholke

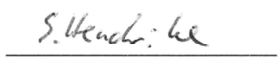

Stephan Hendrikx

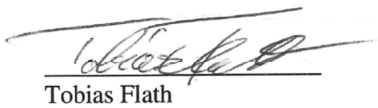

Tobias Flath

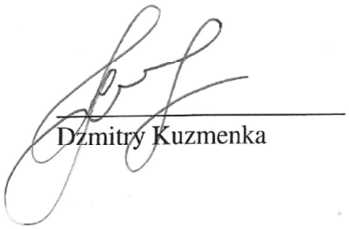

Dzmitry Kuzmenka

Hans-Martin Dörfler

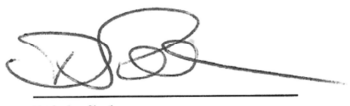

Dirk Schumann

Mathias Gressenbuch

F. Peter Schulze

Michaela Schulz-Siegmund

Michael C. Hacker

CHAPTER 6

Discussion

6.1 MACROMERS FOR BIOMATERIAL DESIGN

As illustrated in Chapter 1, macromer-based materials are interesting due to their high flexibility in chemical design and processability.[87] Macromer chemistry can be adjusted in terms of macromer composition, valence, content of cross-linkable functionalities and molecular weight (Figure 1-4). The versatility of macromer-derived materials greatly increases by the combination of different macromer types which opens potential for precise material tunability on multiple levels. The design flexibility of macromer-based networks motivated the investigation of macromer-based material concepts with regard to macromer processability and material adjustability. Two macromer-derived material platforms were challenged with regard to the following two main aspects:

- Synthesis of adjustable macromer structures from at least two different comonomers.
- Processing of the synthesized macromers into hybrid networks by combination with another oligomeric building block and covalent cross-linking.

On this basis, the following objectives were proposed:

1) To synthesize two types of biodegradable, multi-armed macromers in high yields in order to enable macromer processing into biomaterials with relevant dimensions.
2) To yield purified and well-defined macromer structures based on physico-chemical characteristics, especially chemical composition, molecular weight and reactivity.
3) To characterize macromer processability into covalently cross-linked hybrid matrices, i.e. a soft gelatin-derived hydrogel system and a rigid hybrid glass material, and to establish structure-property relationships.
4) To investigate strategies for the adjustment of material macroporosity, including porogen-leaching and 3D-printing, and to achieve decoupling of porosity and chemical (nano)structure of the cross-linked network.
5) To determine key material properties relevant for regenerative applications, including mechanical properties, *in vitro* matrix degradability and material cytocompatibility.

6) To identify strategies for covalent functionalization of the hybrid materials by post-fabrication functionalization via specifically introduced chemical functionalities to decouple material decoration from the physico-chemical matrix properties.

These aims were selected to refine the macromer-based material concept with regard to the following biomaterial challenges:

I) Hydrogels as artificial extracellular matrices (aECM)

The central presumption of scaffold-based tissue engineering is that cells require a certain 3D biomaterial guidance structure which closely mimics the extracellular matrix (ECM) of the target tissue.[2] To this end, many efforts have been and are still being done to completely understand the physiology of the ECM, especially with respect to matrix structure, chemistry, mechanics and biology.[76] Besides water, collagen and elastin serve as primary structural elements of the ECM.[217] Associated macromolecular glycosaminoglycans (GAG), such as heparan, dermatan, chondroitin and hyaluronan, serve as ECM cross-linkers.[81] Due to their highly negative charge combined with the presence of binding sites for specific proteins, GAG further act as reservoirs for water, growth factors, chemo- and cytokines. Fibronectin, laminin and collagen which all are integrin-binding proteins control cell adhesion and differentiation.[82] The combination of hydrophilic partially cross-linked macromolecules and immobilized as well as free interstitial fluid provides a gel-like ECM consistency.[153] The illustrated complexity of the ECM structure and functionality, however, significantly complicates biomaterial design as functional mimicry. Hydrogels have been identified as ideal candidate materials for tissue engineering due to their viscoelastic properties close to that of the ECM. The diversity of hydrogel-forming polymers enabled specific fine-tuning of matrix properties toward divers target tissues. While traditionally considered for soft tissue regeneration, hydrogels have meanwhile been also established for regeneration of hard tissues, including bone tissue engineering.[218] The implementation of ECM-like functionality, however, remains a great challenge which generally cannot be addressed by a single hydrogel-forming macromolecule. To this end, a great variety of ECM component-derived peptides or bioactive molecules, including cell-adhesive, growth factor-binding and enzyme-sensitive structures, have been used to modify hydrogel matrices.[82]

Cross-linking of isolated ECM structures is one possibility to fabricate ECM-like hydrogels. For example, collagen-based matrices were synthesized by simple EDC cross-linking of collagen or collagenous fragments. This approach can also be extended toward the cross-linking of a mixture

of different ECM components.[125,217] These strategies, however, are limited in terms of the implementation of ECM functionality. While soluble factors can be introduced by diffusion or adsorptive binding, decoration with covalently associated structures is challenging in these gels.

In this regard, macromer-based hydrogels offer great potential in order to better mimic the natural ECM structure with respect to its functionality. On the one hand, their physical matrix properties can be precisely tuned by the variation of macromer chemistry, the combination of different macromer building blocks and the adjustment of cross-linking density (Figure 1-4A-C). On the other hand, the introduction of specific chemical functionalities offers potential for covalent matrix derivatization with functional ECM components (Figure 1-4D-E). Bioconjugation reactions which can be performed under mild conditions are often favored in order to preserve the structure of chemically sensitive protein components (Figure 1-1). These chemistries are often used to introduce functional ECM components immediately during hydrogel synthesis, e.g. by cross-linking of chemically functionalized ECM molecules.[82] The drawback of this approach is that physico-chemical matrix properties strongly depend on the type and content of the immobilized derivatives as these parameters affect the network structure.

The innovative aspect of the hydrogel concept presented in this thesis is to decouple material functionalization from the physico-chemical network properties which has not yet been reported for cross-linked gelatin matrices. To this end, dual-functional macromers (oligo(PEDAS-*co*-DAAm-*co*-MA), oPDMA) were synthesized that can build hydrogels by covalent cross-linking with gelatin via anhydride groups (from MA).[90,91] Methyl ketones (from DAAm) were introduced as second functionality enabling covalent immobilization of hydrazido-functionalized components which can easily be introduced into various types of (bio)molecules.[16,40,136] Following this so-called post-fabrication functionalization strategy, hydrogels can effectively be functionalized under mild conditions and independently of the network properties that have been adjusted by type and concentration of the hydrogel building blocks (Figure 1-4E).

II) Bone regeneration by glass-based scaffolds

Bone is the second most transplanted tissue after blood.[94,206] Currently, many biomaterial approaches focus on the replacement of autografts – still the gold standard – by synthetic substitute materials. In this regard, bioactive glass was detected as one of the most promising bone replacement materials as it can covalently bond to existing bone and be osteoinductive.[38,219,220] Degradability, however, remains a crucial issue of these materials as

particulate residues have been detected up to more than 10 years after implantation which can cause inflammation.[3,181,221] Besides degradability, bone regeneration requires substitutes with specific mechanical properties – more than for any other tissue. Especially load-bearing bone tissues provide high mechanical stability, but are simultaneously characterized by an open-porous structure.[69,70] The realization of high strength and stiffness combined with high porosity, however, is generally crucial as it is known that both mechanical characteristics inversely correlate with material porosity.[4,54,166]

In that regard, macromer-based materials hold great promise due to their design flexibility (Figure 1-4). Matrix degradability can be adjusted by the introduction of degradable functionalities, such as hydrolytically labile esters. This aim can be reached by the application of degradable comonomers, by introduction of degradable functionalities upon copolymerization in macromer synthesis (e.g. by polycondensation), or by the formation of degradable cross-links (Figure 1-4A). The combination of a degradable macromer with another macromer building block offers further potential for the adjustment of material degradation (Figure 1-4B). This approach can be used to synthesize hybrid glass materials by cross-linking of a degradable macromer with a reactive sol-gel-derived glass precursor and therefore to address matrix degradation (macromer) and material stiffness (covalent oligomer/glass hybrid). Matrix mechanics strongly depend on the cross-linking degree which can be adjusted by molecular weight, reactivity and concentrations of the oligomeric building blocks, i.e. macromer and glass precursor (Figure 1-4C). To this end, the macromer concept allows for the versatile tunability of cross-linking degree (almost) independently of the chemistry of a degradable macromer (type and content of degradable functionalities) (Figure 1-4A-C). This level of control is important for bone regeneration as the adjustment of material degradation by macromer chemistry generally also affects material mechanics which have to meet the specific characteristics of the target tissue.

While degradability of purely inorganic glass materials can be inadequately tuned,[222] the design of macromer/glass hybrid materials, however, should provide the required level of control. Different degradable macromers have been covalently integrated into class II hybrid glass matrices. The most studies focused on polycaprolactone (PCL) that was activated by 3-isocyanatopropyltriethoxysilane (ICPTES) and combined with a tetraethoxysilane(TEOS)-derived silica sol.[35,190–192,223,224] Other polyesters, such as polylactide (PLA) and polyglycolide

(PGA), were accordingly processed.[193,225] Furthermore, gelatin was covalently introduced as naturally degradable building block after activation by 3-glycidoxypropyl trimethoxysilane (GPTMS).[36,74,151,187,226,227] Degradable hybrids were also synthesized from chitosan[80,228] and poly(γ-glutamic acid)[37,146,180,229]. These studies, however, were mostly focused on physico-chemical, mechanical and biological material properties, but degradation kinetics were often sparsely investigated.

To this end, one goal of this work was to bring new insights into the degradability of glass-based hybrid materials. In detail, oligo(D,L-lactide) units were introduced into three- (TMPEO, Tx) and four-armed (PETEO, Px) ethoxylated alcohols. Hybrid scaffolds were synthesized by combination with a TEOS-derived silica sol. Long-term degradation studies over 12 months were performed in order to characterize tailorability of the hydrolytic material degradation.

6.2 FUNCTIONAL ANHYDRIDE-CONTAINING MACROMERS AS HYDROGEL BUILDING BLOCKS

Biomimetic hydrogels are promising biomaterials as they are characterized by improved biological performance due to presentation of cell-responsive motifs. The integration of extracellular matrix(ECM)-derived structures serves as a promising strategy in order to promote cell adhesion and proliferation.[101–103] In this regard, gelatin was identified as a promising non-immunogenic building block as this fractionally hydrolyzed collagen derivative is characterized by improved processability, but still contains the relevant cell adhesion sites.[92] Gelatin-derived hydrogels often have been fabricated by chemical cross-linking with glutaraldehyde (GTA) or genipin.[171,172,230] As the most frequently used cross-linker GTA, however, is characterized by relevant toxicity potential due to unreacted aldehyde functionalities, cytocompatible alternatives that ideally can be easily chemically modified are wanted. We have previously synthesized anhydride-containing macromers that can be used as cytocompatible alternative of GTA.[90,91] These macromers were synthesized by free radical polymerization (FRP) of penthaerythritol diacrylate monostearate (PEDAS), *N*-isopropylacrylamide (NiPAAm) and maleic anhydride (MA) to yield oligo(PEDAS-*co*-NiPAAm-*co*-MA) (oPNMA) which was in accordance with a previously established macromer design concept[90,120–122] Oligomer(oPNMA)-cross-linked

gelatin-based hydrogels (cGEL) were characterized by high flexibility, sufficient mechanical stability and promising biological performance.[91,92]

6.2.1 Synthesis of dual-functional macromers

Based on these findings, the motivation of this thesis was to introduce a second chemical functionality into MA-containing macromers in order to enable covalent hydrogel functionalization independent of cross-linking chemistry. In particular, the versatility of FRP was used to exchange NiPAAm by diacetone acrylamide (DAAm) as another functional monomer without significant alterations to synthesis and purification protocols. Ketone-containing DAAm could be successfully copolymerized into oligo(PEDAS-*co*-DAAm-*co*-MA) (oPDMA) macromers. The copolymer solutions could be purified by precipitation and solvent residues were removed by vacuum drying. Low molecular-weight macromers with adjustable composition were obtained that bear anhydride and ketone functionalities in the same oligomer chain (Figure 1-4E). The combination of these chemical functionalities in a single macromer structures was not reported before.

Patenaude et al. have used free radical polymerization to synthesize poly(NiPAAm)-based aldehyde- and ketone-containing macromers.[44] Dual functionality of these macromers together with their reactivity toward hydrazides indicates similarity to oPDMA derivatives presented in this work. Interestingly, hydrazide reactivity of the poly(NiPAAm)-derived macromers was kinetically tunable by variation of the aldehyde to ketone ratio and the total carbonyl content. Nevertheless, two significant differences in comparison with oPDMA can be noted: I) The functional methacrylamide-based carbonyl-containing monomers were not commercially available and therefore had to be synthesized and purified. In this regard, the aldehyde and ketone functionalities had to be protected by acetal and ketal groups, respectively, which had to be removed in the resulting macromers. In contrast, ketone-containing DAAm was available in synthesis quality and could be used without purification and ketone protection. II) Both reactive groups of the poly(NiPAAm)-based macromers (aldehydes and ketones) were reactive toward hydrazides and therefore targeted the same chemical functionality. This strategy cannot be used for decoupling of matrix formation and hydrogel functionalization. In contrast, the oPDMA-based material concept combined macromer reactivity toward amines (anhydrides) and hydrazides (ketones). It was further demonstrated that the ketone-functionalized derivatives

offered cytocompatibility in concentrations of up to 2% (w/v) which was far beyond the physiological relevance for their injectable hydrogel system. This is in accordance with the cytocompatibility of oPDMA/COL hydrogels found in this work. Methyl ketone incorporation via DAAm monomers did not raise any concerns on oPDMA/COL hydrogel cytocompatibility, but yielded formulations that showed superior cell-material interactions as compared to established and ketone-free oPNMA/COL matrices.[91] This was confirmed in a recent study on melanocytes seeded to oPDMA-7.5/COL (3.5%/15%) hydrogels. Melanin production as well as melanotic gene expression was fostered and even considered superior to other substrates including oPNMA-derived gels, electrospun poly(caprolactone) (PCL) matrices, as well as a commercially available full-length collagen material (Collagen Cell Carrier®).[104]

It has been shown that FRP can be used for copolymerization of a great variety of functional monomers that allow for post-polymerization modification.[231] In this regard, the introduction of vinyl-, disulfide-, alkyne- and azide-functionalized derivatives provides a promising perspective for future derivatives as these clickable functionalities enable modification under mild conditions. Nevertheless, these monomers have to be separately synthesized which is quite laborious and cost-extensive. In contrast, all monomers used for oPDMA synthesis were commercially available to moderate prices. The exchange of NiPAAm by DAAm did not require for an adjustment of the synthesis conditions and yielded oligomers with generally comparable molecular weight and monomer conversions.[90] The increased molecular weights and decreased MA conversions in oPDMA macromers can be explained with enhanced tendency of DAAm to homopolymerize.[68] FRP offers potential to adjust macromer composition and molecular weight by composition of the comonomer feed, total monomer concentration, solvent type, type and concentration of the initiator as well as reaction time and temperature[11] which was confirmed for the oPxMA macromers.[95] Copolymerization of MA by FRP, however, is limited which can be assumed from previous failed attempts to copolymerize PEDAS and MA with acrylamide, *N*-vinyl pyrrolidone or dimethylaminoethyl acrylate in comparable comonomer ratios.[95,96] Besides FRP, controlled/living radical polymerization (CRP), including reversible addition-fragmentation chain transfer (RAFT) polymerization and atom transfer radical polymerization (ATRP), offers compatibility to a wide range of monomers.[232] In addition, CRP-derived macromers are characterized by improved dispersity which is a key concern of the macromer concept to yield well-controlled material properties.[27,233] Literature reports on CRP for synthesis of MA-containing macromers, however, is limited to styrene/MA derivatives which is not

suitable for regenerative purposes.[234,235] In this thesis, CRP strategies were not investigated for macromer synthesis. Nevertheless, well-defined oPDMA macromers with low dispersity were synthesized by FRP.

Macromers containing hydrolytically cleavable functionalities are further interesting as they can mediate and control hydrogel degradability. The synthesized oPDMA macromers offer ester functionalities (from PEDAS) which are generally degradable, but the contribution of these lipophilic acrylate esters for oligomer degradability is supposed to be low. Ester functionalities with significant degradability, however, can be introduced by simple polycondensation as demonstrated by Gyawali et al. who synthesized citrate-based macromers from citric acid, PEG and MA.[20] Therein, the MA monomer was introduced by ring-opening polymerization consuming the anhydride reactivity and the reactive C=C double bond remained available for cross-polymerization. This principle is different from MA copolymerization by FRP in which its anhydride functionality is maintained.

6.2.2 Macromer processability into cross-linked oligomer/gelatin hydrogel matrices

In the synthesized oPDMA macromers, a high fraction of incorporated MA units (approximately 70%) remained chemically intact and therefore available for cross-linking of amine-containing macromolecules. To this end, it was aimed to process the synthesized dual-functional macromers into stable hydrogel matrices by covalent cross-linking with gelatinous peptides.

It has been demonstrated that different gelatin types were cross-linkable into oligomer/gelatin hybrid matrices.[9192] This indicated excellent processability of both hydrogel building blocks. Solutions of the synthetic hydrogel building blocks in DMF even in concentrations of up to 35% (w/v) were low viscous and can therefore be easily pipetted. The same holds true for the gelatinous peptides which were processable in water (COL) or in a DMF/water mixture (1:1 (v/v), high molecular-weight peptides). It was found that cross-linking kinetics were adjustable by oPDMA concentration and reactivity as well as peptide concentration and oPDMA/gelatin ratio. All synthesized oPDMA macromers were processable into hydrogel matrices by predominantly cross-linking the flexible low molecular-weight COL component. Overall, more than 30 differently composed oPDMA-containing hydrogels were obtained. This high compositional flexibility is in accordance with that of the previously established oPNMA/gelatin

hydrogel platform,[91,115] but – to our knowledge – was not described for any other hydrogel concept in comparable manner.

Other gelatin-based systems, for example, usually made use of only one cross-linker type (e.g. GTA or genipin).[171,236,237] Flexibility of these concepts was further reduced by cross-linking of a selected gelatin type. Consequently, compositional variability of these matrices was only derived from gelatin and cross-linker concentrations resulting in significantly reduced degree of material engineering freedom when compared to the oPxMA/gelatin platforms. In another poly(NiPAAm)-based hydrogel concept, the variability of macromer composition (type and content of cross-linking functionalities) was used to fabricate 6 differently composed hydrogel formulations.[44] Singh et al. have exhausted the potential of the macromer-based hydrogel design to a higher degree by combining different types of functional PEGDA/alpha-cyclodextrin macromers together with variable PEGDA concentrations.[88] This resulted in 12 different hydrogel formulations, which is less than that of the successfully processable oPDMA/gelatin formulations. Nevertheless, it was demonstrated that this set of PEGDA/alpha-cyclodextrin hydrogel formulations enabled identification of structure-property relationships with high relevance for biomaterial engineering. In another work, we further demonstrated the potential to adapt gelation kinetics of the oligomer/gelatin system by variation of type and concentration of the base used for proton scavenging which was not investigated in this work.[115] In combination with the application of a double syringe delivery system equipped with a static mixing nozzle, this offers great promise to further increase the number of hydrogel compositions by processing even high reactive oPDMA/COL formulations which formed inhomogeneous matrices when processed with the standard hydrogel fabrication method.

The synthesized oPDMA and oPNMA macromers served as effective alternative to glutaraldehyde (GTA) for cross-linking of gelatin.[170–172] In comparison, cross-linker reactivity was better balanced in the oPxMA derivatives which helped to avoid the characteristic turbidity of GTA-derived hydrogels. In this context, two further significant advantages of the anhydride-based macromers became apparent: I) While GTA residues can cause cytocompatibility issues,[238] oPxMA-derived anhydrides that were not reacted with amines will effectively be hydrolyzed in the hydrogel washing and hydration steps. II) GTA acts as simple cross-linker enabling hydrogel formation by gelatin cross-linking into a high molecular-weight network. In contrast, oPxMA serves as hydrogel building block that will introduce specific functionality into the cross-linked

hybrid matrices. Besides GTA, genipin was described as another chemical cross-linker of gelatin with decreased reactivity.[91,236,237] Genipin-cross-linked matrices have shown reduced toxicity, but are characterized by comparatively low cross-linking degrees. These examples illustrate a general correlation between cross-linker effectiveness and toxicity which is often described for established chemical gelatin cross-linkers.[22] In that regard, the anhydride-based macromers offer great potential as they combine cross-linking effectiveness comparable to that of GTA with promising cytocompatibility.

6.2.3 Adjustability of oPxMA/gelatin hydrogel porosity

Different strategies have been reported for fabrication of porous hydrogels.[2,176] In this regard, versatile macromer processability is advantageous in order to enable the application of different concepts for porosity adjustment. As the previously established oPNMA-derived matrices were characterized by low pore sizes which resulted in limited cell migration, it was intended to identify strategies for efficient porosity adjustment of oligomer/gelatin hydrogel matrices.

Versatile processability of the oligomer/gelatin system was used to introduce macroporosity into the oPxMA/gelatin gels and successful application of a high molecular-weight PEG porogen (P8k) was demonstrated. This approach made use of the liquid-liquid immiscibility of P8k and the precursors solutions enabling pore generation by phase separation.[10,239] Effective removal of the incorporated porogen was shown demonstrating the chemical inertness of the anhydride functionalities toward PEG-derived alcohol groups under the applied conditions.[96,162] Network formation was not affected by the presence of PEG beads indicating robustness of the cross-linking chemistry. In another strategy, hydrogel porosity was adjusted by alteration of its nanostructure. The formation of wide-meshed networks was promoted by cross-linking of high molecular-weight gelatin (G160) by oPNMA macromers with low reactivity. Successful processability into stable gels was demonstrated and the combination of high molecular weight with low MA content likely contributed to low cross-link density and therefore increased nanoporosity.

While macroporosity is important in terms of cell penetration, micro- and nanoporosity are also highly relevant in order to control swelling and diffusion properties of a hydrogel.[57,63,143,154] For different macromer-based hydrogel concepts, it has been demonstrated that the hydrogel

nanostructure is controlled by the density of cross-links which can be adjusted by architecture, molecular weight as well as density of reactive functionalities of the macromer (Figure 1-4C).[23,88,240] We were able to confirm these correlations in our oPxMA/gelatin hydrogel concept and a key role of the parameter 'molecular weight per chemically intact MA' on the hydrogel network structure was identified.[90] The application of two hydrogel building blocks was beneficial and versatile combinability opened potential for extended tunability of the network structure (Figure 1-4B).

Various methods have been described to control hydrogel macroporosity and porogen-leaching was identified as the most promising strategy.[59] PEG is known as another promising porogen applicable for engineering of hydrogels due to its hydrophilicity and chemical inertness which makes it easy removable in aqueous medium.[57,144,160,239] The most related study was performed by Lévesque et al. who successfully applied a 10 kDa PEG in concentrations of 1-20 wt%.[57] A shift from micro- to macroporosity was found in a PEG concentration-dependent manner and interconnected pores with sizes of up to 120 µm were detected. In this thesis, the effect of PEG concentration on hydrogel porosity was confirmed which is in accordance with previous results for oPNMA/COL matrices. The generation of ice crystals that act as porogens in a freeze-drying process is another porogen-leaching method which is applicable to nearly all hydrogel systems.[155] As the cross-linked oPxMA/gelatin hydrogels were also freeze-dried immediately after fabrication, corresponding effects on matrix macroporosity can be assumed as indicated by enhanced storage modulus upon freeze-drying (not shown). Recently, many efforts have been done to establish 3D-printing methods for fabrication of macroporous hydrogels.[58] This strategy opens potential for improved control over material pore structure and especially pore interconnectivity.[61,62] In particular, extrusion-based methods are most promising for hydrogel engineering, which, however, requires precise adjustability of the cross-linking kinetics.[61] Extrusion-based printing has been applied for fabrication of UV-cross-linked gelatinous hydrogels.[59] In this thesis, it was shown that the hydrogel fabrication process can be up-scaled toward gels of larger dimensions. Our group further demonstrated that oPNMA-containing formulations can be processed into tubular structures by using an injection-molding procedure.[115] These are valuable fundamentals indicating the potential for applicability of 3D-printing, which was not investigated for the oligomer-cross-linked gelatin networks in this thesis.

6.2.4 Tunability of dual-component hydrogels

6.2.4.1 Post-fabrication hydrogel functionalization. Key aspect of the oPDMA/gelatin-based hydrogel concept was to demonstrate the potential of covalent material functionalization independently of the physico-chemical matrix properties which offers potential for high material tailorability. This was aimed by the combination of two different chemical functionalities in the same macromer.

This aim was successfully achieved as the incorporated methyl ketone functionality (from DAAm) remained intact after hydrogel formation via anhydride-mediated cross-linking. The ketone functionality was therefore available for post-fabrication functionalization and triple-tunable immobilization of a fluorescent hydrazide derivative was shown. In particular, the effects of ligand concentration, medium pH and hydrogel ketone content on hydrazide immobilization were identified. These correlations have not been reported before in context with post-fabrication functionalization of macromer-based materials. It was further shown that the presented functionalization concept was applicable for immobilization of functional ECM (i.e. hydrazido-functionalized HA) derivatives. This demonstrates the potential of oPDMA-cross-linked matrices for fabrication of biomimetic matrices in which gelatin provides the ECM structure, while HA introduces specific matrix functionality. Furthermore, the illustrated release potential of immobilized ligands in the micromolar range holds great promise to mediate relevant effects on surrounding cells.

The Anseth Lab provided important knowledge on the hydrazone formation kinetics for PEG-based hydrogels even at physiological pH.[50,241] Patenaude et al. have investigated injectable poly(NiPAAm)-based hydrogels and demonstrated that hydrazone formation was controlled by adjustment of the ratio of aldehyde-to-ketone functional groups as well as the total number of ketone groups in the hydrazide-reactive macromer.[44,242] Both concepts applied hydrazone chemistry for cross-linking of ketone-/aldehyde- and hydrazide-/hydrazide-functionalized macromers into hydrogel matrices which is different from the oPDMA-based approach.

Effective hydrazone formation under physiologically relevant conditions combined with the high selectivity of hydrazone formation holds promise for immobilization of other sensitive structures, such as growth factors or cytokines, on oPDMA-derived matrices.[67] The Prestwich Lab has extensively studied hydrazido-functionalized hyaluronan (HA) and demonstrated the potential to use this functionality for matrix formation and subsequent hydrogel functionalization.[243] Ossipov

et al. also used hydrazone chemistry for post-fabrication functionalization. HA-based matrices were cross-linked by disulfide groups and an aldehyde functionality enabled covalent immobilization of a hydrazido-bearing poly(vinyl alcohol)(PVA)-doxorubicin conjugate.[17] Therein, matrix formation and functionalization were performed in one step which reduces control over the network structure e.g. by steric effects. These two examples are in contrast with the oPDMA concept which is based on the separation of hydrogel cross-linking and functionalization by different chemical functionalities and in separate steps. Consequently, pre-determined hydrogel properties, such as the cross-linking degree, are not affected by material functionalization (Figure 1-4E). The same strategy was achieved by Kaga et al. who have synthesized dual-functional dendron-polymer conjugates.[84] While methacrylate functionalities contributed to UV-mediated network cross-linking, incorporated alkyne groups enabled functionalization of the cross-linked gels by azide-bearing components, such as biotin-azide.

Overall, decoupling network formation from material functionalization has been enabled by the combination of different chemical strategies.[102,244] Although especially click chemistry offers potential for high versatility in this regard, the introduction of *in vivo c*lickable functionalities is comparatively laborious and cost-extensive. In this context, the oPDMA-based hydrogel concept offers great potential as hydrazide functionalization is comparatively simple and can be performed for a variety of ECM components.[16,40,136]

The release potential of immobilized ligands which was demonstrated for this concept can be highly relevant for providing effects on the surrounding tissue. Covalent coupling of protein ligands, such as growth factors, however, might be challenging as it can result in reduced biological activity of the immobilized derivative. *In-silico* modeling, including molecular docking experiments, is a promising strategy in order to detect uncritical region for hydrazide functionalization and subsequent covalent immobilization into a hydrogel network.[245] In this context, it was found that the introduction of a spacer structure between ligand and the cross-linked network can be beneficial in order to maintain the biological activity of a complex 3D structure.[22,246] Besides covalent immobilization, the potential of the oPxMA-derived matrices for non-covalent loading with siRNA poly- and lipoplexes has been recently shown which is based on electrostatic interactions between positively charged siRNA nanocomplexes and the negatively charged hydrogel matrix.[168]

6.2.4.2 Adjustability of hydrogel matrix properties. The dual-functional macromer design was selected in order to decouple hydrogel functionalization from physico-chemical network properties. The cross-linked matrix was exclusively formed by consumption of anhydride units, before methyl ketones enabled covalent immobilization of functional ligands. This strategy is different from that previously shown for oPNMA-cross-linked matrices in which macromers were pre-derivatized with functional compounds by anhydride aminolysis before cross-linking.[90,115,247] In this regard, the oPDMA-based hydrogel concept offers potential for enhanced degree of engineering freedom and therefore improved material versatility (Figure 1-4).

The physico-chemical hydrogel properties were generally tunable by macromer composition, gelatin type and content of both building blocks in the hydrogel matrix. The large set of processable formulations (section 6.2.2) allowed for detection of correlations between hydrogel properties with macromer parameters. This is exemplarily discussed in context with the mechanical hydrogel properties.

Contents of anhydride and amine functionalities in the reaction feed were detected as factors that significantly determine hydrogel mechanics as these parameters control cross-linking density (Figure 1-4C). Hydrogel stiffness was further affected by the oPDMA type which varied in reactivity, molecular weight and hydrophilicity. Single effects of these three specific macromer characteristics on material mechanics are known in the literature,[88,248] but have not been statistically assessed herein. The application of a PEG porogen into the oPxMA/gelatin system did not affect hydrogel mechanics. Overall, the fabricated oPxMA gels were comparatively rigid and free-standing gel disks were obtained which allowed for proper handling without damaging the gel structure. The cross-linked hybrid matrices were characterized by high storage moduli of 1-10 kPa which correspond to elastic moduli of 3-30 kPa (according to the common approximation of $E = 3G'$).[125] The exchange of NiPAAm by DAAm in oPDMA macromers resulted in increased gel rigidity when compared to analogous oPNMA-derived networks. For GTA-cross-linked gelatin-based hydrogels, elastic moduli of 1.5-7.4 kPa and 3.5-7.3 kPa, respectively, were reported.[173,174] Similar rigidity was obtained for EDC-cross-linked collagen/HA hydrogels (E = 4.3-6.7 kPa).[249] Elastic moduli of these hydrogels corresponded to the lower end of the broad mechanics range obtained for oPxMA/gelatin hydrogels demonstrating the significant contribution of the macromer hydrogel building blocks to the hydrogel network structure (Figure 1-4C). These findings underline the benefit of macromer-

based two-component concepts over conventional cross-linking by GTA or other low molecular-weight and non-functional cross-linkers with regard to material adjustability.

6.3 MULTI-ARMED LACTIDE-BASED MACROMERS AS BUILDING BLOCKS FOR SOL-GEL GLASS-BASED HYBRID SCAFFOLDS

The second concept of a macromer-based material investigated in this thesis addressed the insufficient degradability of glass-based materials.[3,93,94,181] In this regard, sol-gel-derived glasses already hold promise due to improved degradability over sintered glasses.[3,94] Sol-gel processing further enables the introduction of organic components to control material degradability. This has been demonstrated for several natural as well as synthetic components, including gelatin and different polyesters.[74,191,193,225] Covalent incorporation of the organic phase (class II hybrid) is generally advantageous in order to achieve congruent and well-controllable degradation.[36,80,250] We have previously established a class II hybrid material consisting of a TEOS-derived silica sol and synthetic oligovalent PEG-based cross-linkers which, however, were not hydrolytically degradable.[54,150,251] Based on this hybrid concept, it was the purpose of this work to fabricate hydrolytically degradable hybrids by the introduction of oligoester-containing macromers as organic component.

6.3.1 Synthesis of hydrolytically degradable macromers

It was aimed to synthesize hydrolytically degradable multi-armed oligomers by ring-opening polymerization (ROP).[53] In detail, tri- (Tx) and tetravalent ethoxylated alcohol cores (Px) of different molecular weights were functionalized with oligo(D,L-lactide) units of varying length (LAy) to obtain TxLAy and PyLAy derivatives. The macromer design was derived from previously established methacrylated TxLAy derivatives that mediated promising degradation characteristics of cross-polymerized scaffolds over several months.[53] The incorporation of relatively short oligolactide domains of 3-6 units was used in order to optimize the less predictable degradation of high molecular-weight PLA-derived polymers. This behavior is caused by self-catalytic hydrolysis and can result in significant inflammatory response.[38,201] The combination of oligoester domains and PEG-derived structures has been widely investigated,

especially in context with hydrogel-forming macromers. This combination enabled adjustability of matrix hydrophilicity which is highly relevant with respect to material degradability.[28,201,210] The oligomers offered well-controlled chemical composition and were effectively purified by precipitation and subsequent vacuum-drying. Macromers with narrow molecular weight distributions were obtained which was enabled by ROP in presence of stannous octoate supporting "living"-like polymerization by reversible de-/polymerization of oligo-/lactide.[10] Consequently, this synthesis setup serves as the method of choice for the introduction of oligolactide domains into differently structured alcohol cores.[53,79,248] Chain-end functionalization with 3-isocyanatopropyltriethoxysilane (ICPTES) in melt served as activation strategy to yield silane-reactive oligomers (TxLAy-Si and PxLAy-Si) and effectively activated macromers were obtained. Overall, 18 differently composed multi-armed macromers were synthesized. This large set of chemically different formulations is an outstanding characteristic of this work and cannot be found in comparable manner in the literature.

Derivatization with ICPTES is a commonly known strategy for effective functionalization of hydroxy-terminated structures and therefore offers great potential for synthesis of degradable covalently cross-linked (class II) hybrid networks.[190–193] The chemical design of the TxLAy-Si and PxLAy-Si macromers has not been described before, although some similar concepts exist. Macromer structures with the most similarity in design have been reported by Helminen et al. who have synthesized linear, 4- and 6-armed PLA-based oligomers (2.5-16 kDa) that have been activated with ICPTES.[193] Unlike our TxLAy-Si and PxLAy-Si derivatives, these macromers were of significantly higher molecular weights and did not contain oligo(ethylene oxide) units in their core alcohols. To this end, impaired macromer processability and reduced adjustability of material hydrophilicity are significant differences when compared to our concept. Oligomeric ethylene oxide units can be found in linear LA-based macromers reported by Mazzocchetti et al., but the application of only one type of alcohol core (tri(ethylene glycol)) limits macromer flexibility.[196] The most frequently reported hydrolytically degradable silane-reactive macromers, however, comprise PCL-derived oligoesters.[190–192,224] As all these derivatives were based on commercially available PCL diols (di(ethylene glycol) as core alcohol), the molecular weight (M_n: 2000 Da or 4000 Da) was the only degree of engineering freedom of these linear macromers. In all these reports, only a few chemically different macromers have been reported (8 in maximum[193]) which is significantly less than that of the TxLAy and PxLAy derivatives (18 macromers) synthesized in this work. The applied macromer design generally offers

potential for further versatility, such as the introduction of other oligoester structures[53] and/or other types of multi-armed alcohol cores.[252]

6.3.2 Processability into macromer/sol-gel glass-derived hybrid scaffolds

The aim of this macromer concept was to synthesize sol-gel-derived class II hybrid matrices. Such a covalent integration of the degradable organic component into the TEOS-based silica sol was performed in order to achieve enhanced control over material degradability when compared with non-covalently cross-linked hybrids.[3,253,254] In this context, the functionalization of each oligomer arm with reactive triethoxysilane groups by ICPTES derivatization was of significant relevance. It has been demonstrated that ICPTES-functionalized lactide- and PCL-based as well as gelatin-derived macromers can be polymerized into class II hybrid matrices, even without the addition of a silica sol.[193,224,255] We have previously demonstrated radical cross-polymerization of methacrylated TxLAy derivatives which resulted in purely organic networks.[256–258] Polymerization of ICPTES-functionalized macromers offers potential for increased cross-linking density when compared with that of methacrylated derivatives due to the introduction of three (ICPTES) vs. one (methacrylate) reactive functionality/-ies per macromer arm. Shirazi et al. even have combined both cross-linking strategies in order to fabricate gelatin-derived hybrids with improved elasticity.[227] In contrast to these concepts, we have used a pre-cured TEOS-derived silica sol as another oligomeric building block for hybrid synthesis. This design enables enhanced degree of material engineering freedom (Figure 1-4B) and likely enhanced control over the hybrid degradability.

Macromer mixtures with the TEOS-derived silica sol offered different viscosities which were dependent on macromer type and content in the hybrid formulation. Nevertheless, all of the investigated formulations could be processed into homogeneous hybrid scaffolds as viscosity differences of the macromer/sol mixtures were compensated by the applied indirect rapid prototyping method[54]. This resulted in a total of 85 chemically different hybrids. There is no study on TEOS-derived class II hybrids available which contains a comparably large set of data. For example, one report containing lactide-based macromers has been found.[196] Although only two different (linear) macromers were described therein, a total number of 20 hybrid formulations provided systematic data sets. Several reports on PCL-derived hybrids are available which only describe a few hybrid formulations each and aimed at illustrating the potential of this

hybrid type for versatile regenerative applications.[190–192,224] Mahony et al. have synthesized degradable gelatin-derived hybrids.[36,74] Interestingly, although just three different hybrid formulations have been described, they were able to detect a variety of correlations between material characteristics and macromer as well as hybrid parameters.

The applied indirect rapid prototyping method enabled the adjustment of scaffold porosity (44-68%) and pore size (160-330 µm) independently of each other. This method was previously established by us for fabrication of lactide-free macromer/TEOS hybrids,[54] but has not yet been described for processing of hydrolytically degradable hybrid formulations. Indirect rapid prototyping opens potential to design materials with complex 3D shape and size which is beneficial for precise biomaterial tailoring toward the geometry of the implant site.[2] Advantage of the indirect processing is that this method is compatible with a wide range of formulation viscosities and gelation kinetics when compared to direct printing. Consequently, this method has been used for fabrication of porous devices of different materials including polymers, ceramics and composites.[259–261] Glass-based formulations have also been processed into porous matrices by other techniques.[143,262] For example, Luo et al. have fabricated alginate/glass composite scaffolds by 3D plotting.[149] The characteristic XXYY pattern of the scaffold structure was almost equal to that of the PCL templates used in our studies.[54,263] Gao et al. have fabricated gelatin-based hybrid scaffolds by robocasting demonstrating the applicability of 3D printing for processing of sol-gel-derived materials.[148] Porous hybrid materials have further been fabricated by various other methods including foaming, freeze-drying, electrospinning and salt-leaching.[36,80,226,228] These techniques may ask for lower optimization of the hybrid formulation when compared to 3D printing, but in fact will result in less defined scaffold structures.

6.3.3 Tunability of macromer/glass hybrid material properties

6.3.3.1 Hybrid degradability. Characterization of material degradability was a central aspect of the hybrid glass concept as the adaption of degradation kinetics toward physiological relevance is still an unmet challenge of glass-based material engineering.[93,94] To this end, an *in vitro* degradation study in PBS was performed over one year. The scaffolds degraded within 6-12 months which is a physiologically relevant time frame. An almost linear weight loss rate was detected. This is a significant advantage when compared with the complex and less predictable degradation behavior of linear polyesters.[9,193,264] In particular, abrupt release of acidic

degradation products, especially in late degradation stages, often causes inflammatory response and can impair tissue regeneration.[5,182,186,265] In our hybrid concept, oligoester domains have been incorporated instead of polymeric segments and the obtained homogeneous degradation is a promising result in the illustrated context. It is known that covalent macromer incorporation into the hybrid network promotes congruent degradation of the organic and inorganic phases.[3,36] Lei et al. reported linear biodegradation behavior *in vitro* for gelatin-derived class II hybrids which is in accordance with our results.[187] Weight loss was well-controlled by the content of degradable functionalities (here: oligoester) in the hybrid which is in accordance with gelatin- and chitosan-containing glass-based hybrids.[36,80] Interestingly, the LA/EO weight ratio was even a better predictor of weight loss indicating the contribution of matrix hydrophilicity. Due to the dual-component material concept, these parameters were adjustable by macromer composition and content of the synthetic building block in the macromer/sol mixture (Figure 1-4B).

Many studies of class II hybrids lack of relevant long-term degradation data. In addition, material degradation is often sparsely investigated by only one or two parameters. For example, Rhee et al. characterized the *in vitro* degradation of a PCL-derived hybrid over 56 days by weight loss and Si release.[191] Degradation of another PCL-based hybrid was performed for 84 days, but was only monitored by weight loss.[224] The most extensive study so far characterized degradability of a lactide-derived hybrid material over 140 days by weight loss, water absorption and thermal analysis (DSC), but only one formulation was investigated.[193] In this context, our degradation study represents the longest and most extensively characterized long-term investigation of class II hybrids. As it is known that oligoester hydrolysis proceeds almost independently of enzyme action, it can be assumed that the *in vitro* data serve as crude approximation of the *in vivo* situation.[75,197] However, before the hybrid scaffolds can be used for regenerative, especially load-bearing, applications *in vivo*, the significant initial decrease of mechanical stability has to be optimized.

6.3.3.2 Structure-property relationships. The entire set of 85 differently composed hybrid formulations could be processed into stable scaffolds. This versatility of hybrid formulations was derived from I) high macromer adjustability, II) the combination of two oligomeric hybrid building blocks (Figure 1-4) and III) the adjustment of material porosity independent of hybrid chemistry, and motivated for investigation of relevant structure-property relationships.

As the entire set of scaffolds was characterized with regard to compressive strength and compressive modulus, these mechanical parameters were used for relationship assessment. Total content, oligo(ethylene oxide) content, oligo(lactide) content and molecular weight of the oligomeric cross-linkers as well as material porosity were identified as the main factors determining hybrid mechanics. The obtained relationships between material characteristics and mechanics are in accordance with reports for other macromer-based materials. For example, the correlation between increased oligomer content and increased compressive strength as well as decreased compressive modulus has been previously reported for PCL-, gelatin- and chitosan-based materials.[74,80,192] The effects of LA and EO content are known from cross-linked PLA/PEG matrices,[53,79] but not yet for hybrid materials. Overall, these findings extend our previous results for LA-free hybrids,[54] but this versatility of correlations has not been reported before for any degradable hybrid material. In this regard, one of the most comprehensive study was performed by Mahony et al. who identified the effects of overall six parameters of gelatin-derived hybrid matrices on compressive strength and modulus.[74] The mechanical properties of chemically cross-linked materials generally strongly depend on the cross-linking degree but its determination in macromer/sol-derived hybrids is difficult. In this regard, the molar ratio of silane-coupling agent (e.g. ICPTES, GPTMS) to organic component (C-factor) can be used in order to estimate the cross-linking degree.[36] Although both parameters were not determined for the TxLAy- and PxLAy-derived hybrids, cross-linking density is affected by all of the illustrated compositional parameters. To this end, our characterization represents an extended differentiation of the hybrid network properties. Furthermore, the identified effects of scaffold porosity on compressive strength and modulus were almost equal to the literature.[4,54,73,166]

Hybrid degradability was significantly controlled by content of degradable oligoester domains and LA/EO weight ratio representing matrix hydrophilicity as illustrated in section 6.3.3.1. These correlations have been described for different hybrids, e.g. materials based on gelatin and chitosan.[36,80] The effect of matrix hydrophilicity on water accessibility toward the hydrolytically degradable groups has been described for many polyester/PEG materials.[30,38,210] Such a correlation, however, was not reported for any glass based hybrid material and was often even undetectable when matrix hydrophilicity was not adjustable independent of the content of degradable functionalities.

Overall, the identified correlations are generally known from literature, but have not yet been reported for the same macromer-based material.

When compared to most other reports for class II hybrids, the number of detected correlations combined with high data density is unique. For example, Rhee and co-workers have characterized the mechanical and degradative properties of PCL-based hybrids in separate reports and by only three and two different formulations, respectively.[191,192] Consequently, statistically relevant correlations have not been described. Furthermore, although Helminen et al. have synthesized 8 different hybrids, only a fraction was characterized with regard to mechanical (6 formulations) and degradative properties (1 formulation).[193] The most extensive study has been performed by Mahony et al. who investigated the effects of 7 structure and process variables on overall 12 different material characteristics.[74] As the most correlations were derived from only 3 different hybrid formulations, however, only trends were usually discussed.

6.4 SIGNIFICANCE OF THE MACROMER-BASED DESIGN

Each macromer-based material concept requires oligo- or polymeric precursors with reactive functional groups enabling cross-linking or cross-polymerization into polymeric networks (Figure 1-1).[19] In this regard, a great variety of strategies has been established for macromer synthesis.[5,10,49] In the present thesis, two different chemistries were used which are both characterized by high flexibility. FRP is applicable for a large number of (meth-)acrylate- and vinyl-based monomers and accordingly functionalized oligo- and polymers.[11] For example, a great variety of hydroxyl and/or amino group-containing derivatives can be effectively methacrylated by methacryloyl chloride and methacryloyl anhydride, respectively.[122,266] As ROP requires cyclic esters, the versatility of this synthetic route is reduced when compared to FRP, although a set of chemically different lactones is available.[10] Different oligoester types can also be combined in a macromer as demonstrated by Davis et al. who have synthesized poly(lactic acid-*co*-caproic acid) diethylene glycol based oligomers.[30] In macromer concepts, reactive functionalities are introduced which either should offer a certain chemical stability or should be protected from inactivation. While (meth-)acrylates can be stabilized by light protection and the addition of hydroquinone ethers,[53,267] clickable functionalities generally offer enhanced stability due to their highly specific reactivity.[12] The sensitivity of reactive macromers was confirmed in

this thesis as partial hydrolysis of reactive functionalities during synthesis and purification was observed in both material concepts. The application of permanent inert degassing, even during macromer purification, might be one strategy in order to improve macromer quality. Once the reactive functionalities were hydrolyzed, a reactivation is generally critical as previously shown for oPNMA derivatives.[96,268] Nevertheless, it was possible to introduce at least two reactive functionalities per macromer molecule into each derivative. To this end, all macromers synthesized in this thesis were able to act as cross-linkers or to support cross-polymerization.

A key aspect of this thesis was to process the synthesized macromers into biomaterials of relevant sizes for which considerable macromer amounts were required. However, limited time-dependent stability of the reactive groups has to be considered when increasing the macromer batch size. All macromers were synthesized in batches of adaptable sizes (yields: 10-30 g), but were storable under different conditions. Storage of the oPDMA macromers in vacuum enabled efficient preservation of the anhydride functionalities over 2-3 months.[96] As an application of reduced pressure for ethanol removal would likely initiate siloxane polymerization in TxLAy-Si and PxLAy-Si derivatives due to ethanol evaporation,[193,196] these conditions were not applicable for storage of these LA-containing macromer derivatives. Consequently, the non-silanized oligomer intermediates were functionalized with ICPTES immediately before processing into glass-based hybrids.

Besides reproducible synthesis strategies, thorough analytical characterization was required for fabrication of adjustable biomaterials.[89] Macromer composition is generally characterized by NMR spectroscopy, although high-resolution techniques, such as 2D NMR, are only applicable for selected derivatives due to the generally broad signals of oligo-/polymeric structures.[250,269] In this thesis, good control over the chemical macromer composition was shown by ^{1}H and ^{13}C NMR spectroscopy which are the most widely used methods.[270] Molecular weight was characterized by size exclusion chromatography (GPC/SEC) and the synthesis of low molecular-weight derivatives (< 10 kDa) was confirmed which fits to the criteria of the macromer concept.[19]

Overall, independent control over different characteristics of the macromer structure is favorable in order to enable specific tunability of macromer-based materials.[53] This flexibility of the macromer structure was demonstrated for both macromer concepts. Macromer composition, especially anhydride (oPxMA) and ketone content (oPDMA) was tunable by composition of the

comonomer feed. Molecular weight can be adjusted by variation of initiator concentration and/or reaction time as previously demonstrated.[95] MA content, however, was not adjustable without affecting molecular weight which is a certain limitation of adjustability of the oPxMA macromers. Nevertheless, the obtained indirect correlation between both variables offers potential to control network properties by variation of the oPDMA type. This can be nicely illustrated by calculating the 'molecular weight per chemically intact MA' which represents a rough estimation of the 'molecular weight between cross-links (M_c)' (section 4.1).[90] For the degradable LA-based macromers, oligo(lactide) content was precisely controlled by the ratio of D,L-lactide to core alcohol in the synthesis feed. Macromer chain-end functionalization by ICPTES further offers great promise to adjust macromer reactivity independently of its molecular weight enabling improved fine-tuning of the final hybrid network structure. Tunability of macromer reactivity, however, is limited in this concept as two out of the three (TxLAy) or four (PxLAy) arms have to be activated to render the macromers efficient cross-linkers. In this regard, increased flexibility might be achieved by the synthesis of more branched structures, such as 5- or 6-armed macromers as shown by Hao et al.[271]

The flexibility of macromer-based materials is a result of high processing flexibility of the low molecular-weight oligo- or polymeric precursors. In that regard, macromer solubility is a key criterion, because good solubility characteristics enables adaption of the macromer concentration over a wide range.[53] Anhydride-containing oPxMA (oPDMA and oPNMA) macromers were soluble in THF, chloroform, dichloromethane, acetone, DMF, DMSO as well as in FDA-approved[272] *N*-methyl-2-pyrrolidone (NMP), and in concentrations of up to more than 50% (w/v). For example, effective cross-linking of model polyetheramines (different Jeffamine® types) was shown in acetonic solution.[90] DMF and acetone were used to perform covalent macromer derivatization with different functional amines.[98,115] Solubility in aqueous medium was further shown which, however, is accompanied by anhydride hydrolysis. Consequently, water-soluble gelatinous peptides were not cross-linkable in purely aqueous medium, but the fast cross-linking reaction enabled gelation in organic-aqueous medium.[91,98] The set of LA-derived macromers was also soluble in common organic solvents, including THF, chloroform, DMSO and ethanol. Water solubility of the hydrophilic silane-functionalized macromers can be assumed, but an aqueous environment would immediately initiate siloxane polymerization. The fluidity of these macromers was used for solvent-free processing. This strategy is novel for macromer processing into degradable glass-based hybrids as it was previously described only in

context with non-degradable macromers.[36,19054] Overall, the low viscosity of the macromers (TxLAy, PxLAy) or their solutions (oPxMA) has to be pointed out as important requirement in order to enable processing of different macromer types by versatile techniques.[58]

With particular respect to regenerative purposes, the fabrication of macroporous scaffolds is promising in order to enable cell migration.[273] Besides conventional strategies, including porogen-leaching[53,56] and freeze-drying[145], macromers can meanwhile even be processed by challenging techniques, such as direct 3D-printing which requires precise adjustability of cross-linking kinetics.[148,149] In this regard, solid scaffold materials offer excellent potential as their porosity can be adjusted by application of versatile methods and over a wide range.[69,176] The adjustability of macroporosity is generally reduced in case of hydrogels due to their fragility.[59,157] Nevertheless, these soft matrices hold great promise for tissue regeneration due to their high similarity with natural ECM and their physico-chemical properties including elasticity and diffusivity.[7–10] To this end, versatile tissue types can be targeted by hydrogel matrices including hard tissues,[152,218] although load-bearing applications can be better addressed by stiff and mechanically stable solid scaffolds.[274] In this thesis, it was demonstrated that two macromer-based material platforms with significantly different rigidity were processable into macroporous matrices. Processability of the LA-containing macromers within hybrid sol mixtures by indirect rapid prototyping was achieved by the application of reduced and adjustable pressure during template filling. In the oPxMA/gelatin hydrogel concept, cross-linking kinetics were crucial for hydrogel homogeneity, while cross-linking density controlled material stability as also previously described.[91,92] We have recently found that optimized mixing of the oligomeric hydrogel precursors can improve hydrogel homogeneity and can be used for hydrogel molding and structuring.[115,247] In particular, the application of a double syringe delivery system equipped with a static mixer enabled fabrication of homogeneous hydrogels from formulations which were not accordingly processable with the conventional method based on vortexing.[91]

Versatility of the macromer-based materials established in this thesis was derived from: I) synthesis of differently composed macromers, II) combination of the macromers with a second oligomeric building block, and III) flexible macromer processability of these dual-component hybrids. With regard to the material properties, this resulted in two key advantages:

- Adjustability of material properties over a wide range.

- Specific tunability of material characteristics toward the requirements of a certain target tissue.

The independent control over different material properties is of particular interest for material tailorability.[38,53,74] In the material concepts investigated in this thesis, this was generally achieved for the following material characteristics: covalent post-functionalization vs. pre-determined material characteristics (oPDMA/gelatin), degradability vs. mechanics and porosity vs. pore size (LA-containing hybrid glass). In both material concepts, however, the degree of engineering freedom was limited to a certain degree. In case of the oPxMA-derived hydrogels, flexibility of the macromer structure is reduced, because the variation of oligomer anhydride content also affected its molecular weight and ketone content. To this end, hydrogel post-fabrication functionalization could not be completely decoupled from the cross-linking density. Furthermore, composition of the oPxMA/gelatin matrices immediately affected hydrogel stiffness as well as material porosity. In this context, porogen-leaching approach by using P8k was identified as a promising strategy to adjust hydrogel porosity independently of the network structure. In comparison, the hybrid glass platform, to date, allows for material adjustment over a wider range of properties which can be explained by a variable macromer design combined with the highly flexible indirect 3D-printing method.[54,251] While LA content of the macromer was precisely adjustable, the variation of EO content was limited by the commercial availability of corresponding core alcohols. Furthermore, despite the independent control over LA and EO content, both parameters strongly triggered molecular weight of the macromers which in turn controlled cross-linking density of the hybrid network. In addition, macromer reactivity was adjustable only under the precondition to obtain at least two reactive groups per molecule for effective cross-linking.[54]

From a biomaterial researcher´s perspective, the identification of relevant structure-property relationships is a fundamental goal of material characterization in order to demonstrate material tailorability for different regenerative purposes.[63] Correlations between different material characteristics and macromer parameters have been reported for versatile biomaterial concepts.[36,88] The identified correlations, however, were often derived from a low number of different formulations.[191] The macromer-based materials in this thesis allowed for the characterization of a large number of formulations. This allowed for statistical confirmation of the observed trends, especially in the glass-based hybrid material. In the oPxMA/gelatin system,

not all formulations could be included due to inhomogeneous cross-linking of highly reactive formulations inherent to the fabrication technique. Nevertheless, a large number of analyzable formulations remained and formulation-property correlations could be derived.

6.5 OUTLOOK

This thesis illustrated the design and processing flexibility of two macromer-based biomaterials. For regenerative purposes, the applicability of strategies for porosity adaption independent of the physico-chemical material properties, including mechanics and degradability, is a critical design advantage in order to fabricate open macroporous materials with sufficient mechanical stability.[74] The indirect rapid prototyping method enabled processing of various macromer-sol mixtures into hybrid glass scaffolds with accurately defined geometry and porosity. The oPxMA-derived hydrogel platform, however, was not yet processable into such precisely structured matrices. Nevertheless, it was shown that both oligomeric hydrogel building blocks can be dissolved in high concentrations, that the hydrogel fabrication process can be up-scaled and that gelation kinetics are adjustable on versatile levels. These are important fundamentals for the applicability of 3D-printing which is clearly arising in the recent years.[58] In this regard, one could imagine applicability of extrusion-based methods, such as direct printing of macromer/gelatin mixtures immediately after mixing which is similar to the injection-molding technique that has already been successfully applied for oPNMA/COL processing.[115,247] Besides, the extrusion of a gelatin solution into a oPxMA macromer bath might be another strategy similar to 3D-printing of calcium-cross-linked alginate gels.[59]

The tunability of gelation kinetics is further relevant for the development of *in situ*-gelling hydrogel systems.[115] In that regard, however, the replacement of the toxic DMF by a more cytocompatible solvent, such as the FDA-approved NMP,[247,275] and the reduction of the amount of organic solvent are key issues that have to be addressed before. Especially the latter strategy is a critical aspect for the established oPxMA-based systems as these macromers form colloidal precipitations in water-rich media. An introduction of more hydrophilic co-monomers might serve as sufficient approach to address this issue[122,276] which is currently being investigated. Nevertheless, injectability of pre-gelled oPNMA/COL formulations by shear thinning was already demonstrated.[247]

The introduction of biological activity is a key issue of biomaterial synthesis. To this end, biomimetic matrices are wanted that combine physico-chemical properties of the ECM with its functionality. In this regard, hydrogels are ideal matrices for post-fabrication functionalization due to their excellent diffusivity and the applicability of versatile bioconjugation strategies.[49] It was shown that the oPDMA/gelatin hydrogel systems offers great promise for covalent material functionalization by partial anhydride conversion and/or post-fabrication functionalization of ketone-containing gels as shown by model ligands. It would be of high relevance to extend the covalent post-fabrication functionalization strategies by:

- Immobilization of other functional ECM components.
- Characterization of the biological activity of immobilized derivatives.
- Investigation of the release potential of temporally immobilized ligands.

In terms of controlled release applications, particulate carriers are also relevant. While processability of the oPxMA/gelatin system into microparticles has already been demonstrated,[91] covalently functionalized oPDMA-based nanoparticles might be of relevance for systemic applications. To this end, oPxMA-cross-linked particulate systems will be subject of future work.

In the context of biomimetic material design, a post-fabrication functionalization of solid scaffolds with ECM components is generally almost limited to surface modification due to reduced matrix diffusivity, especially of hydrophobic materials.[140,258] The hydrophilic silica-based network of the degradable hybrid scaffolds described in this thesis, however, might open potential for matrix functionalization. Furthermore, the sol-gel process can be used to covalently introduce functional components into glass-based materials.[36,188] In this regard, an introduction of calcium ions into the hybrid matrix is another important bulk modification with respect to bone regeneration which, however, is generally challenging for sol-gel-derived glass-based networks.[219] We meanwhile know that adaption of the curing conditions can serve as sufficient strategy to reduce the wash out of calcium ions from LA-free hybrids.[150] Controllable degradability of the LA-containing hybrid matrices might be helpful to achieve long-term retention and release of incorporated calcium salts.[38] The oligolactide-derived ester functionalities further offer potential for calcium ion accumulation from the environment.[215] These aspects motivate further characterization of the TxLAy- and PxLAy-derived hybrids.

CHAPTER 7

Summary

Modern biomaterial research in Tissue Engineering and Regenerative Medicine is based on the adaption of material characteristics, especially material chemistry, mechanical properties, porosity, degradability and defect geometry, toward the specific requirements of the target tissue or defect. These material characteristics have been identified by collaboration of researchers in different scientific fields.[63,76] Besides the versatility of different human tissues, variability even within the same type of tissue between humans is known. This can be explained by different localization and (disease-related) differences in metabolism and complicates biomaterial development.[51,72] To this end, materials are wanted, whose properties can precisely be adjusted over a broad range and preferably independently of each other.[165] Macromer-based systems are promising biomaterials in this regard, because the application of chemically well-defined oligomeric building blocks enables flexible tunability of material properties.[20] At the same time, macromers are easily processable due to their low molecular weight which makes them accessible for versatile fabrication methods and allow for the creation of implants of adaptable size, shape and porosity.

In this context, this thesis aimed at advancing two different macromer-based material platforms which were derived from previously established concepts: A) Oligomer-cross-linked gelatinous hydrogels with inherent reactivity for post-fabrication functionalization and B) sol-gel hybrid glass scaffolds from hydrolytically degradable multi-armed macromers. The key aspect of this work was to demonstrate the versatile tunability of these macromer-based materials, while focusing on different specific questions in each platform.

The hydrogel concept is based on cross-linking of gelatinous peptides by anhydride-containing macromers that also act as property determining building blocks as cytocompatible and functional alternative of glutaraldehyde.[90,91] Objective of the present work was to enable decoupling of covalent post-fabrication functionalization of the hydrogel matrix from its cross-linking chemistry. This can be achieved by the combination of two types of reactive functionalities in the same macromer.[84] The set of previously synthesized macromers (oPNMA-x), however, only offered one type of reactive functional groups (anhydrides). To this end, a second functionality was introduced into the hydrogel system by the adaption of macromer composition, namely diacetone acrylamide (DAAm). This comonomer was used as methyl ketone-containing structure which was copolymerized with maleic anhydride (MA) and pentaerythritol diacrylate monostearate (PEDAS) by free radical polymerization to yield dual-

functional oligo(PEDAS-*co*-DAAm-*co*-MA) (oPDMA) macromers. Low molecular-weight oligomers (M_n < 7500 Da) of controlled composition were obtained. Fractions of chemically intact anhydrides of around 70% enabled effective cross-linking of amine-containing macromolecules. Macromer processability into dual-component hydrogel matrices by cross-linking of gelatinous peptides (type B) by adaption of a previously established fabrication procedure was shown.[91] The tunability of hydrogel properties by macromer composition, gelatin type and concentrations of both hydrogel-forming building blocks was demonstrated and elastic moduli of up to 30 kPa indicated the formation of rigid hydrogels. Reactivity of the incorporated methyl ketone functionality toward hydrazides and hydrazines was shown on the macromer level and in the hydrogel state by different strategies. Firstly, pre-fabricated hydrogels were successfully reinforced by secondary cross-linking with adipic acid dihydrazide (ADH). Secondly, pH-dependent immobilization of 2,4-dinitrophenylhydrazine (DNPH) to acid-soluble macromer derivatives as well as cross-linked oPDMA/COL matrices was demonstrated. Thirdly, reversible immobilization of a fluorescent hydrazide (AFH) was shown which was controlled by hydrogel ketone content, hydrazide ligand concentration and medium pH. Lastly, proof-of-concept experiments with hydrazido-functionalized hyaluronan (ATTO-hyHA) demonstrated the potential for covalent post-fabrication hydrogel decoration with ECM components. Cell culture experiments further indicated that the ketone functionality did not negatively affect cytocompatibility. In contrast, the incorporation of the dual-functional building block rather improved cell adhesion and proliferation when oPDMA-derived hydrogels were compared to ketone-free oPNMA-containing analogs. For regenerative purposes, material porosity is known as another important parameter of a scaffold structure determining tissue penetration characteristics.[57,143] To this end, two different strategies were followed to enhance hydrogel porosity on the macro- and nanoscale, respectively. The introduction of macropores was attempted by hydrogel cross-linking in presence of poly(ethylene glycol) (M_n = 8000 Da, P8k). This polymer acted as porogen by phase separation during hydrogel formation. It was found that P8k was effectively extracted from the cross-linked matrix, while physico-chemical hydrogel properties remained unchanged. The other approach aimed at increasing mesh size of the cross-linked network by using hydrogel building blocks with increased molecular weights. In particular, high molecular-weight gelatin (160 Bloom, G160) was cross-linked by low-reactive macromers. Homogeneous and mechanically stable hydrogels were obtained and physico-

chemical properties were determined. An increase of hydrogel porosity was functionally shown by enhanced cell migration and improved release profile of incorporated nanoparticles.[168]

A novel macromer/glass hybrid concept was based on the covalent incorporation of multi-armed oligomeric cross-linkers into a sol-gel-derived silica network in order to improve mechanical stability and to control network properties.[54] The purpose of this work was to introduce adjustable degradability into this hybrid material in order to address the commonly known biodegradability limitations of glass-derived matrices.[93,94] As previously established cross-linkers were not degradable, a novel set of sol-gel-glass reactive macromers with hydrolytically cleavable functionalities was designed. To this end, a macromer platform was synthesized from three- (TMPEO, Tx) or four-armed (PETEO, Px) ethoxylated alcohol cores by ring-opening polymerization with D,L-lactide (LA) which is a common strategy to synthesize biodegradable materials.[53] Low molecular-weight oligomers (TxLAy and PxLAy, M_n = 1100-3200 Da) with variable oligo(ethylene oxide) (EO) content and precisely adjustable degree of oligo(lactide) (LA) derivatization were obtained. Oligomer functionalization with reactive triethoxysilane groups enabled effective cross-linking of a tetraethoxysilane(TEOS)-derived silica sol into class II hybrid glasses. Processability of the macromer/sol mixtures into macroporous scaffolds by using an indirect 3D-printing method was demonstrated. This procedure allowed for the adjustment of pore size and total porosity independently of each other. Overall, 85 hybrid scaffold formulations were fabricated by processing a set of 18 differently composed macromers in different concentrations which enabled the identification of relevant structure-property relationships. Precise adjustability of the mechanical properties (compressive strength: 2-30 MPa, compressive modulus: 44-716 MPa) covering the range described for cancellous bone and beyond was demonstrated.[70,186] By statistical analysis, total content, oligo(ethylene oxide) content, oligo(lactide) content and molecular weight of the organic component were determined as factors determining hybrid mechanics. This material property was further adjustable by material porosity independent of hybrid composition. Uniform *in vitro* degradation of the hybrid scaffolds with almost linear weight loss profiles and only moderate material swelling was found. Hybrid glasses degraded at physiologically relevant rates of 0.2-0.5 wt%/d. Rate was controlled by oligoester content and the ratio of LA content to EO content. This indicated the significance of material hydrophilicity as an additional key factor besides content of degradable functionalities. Hybrid cytocompatibility was demonstrated by direct contact experiments with

human adipose tissue-derived stem cells (hASC). Cells were able to infiltrate the entire pore network, to proliferate and to differentiate toward the osteogenic lineage.

In summary, chemically well-defined macromers were developed by application of reproducible and economic synthesis strategies and were extensively characterized. Flexible macromer processability was demonstrated by the fabrication of covalently cross-linked dual-component hydrogel as well as hybrid glass matrices, and by application of different strategies to adjust material porosity. Precise tunability of these macromer-based materials was shown while focusing on covalent post-functionalization independently of the physico-chemical matrix properties (hydrogels) and the adjustability of mechanical and degradative properties (hybrid glasses). In particular, the independent control over different material characteristics as demonstrated for both macromer-based concepts holds great promise for tailoring material characteristics toward specific regenerative applications.

CHAPTER 8

Zusammenfassung

Die moderne Entwicklung von Biomaterialien für Tissue Engineering und Regenerative Medizin basiert auf der gezielten Anpassung der Materialeigenschaften an die Anforderungen des jeweiligen Zielgewebes oder Gewebedefektes. Dabei stehen vor allem Chemie, mechanische Eigenschaften, Porosität, Abbaubarkeit und Geometrie des Biomaterials im Vordergrund. Diese Materialcharakteristika konnten durch interdisziplinäre Zusammenarbeit unterschiedlicher Forschergruppen identifiziert werden.[63,76] Neben der Vielseitigkeit der verschiedenen humanen Gewebe ist auch eine gewisse Variabilität innerhalb des gleichen Gewebes zwischen verschiedenen Individuen bekannt. Dies kann mit unterschiedlicher Lokalisation und (krankheitsbedingten) Unterschieden im Metabolismus erklärt werden und erschwert die Entwicklung neuer Biomaterialien.[51,72] Aus diesem Grund werden Materialien benötigt, deren Eigenschaften präzise über einen breiten Bereich und vorzugsweise unabhängig voneinander eingestellt werden können.[165] In dieser Hinsicht stellen Makromer-basierte Systeme vielversprechende Biomaterialien dar, weil die Verwendung von chemisch wohldefinierten oligomeren Materialbausteinen eine flexible Einstellbarkeit der Materialeigenschaften ermöglicht.[20] Gleichzeitig sind Makromere aufgrund ihres niedrigen Molekulargewichtes einfach prozessierbar, weshalb sie für vielfältige Herstellungsmethoden zugänglich sind und die Herstellung von Implantaten mit anpassbarer Größe, Form und Porosität erlauben.

In diesem Kontext zielte die vorliegende Dissertation auf die Weiterentwicklung zweier unterschiedlicher Makromer-basierter Materialplattformen, die von bereits etablierten Konzepten abgeleitet wurden: A) Oligomer-vernetzte gelatine-artige Hydrogele mit inhärenter Reaktivität zur Realisierung von *post-fabrication*-Hydrogel-Funktionalisierung sowie B) Sol-Gel Hybrid-Glas Scaffolds aus hydrolytisch spaltbaren, mehrarmigen Makromeren. Hauptaugenmerk dieser Arbeit lag darauf, die vielseitige Anpassbarkeit dieser Makromer-basierten Systeme zu zeigen, wobei in jeder Plattform auf unterschiedliche spezifische Fragestellungen fokussiert wurde.

Das Hydrogel-Konzept basiert auf der Quervernetzung von gelatine-artigen Peptiden durch Anhydrid-haltige Makromere, welche als eigenschaftsbestimmende Bausteine dienen und zytokompatible sowie funktionelle Alternativen von Glutaraldehyd darstellen.[90,91] Zielsetzung der vorliegenden Arbeit war es, eine Entkopplung der kovalenten *post-fabrication*-Funktionalisierung der Hydrogelmatrix von deren Quervernetzungschemie zu ermöglichen. Dies kann prinzipiell durch die Kombination zweier Typen von reaktiven Funktionalitäten im gleichen Makromer erreicht werden.[84] Die zuvor synthetisierten Makromere (oPNMA-x)

enthielten lediglich einen Typ funktioneller Gruppen (Anhydride). Daher wurde eine zweite Funktionalität in das Hydrogel-System durch die Anpassung der Makromer-Zusammensetzung eingeführt: Diacetonacrylamid (DAAm). Dieses Methylketon-haltige Comonomer wurde mit Maleinsäureanhydrid (MA) und Pentaerythritoldiacrylatmonostearat (PEDAS) durch freie radikalische Polymerisation copolymerisiert, um zweifach-funktionelle oligo(PEDAS-*co*-DAAm-*co*-MA)(oPDMA)-Makromere zu erhalten. Oligomere mit niedrigem Molekulargewicht (M_n < 7500 Da) und kontrollierter Zusammensetzung wurden erhalten. Anteile chemisch intakter Anhydride von rund 70% ermöglichten die effektive Quervernetzung von Amin-haltigen Makromolekülen. Die Prozessierbarkeit der Makromere in Zweikomponenten-Hydrogel-Matrizes durch Quervernetzung gelatine-artiger Peptide (Typ B) unter Anwendung eines zuvor etablierten Herstellungsverfahrens wurde gezeigt.[91] Die Einstellbarkeit der Hydrogel-Eigenschaften durch die Makromer-Zusammensetzung, den Gelatine-Typ sowie die Konzentrationen beider Hydrogel-bildender Materialbausteine wurde dargestellt. E-Modul-Werte von bis zu 30 kPa deuteten die Bildung rigider Hydrogele an. Die Reaktivität der eingeführten Methylketon-Funktionalität gegenüber Hydraziden und Hydrazinen wurde sowohl auf Makromer-Ebene als auch im Hydrogel-Zustand durch unterschiedliche Strategien gezeigt. Erstens: Bereits vernetzte Hydrogele wurden durch sekundäre Quervernetzung mittels Adipinsäuredihydrazid (ADH) erfolgreich verfestigt. Zweitens: Die pH-abhängige Immobilisierung von 2,4-Dinitrophenylhydrazin (DNPH) an säurelösliche Makromer-Derivate sowie quervernetzte oPDMA/COL-Matrizes wurde demonstriert. Drittens: Die reversible Immobilisierung eines fluoreszierenden Hydrazids (AFH) wurde bewiesen. Die AFH-Immobilisierung wurde kontrolliert durch den Keton-Gehalt im Hydrogel, die Konzentration des Hyrazid-Liganden und den pH-Wert des Mediums. Schließlich zeigten *proof-of-concept*-Experimente mit Hydrazido-funktionalisiertem Hyaluronan (ATTO-hyHA) das Potenzial zur Hydrogel-Dekoration mit Extrazellulärmatrix(ECM)-Komponenten unter Verwendung von kovalenter *post-fabrication*-Funktionalisierung auf. Zellkultur-Experimente deuteten ferner an, dass die Keton-Funktionalität die Zytokompatibilität nicht negativ beeinflusst. Im Gegenteil trug die Einführung des zweifach-funktionellen Bausteins im Vergleich zu Keton-freien oPNMA-haltigen Hydrogel-Analoga sogar zur Verbesserung der Zelladhäsion und -Proliferation bei. Im Hinblick auf regenerative Anwendungen ist die Materialporosität als ein weiterer wichtiger Parameter der Scaffold-Struktur bekannt, der das Penetrationsvermögen eines regenerierenden Gewebes bestimmt.[57,143] Aus diesem Grund wurden zwei unterschiedliche Strategien verfolgt,

um die Hydrogel-Porosität makro- bzw. nano-skalig zu erhöhen. Die Erzeugung von Makroporen wurde durch Hydrogel-Quervernetzung in Anwesenheit von Polyethylenglykol (M_n = 8000 Da, P8k) versucht. Dieses Polymer wirkte durch Phasentrennung während der Hydrogel-Quervernetzung als Porogen. P8k konnte effektiv aus der quervernetzten Matrix extrahiert werden, während die physikochemischen Hydrogel-Eigenschaften erhalten blieben. Ein zweiter Ansatz zielte auf die Erhöhung der Maschenweite des quervernetzten Netzwerks durch die Verwendung von Hydrogel-Bausteinen mit erhöhtem Molekulargewicht. Konkret wurde hochmolekulare Gelatine (160 Bloom, G160) mittels niedrig reaktiver Makromere quervernetzt. Homogene und mechanisch stabile Hydrogele wurden erhalten und die physikochemischen Eigenschaften wurden ermittelt. Eine Erhöhung der Hydrogel-Porosität wurde funktionell durch verstärkte Zellmigration sowie optimierte Freisetzungsprofile eingeschlossener Nanopartikel bewiesen.[168]

Ein neuartiges Makromer/Glas-Hybrid-Konzept beruhte auf der kovalenten Einführung mehrarmiger oligomerer Quervernetzer in ein Sol-Gel-basiertes Silikat-Netzwerk, um dessen mechanische Stabilität zu verbessern und die Netzwerkeigenschaften zu kontrollieren.[54] Diesbezüglich war die Zielsetzung dieser Arbeit die Einführung einstellbarer Abbaubarkeit in dieses Hybrid-Material, um die allgemein bekannten Abbaubarkeitsprobleme Glas-basierter Matrizes zu adressieren.[93,94] Da die zuvor etablierten Quervernetzer nicht abbaubar waren, wurden neuartige Sol-Gel-Glas-reaktive Makromere mit hydrolytisch spaltbaren Funktionalitäten entwickelt. Eine Makromer-Plattform wurde ausgehend von drei- (TMPEO, Tx) oder vierarmigen ethoxylierten Alkohol-Kernen (PETEO, Px) durch Ringöffnungspolymerisation mit D,L-Lactid (LA) synthetisiert, was eine übliche Strategie zur Synthese bioabbaubarer Materialien darstellt.[53] Niedermolekulare Oligomere (TxLAy und PxLAy, M_n = 1100-3200 Da) mit variablem Oligo(ethylenoxid)(EO)-Gehalt und präzise einstellbarem Grad an Oligo(lactid)-Derivatisierung wurden erhalten. Die Oligomer-Funktionalisierung mit reaktiven Triethoxysilan-Gruppen ermöglichte die effektive Quervernetzung eines Tetraethoxysilan(TEOS)-basierten Silikat-Sols in Hybrid-Gläser der Klasse II. Die Prozessierbarkeit der Makromer/Sol-Mischungen in makroporöse Scaffolds unter Verwendung einer indirekten 3D-Druck-Methode wurde bewiesen. Diese Prozedur erlaubte die Einstellung von Porengröße und Gesamtporosität unabhängig voneinander. Durch Prozessieren eines Sets aus 18 unterschiedlich zusammengesetzten Makromeren in verschiedenen Konzentrationen konnten insgesamt 85 unterschiedliche Hybrid-Scaffold-Formulierungen hergestellt werden, was die Identifizierung

relevanter Struktur-Eigenschafts-Beziehungen ermöglichte. Die präzise Einstellbarkeit der mechanischen Eigenschaften (Druckfestigkeit: 2-30 MPa, Kompressionsmodul: 44-716 MPa), die den für spongiösen Knochen beschriebenen Bereich abdecken beziehungsweise übertreffen, wurde gezeigt.[70,186] Durch statistische Analyse der Ergebnisse konnten Gesamtgehalt, Oligo(ethylenoxid)-Gehalt, Oligo(lactid)-Gehalt und Molekulargewicht der organischen Komponente als Hybrid-Mechanik-bestimmende Faktoren ermittelt werden. Die Material-Mechanik war ferner anpassbar über die Materialporosität, was unabhängig von der Hybrid-Zusammensetzung gelang. Ein gleichmäßiger *in vitro*-Abbau der Hybrid-Scaffolds mit nahezu linearen Masseverlust-Profilen und lediglich moderater Material-Quellung wurde gefunden. Die Hybrid-Gläser bauten sich mit physiologisch relevanten Raten von 0,2-0,5 Gew.%/Tag ab. Die Abbaurate wurde durch den Oligoester-Gehalt und das Verhältnis aus LA-Gehalt zu EO-Gehalt kontrolliert. Dies verdeutlicht die Bedeutung der Materialhydrophilie als einen zusätzlichen Schlüsselfaktor neben dem Gehalt abbaubarer Funktionalitäten. Die Zytokompatibilität der Hybride wurde durch Experimente gezeigt, in denen die Hybride in direkten Kontakt mit aus humanem Fettgewebe gewonnenen Stammzellen (hASC) kamen. Die Zellen waren zur Einwanderung in das gesamte Porennetzwerk, zur Proliferation und zur osteogenen Differenzierung befähigt.

Zusammenfassend wurden chemisch wohldefinierte Makromere durch Anwendung reproduzierbarer und ökonomischer Synthesestrategien entwickelt und umfassend charakterisiert. Die vielseitige Prozessierbarkeit der Makromere wurde anhand der Herstellung von kovalent vernetzten Zweikomponenten-Hydrogelen sowie Hybrid-Glas-Matrizes, und durch die Anwendung unterschiedlicher Strategien zur Einstellung der Materialporosität demonstriert. Die präzise Einstellbarkeit dieser Makromer-basierten Materialien wurde bewiesen mit dem Fokus auf der kovalenten Post-Funktionalisierung bereits vernetzter Matrizes unabhängig von den physikochemischen Matrix-Eigenschaften (Hydrogele) beziehungsweise einer Anpassbarkeit der Material-Mechanik und -Abbaubarkeit (Hybrid-Gläser). Insbesondere die unabhängige Kontrolle über unterschiedliche Materialcharakteristika, die für beide Makromer-basierte Konzepte gezeigt wurde, bietet großes Potential, um die Materialeigenschaften für spezifische regenerative Anwendungen maßzuschneidern.

REFERENCES

(1) OPTN/UNOS Public Comment. *https://optn.transplant.hrsa.gov/* **2017**.

(2) Billiet, T.; Vandenhaute, M.; Schelfhout, J.; Van Vlierberghe, S.; Dubruel, P. *Biomaterials* **2012**, *33* (26), 6020–6041.

(3) Jones, J. R. *Acta Biomater.* **2013**, *9* (1), 4457–4486.

(4) Fu, Q.; Saiz, E.; Rahaman, M. N.; Tomsia, A. P. *Adv. Funct. Mater.* **2013**, *23* (44), 5461–5476.

(5) Puppi, D.; Chiellini, F.; Piras, a. M. M.; Chiellini, E. *Prog. Polym. Sci.* **2010**, *35* (4), 403–440.

(6) Patterson, J.; Martino, M. M.; Hubbell, J. A. *Mater. Today* **2010**, *13* (1–2), 14–22.

(7) Hoffman, A. S. *Adv. Drug Deliver. Rev.* **2012**, *64*, 18–23.

(8) Dimitriou, R.; Jones, E.; McGonagle, D.; Giannoudis, P. V. *BMC Med.* **2011**, *9*, 66.

(9) Amass, W.; Amass, A.; Tighe, B. *Polym. Int.* **1998**, *47* (2), 89–144.

(10) Fakirov, S. *Biodegradable Polyesters*, First Edit.; Wiley-VCH, Weinheim, 2015.

(11) Odian, G. *Principles of Polymerization*, Fourth Edi.; Wiley InterScience, 2004.

(12) Uliniuc, A.; Popa, M.; Hamaide, T.; Dobromir, M. *Cell. Chem. Technol.* **2012**, *46* (1–2), 1–11.

(13) Van Vlierberghe, S.; Dubruel, P.; Schacht, E. *Biomacromolecules* **2011**, *12* (5), 1387–1408.

(14) Lau, H. K.; Kiick, K. L. *Biomacromolecules* **2015**, *16* (1), 28–42.

(15) Ahadian, S.; Sadeghian, R. B.; Salehi, S.; Ostrovidov, S.; Bae, H.; Ramalingam, M.; Khademhosseini, A. *Bioconjug. Chem.* **2015**, *26* (10), 1984–2001.

(16) Algar, W. R.; Prasuhn, D. E.; Stewart, M. H.; Jennings, T. L.; Blanco-Canosa, J. B.; Dawson, P. E.; Medintz, I. L. *Bioconjug. Chem.* **2011**, *22* (5), 825–858.

(17) Ossipov, D.; Kootala, S.; Yi, Z.; Yang, X.; Hilborn, J. *Macromolecules* **2013**, *46* (10), 4105–4113.

(18) Vert, M. *Biomacromolecules* **2004**, *6* (2), 538–546.

(19) Nic, M.; Jirát, J.; Košata, B.; Jenkins, A.; McNaught, A.; Wilkinson, A. *IUPAC, Research Triangle Park, NC* **2014**.

(20) Hacker, M. C.; Nawaz, H. A. *Int. J. Mol. Sci.* **2015**, *16* (11), 27677–27706.

(21) Camci-Unal, G.; Cuttica, D.; Annabi, N.; Demarchi, D.; Khademhosseini, A. *Biomacromolecules* **2013**, *14* (4), 1085–1092.

(22) Li, Y.; Rodrigues, J.; Tomás, H. *Chem. Soc. Rev.* **2012**, *41* (6), 2193–2221.

(23) Ravichandran, R.; Mirazul Islam, M.; Alarcon, E.; Samanta, A.; Wang, S.; Lundström, P.; Hilborn, J.; Griffith, M.; Phopase, J. *J. Mater. Chem. B* **2015**, *4*, 318–326.

(24) Hutson, C. B.; Nichol, J. W.; Aubin, H.; Bae, H.; Yamanlar, S.; Al-Haque, S.; Koshy, S. T.; Khademhosseini, A. *Tissue Eng. Part A* **2011**, *17* (13–14), 1713–1723.

(25) Durst, C. A.; Cuchiara, M. P.; Mansfield, E. G.; West, J. L.; Grande-Allen, K. J. *Acta Biomater.* **2011**, *7* (6), 2467–2476.

(26) Pedrón, S.; Peinado, C.; Bosch, P.; Anseth, K. S. *Acta Biomater.* **2010**, *6* (11), 4189–4198.

(27) Klouda, L. *Eur. J. Pharm. Biopharm.* **2015**, *97*, 338–349.

(28) Lee, S.; Kim, S. H.; Kim, Y. H.; Han, Y. *Macromol. Res.* **2002**, *10* (2), 85–90.

(29) Metters, A. T.; Anseth, K. S.; Bowman, C. N. *Polymer* **2000**, *41* (11), 3993–4004.

(30) Davis, K. A.; Burdick, J. A.; Anseth, K. S. *Biomaterials* **2003**, *24* (14), 2485–2495.

(31) Zhu, A.; Pan, Y.; Liao, T.; Zhao, F.; Chen, T. *J. Biomed. Mater. Res. B Appl. Biomater.* **2008**, *85B* (2), 489–495.

(32) Behravesh, E.; Shung, A. K.; Jo, S.; Mikos, A. G. *Biomacromolecules* **2002**, *3* (1), 153–158.

(33) Shin, H.; Temenoff, J. S.; Mikos, A. G. *Biomacromolecules* **2003**, *4* (3), 552–560.

(34) Maaref, S.; Roz, Z.; Sun, S.-S.; Seo, K.; Winston, K.; Bonner, C. E. *J. Appl. Polym. Sci.* **2004**, *92* (1), 317–322.

(35) Tian, D.; Dubois, P. H.; Jérôme, R. *J. Polym. Sci. A Polym. Chem.* **1997**, *35* (11), 2295–2309.

(36) Mahony, O.; Tsigkou, O.; Ionescu, C.; Minelli, C.; Ling, L.; Hanly, R.; Smith, M. E.; Stevens, M. M.; Jones, J. R. *Adv. Funct. Mater.* **2010**, *20* (22), 3835–3845.

(37) Poologasundarampillai, G.; Ionescu, C.; Tsigkou, O.; Murugesan, M.; Hill, R. G.; Stevens, M. M.; Hanna, J. V; Smith, M. E.; Jones, J. R. *J. Mater. Chem.* **2010**, *20* (40), 8952–8961.

(38) Valliant, E. M.; Jones, J. R. *Soft Matter* **2011**, *7* (11), 5083–5095.

(39) Jiang, Y.; Chen, J.; Deng, C.; Suuronen, E. J.; Zhong, Z. *Biomaterials* **2014**, *35* (18), 4969–4985.

(40) Pouyani, T.; Prestwich, G. D. *Bioconjug. Chem.* **1994**, *5* (4), 339–347.

(41) Martinez-Sanz, E.; Ossipov, D. A.; Hilborn, J.; Larsson, S.; Jonsson, K. B.; Varghese, O. P. *J. Control. Release* **2011**, *152* (2), 232–240.

(42) Ito, T.; Yeo, Y.; Highley, C. B.; Bellas, E.; Kohane, D. S. *Biomaterials* **2007**, *28* (23), 3418–3426.

(43) Boehnke, N.; Cam, C.; Bat, E.; Segura, T.; Maynard, H. D. *Biomacromolecules* **2015**, *16* (7), 2101–2108.

(44) Patenaude, M.; Campbell, S.; Kinio, D.; Hoare, T. *Biomacromolecules* **2014**, *15* (3), 781–790.

(45) Dirksen, A.; Dawson, P. E. *Bioconjug. Chem.* **2008**, *19* (12), 2543–2548.

(46) Popescu, I.; Suflet, D. M.; Pelin, I. M.; Chiţanu, G. C. *Rev. Roum. Chim.* **2011**, *56* (3), 173–188.

(47) Guan, J.; Hong, Y.; Ma, Z.; Wagner, W. R. *Biomacromolecules* **2008**, *9* (4), 1283–1292.

(48) Truong, V. X.; Tsang, K. M.; Simon, G. P.; Boyd, R. L.; Evans, R. A.; Thissen, H.; Forsythe, J. S. *Biomacromolecules* **2015**, *16* (7), 2246–2253.

(49) Nimmo, C. M.; Shoichet, M. S. *Bioconjug. Chem.* **2011**, *22* (11), 2199–2209.

(50) McKinnon, D. D.; Domaille, D. W.; Cha, J. N.; Anseth, K. S. *Chem. Mater.* **2014**, *26* (7), 2382–2387.

(51) Hutmacher, D. W.; Schantz, J. T.; Lam, C. X. F.; Tan, K. C.; Lim, T. C. *J. Tissue Eng. Regen. Med.* **2007**, *1* (4), 245–260.

(52) Evchuk, I. Y.; Musii, R. I.; Makitra, R. G.; Pristanskii, R. E. *Russ. J. Appl. Chem.* **2005**, *78* (10), 1576–1580.

(53) Loth, R.; Loth, T.; Schwabe, K.; Bernhardt, R.; Schulz-Siegmund, M.; Hacker, M. C. *Acta Biomater.* **2015**, *26*, 82–96.

(54) Hendrikx, S.; Kascholke, C.; Flath, T.; Schumann, D.; Gressenbuch, M.; Schulze, P.; Hacker, M. C.; Schulz-Siegmund, M. *Acta Biomater.* **2016**, *35*, 318–329.

(55) Lee, S. B.; Kim, Y. H.; Chong, M. S.; Hong, S. H.; Lee, Y. M. *Biomaterials* **2005**, *26* (14), 1961–1968.

(56) Hacker, M.; Ringhofer, M.; Appel, B.; Neubauer, M.; Vogel, T.; Young, S.; Mikos, A. G.; Blunk, T.; Göpferich, A.; Schulz, M. B. *Biomaterials* **2007**, *28* (24), 3497–3507.

(57) Lévesque, S. G.; Lim, R. M.; Shoichet, M. S. *Biomaterials* **2005**, *26* (35), 7436–7446.

(58) Mandrycky, C.; Wang, Z.; Kim, K.; Kim, D. H. *Biotechnol. Adv.* **2016**, *34* (4), 422–434.

(59) Kirchmajer, D. M.; Gorkin III, R.; in het Panhuis, M. *J. Mater. Chem. B* **2015**, *3* (20), 4105–4117.

(60) Hoch, E.; Hirth, T.; Tovar, G. E. M.; Borchers, K. *J. Mater. Chem. B* **2013**, *1* (41), 5675–5685.

(61) Pantani, R.; Turng, L.-S. *J. Appl. Polym. Sci.* **2015**, *132* (48), 42458.

(62) Maher, P. S.; Keatch, R. P.; Donnelly, K.; Mackay, R. E.; Paxton, J. Z. *Rapid Prototyp. J.* **2009**, *15* (3), 204–210.

(63) Hilderbrand, A. M.; Ovadia, E. M.; Rehmann, M. S.; Kharkar, P. M.; Guo, C.; Kloxin, A. M. *Curr. Opin. Solid St. M.* **2016**, *20* (4), 212–224.

(64) Rzaev, Z. M. O.; Dinçer, S.; Pişkin, E. *Prog. Polym. Sci.* **2007**, *32* (5), 534–595.

(65) Cohn, D.; Younes, H. *J. Biomed. Mater. Res.* **1988**, *22* (11), 993–1009.

(66) Niu, X.; Luo, Y.; Li, Y.; Fu, C.; Chen, J.; Wang, Y. *J. Biomed. Mater. Res. A* **2008**, *84* (4), 908–916.

(67) Tian, W. M.; Zhang, C. L.; Hou, S. P.; Yu, X.; Cui, F. Z.; Xu, Q. Y.; Sheng, S. L.; Cui, H.; Li, H. D. *J. Control. Release* **2005**, *102* (1), 13–22.

(68) Dinçer, S.; Köseli, V.; Kesim, H.; Rzaev, Z. M. O.; Pişkin, E. *Eur. Polym. J.* **2002**, *38* (11), 2143–2152.

(69) Karageorgiou, V.; Kaplan, D. *Biomaterials* **2005**, *26* (27), 5474–5491.

(70) Hench, L. L.; Wilson, J. *World Scientific Publishing Company, Singapore* **1993**.

(71) Fratzl, P.; Gupta, H. S.; Paschalis, E. P.; Roschger, P. *J. Mater. Chem.* **2004**, *14* (14), 2115–2123.

(72) Fu, Q.; Saiz, E.; Rahaman, M. N.; Tomsia, A. P. *Mater. Sci. Eng. C* **2011**, *31* (7), 1245–1256.

(73) Thomson, R. C.; Yaszemski, M. J.; Powers, J. M.; Mikos, A. G. *J. Biomat. Sci.-Polym. E.* **1995**, *7* (1), 23–38.

(74) Mahony, O.; Yue, S.; Turdean-Ionescu, C.; Hanna, J. V.; Smith, M. E.; Lee, P. D.; Jones, J. R. *J. Sol-Gel Sci. Technol.* **2014**, *69* (2), 288–298.

(75) Eglin, D.; Mortisen, D.; Alini, M. *Soft Matter* **2009**, *5* (5), 938–947.

(76) Burdick, J. A.; Murphy, W. L. *Nat. Commun.* **2012**, *3*, 1269.

(77) Watarai, A.; Schirmer, L.; Thönes, S.; Freudenberg, U.; Werner, C.; Simon, J. C.; Anderegg, U. *Acta Biomater.* **2015**, *25*, 65–75.

(78) Clapper, J. D.; Skeie, J. M.; Mullins, R. F.; Guymon, C. A. *Polymer* **2007**, *48* (22), 6554–6564.

(79) Dai, X.; Chen, X.; Yang, L.; Foster, S.; Coury, A. J.; Jozefiak, T. H. *Acta Biomater.* **2011**, *7* (5), 1965–1972.

(80) Wang, D.; Romer, F.; Connell, L.; Walter, C.; Saiz, E.; Yue, S.; Lee, P. D.; McPhail, D. S.; Hanna, J. V.; Jones, J. R. *J. Mater. Chem. B* **2015**, *3* (38), 7560–7576.

(81) Aamodt, J. M.; Grainger, D. W. *Biomaterials* **2016**, *86*, 68–82.

(82) Zhu, J.; Marchant, R. E. *Expert Rev. Med. Devices* **2011**, *8* (5), 607–626.

(83) Freudenberg, U.; Hermann, A.; Welzel, P. B.; Stirl, K.; Schwarz, S. C.; Grimmer, M.; Zieris, A.; Panyanuwat, W.; Zschoche, S.; Meinhold, D.; Storch, A.; Werner, C. *Biomaterials* **2009**, *30* (28), 5049–5060.

(84) Kaga, S.; Yapar, S.; Gecici, E. M.; Sanyal, R. *Macromolecules* **2015**, *48* (15), 5106–5115.

(85) Luo, Y.; Prestwich, G. D. *Bioconjug. Chem.* **1999**, *10* (5), 755–763.

(86) DeForest, C. A.; Polizzotti, B. D.; Anseth, K. S. *Nat. Mater.* **2009**, *8* (8), 659–664.

(87) DeForest, C. A.; Anseth, K. S. *Nat. Chem.* **2011**, *3* (12), 925–931.

(88) Singh, A.; Zhan, J.; Ye, Z.; Elisseeff, J. H. *Adv. Funct. Mater.* **2013**, *23* (5), 575–582.

(89) Hacker, M. C. *Habil. Univ. Leipzig, Fak. für Biowissenschaften, Pharm. und Psychol.* **2016**.

(90) Loth, T.; Hennig, R.; Kascholke, C.; Hötzel, R.; Hacker, M. C. *React. Funct. Polym.* **2013**, *73* (11), 1480–1492.

(91) Loth, T.; Hötzel, R.; Kascholke, C.; Anderegg, U.; Schulz-Siegmund, M.; Hacker, M. C. *Biomacromolecules* **2014**, *15* (6), 2104–2118.

(92) Loth, T. *Diss. Univ. Leipzig, Fak. für Biowissenschaften, Pharm. und Psychol.* **2016**.

(93) Hamadouche, M.; Meunier, A.; Greenspan, D. C.; Blanchat, C.; Zhong, J. P.; La Torre, G. P.; Sedel, L. *J. Biomed. Mater. Res.* **2001**, *54* (4), 560–566.

(94) Martin, R. A.; Yue, S.; Hanna, J. V.; Lee, P. D.; Newport, R. J.; Smith, M. E.; Jones, J. R. *Philos. Trans. A Math. Phys. Eng. Sci.* **2012**, *370* (1963), 1422–1443.

(95) Hennig, R. *Dipl. Univ. Leipzig, Fak. für Biowissenschaften, Pharm. und Psychol.* **2010**.

(96) Kascholke, C. *Dipl. Univ. Leipzig, Fak. für Biowissenschaften, Pharm. und Psychol.* **2011**.

(97) Wang, R.; Wang, J.; Lv, W.; Guo, J.; He, Y.; Jiang, M. *J. Appl. Polym. Sci.* **2011**, *120* (5), 3109–3117.

(98) Kascholke, C.; Loth, T.; Kohn-Polster, C.; Möller, S.; Bellstedt, P.; Schulz-Siegmund, M.; Schnabelrauch, M.; Hacker, M. C. *Biomacromolecules* **2017**, *18* (3), 683–694.

(99) Volpi, N.; Maccari, F.; Titze, J. *J. Chromatogr. B* **2005**, *820* (1), 131–135.

(100) Storey, R. F.; Sherman, J. W. *Macromolecules* **2002**, *35* (5), 1504–1512.

(101) Shin, H.; Jo, S.; Mikos, A. G. *Biomaterials* **2003**, *24* (24), 4353–4364.

(102) Zhu, J. *Biomaterials* **2010**, *31* (17), 4639–4656.

(103) Hynd, M. R.; Frampton, J. P.; Dowell-Mesfin, N.; Turner, J. N.; Shain, W. *J. Neurosci.*

Methods **2007**, *162* (1–2), 255–263.

(104) Sülflow, K.; Schneider, M.; Loth, T.; Kascholke, C.; Schulz-Siegmund, M.; Hacker, M. C.; Simon, J.-C.; Savkovic, V. *J. Biomed. Mater. Res. A* **2016**, *104* (12), 3115–3126.

(105) Nakayama, Y. *Prog. Org. Coatings* **2004**, *51* (4), 280–299.

(106) Neuberg, C.; Grauer, A.; Pisha, B. V. *Anal. Chim. Acta* **1952**, *7* (3), 238–242.

(107) Alves, M. H.; Young, C. J.; Bozzetto, K.; Poole-Warren, L. A.; Martens, P. J. *Biomed. Mater.* **2012**, *7* (2), 24106.

(108) Lee, K. Y.; Bouhadir, K. H.; Mooney, D. J. *Macromolecules* **2000**, *33* (1), 97–101.

(109) Lu, C.; Wang, X.; Wu, G.; Wang, J.; Wang, Y.; Gao, H.; Ma, J. *J. Biomed. Mater. Res. A* **2014**, *102* (3), 628–638.

(110) Patenaude, M.; Hoare, T. *Biomacromolecules* **2012**, *13* (2), 369–378.

(111) Roberts, J. J.; Naudiyal, P.; Jugé, L.; Bilston, L. E.; Granville, A. M.; Martens, P. J. *ACS Biomater. Sci. Eng.* **2015**, *1* (12), 1267–1277.

(112) Zhang, J. H.; Lin, X. N.; Liu, J. J.; Zhao, J. Q.; Dong, H. X.; Deng, L. D.; Liu, J. F.; Dong, A. J. *J. Mater. Chem. B* **2013**, *1* (36), 4667–4677.

(113) Lu, Y.; Mbong, G. N. N.; Liu, P.; Chan, C.; Cai, Z.; Weinrich, D.; Boyle, A. J.; Reilly, R. M.; Winnik, M. A. *Biomacromolecules* **2014**, *15* (6), 2027–2037.

(114) Uzu, S.; Kanda, S.; Imai, K.; Nakashima, K.; Akiyama, S. *Analyst* **1990**, *115* (11), 1477–1482.

(115) Kohn, C.; Klemens, J. M.; Kascholke, C.; Murthy, N. S.; Kohn, J.; Brandenburger, M.; Hacker, M. C. *Biomater. Sci.* **2016**, *4*, 1605–1621.

(116) Kunze, R.; Roesler, M.; Moeller, S.; Schnabelrauch, M.; Riemer, T.; Hempel, U.; Dieter, P. *Glycoconj. J.* **2010**, *27* (1), 151–158.

(117) Luo, Y.; Kirker, K. R.; Prestwich, G. D. *J. Control. Release* **2000**, *69* (1), 169–184.

(118) Creuzet, C.; Kadi, S.; Rinaudo, M.; Auzély-Velty, R. *Polymer* **2006**, *47* (8), 2706–2713.

(119) Salbach-Hirsch, J.; Ziegler, N.; Thiele, S.; Moeller, S.; Schnabelrauch, M.; Hintze, V.; Scharnweber, D.; Rauner, M.; Hofbauer, L. C. *J. Cell. Biochem.* **2014**, *115* (6), 1101–1111.

(120) Klouda, L.; Hacker, M. C.; Kretlow, J. D.; Mikos, A. G. *Biomaterials* **2009**, *30* (27), 4558–4566.

(121) Klouda, L.; Perkins, K. R.; Watson, B. M.; Hacker, M. C.; Bryant, S. J.; Raphael, R. M.; Kasper, F. K.; Mikos, A. G. *Acta Biomater.* **2011**, *7* (4), 1460–1467.

(122) Hacker, M. C.; Klouda, L.; Ma, B. B.; Kretlow, J. D.; Mikos, A. G. *Biomacromolecules* **2008**, *9* (6), 1558–1570.

(123) Coleman, L. E.; Bork, J. F.; Wyman, D. P.; Hoke, D. I. *J. Polym. Sci. Part A* **1965**, *3* (4PA), 1601–1608.

(124) Taylor, L. D.; Cerankowski, L. D. *J. Polym. Sci.* **1975**, *13* (11), 2551–2570.

(125) Kniazeva, E.; Kachgal, S.; Putnam, A. J. *Tissue Engineering Part A*. 2011, pp 905–914.

(126) Wang, L.-S.; Boulaire, J.; Chan, P. P. Y.; Chung, J. E.; Kurisawa, M. *Biomaterials* **2010**, *31* (33), 8608–8616.

(127) Tillet, G.; Boutevin, B.; Ameduri, B. *Prog. Polym. Sci.* **2011**, *36* (2), 191–217.

(128) Sung, H. J.; Sakala Labazzo, K. M.; Bolikal, D.; Weiner, M. J.; Zimnisky, R.; Kohn, J. *Eur. Cell. Mater.* **2008**, *15*, 77–87.

(129) Demko, P. R. *J. Chromatogr.* **1979**, *179* (2), 361–364.

(130) Nayeem, S. M.; Deep, S. *J. Mol. Recognit.* **2014**, *27* (8), 471–481.

(131) Fan, H.; Vitharana, S. N.; Chen, T.; O'Keefe, D.; Middaugh, C. R. *Mol. Pharm.* **2007**, *4* (2), 232–240.

(132) Burnat, G.; Rau, T.; Elshimi, E.; Hahn, E. G.; Konturek, P. C. *Scand. J. Gastroenterol.* **2007**, *42* (12), 1460–1465.

(133) Liu, Y.; Kalén, A.; Risto, O.; Wahlström, O. *Platelets* **2003**, *14* (4), 233–237.

(134) Kalén, A.; Wahlström, O.; Linder, C. H.; Magnusson, P. *Biochem. Biophys. Res. Commun.* **2008**, *375* (2), 261–264.

(135) Schwartz, D. A.; Abrams, M. J.; Hauser, M. M.; Gaul, F. E.; Larsen, S. K.; Rauh, D.; Zubieta, J. A. *Bioconjug. Chem.* **1991**, *2* (5), 333–336.

(136) Zhang, X.; Breslav, M.; Grimm, J.; Guan, K.; Huang, A.; Liu, F.; Maryanoff, C. A.; Palmer, D.; Patel, M.; Qian, Y.; Shaw, C.; Sorgi, K.; Stefanick, S.; Xu, D. *J. Org. Chem.* **2002**, *67* (26), 9471–9474.

(137) Dirksen, A.; Dirksen, S.; Hackeng, T. M.; Dawson, P. E. *J. Am. Chem. Soc.* **2006**, *128* (49), 15602–15603.

(138) King, T. P.; Zhao, S. W.; Lam, T. *Biochemistry* **1986**, *25* (19), 5774–5779.

(139) Chim, H.; Miller, E.; Gliniak, C.; Alsberg, E. *Cell Tissue Res.* **2012**, *350* (1), 89–94.

(140) Steinhagen, M.; Hoffmeister, P.-G.; Nordsieck, K.; Hötzel, R.; Baumann, L.; Hacker, M. C.; Schulz-Siegmund, M.; Beck-Sickinger, A. G. *ACS Appl. Mater. Interfaces* **2014**, *6* (8), 5891–5899.

(141) Shoichet, M. S. *Macromolecules* **2010**, *43* (2), 581–591.

(142) Moore, M. J.; Jabbari, E.; Ritman, E. L.; Lu, L.; Currier, B. L.; Windebank, A. J.; Yaszemski, M. J. *J. Biomed. Mater. Res. A* **2004**, *71* (2), 258–267.

(143) Baino, F.; Fiorilli, S.; Vitale-Brovarone, C. *Acta Biomater.* **2016**, *42*, 18–32.

(144) Columbus, S.; Krishnan, L. K.; Krishnan, V. K. *J. Biomed. Mater. Res. B Appl. Biomater.* **2014**, *102* (4), 789–796.

(145) Whang, K.; Thomas, C. H.; Healy, K. E.; Nuber, G. *Polymer* **1995**, *36* (4), 837–842.

(146) Poologasundarampillai, G.; Yu, B.; Tsigkou, O.; Valliant, E.; Yue, S.; Lee, P. D.; Hamilton, R. W.; Stevens, M. M.; Kasuga, T.; Jones, J. R. *Soft Matter* **2012**, *8* (17), 4822–4832.

(147) Savkovic, V.; Flämig, F.; Schneider, M.; Sülflow, K.; Loth, T.; Lohrenz, A.; Hacker, M. C.; Schulz-Siegmund, M.; Simon, J. C. *J. Biomed. Mater. Res. A* **2016**, *104* (1), 26–36.

(148) Gao, C.; Rahaman, M. N.; Gao, Q.; Teramoto, A.; Abe, K. *J. Biomed. Mater. Res. A* **2013**, *101A* (7), 2027–2037.

(149) Luo, Y.; Wu, C.; Lode, A.; Gelinsky, M. *Biofabrication* **2013**, *5* (1), 15005.

(150) Hendrikx, S.; Kuzmenka, D.; Köferstein, R.; Flath, T.; Uhlig, H.; Enke, D.; Schulze, F. P.; Hacker, M. C.; Schulz-Siegmund, M. *J. Sol-Gel Sci. Technol.* **2017**, *83* (1), 143–154.

(151) Lao, J.; Dieudonné, X.; Fayon, F.; Montouillout, V.; Jallot, E. *J. Mater. Chem. B* **2016**, *4* (14), 2486–2497.

(152) Gyles, D. A.; Castro, L. D.; Carrera Silva, J. O.; Ribeiro-Costa, R. M. *Eur. Polym. J.* **2017**, *88* (1), 373–392.

(153) Slaughter, B. V.; Khurshid, S. S.; Fisher, O. Z.; Khademhosseini, A.; Peppas, N. A. *Adv. Mater.* **2009**, *21* (32–33), 3307–3329.

(154) Brandl, F.; Sommer, F.; Goepferich, A. *Biomaterials* **2007**, *28* (2), 134–146.

(155) Lai, J.; Li, Y. **2010**, 1387–1397.

(156) Khutoryanskaya, O. V; Mayeva, Z. A.; Mun, G. A.; Khutoryanskiy, V. V. *Biomacromolecules* **2008**, *9* (12), 3353–3361.

(157) Dadsetan, M.; Hefferan, T. E.; Szatkowski, J. P.; Mishra, P. K.; Macura, S. I.; Lu, L.; Yaszemski, M. J. *Biomaterials* **2008**, *29* (14), 2193–2202.

(158) Van Vlierberghe, S.; Cnudde, V.; Dubruel, P.; Masschaele, B.; Cosijns, A.; De Paepe, I.; Jacobs, P. J. S.; Van Hoorebeke, L.; Remon, J. P.; Schacht, E. *Biomacromolecules* **2007**, *8* (2), 331–337.

(159) Rose, J. C.; Torres, M. C.; Rahimi, K.; Köhler, J.; Moeller, M.; De Laporte, L. *Nano Lett.* **2017**, *17* (6), 3782–3791.

(160) Scott, E. A.; Nichols, M. D.; Kuntz-Willits, R.; Elbert, D. L. *Acta Biomater.* **2010**, *6* (1), 29–38.

(161) Zhu, L.; Yi, Z.; Liu, F.; Wei, X.; Zhu, B.; Xu, Y. *Eur. Polym. J.* **2008**, *44* (6), 1907–1914.

(162) Atta, A. M.; El-Hamouly, S. H.; AlSabagh, A. M.; Gabr, M. M. *J. Appl. Polym. Sci.* **2007**, *105* (4), 2113–2120.

(163) Rietman, E. A.; Kaplan, M. L. *J. Polym. Sci. Pol. Lett.* **1990**, *28* (6), 187–191.

(164) Xu, J.; Filion, T. M.; Prifti, F.; Song, J. *Chem. Asian J.* **2011**, *6* (10), 2730–2737.

(165) DeForest, C. A.; Anseth, K. S. *Annu. Rev. Chem. Biomol. Eng.* **2012**, *3*, 421–444.

(166) Wagoner Johnson, A. J.; Herschler, B. A. *Acta Biomater.* **2011**, *7* (1), 16–30.

(167) Mezger, T. *Das Rheologie-Handbuch*, First Edit.; Vincentz Network, Hannover, 2000.

(168) Schwabe, K.; Ewe, A.; Kohn, C.; Loth, T.; Aigner, A.; Hacker, M. C.; Schulz-Siegmund, M. *Int. J. Pharm.* **2017**, *526* (1–2), 178–187.

(169) Dawlee, S.; Sugandhi, A.; Balakrishnan, B.; Labarre, D.; Jayakrishnan, A. *Biomacromolecules* **2005**, *6* (4), 2040–2048.

(170) Kang, H. W.; Tabata, Y.; Ikada, Y. *Biomaterials* **1999**, *20* (14), 1339–1344.

(171) Bigi, A.; Cojazzi, G.; Panzavolta, S.; Rubini, K.; Roveri, N. *Biomaterials* **2001**, *22* (8), 763–768.

(172) Sisson, K.; Zhang, C.; Farach-Carson, M. C.; Chase, D. B.; Rabolt, J. F. *Biomacromolecules* **2009**, *10* (7), 1675–1680.

(173) Rattanaruengsrikul, V.; Pimpha, N.; Supaphol, P. *Macromol. Biosci.* **2009**, *9* (10), 1004–1015.

(174) Sheu, M. T.; Huang, J. C.; Yeh, G. C.; Ho, H. O. *Biomaterials* **2001**, *22* (13), 1713–1719.

(175) Ren, L.; Tsuru, K.; Hayakawa, S.; Osaka, A. *Biomaterials* **2002**, *23* (24), 4765–4773.

(176) Yang, X.-Y.; Chen, L.-H.; Li, Y.; Rooke, J. C.; Sanchez, C.; Su, B.-L. *Chem. Soc. Rev.* **2017**, *46* (2), 481–558.

(177) Harrar, K.; Hamami, L. *J. Med. Biol. Eng.* **2013**, *33* (6), 569–575.

(178) Nakayama, H.; Burns, D. M.; Kawase, T. *J. Nondestruct. Eval.* **2011**, *30* (2), 71–80.

(179) Rahaman, M. N.; Day, D. E.; Sonny Bal, B.; Fu, Q.; Jung, S. B.; Bonewald, L. F.; Tomsia, A. P. *Acta Biomater.* **2011**, *7* (6), 2355–2373.

(180) Valliant, E. M.; Romer, F.; Wang, D.; McPhail, D. S.; Smith, M. E.; Hanna, J. V.; Jones,

J. R. *Acta Biomater.* **2013**, *9* (8), 7662–7671.

(181) Wang, Z.; Yu, L.; Ding, M.; Tan, H.; Li, J.; Fu, Q. *Polym. Chem.* **2011**, *2* (3), 601–607.

(182) Rezwan, K.; Chen, Q. Z.; Blaker, J. J.; Boccaccini, A. R. *Biomaterials* **2006**, *27* (18), 3413–3431.

(183) Luckachan, G. E.; Pillai, C. K. S. *J. Polym. Environ.* **2011**, *19* (3), 637–676.

(184) Roether, J. A.; Boccaccini, A. R.; Hench, L. L.; Maquet, V.; Gautier, S.; Jérôme, R. *Biomaterials* **2002**, *23* (18), 3871–3878.

(185) Blaker, J. J.; Nazhat, S. N.; Maquet, V.; Boccaccini, A. R. *Acta Biomater.* **2011**, *7* (2), 829–840.

(186) Zhou, H.; Lawrence, J. G.; Bhaduri, S. B. *Acta Biomater.* **2012**, *8* (6), 1999–2016.

(187) Lei, B.; Wang, L.; Chen, X.; Chae, S.-K. *J. Mater. Chem. B* **2013**, *1* (38), 5153–5162.

(188) Trujillo, S.; Pérez-Román, E.; Kyritsis, A.; Gómez Ribelles, J. L.; Pandis, C. *J. Polym. Sci. Pol. Phys.* **2015**, *53* (19), 1391–1400.

(189) Litschauer, M.; Neouze, M. A.; Haimer, E.; Henniges, U.; Potthast, A.; Rosenau, T.; Liebner, F. *Cellulose* **2011**, *18* (1), 143–149.

(190) Rhee, S.-H.; Choi, J.-Y.; Kim, H.-M. *Biomaterials* **2002**, *23* (24), 4915–4921.

(191) Rhee, S.-H. *Biomaterials* **2003**, *24* (10), 1721–1727.

(192) Rhee, S.-H. *Biomaterials* **2004**, *25* (7–8), 1167–1175.

(193) Helminen, A.; Korhonen, H.; Seppälä, J. *Polymer* **2001**, *42* (8), 3345–3353.

(194) Rhee, S.-H.; Lee, S. J. *J. Biomed. Mater. Res. A* **2007**, *83A* (3), 799–805.

(195) Poologasundarampillai, G.; Yu, B.; Jones, J. R.; Kasuga, T. *Soft Matter* **2011**, *7* (21), 10241–10251.

(196) Mazzocchetti, L.; Sandri, S.; Scandola, M. *Biomacromolecules* **2007**, *8* (2), 672–678.

(197) Ikada, Y.; Tsuji, H. *Macromol. Rapid Comm.* **2000**, *21* (3), 117–132.

(198) Schulze, P.; Flath, T.; Dörfler, H.-M.; Schulz-Siegmund, M.; Hacker, M.; Hendrikx, S.; Kascholke, C.; Gressenbuch, M.; Schumann, D. *Ger. Pat. No. DE102014224654A1* **2016**.

(199) Lieb, E.; Milz, S.; Vogel, T.; Hacker, M.; Dauner, M.; Schulz, M. B. *Tissue Eng.* **2004**, *10* (9–10), 1399–1413.

(200) Wang, D. K.; Varanasi, S.; Hill, D. J. T.; Rasoul, F.; Symons, A. L.; Whittaker, A. K. *J. Mater. Chem.* **2012**, *22* (14), 6994–7004.

(201) Peng, H.; Varanasi, S.; Wang, D. K.; Blakey, I.; Rasoul, F.; Symons, A.; Hill, D. J. T.; Whittaker, A. K. *Eur. Polym. J.* **2016**, *84*, 448–464.

(202) Sadeghi, R.; Jahani, F. *J. Phys. Chem. B* **2012**, *116* (17), 5234–5241.

(203) Albertsson, A.-C.; Varma, I. K. *Biomacromolecules* **2003**, *4* (6), 1466–1486.

(204) Messori, M.; Toselli, M.; Pilati, F.; Fabbri, E.; Fabbri, P.; Pasquali, L.; Nannarone, S. *Polymer* **2004**, *45* (3), 805–813.

(205) Chung, J. J.; Li, S.; Stevens, M. M.; Georgiou, T. K.; Jones, J. R. *Chem. Mater.* **2016**, *28* (17), 6127–6135.

(206) Giannoudis, P. V; Dinopoulos, H.; Tsiridis, E. *Injury* **2005**, *36* (3), 20–27.

(207) Babis, G. C.; Soucacos, P. N. *Injury* **2005**, *36* (4), S38–S44.

(208) Oliver, M. S.; Dubois, G.; Sherwood, M.; Gage, D. M.; Dauskardt, R. H. *Adv. Funct. Mater.* **2010**, *20* (17), 2884–2892.

(209) Maçon, A. L.; Page, S. J.; Chung, J. J.; Amdursky, N.; Stevens, M. M.; Weaver, J. V. M.; Hanna, V.; Jones, J. R. *Phys. Chem. Chem. Phys.* **2015**, *17* (43), 29124–29133.

(210) Kumar, N.; Ravikumar, M. N. V; Domb, A. J. *Adv. Drug Deliver. Rev.* **2001**, *53* (1), 23–44.

(211) Li, S. M.; Rashkov, I.; Espartero, J. L.; Manolova, N.; Vert, M. *Macromolecules* **1996**, *29* (1), 57–62.

(212) Tsuji, H. *Macromol. Biosci.* **2005**, *5* (7), 569–597.

(213) Jansen, E. J. P.; Pieper, J.; Gijbels, M. J. J.; Guldemond, N. A.; Riesle, J.; Van Rhijn, L. W.; Bulstra, S. K.; Kuijer, R. *J. Biomed. Mater. Res. A* **2009**, *89* (2), 444–452.

(214) Sherwood, J. K.; Riley, S. L.; Palazzolo, R.; Brown, S. C.; Monkhouse, D. C.; Coates, M.; Griffith, L. G.; Landeen, L. K.; Ratcliffe, A. *Biomaterials* **2002**, *23* (24), 4739–4751.

(215) Maçon, A. L. B.; Li, S.; Chung, J. J.; Nommeots-Nomm, A.; Solanki, A. K.; Stevens, M. M.; Jones, J. R. *J. Mater. Chem. B* **2016**, *4* (36), 6032–6042.

(216) Nooeaid, P.; Salih, V.; Beier, J. P.; Boccaccini, A. R. *J. Cell. Mol. Med.* **2012**, *16* (10), 2247–2270.

(217) Wang, H. M.; Chou, Y. T.; Wen, Z. H.; Wang, Z. R.; Chen, C. H.; Ho, M. L. *PLoS One* **2013**, *8* (6), 2–12.

(218) Guarino, V.; Gloria, A.; Raucci, M. G.; Ambrosio, L. *Polymers* **2012**, *4* (3), 1590–1612.

(219) Hench, L. L.; Jones, J. R. *Front. Bioeng. Biotechnol.* **2015**, *3* (194), 1–12.

(220) Hench, L. L.; Polak, J. M. *Science* **2002**, *295* (5557), 1014–1017.

(221) Lindfors, N. C.; Koski, I.; Heikkilä, J. T.; Mattila, K.; Aho, A. J. *J. Biomed. Mater. Res. B Appl. Biomater.* **2010**, *94B* (1), 157–164.

(222) Yao, A.; Wang, D.; Huang, W.; Fu, Q.; Rahaman, M. N.; Day, D. E. *J. Am. Ceram. Soc.* **2007**, *90* (1), 303–306.

(223) Rhee, S.-H.; Lee, Y.-K.; Lim, B.-S.; Yoo, J. J.; Kim, H. J. *Biomacromolecules* **2004**, *5* (4), 1575–1579.

(224) Song, S. H.; Lee, S. J.; Rhee, S. H. *J. Biomed. Mater. Res. B Appl. Biomater.* **2012**, *100B* (5), 1289–1297.

(225) Obata, A.; Ito, S.; Iwanaga, N.; Mizuno, T.; Jones, J. R.; Kasuga, T. *RSC Adv.* **2014**, *4* (94), 52491–52499.

(226) Gao, C.; Gao, Q.; Li, Y.; Rahaman, M. N.; Teramoto, A.; Abe, K. *J. Appl. Polym. Sci.* **2013**, *127* (4), 2588–2599.

(227) Negahi Shirazi, A.; Fathi, A.; Suarez, F. G.; Wang, Y.; Maitz, P. K.; Dehghani, F. *ACS Appl. Mater. Interfaces* **2016**, *8* (3), 1676–1686.

(228) Shiu, J. C.; Ho, M. H.; Yu, S. H.; Chao, A. C.; Su, Y. R.; Chen, W. J.; Chiang, Z. C.; Yang, W. P. *Carbohydr. Polym.* **2010**, *79* (3), 724–730.

(229) Poologasundarampillai, G.; Yu, B.; Tsigkou, O.; Wang, D.; Romer, F.; Bhakhri, V.; Giuliani, F.; Stevens, M. M.; McPhail, D. S.; Smith, M. E.; Hanna, J. V.; Jones, J. R. *Chem. Eur. J.* **2014**, *20* (26), 8149–8160.

(230) Rose, J. B.; Pacelli, S.; El Haj, A. J.; Dua, H. S.; Hopkinson, A.; White, L. J.; Rose, F. R. A. J. *Materials* **2014**, *7* (4), 3106–3135.

(231) Gauthier, M. A.; Gibson, M. I.; Klok, H.-A. *Angew. Chemie Int. Ed.* **2009**, *48* (1), 48–58.

(232) Schilli, C. M.; Müller, A. H. E.; Rizzardo, E.; Thang, S. H.; Chong, B. Y. K. In *Advances in Controlled/Living Radical Polymerization*; 2003; Vol. 854, pp 603–618.

(233) Lü, S.; Li, B.; Ni, B.; Sun, Z.; Liu, M.; Wang, Q. *Soft Matter* **2011**, *7* (22), 10763–10772.

(234) Park, E.-S.; Kim, M.-N.; Lee, I.-M.; Lee, H. S.; Yoon, J.-S. *J. Polym. Sci. Pol. Chem.* **2000**, *38* (12), 2239–2244.

(235) Lessard, B. H.; Mackay, S.; Métafiot, A.; Marić, M. *Macromol. Res.* **2016**, *24* (8), 710–715.

(236) Bigi, A.; Cojazzi, G.; Panzavolta, S.; Roveri, N.; Rubini, K. *Biomaterials* **2002**, *23* (24), 4827–4832.

(237) Liang, H. C.; Chang, W. H.; Liang, H. F.; Lee, M. H.; Sung, H. W. *J. Appl. Polym. Sci.* **2004**, *91* (6), 4017–4026.

(238) Speer, D. P.; Chvapil, M.; Eskelson, C. D.; Ulreich, J. *J. Biomed. Mater. Res.* **1980**, *14*

(6), 753–764.

(239) Rose, J. C.; Torres, M. C.; Rahimi, K.; Köhler, J.; Moeller, M.; De Laporte, L. *Nano Lett.* **2017**, *17* (6), 3782–3791.

(240) Kirchhof, S.; Brandl, F. P.; Hammer, N.; Goepferich, A. M. *J. Mater. Chem. B* **2013**, *1* (37), 4855.

(241) McKinnon, D. D.; Domaille, D. W.; Brown, T. E.; Kyburz, K. a; Kiyotake, E.; Cha, J. N.; Anseth, K. S. *Soft Matter* **2014**, *10*, 9230–9236.

(242) Patenaude, M.; Hoare, T. *ACS Macro Lett.* **2012**, *1* (3), 409–413.

(243) Prestwich, G. D.; Marecak, D. M.; Marecek, J. F.; Vercruysse, K. P.; Ziebell, M. R. *J. Control. Release* **1998**, *53* (1–3), 93–103.

(244) Beria, L.; Gevrek, T. N.; Erdog, A.; Sanyal, R.; Pasini, D.; Sanyal, A. *Biomater. Sci.* **2014**, *2* (1), 67–75.

(245) Atkovska, K.; Samsonov, S. A.; Paszkowski-Rogacz, M.; Pisabarro, M. T. *Int. J. Mol. Sci.* **2014**, *15* (2), 2622–2645.

(246) Costa, F.; Carvalho, I. F.; Montelaro, R. C.; Gomes, P.; Martins, M. C. L. *Acta Biomater.* **2011**, *7* (4), 1431–1440.

(247) Kohn-Polster, C.; Bhatnagar, D.; Woloszyn, D. J.; Richtmyer, M.; Starke, A.; Springwald, A. H.; Franz, S.; Schulz-Siegmund, M.; Kaplan, H. M.; Kohn, J.; Hacker, M. C. *Int. J. Mol. Sci.* **2017**, *18* (5), 1104.

(248) Burdick, J. A.; Philpott, L. M.; Anseth, K. S. *J. Polym. Sci. Pol. Chem.* **2001**, *39* (5), 683–692.

(249) Davidenko, N.; Campbell, J. J.; Thian, E. S.; Watson, C. J.; Cameron, R. E. *Acta Biomater.* **2010**, *6* (10), 3957–3968.

(250) Russo, L.; Gabrielli, L.; Valliant, E. M.; Nicotra, F.; Jiménez-Barbero, J.; Cipolla, L.; Jones, J. R. *Mater. Chem. Phys.* **2013**, *140* (1), 168–175.

(251) Hendrikx, S. A. G. *Diss. Univ. Leipzig, Fak. für Biowissenschaften, Pharm. und Psychol.* **2016**.

(252) Södergård, A.; Stolt, M. *Prog. Polym. Sci.* **2002**, *27* (6), 1123–1163.

(253) Novak, B. M. *Adv. Mater.* **1993**, *5* (6), 422–433.

(254) Valliant, E. M.; Jones, J. R. *Soft Matter* **2011**, *7* (11), 5083.

(255) Ren, L.; Tsuru, K.; Hayakawa, S.; Osaka, A. *J. Non-Cryst. Solids* **2001**, *285* (1–3), 116–122.

(256) Loth, R.; Loth, T.; Schwabe, K.; Bernhardt, R.; Schulz-Siegmund, M.; Hacker, M. C. *Acta Biomater.* **2015**, *26*, 82–96.

(257) Picke, A.-K.; Salbach-Hirsch, J.; Hintze, V.; Rother, S.; Rauner, M.; Kascholke, C.; Möller, S.; Bernhardt, R.; Rammelt, S.; Pisabarro, M. T.; Ruiz-Gómez, G.; Schnabelrauch, M.; Schulz-Siegmund, M.; Hacker, M. C.; Scharnweber, D.; Hofbauer, C.; Hofbauer, L. C. *Biomaterials* **2016**, *96*, 11–23.

(258) Müller, B. M.; Loth, R.; Hoffmeister, P.-G.; Zühl, F.; Kalbitzer, L.; Hacker, M. C.; Schulz-Siegmund, M. *Acta Biomater.* **2017**, *51*, 148–160.

(259) Lee, M.; Dunn, J. C. Y.; Wu, B. M. *Biomaterials* **2005**, *26* (20), 4281–4289.

(260) Schumacher, M.; Deisinger, U.; Ziegler, G.; Detsch, R. *J. Mater. Sci. Mater. Med.* **2010**, *21* (12), 3119–3127.

(261) Taboas, J. M.; Maddox, R. D.; Krebsbach, P. H.; Hollister, S. J. *Biomaterials* **2003**, *24* (1), 181–194.

(262) Zhang, J.; Zhao, S.; Zhu, Y.; Huang, Y.; Zhu, M.; Tao, C.; Zhang, C. *Acta Biomater.* **2014**, *10* (5), 2269–2281.

(263) Kascholke, C.; Hendrikx, S.; Flath, T.; Kuzmenka, D.; Dörfler, H.-M.; Schumann, D.; Gressenbuch, M.; Schulze, F. P.; Schulz-Siegmund, M.; Hacker, M. C. *Acta Biomater.* **2017**, *63*, 336–349.

(264) Siparsky, G. L.; Voorhees, K. J.; Miao, F. *J. Environ. Polym. Degr.* **1998**, *6* (1), 31–41.

(265) Sheikh, Z.; Najeeb, S.; Khurshid, Z.; Verma, V.; Rashid, H.; Glogauer, M. *Materials* **2015**, *8* (9), 5744–5794.

(266) Duffy, C. V.; David, L.; Crouzier, T. *Acta Biomater.* **2015**, *20*, 51–59.

(267) Smeets, N. M. B.; Patenaude, M.; Kinio, D.; Yavitt, F. M.; Bakaic, E.; Yang, F.-C.; Rheinstädter, M.; Hoare, T. *Polym. Chem.* **2014**, *5* (23), 6811–6823.

(268) Świtała-Żeliazkow, M. *Polym. Degrad. Stab.* **2001**, *74* (3), 579–584.

(269) Pouyani, T.; Brook, S.; Prestwich, G. D. *US Pat. No. 5,616,568* **1997**.

(270) Mikos, A. G.; Hacker, M. C. *US Pat. No. 8,349,982* **2008**.

(271) Hao, Q.; Li, F.; Li, Q.; Li, Y.; Jia, L.; Yang, J.; Fang, Q.; Cao, A. *Biomacromolecules* **2005**, *6* (4), 2236–2247.

(272) Jouyban, A.; Fakhree, M. A. A.; Shayanfar, A. *J. Pharm. Pharm. Sci.* **2010**, *13* (4), 524–535.

(273) Hulbert, S. F.; Young, F. A.; Mathews, R. S.; Klawitter, J. J.; Talbert, C. D.; Stelling, F.

H. *J. Biomed. Mater. Res. A* **1970**, *4* (3), 433–456.

(274) Utech, S.; Boccaccini, A. R. *J. Mater. Sci.* **2016**, *51* (1), 271–310.

(275) Kondiah, P. J.; Choonara, Y. E.; Kondiah, P. P. D.; Marimuthu, T.; Kumar, P.; Du Toit, L. C.; Pillay, V. *Molecules* **2016**, *21* (11).

(276) Kretlow, J. D.; Hacker, M. C.; Klouda, L.; Ma, B. B.; Mikos, A. G. *Biomacromolecules* **2010**, *11* (3), 797–805.

APPENDIX

List of Abbreviations

Curriculum Vitae

List of Publications

Declaration of Authorship

Acknowledgements

LIST OF ABBREVIATIONS

µCT	micro-computed tomography
ADH	adipic acid dihydrazide
aECM	artificial extracellular matrix
AFH	Alexa Fluor 350 hydrazide
AIBN	azobisisobutyronitrile, 2,2'-azobis(2-methylpropionitrile)
ALP	alkaline phosphatase
ATRP	atom transfer radical polymerization
ATTO	fluorescent marker
ATTO-hyHA	fluorescently labeled and hydrazido-functionalized hyaluronan
BMP-2	bone morphogenetic protein-2
brine	saturated aqueous sodium chloride solution
BSA	bovine serum albumin
C	total content of oligomer in hybrid
CAD	computer-aided design
$CDCl_3$	chloroform
cGEL	oligomer(oPxMA)-cross-linked gelatinous hydrogels
CLSM	confocal laser scanning microscopy
COL	Collagel
CRP	controlled/living radical polymerization
DAAm	diacetone acrylamide
DAPI	4',6-diamidino-2-phenylindole
DEED	*N,N*-diethylethylenediamine
DIPE	diisopropyl ether
$Đ_M$	molecular-weight dispersity
DMEM	Dulbecco's modified eagle medium
DMF	dimethylformamide
DMSO-d_6	deuterated dimethyl sulfoxide
DNPH	2,4-dinitrophenylhydrazine
DSC	differential scanning calorimetry
DW / w_{dry}	dry weight
E	elastic modulus
ECM	extracellular matrix
EDC	1-ethyl-3-(3-dimethylaminopropyl)carbodiimide
EO	oligo(ethylene oxide)
FBS	fetal calf serum

FDA	US Food and Drug Administration
FGF	fibroblast growth factor
FRP	free radical polymerization
G´	storage modulus
G´´	loss modulus
G160	gelatin 160 Bloom
G50	gelatin 50 Bloom
GAG	glycosaminoglycan
GPC	gel permeation chromatography
GPTMS	3-glycidoxypropyl trimethoxysilane
GTA	glutaraldehyde
HA	hyaluronan
hASC	human adipose tissue-derived stem cells
HPLC	high-performance liquid chromatography
HTWK	Hochschule für Technik, Wirtschaft und Kultur
hyHA	hydrazido-modified hyaluronan
ICI	interconnectivity index
ICPTES	3-isocyanatopropyltriethoxysilane
IgG	immunglobulin G
ISO	International Organization for Standardization
IUPAC	International Union of Pure and Applied Chemistry
LA	oligo(D,L-lactide)
LSM	laser scanning microscopy
MA	maleic anhydride
MIP	mercury intrusion porosimetry
M_n	number average molecular weight
M_n(EO)	oligo(ethylene oxide)-derived molecular weight
M_n(LA)	oligo(lactide)-derived molecular weight
M_n(total)	total molecular weight
M_w	weight average molecular weight
N	oligomer valence
$NaCNBH_3$	sodium cyanoborohydride
NHS	*N*-hydroxysuccinimide
NiPAAm	*N*-isopropylacrylamide
NMP	*N*-methyl-2-pyrrolidone
NMR	nuclear magnetic resonance
oPDMA	oligo(PEDAS-*co*-DAAm-*co*-MA)
$oPDMA^{+DEED}$	DEED-functionalized oPDMA

oPNMA	oligo(PEDAS-*co*-NiPAAm-*co*-MA)
OPTN	Organ Procurement and Transplantation Network
oPxMA	oPDMA or oPNMA
P8k	poly(ethylene glycol) with average molecular weight (M_n) = 8000 Da
PBS	phosphate buffered saline
PCL	poly(ε-caprolactone)
PDGF	platelet derived growth factor
PEDAS	pentaerythritol diacrylate monostearate
PEG	poly(ethylene glycol)
PETEO / Px	pentaerythritol ethoxylate with x representing its molecular weight (M_n)
PGA	polyglycolide
PLA	polylactide
PLGA	poly(lactide-*co*-glycolide)
PTFE	polytetrafluoroethylene
PVA	poly(vinyl alcohol)
PxLAy	four-armed LA-containing PETEO-derived oligomer
PxLAy-Si	silanized four-armed LA-containing PETEO-derived macromer
RAFT	reversible addition-fragmentation chain transfer
RFU	relative fluorescence units
RGD	arginylglycylaspartic acid
ROP	ring-opening polymerization
rt	room temperature
SD	standard deviation
SDF-1α	stromal cell-derived factor-1α
SEC	size exclusion chromatography
SEM	scanning electron microscopy
siRNA	small interfering RNA
$Sn(Oct)_2$	tin(II) 2-ethylhexanoate
SRTR	Scientific Registry of Transplant Recipients
TEA	triethylamine
TEOS	tetraethoxysilane
TFAA	trifluoroacetic anhydride
TGF-β	transforming growth factor beta
THF	tetrahydrofuran
TMPEO / Tx	trimethylolpropane ethoxylate with x representing its molecular weight (M_n)
TNBS	2,4,6-trinitrobenzenesulfonic acid
TW	theoretical (dry) weight
TxLAy	three-armed LA-containing TMPEO-derived oligomer
TxLAy-Si	silanized three-armed LA-containing TMPEO-derived macromer

v_{dry}	dry volume
VEGF	vascular endothelial growth factor
v_{wet}	wet volume
WW / w_{wet}	wet weight
η^*	complex viscosity

CURRICULUM VITAE

PERSONAL DATA

Date and place of birth	July 2, 1988 in Poessneck
Civil status	Married, 2 children
Nationality	German

PROFESSIONAL EXPERIENCE

06/2017 - today	**Project Manager**, mibe GmbH Arzneimittel, Brehna
12/2011 - 05/2017	**PhD candidate**, Institute of Pharmacy, Pharmaceutical Technology, Leipzig University
	Parental leave (02/12/2015 - 04/11/2015)
01/2012	**Licensure as Pharmacist** (final grade: 1.34)
05/2011 - 10/2011	Pharmaceutical traineeship, public pharmacy, Apotheke am Sanct Georg, Leipzig
10/2010 - 04/2011	**Diploma thesis**, Institute of Pharmacy, Pharmaceutical Technology, Leipzig University
	"Synthese und Charakterisierung von Maleinsäureanhydrid-haltigen oligomeren Quervernetzern" (grade: 1.0, 09/2011)
10/2006 - 09/2010	Pharmaceutical studies, Friedrich-Schiller University, Jena

EDUCATION

09/1998 - 05/2006	**High school**, Gymnasium "Am Weissen Turm", Poessneck (final grade: 1.0)
08/1994 - 07/1998	Elementary school, Grundschule "Am Park", Poessneck

LIST OF PUBLICATIONS

PUBLICATIONS (PEER-REVIEWED PAPERS)

Biodegradable and adjustable sol-gel glass based hybrid scaffolds from multi-armed oligomeric building blocks

C. Kascholke, S. Hendrikx, T. Flath, D. Kuzmenka, H.-M. Dörfler, D. Schumann, M. Gressenbuch, F. P. Schulze, M. Schulz-Siegmund, M. C. Hacker. *Acta Biomaterialia*, **2017**, Accepted Manuscript, doi: 10.1016/j.actbio.2017.09.024

Dual-functional hydrazide-reactive and anhydride-containing oligomeric hydrogel building blocks

C. Kascholke, T. Loth, S. Möller, P. Bellstedt, M. Schulz-Siegmund, M. Schnabelrauch, M. C. Hacker. *Biomacromolecules*, March **2017**, Volume 18, No. 3, Pages 683–694

Dual-component collagenous peptide/reactive oligomer hydrogels as potential nerve guidance materials – from characterization to functionalization

C. Kohn, J. M. Klemens, C. Kascholke, N. S. Murthy, J. Kohn, M. Brandenburger, M. C. Hacker. *Biomaterials Science*, October **2016**, Volume 4, No. 11, Pages 1605-1621

Melanocytes from the outer root sheath of human hair and epidermal melanocytes display improved melanotic features in the niche provided by cGEL, oligomer-cross-linked gelatin-based hydrogel

K. Sülflow, M. Schneider, T. Loth, C. Kascholke, M. Schulz-Siegmund, M. C. Hacker, J.-C. Simon, V. Savkovic. *Journal of Biomedical Materials Research Part A*, December **2016**, Volume 104, No. 12, Pages 3115-3126

Sulfated hyaluronan improves bone regeneration of diabetic rats by scavenging sclerostin and enhancing osteoblast function

A.-K. Picke, J. Salbach-Hirsch, V. Hintze, S. Rother, M. Rauner, S. Möller, C. Kascholke, M. C. Hacker, M. Schulz-Siegmund, S. Rammelt, M. Schnabelrauch, D. Scharnweber, C. Hofbauer, L. C. Hofbauer. *Biomaterials*, July **2016**, Volume 96, Pages 11-23

Indirect rapid prototyping of sol-gel hybrid glass scaffolds for bone regeneration - effects of organic crosslinker valence, content and molecular weight on mechanical properties

S. Hendrikx, C. Kascholke, T. Flath, D. Schumann, M. Gressenbuch, P. Schulze, M. C. Hacker, M. Schulz-Siegmund. *Acta Biomaterialia*, April **2016**, Volume 35, Pages 318-329

Gelatin-based biomaterial engineering with anhydride-containing oligomeric cross-linkers

T. Loth, R. Hötzel, C. Kascholke, U. Anderegg, M. Schulz-Siegmund, M. C. Hacker. *Biomacromolecules*, May **2014**, Volume 15, No. 6, Pages 2104-2118

Reactive and stimuli-responsive maleic anhydride containing macromers – multi-functional cross-linkers and building blocks for hydrogel fabrication

T. Loth*, R. Hennig*, C. Kascholke*, R. Hötzel, M. C. Hacker (*Contributed equally). *Reactive and Functional Polymers*, November **2013**, Volume 73, No. 11, Pages 1480-1492

PATENTS

Makroporöse, bioabbaubare organisch-vernetzte Silikat-Hybridmaterialien zur Implantation

P. Schulze, T. Flath, H.-M. Dörfler, M. Schulz-Siegmund, M. Hacker, S. Hendrikx, C. Kascholke, M. Gressenbuch, D. Schumann. *German Patent*, June **2016**, No. 10 2014 224 654A1

CONFERENCE ABSTRACTS (POSTER PRESENTATIONS)

Modification Potential of Oligomer-cross-linked Gelatin Gels Containing Ketone Groups

C. Kascholke, S. Krusch, C. Kohn, M. Schulz-Siegmund, M. C. Hacker

13th Research Festival, Leipzig, Germany, December 18, **2014**

Dual-functional oligomeric cross-linkers for gelatin hydrogel formation - Physico-chemical characterization

C. Kascholke, S. Krusch, C. Kohn, M. Schulz-Siegmund, M. C. Hacker

Annual Meeting of the German Society for Biomaterials (DGBM), Dresden, Germany, November 6-8, **2014**

Novel cross-linked gelatin-based hydrogels - Effects of cross-linker chemistry on material properties

T. Loth, C. Kascholke, R. Hötzel, M. Schulz-Siegmund, M. C. Hacker

Controlled Release Society (CRS), German Chapter Annual Meeting, Ludwigshafen, Germany, March 21-22, **2013**

DECLARATION OF AUTHORSHIP

Hiermit erkläre ich, dass ich die vorliegende Dissertation mit dem Thema „Novel Oligomeric Biodegradable Crosslinkers For Hybrid Biomaterial Fabrication For Regenerative Purposes“ eigenständig verfasst und alle verwendeten Quellen im Literaturverzeichnis angegeben habe. Ich bestätige, dass ich die Kapitel 1, 2, 6, 7 und 8 in alleiniger Urheberschaft verfasst habe.

Zitate aus der Literatur sind als solche gekennzeichnet. Abbildungen und Tabellen sind von mir selbst erstellt worden oder mit einem entsprechenden Literaturverweis versehen.

Ich versichere, dass

- die vorliegende Arbeit ohne unzulässige Hilfe und ohne Benutzung anderer als der angegebenen Hilfsmittel angefertigt wurde und dass die aus fremden Quellen direkt oder indirekt übernommenen Gedanken in der Arbeit als solche kenntlich gemacht worden sind;
- keine weiteren Personen als die genannten Coautoren und die in der Danksagung erwähnten Personen in dem jeweils genannten Umfang an der Auswahl und Auswertung des Materials sowie bei der Herstellung des Manuskripts beteiligt waren;
- keine Hilfe eines Promotionsberaters in Anspruch genommen wurde und dass Dritte weder unmittelbar noch mittelbar geldwerte Leistungen für Arbeiten erhalten haben, die im Zusammenhang mit dem Inhalt der vorgelegten Dissertation stehen;
- die vorgelegte Arbeit in gleicher oder in ähnlicher Form keiner anderen wissenschaftlichen Einrichtung zum Zwecke einer Promotion oder eines anderen Prüfungsverfahrens vorgelegt und auch veröffentlicht wurde;
- bisher keine erfolglosen Promotionsversuche stattgefunden haben;
- die Art und der Umfang der Coautoren an der wissenschaftlichen Leistung der vorgelegten Publikationen vollständig angegeben sind.

Leipzig, den 13.11.2017

_____

Christian Kascholke

ACKNOWLEDGEMENTS

Frau Prof. Dr. Michaela Schulz-Siegmund danke ich für die Möglichkeit, ein Teil ihres Forschungsteams sein zu können sowie für die kontinuierliche Unterstützung beim Fortgang meiner Arbeit. Bereits durch die Aufnahme in ihre Arbeitsgruppe als Diplomand trug sie maßgeblich dazu bei, mein Interesse am Forschungsgebiet zu wecken. Die während dieser Zeit erworbenen Erfahrungen ermöglichten mir zudem einen optimalen Einstieg in die Doktorandenzeit. Ebenfalls danke ich ihr für die Möglichkeit zur flexiblen Planung der Arbeitszeit, die es mir ermöglichte, Doktorandenzeit und Familie miteinander zu vereinbaren.

Herrn PD Dr. Michael Hacker danke ich dafür, insgesamt drei unterschiedliche Biomaterial-Projekte bearbeiten zu dürfen und für das dabei entgegengebrachte Vertrauen. Vielen Dank für die wertvolle Unterstützung bei der Planung der Experimente, der kritischen Diskussion der Ergebnisse und beim Verfassen der Publikationen sowie der vorliegenden Arbeit. Besonders bedanken möchte ich mich für die Möglichkeit zur Teilnahme an zwei nationalen Konferenzen und die Aufnahme in ein interdisziplinäres DFG-Projekt, durch das ich meine wissenschaftlichen Kompetenzen maßgeblich erweitern konnte.

Für die finanzielle Unterstützung danke ich der Deutschen Forschungsgemeinschaft (DFG, SFB/Transregio 67, Teilprojekt A1), sowie der AiF Projekt GmbH (Förderungs-Nr.: KF2734502MU1).

Ich danke Dr. Stephan Hendrikx, Dzmitry Kuzmenka (Institut für Pharmazie, Pharmazeutische Technologie, Universität Leipzig), Tobias Flath, Hans-Martin Dörfler, Prof. Dr. Peter Schulze (Fakultät für Maschinenbau und Energietechnik, HTWK Leipzig), Dr. Mathias Gressenbuch (DMG Chemie GmbH, Leipzig) und Dr. Dirk Schumann (intelligent fluids GmbH, Leipzig) für die konstruktive Kooperation im ‚HySiBone'-Projekt, auch wenn es letztendlich nicht gelang, einen Bioglas-Körper in Form eines Messers herzustellen.

Großer Dank gilt Dr. Robert Hennig, Dr. Tina Loth, Caroline Kohn-Polster und Hafiz Awais Nawaz (Institut für Pharmazie, Pharmazeutische Technologie, Universität Leipzig) für die enge Zusammenarbeit im oPxMA/Gelatine-Hydrogel-Projekt. Durch stetes Miteinander konnte die Materialentwicklung optimal vorangetrieben werden und die routinemäßige Makromer-Synthese und Materialherstellung für Kooperationspartner auf mehrere Schultern verteilt werden.

Vielen Dank an Dr. Rudi Loth, Jan Krieghoff und Benno Müller (Institut für Pharmazie, Pharmazeutische Technologie, Universität Leipzig) für die Unterstützung bei der Bearbeitung des TriLA-Material-Projektes. Auch hier musste ein Spagat aus eigenem Forschungsfortschritt und der Materialsynthese für den Forschungsverbund gefunden werden, der allein nicht möglich gewesen wäre.

Ein ganz besonderer Dank gilt Annett Starke (Institut für Pharmazie, Pharmazeutische Technologie, Universität Leipzig), die in allen drei Projekten wertvolle Zuarbeit leistete. Dies betraf vor allem Routine-Aufgaben, die sie sehr gewissenhaft und zuverlässig erledigte. Vielen Dank auch für die regelmäßige Erinnerung an die Einhaltung des Arbeitsschutzes im Labor.

Für die erfolgreiche Kooperation im DFG-Projekt ‚SFB/Transregio 67' danke ich Marie Schneider / Dr. Vuk Savkovic (Translationszentrum für Regenerative Medizin, Leipzig), Dr. Ann-Kristin Picke / Prof. Dr. Lorenz Hofbauer (Klinik und Poliklinik für Innere Medizin III, TU Dresden), Stephan Thönes / PD Dr. Ulf Anderegg und Nadine Lohmann / Dr. Sandra Franz (Klinik und Poliklinik für Dermatologie, Venerologie und Allergologie, Universität Leipzig). Dabei stand vor allem die *in vitro*- und *in vivo*-Charakterisierung der Zytokompatibilität der synthetisierten Materialien im Mittelpunkt. Ganz besonders möchte ich die Zusammenarbeit mit Dr. Stephanie Möller / Dr. Matthias Schnabelrauch (Innovent e. V., Bereich Biomaterialien, Jena) hervorheben. Auch wenn Stephanie in unzählige weitere Projekte involviert war, investierte sie viel Zeit in die Herstellung Hydrazido-funktionalisierter Hyaluronan-Derivate und ermöglichte damit eine Veröffentlichung des oPDMA/Gelatine-Materialkonzeptes in *Biomacromolecules*.

Ich danke Dr. Lothar Hennig (Institut für Organische Chemie, Universität Leipzig) für die Unterstützung bei der NMR-Analytik. Er ermöglichte stets einen kurzfristigen Zugang zu den Spektrometern. Gleichzeitig hatte er immer ein offenes Ohr für sich stellende Probleme und konnte durch seine umfassende Expertise einen großen Beitrag zu deren Lösung leisten.

Großer Dank gilt Jonas Steiner, Franziska Tischer, Saskia Krusch und Anne Dießler (Institut für Pharmazie, Pharmazeutische Technologie, Universität Leipzig), die durch ihre Tätigkeiten im Wahlpflichtfach wertvolle Forschungsarbeit leisteten. Durch enge Zusammenarbeit gelang es dabei, in nur kurzer Zeit publikationsreife Methoden zu etablieren und Daten zu generieren.

Ich danke Ingo Kannetzky (Werkstatt der Fakultät für Lebenswissenschaften, Universität Leipzig), dessen technische Fähigkeiten sehr hilfreich waren. Vor allem hinsichtlich der Reparatur defekter Geräte war seine Hilfe Gold wert, da er durch seinen Einsatz die eine oder andere kostenintensive Reparatur beim Hersteller vermeiden konnte.

Vielen Dank an alle ehemaligen Kollegen für die Unterstützung im Doktorandenalltag, vor allem hinsichtlich der Organisation im Labor und der Studentenbetreuung. Danke, dass ihr meine Musik im Labor ertragen habt. Ich danke euch auch für die erheiternden Mittagspausen im Seminarraum oder unter freiem Himmel, die einer effektiven Erholung dienten und neue Kraft für den Nachmittag gaben. Sandra Müller und Tobias Flath danke ich sehr für die Hilfe bei der Organisation der ‚1st International Lab Olympics' im April 2017 – einem unvergesslichen Event, das den krönenden Abschluss meiner Doktorandenzeit darstellte.

Unendlicher Dank gilt meiner lieben Frau Annemarie und meinen Kindern Sophia und Jonas für die seelische und moralische Unterstützung während meiner Doktorandenzeit. Ihr bereichert meinen Alltag und seid jeden Tag aufs Neue eine große Motivation. Danke, dass ihr immer an mich geglaubt habt und mich nach Kräften in jeder Hinsicht unterstützt habt. Bitte entschuldigt, dass ihr insbesondere in der Endphase der Fertigstellung dieser Arbeit deutlich zu kurz gekommen seid.